INHIBITION OF THE CORROSION OF MILD STEEL AND ALUMINIUM IN ACIDIC MEDIA BY SOME PURINES

By

HABIBAT MOMOH-YAHAYA

DEPARTMENT OF CHEMISTRY,
FACULTY OF SCIENCE,
AHMADU BELLO UNIVERSITY, ZARIA
NIGERIA

MARCH, 2014

INHIBITION OF THE CORROSION OF MILD STEEL AND ALUMINIUM IN ACIDIC MEDIA BY SOME PURINES

By

Habibat MOMOH-YAHAYA
B.Sc (Hons) (Jos) 1998, M.Sc (Ibadan) 2003
Ph.D / SCIEN / 04406 / 2009-2010

A DISSERTATION SUBMITTED TO THE SCHOOL OF POSTGRADUATE STUDIES, AHMADU BELLO UNIVERSITY, ZARIA, IN PARTIAL FULFILMENT OF THE REQUIREMENTS FOR THE AWARD OF DOCTOR OF PHILOSOPHY (Ph.D) IN PHYSICAL CHEMISTRY

DEPARTMENT OF CHEMISTRY,
FACULTY OF SCIENCE,
AHMADU BELLO UNIVERSITY, ZARIA
NIGERIA

MARCH, 2014

DECLARATION

I declare that the work in this dissertation entitled **'INHIBITION OF THE CORROSION OF MILD STEEL AND ALUMINIUM IN ACIDIC MEDIA BY SOME PURINES'** was performed by me in the Department of Chemistry, under the supervision of Prof. J. F. Iyun, Dr. N. O. Eddy, Prof. C. E. Gimba and Dr. E. E. Oguzie. The information derived from the literature has been duly acknowledged in the text and a list of references provided. No part of this dissertation has been previously presented for another Degree or Diploma at any Institution.

Habibat MOMOH-YAHAYA	**----------**	**----------**
Name of Student	Signature	Date

CERTIFICATION

This dissertation entitled **'INHIBITION OF THE CORROSION OF MILD STEEL AND ALUMINIUM IN ACIDIC MEDIA BY SOME PURINES'** by Habibat MOMOH-YAHAYA, meets the regulations governing the award of Doctor of Philosophy (Ph.D) in Physical Chemistry of Ahmadu Bello University, and is approved for its contribution to knowledge and literary presentation.

Prof. J.F. Iyun Chairman, Supervisory Committee	Signature	Date
Dr. N.O. Eddy Member, Supervsiory Committee	Signature	Date
Prof. C.E. Gimba Member, Supervisory Committee	Signature	Date
Dr. E.E Oguzie Member, Supervisory Committee Department of Chemistry, FUTO, Owerri.	Signature	Date
Prof. A. Uzairu Ag. Head of Department	Signature	Date
Prof. A.A. Joshua Dean, School of Postgraduate Studies	Signature	Date

DEDICATION

This work is dedicated to my Heavenly Father, Jesus my Saviour and Lord, and the Sweet Holy Spirit. “ But thou, O Lord, art a shield for me, my glory and the lifter up of mine head”. Ps 3:3

ACKNOWLEDGEMENTS

My utmost appreciation goes to the Almighty God, the Father of all flesh and spirits for uncommon favour, grace, strength and divine supplies in the course of this research. I am most grateful to my supervisors, Prof. J.F. Iyun, Dr. N.O. Eddy, Prof. C.E. Gimba,all of the Department of Chemistry, Ahmadu Bello University Zaria and Dr. E.E. Oguzie of the Department of Chemistry (Electrochemistry and Material Science Unit), Federal University of Technology (FUTO), Owerri, for their guidance and effective supervision. I acknowledge the support of the Chief Technologists viz: Mrs O.R.A. Iyun and Mr. S. Ekwuribe, Mr. C.A. Ochigbo a Senior Technologist and the rest of staff of the Department of Chemistry, Ahmadu Bello University Zaria. I am much indebted to Prof. G.I. Ndukwe and late Prof. J.A. Kagbu of blessed memory, for their valuable advice and suggestions. I also like to thank Dr. M. Abdulwahab, Dr. V.O. Aigbodion and Mr E.O. Ochuokpa all of the Department of Metallurgical Engineering for their constant support and helpful discussions on this research. Mr D. Zang of Metallurgical Engineering workshop is specially acknowledged for machining the metal sheets into coupons. My appreciation and gratitude also go to the Management and staff of the Kaduna Refinery and Petrochemicals Company (KRPC), particularly the staff of the Chemical Laboratory, for allowing me access to their facilities and some reagents in carrying out the weight loss studies. Special thanks go to Mr. El-Idris (D.O. Quality Control) and all the staff in Lubes, Fuels and Water Units for their friendship and technical support. I want to thank all the members of the Materials and Corrosion group, Department of Chemistry, FUTO for their assistance and knowledge sharing on the use of the electrochemical workstation for electrochemical studies. Thanks go to Arinze, Mr. C.O. Akalezi and Dr. C.K. Enenebeaku. My special gratitude goes to the Tertiary Educational Trust Fund (TETFUND), Federal University of Agriculture Makurdi for providing financial support for this work. I am indebted to my colleaques at the Department of Chemistry, Federal University of Agriculture Makurdi for holding the fort while I was on study leave. I am grateful to the Dean of the College of Science, Prof. R. Sha'ato and the Head of Department of Chemistry, Dr. I.S. Eneji for their valuable advice and support. I wish to thank my friends Terga (sis T), Mordecaia Chahul, Chinyere Okam, Joseph Ocholi, Ivy Bem, Nosiru Adenuga, Kunle Osunlaja, Ahmed Adetoro, Dr. Benny Atolaiye, Mrs C.N. Diri and family, Mr and Mrs Gudi Kreni, for their love, moral and spiritual support, and to all my pastors for their spiritual support. My appreciation goes to Chief O. Onuminya and family for their kind support and assistance in the course of this research. Lastly, my regards go to my siblings Shehu and family, Abdul (Dube), Adams, Musa, Fati, Hauwa, Hassan, Ibro, Rakiya, Aisha and my parents, (Rtd) Capt. and Mrs Yahaya Momoh for their love, understanding, prayers and support. Thank you for always being there for me, I love you all!

ABSTRACT

Studies on the corrosion inhibition potentials of adenine (AD), guanine (GU), hypoxanthine (HYP) and xanthine (XN) on mild steel and aluminium in 0.1 M solutions of HCl, H_2SO_4 and H_3PO_4 were carried out using electrochemical impedance spectroscopy (EIS), potentiodynamic polarisation and gravimetric techniques. The study was carried out at 303 and 333 K respectively. The results obtained revealed that AD, GU, HYP and XN had moderate inhibitive effects on corrosion of mild steel in the three acid media in the decreasing order: AD> HYP> GU> XN in HCl; HYP> AD> GU> XN in H_2SO_4 and GU> AD> HYP> XN in H_3PO_4 at 303 K. The results obtained also showed that AD, GU, HYP and XN inhibited the corrosion of aluminium in HCl in the order: GU> HYP> AD> XN. It was observed that only HYP inhibited the corrosion of aluminium in H_2SO_4 solution while none of the purines inhibited the corrosion of aluminium in H_3PO_4 solution. Potentiodynamic polarisation studies showed that the purines surpressed both the anodic and cathodic half reactions of the corrosion processes, thereby acting as mixed inhibitors, while impedance data indicated that inhibition was achieved via adsorption of the inhibitor species on the mild steel and aluminium surfaces. Synergistic effects slightly increased the efficiency of the inhibitors in the presence of iodide ions. Among several adsorption isotherms assessed, Langmuir adsorption isotherm was found to best describe the adsorption behaviour of the inhibitors on the metal surfaces. According to Langmuir isotherm, calculated values of free energy of adsorption, $\Delta G_{ads}°$, for the corrosion of mild steel in the presence of AD, GU, HYP and XN are as follows: -22.30 to -25.78 kJ mol^{-1} and 5.38 to -28.33 kJ mol^{-1} in HCl at 303 and 333 K respectively; -3.19 to -27.52 kJ mol^{-1} and -11.12 to -21.19 kJ mol^{-1} in H_2SO_4 at 303 and 333 K respectively; -6.70 to -27.52 kJ mol^{-1} and -18.39 to -30.25 kJ mol^{-1} in H_3PO_4 at 303 and 333 K respectively. Calculated $\Delta G_{ads}°$ values for the corrosion of aluminium in the presence of AD, GU, HYP and XN are as follows: -10.12 to -24.04 kJ mol^{-1} and -24.19 to 30.25 kJ mol^{-1} in HCl at 303 and 333 K respectively; -10.12 kJ mol^{-1} and -11.12 kJ mol^{-1} for HYP in H_2SO_4 at 303 and 333 K

respectively. Calculated activation energy (E_a) values for the corrosion of mild steel in the presence of AD, GU, HYP and XN and the blank are as follows: 49.02 to 60.81 kJ mol^{-1} and 49.02 kJ mol^{-1} (blank) in HCl; 18.99 to 33.90 kJ mol^{-1} and 34.86 kJ mol^{-1} (blank) in H_2SO_4; 27.79 to 30.94 kJ mol^{-1} and 29.87 kJ mol^{-1} (blank) in H_3PO_4. Calculated E_a values for the corrosion of aluminium in the presence of AD, GU, HYP and XN and the blank are as follows: 61.51 to 88.98 kJ mol^{-1} and 52.13 kJ mol^{-1} (blank) in HCl; 54.27 to 72.19 kJ mol^{-1} and 50.54 kJ mol^{-1} (blank) respectively in H_2SO_4; 55.05 to 56.99 kJ mol^{-1} and 52.08 kJ mol^{-1} (blank) in H_3PO_4. Calculated values of heats of adsorption, ΔQ_{ads}, of AD, GU, HYP and XN on mild steel surfaces are as follows: -3.86 to -10.58 kJ mol^{-1} respectively in HCl; 2.31 to 10.47 kJ mol^{-1} in H_2SO_4; 0.66 kJ mol^{-1}, 0.40 to 9.27 kJ mol^{-1} in H_3PO_4. Calculated ΔQ_{ads} values for the adsorption of AD, GU, HYP and XN on aluminium surfaces are as follow: -8.86 to -24.37 kJ mol^{-1} in HCl. The negative ΔG_{ads} values obtained in the study indicate the spontaneity of the adsorption processes while the calculated values of activation energy (E_a) for the adsorption of the purines on the metal surfaces shows that the adsorption mechanism may not be purely physisorption. The inhibition mechanisms, estimated from the temperature dependence of inhibition efficiency as well from activation energy (E_a) and heat of adsorption (ΔQ_{ads}) parameters show that the purines functioned via mixed inhibition mechanism which was confirmed by polarization curves. The SEM micrographs, FTIR and impedance spectra of the metals in the presence of the inhibitors as well as molecular dynamics modeling of the adsorption of the single molecules on the metal surface confirmed the presence of protective layers over the mild steel and aluminium surfaces thereby providing evidence for the inhibition of the corrosion of the metals.

TABLE OF CONTENTS

Title page - - - - - - - - - iii

Declaration - - - - - - - - - iv

Certification - - - - - - - - - v

Dedication - - - - - - - - - vi

Acknowledgements - - - - - - - - - vii

Abstract - - - - - - - - - viii

Table of Contents - - - - - - - - - x

List of Figures - - - - - - - - - - xv

List of Tables - - - - - - - - - xxiii

List of Appendices - - - - - - - - - xxv

Abbreviations and Symbols - - - - - - - - xxviii

CHAPTER ONE

INTRODUCTION

1.1 Background to the Study - - - - - - 1

1.2 Forms of Corrosion - - - - - - - 3

1.2.1 Uniform corrosion - - - - - - - - 3

1.2.2 Galvanic corrosion - - - - - - - - 3

1.2.3 Pitting corrosion - - - - - - - - 3

1.2.4 Crevice corrosion - - - - - - - - 4

1.2.5 Intergranular corrosion - - - - - - - 4

1.2.6 Erosion corrosion - - - - - - - - 4

1.2.7 Cavitation corrosion - - - - - - - - 5

1.2.8 Interfilm corrosion - - - - - - - - 5

1.2.9 Fretting corrosion - - - - - - - 5

1.3 Corrosion Monitoring Techniques - - - - - 6

1.3.1 Gravimetric technique- - - - - - - 6

1.3.2 Gasometric technique - - - - - - - 7

1.3.3 Thermometric technique - - - - - - 8

1.3.4 Potentiodynamic polarisation techniques - - - - 8

1.3.5 Linear polarisation resistance (LPR) - - - - - 9

1.3.6 Electochemical noise - - - - - - - 9

1.3.7 Electrochemical impedance spectroscopy (EIS) - - - 9

1.3.8 Galvanic/potential monitoring - - - - - 10

1.4 Common Methods of Corrosion Prevention - - - 11

1.4.1 Selection of materials and design against corrosion - - - 11

1.4.2 Cathodic protection - - - - - - - 12

1.4.3 Protective coatings - - - - - - - 12

1.4.4 Environment modification and addition of inhibitors- - - 12

1.5 **Inhibitors** - - - - - - - - 13

1.5.1 Classification of inhibitors - - - - - - 13

1.6 Adsorption Isotherms - - - - - - 18

1.6.1 Langmuir adsorption isotherm - - - - - 19

1.6.2 Freundlich isotherm - - - - - - - 19

1.6.3 Temkin adsorption isotherm - - - - - - 19

1.6.4 Flory-Huggins adsorption isotherm - - - - - 20

1.6.5 El-Awady *et al.* kinetic-thermodynamic adsorption isotherm - 20

1.6.6 Frumkin adsorption isotherm - - - - - - 21

1.7 Purines - - - - - - - - 22

1.7.1 Adenine - - - - - - - - 22

1.7.2 Guanine - - - - - - - - 23

1.7.3 Hypoxanthine - - - - - - - - 23

1.7.4 Xanthine - - - - - - - - 23

1.8 Statement of the Problem - - - - - - 23

1.9 Justification for the Choice of Purines as Corrosion Inhibitors - 24

1.10 Aims of the Research - - - - - - 26

1.11 Objectives of the Research - - - - - - 26

CHAPTER TWO

LITERATURE REVIEW

2.1 Corrosion Inhibitors - - - - - - - 28

2.1.1 Triazoles and benzotriazoles derivatives as corrosion inhibitors - 28

2.1.2 Dyes as corrosion inhibitors - - - - - - 30

2.1.3 Amino acids as corrosion inhibitors - - - - - 32

2.1.4 Schiff bases as corrosion inhibitors - - - - - 33

2.1.5 Imidazoles as corrosion inhibitors - - - - - 33

2.1.6 Purines as Corrosion Inhibitors - - - - - 34

CHAPTER THREE

MATERIALS AND METHODS

3.1 Material Preparation - - - - - - 37

3.2 Gravimetric Method - - - - - - - 37

3.3 Electrochemical Impedance Spectroscopy (EIS) - - - 38

3.4 Potentiodynamic Polarisation - - - - - 39

3.5 Synergistic Effects - - - - - - - 39

3.6 Fourier Transform Infrared Spectrophotometery(FTIR) - 39

3.7 Scanning Electron Microscopy (SEM) - - - - 40

3.8 Computational and Theoretical Considerations - - - 40

3.8.1 Quantum chemical calculations - - - - - 40

3.8.2 Molecular dynamics simulation - - - - - 41

CHAPTER FOUR

RESULTS

4.1 Gravimetric Measurements - - - - - - - 42

4.2 Half Lives ($t_{1/2}$) of Mild Steel and Aluminium in the Test Solutions 63

4.3 Electrochemical Tests at 303 K - - - - - 68

4.4 Synergistic Considerations - - - - - - 77

4.5 Infrared Spectroscopy Analysis - - - - - 77

4.6 Scanning Electron Microscopy - - - - - 77

4.7 Quantum Chemical Calculations - - - - - 77

4.8 Molecular Dynamics - - - - - - - 78

CHAPTER FIVE

DISCUSSION

5.1 Gravimetric Measurements - - - - - - - 102

5.2 Half Lives ($t_{1/2}$) of Mild Steel and Aluminium in the Test Solutions 106

5.3 Effect of Temperature /Thermodynamics Study - - - 123

5.4 Adsorption Study - - - - - - - 130

5.5 Electrochemical Tests at 303 K - - - - - 170

5.5.1. Electrochemical impedance measurements - - - - 170

5.5.2 Potentiodynamic polarization measurements - - - - 172

5.6 Synergistic Considerations - - - - - - 173

5.7 Infrared Spectroscopic Analysis - - - - - 175

5.8 Scanning Electron Microscopy - - - - - 178

5.9 Quantum Chemical Calculations - - - - - 179

5.10 Molecular Dynamics Simulations - - - - - 180

5.11 Mechanism of Inhibition - - - - - - 182

CHAPTER SIX

SUMMARY, CONCLUSIONS AND RECOMMENDATIONS

6.1 Summary and Conclusions - - - - - - 186

6.2 Recommendations - - - - - - - 188

REFERENCES - - - - - - - - 189

APPENDICES - - - - - - - - - 202

LIST OF FIGURES

Figure(s)		Page
1.1	Chemical structures of (a) Adenine (b) Guanine (c) Hypoxanthine and (d) Xanthine - - - - - - -	25
4.1	Variation of weight loss with time (hrs) for the corrosion of mild steel in 0.1 M (a). HCl (b). H_2SO_4 and (c) H_3PO_4 containing various concentrations of adenine (AD) at 303 K - - - -	43
4.2.	Variation of weight loss with time (hrs) for the corrosion of mild steel in 0.1 M (a). HCl (b). H_2SO_4 and (c). H_3PO_4 containing various concentrations of adenine (AD) at 333 K. - - - -	44
4.3.	Variation of weight loss with time (hrs) for the corrosion of mild steel in 0.1 M (a). HCl (b). H_2SO_4 and (c). H_3PO_4 containing various concentrations of guanine (GU) at 303 K. - - - -	45
4.4.	Variation of weight loss with time (hrs) for the corrosion of mild steel in 0.1 M (a). HCl (b). H_2SO_4 and (c). H_3PO_4 containing various concentrations of guanine (GU) at 333 K. - - - -	46
4.5.	Variation of weight loss with time (hrs) for the corrosion of mild steel in 0.1 M (a). HCl (b). H_2SO_4 and (c). H_3PO_4 containing various concentrations of hypoxanthine (HYP) at 303 K. - - -	47
4.6.	Variation of weight loss with time (hrs) for the corrosion of mild steel in 0.1 M (a). HCl (b). H_2SO_4 and (c). H_3PO_4 containing various concentrations of hypoxanthine (HYP) at 333 K. - - -	48
4.7.	Variation of weight loss with time (hrs) for the corrosion of mild steel in 0.1 M (a). HCl (b). H_2SO_4 and (c). H_3PO_4 containing various concentrations of xanthine (XN) at 303 K. - - - -	49
4.8.	Variation of weight loss with time (hrs) for the corrosion of mild steel in 0.1 M (a). HCl (b). H_2SO_4 (c). H_3PO_4 containing various concentrations of xanthine (XN) at 333 K. - - - -	50
4.9.	Variation of weight loss with time (hrs) for the corrosion of aluminium in 0.1 M (a). HCl (b). H_2SO_4 and (c). H_3PO_4 containing various concentrations of adenine (AD) at 303 K. - - - -	51
4.10.	Variation of weight loss with time (hrs) for the corrosion of aluminiumin 0.1 M (a). HCl (b). H_2SO_4 and (c). H_3PO_4 containing various concentrations of adenine (AD) at 333 K. - - - -	52
4.11.	Variation of weight loss with time (hrs) for the corrosion of aluminium in 0.1 M (a). HCl (b). H_2SO_4 and (c). H_3PO_4 containing various concentrations of guanine (GU) at 303 K. - - - -	53

4.12. Variation of weight loss with time (hrs) for the corrosion of aluminium in 0.1 M (a). HCl (b). H_2SO_4 and (c). H_3PO_4 containing various concentrations of guanine (GU) at 333 K. - - - - 54

4.13. Variation of weight loss with time (hrs) for the corrosion of aluminium in 0.1 M (a). HCl (b). H_2SO_4 and (c). H_3PO_4 containing various concentrations of hypoxanthine (HYP) at 303 K. - - - 55

4.14. Variation of weight loss with time (hrs) for the corrosion of aluminium in 0.1 M (a). HCl (b). H_2SO_4 and (c). H_3PO_4 containing various concentrations of hypoxanthine (HYP) at 333 K. - - - 56

4.15. Variation of weight loss with time (hrs) for the corrosion of aluminium in 0.1 M (a). HCl (b). H_2SO_4 and (c). H_3PO_4 containing various concentrations of xanthine (XN) at 303 K. - - - - 57

4.16. Variation of weight loss with time (hrs) for the corrosion of aluminium in 0.1 M (a). HCl (b). H_2SO_4 and (c). H_3PO_4 containing various concentrations of xanthine (XN) at 333 K. - - - - 58

4.17. Impedance spectra of the corrosion of mild steel in 0.1 M HCl, H_2SO_4 and H_3PO_4 in the absence and presence of 0.01 M adenine (AD), guanine (GU), hypoxanthne (HYP) and xanthine (XN) at 303 K. - - - - - - - - 69

4.18. Impedance spectra of the corrosion of aluminium in 0.1 M HCl, H_2SO_4 and H_3PO_4 in the absence and presence of 0.01 M adenine (AD), guanine (GU), hypoxanthine (HYP) and xanthine (XN) at 303 K. - - - - - - - - 70

4.19. Polarisation curves of the corrosion of mild steel in 0.1 M HCl, H_2SO_4 and H_3PO_4 in the absence and presence of 0.01 Madenine (AD), guanine (GU), hypoxanthine (HYP) and xanthine (XN) at 303 K. - - - - - - - - 71

4.20. Polarisation curves of the corrosion of aluminium in 0.1 M solution of HCl, H_2SO_4 and H_3PO_4 in the absence and presence of 0.01 M adenine (AD), guanine (GU), hypoxanthine (HYP) and xanthine (XN) at 303 K. - - - - - - - 72

4.21. FTIR spectra of (a). adenine (AD) powder alone and (b). corrosion product of mild steel obtained in the presence of adenine (AD) in 0.1 M HCl solution. - - - - - - 82

4.22. FTIR spectra of (a). adenine (AD) powder alone and (b). corrosion product of aluminium obtained in the presence of adenine (AD) in 0.1 M HCl solution. - - - - - - 83

4.23. FTIR spectra of (a). guanine (GU) powder alone and (b). corrosion product of mild steel obtained in the presence of guanine (GU) in 0.1 M HCl solution. - - - - - - 84

4.24. FTIR spectra of (a). guanine (GU) powder alone and (b). corrosion product of aluminium obtained in the presence of guanine (GU) in 0.1 M HCl. - - - - - - - - 85

4.25. FTIR spectra of (a). hypoxanthine (HYP) powder alone and (b). corrosion product of mild steel obtained in the presence of hypoxanthine (HYP) in 0.1 M HCl solution. - - - - 86

4.26. FTIR spectra of (a). hypoxanthine (HYP) powder alone and (b). corrosion product of aluminium obtained in the presence of hypoxanthine (HYP) in 0.1 M HCl. - - - - - 87

4.27. FTIR spectra of (a). xanthine (XN) powder alone and (b). corrosion product of mild steel obtained in the presence of xanthine (XN) in 0.1 M HCl. - - - - - - - - 88

4.28. FTIR spectra of (a). xanthine (XN) powder alone and (b). corrosion product of aluminium obtained in the presence of xanthine (XN) in 0.1 M HCl. - - - - - - - - 89

4.29. Micrographs of mild steel after dipping in 0.1 M HCl solution for 2 days at x 5,000 magnification (a). mild steel alone and in the presence of (b). adenine (AD) (c). guanine (GU) and (d). hypoxanthine (HYP). - - - - - - - 90

4.30. Micrographs of aluminium after dipping in 0.1 M HCl solution for 2 days at x 5,000 magnification (a). aluminium alone and in the presence of (b). adenine (AD) (c). guanine (GU) and (d). hypoxanthine (HYP). - - - - - - - 91

4.31. Electronic structure properties of adenine (AD). - - - 92

4.32. Electronic structure properties of guanine (GU). - - - 93

4.33. Electronic structure properties of hypoxanthine (HYP). - - 94

4.34. Electronic structure properties of xanthine (XN). - - - 95

4.35. Adsorption of single molecules of adenine (AD), guanine (GU), hypoxanthine (HYP) and xanthine (XN) on a Fe (110) surface. - 97

4.36. Adsorption of single molecules of adenine (AD), guanine (GU), hypoxanthine (HYP) and xanthine (XN) on Al (110) surface. - 98

4.37. Representative snapshots of the on-top views of adenine (AD), guanine (GU), hypoxanthine (HYP) and xanthine (XN) on Fe (110) surface. - - - - - - - 99

4.38. Representative snapshots of the on-top views of adenine (AD), guanine (GU), hypoxanthine (HYP) and xanthine (XN) on Al (110) surface. - - - - - - - 100

5.1. Plots of –log weight loss (g) versus time (hrs) for the corrosion of mild steel in 0.1 M HCl, H_2SO_4 and H_3PO_4 containing various concentrations of adenine (AD) at 303 K. - - - - 107

5.2. Plots of –log weight loss (g) versus time (hrs) for the corrosion of mild steel in 0.1 M HCl, H_2SO_4 and H_3PO_4 containing various concentrations of adenine (AD) at 333 K. - - - - 108

5.3. Plots of –log weight loss (g) versus time (hrs) for the corrosion of mild steel in 0.1 M HCl, H_2SO_4 and H_3PO_4 containing various concentrations of guanine (GU) at 303 K. - - - - 109

5.4. Plots of –log weight loss (g) versus time (hrs) for the corrosion of mild steel in 0.1 M HCl, H_2SO_4 and H_3PO_4 containing various concentrations of guanine (GU) at 333 K. - - - - 110

5.5. Plots of –log weight loss (g) versus time (hrs) for the corrosion of mild steel in 0.1 M HCl, H_2SO_4 and H_3PO_4 containing various concentrations of hypoxanthine (HYP) at 303 K. - - - 111

5.6. Plots of –log weight loss (g) versus time (hrs) for the corrosion of mild steel in 0.1 M HCl, H_2SO_4 and H_3PO_4 containing various concentrations of hypoxanthine (HYP) at 333 K. - - - 112

5.7. Plots of –log weight loss (g) versus time (hrs) for the corrosion of mild steel in 0.1 M HCl, H_2SO_4 and H_3PO_4 containing various concentrations of xanthine (XN) at 303 K. - - - - 113

5.8. Plots of –log weight loss (g) versus time (hrs) for the corrosion of mild steel in 0.1 M HCl, H_2SO_4 and H_3PO_4 containing various concentrations of xanthine (XN) at 333 K. - - - - 114

5.9. Plots of –log weight loss (g) versus time (hrs) for the corrosion of aluminium in 0.1 M HCl, H_2SO_4 and H_3PO_4 containing various concentrations of adenine (AD) at 303 K. - - - - 115

5.10. Plots of –log weight loss (g) versus time (hrs) for the corrosion of aluminium in 0.1 M HCl, H_2SO_4 and H_3PO_4 containing various concentrations of adenine (AD) at 333 K. - - - - 116

5.11. Plots of –log weight loss (g) versus time (hrs) for the corrosion of aluminium in 0.1 M HCl, H_2SO_4 and H_3PO_4 containing various concentrations of guanine (GU) at 303 K. - - - - 117

5.12. Plots of –log weight loss (g) versus time (hrs) for the corrosion of aluminium in 0.1 M HCl, H_2SO_4 and H_3PO_4 containing various concentrations of guanine (GU) at 333 K. - - - - 118

5.13. Plots of –log weight loss (g) versus time (hrs) for the corrosion of aluminium in 0.1 M HCl, H_2SO_4 and H_3PO_4 containing various concentrations of hypoxanthine (HYP) at 303 K. - - - 119

5.14. Plots of –log weight loss (g) versus time (hrs) for the corrosion of aluminium in 0.1 M HCl, H_2SO_4 and H_3PO_4 containing various concentrations of hypoxanthine (HYP) at 333 K. - - - 120

5.15. Plots of –log weight loss (g) versus time (hrs) for the corrosion of aluminium in 0.1 M HCl, H_2SO_4 and H_3PO_4 containing various concentrations of xanthine (XN) at 303 K. - - - - 121

5.16. Plots of –log weight loss (g) versus time (hrs) for the corrosion of aluminium in 0.1 M HCl, H_2SO_4 and H_3PO_4 containing various concentrations of xanthine (XN) at 333 K. - - - - 122

5.17. Langmuir isotherm for the adsorption of adenine (AD) on mild steel surface in 0.1 M solutions of HCl, H_2SO_4 and H_3PO_4 at 303 and 333 K. - - - - - - - - 132

5.18. Langmuir isotherm for the adsorption of guanine (GU) on mild steel surface in 0.1 M solutions of HCl, H_2SO_4 and H_3PO_4 at 303 and 333 K. - - - - - - - - 133

5.19. Langmuir isotherm for the adsorption of hypoxanthine (HYP) on mild steel surface in 0.1 M solutions of HCl, H_2SO_4 and H_3PO_4 at 303 and 333 K. - - - - - - - 134

5.20. Langmuir isotherm for the adsorption of xanthine (XN) on mild steel surface in 0.1 M solutions of HCl, H_2SO_4 and H_3PO_4 at 303 and 333 K. - - - - - - - - 135

5.21. Langmuir isotherm for the adsorption of adenine (AD), guanine (GU) and xanthine (XN) on aluminium surface in 0.1 M solution of HCl, H_2SO_4 and H_3PO_4 at 303 and 333 K. - - - 136

5.22. Langmuir isotherm for the adsorption of hypoxanthine (HYP) on aluminium surface in 0.1 M solutions of HCl and H_2SO_4 at 303 and 333 K. - - - - - - - - 137

5.23. Freundlich isotherm for the adsorption of adenine (AD) on mild steel surface in 0.1 M solutions of HCl, H_2SO_4 and H_3PO_4 at 303 and 333 K. - - - - - - - - 138

5.24. Freundlich isotherm for the adsorption of guanine (GU) on mild steel surface in 0.1 M solutions of HCl, H_2SO_4 and H_3PO_4 at 303 and 333 K. - - - - - - 139

5.25. Freundlich isotherm for the adsorption of hypoxanthine (HYP) on mild steel surface in 0.1 M solutions of HCl, H_2SO_4 and H_3PO_4 at 303 and 333 K. - - - - - - 140

5.26. Freundlich isotherm for the adsorption of xanthine (XN) on mild steel surface in 0.1 M solutions of HCl, H_2SO_4 and H_3PO_4 at 303 and 333 K. - - - - - - 141

5.27. Freundlich isotherm for the adsorption of adenine (AD), guanine (GU) and xanthine (XN) on aluminium surface in 0.1 M solutions of HCl at 303 and 333 K. - - - - - - 142

5.28. Freundlich isotherm for the adsorption of hypoxanthine (HYP) on aluminium surface in 0.1 M solutions of HCl and H_2SO_4 at 303 and 333 K. - - - - - - - 143

5.29. Temkin isotherm for the adsorption of adenine (AD) on mild steel surface in 0.1 M solutions of HCl, H_2SO_4 and H_3PO_4 at 303 and 333 K. - - - - - - - 144

5.30. Temkin isotherm for the adsorption of guanine (GU) on mild steel surface in 0.1 M solutions of HCl, H_2SO_4 and H_3PO_4 at 303 and 333 K. - - - - - - - 145

5.31. Temkin isotherm for the adsorption of hypoxanthine (HYP) on mild steel surface in 0.1 M solutions of HCl, H_2SO_4 and H_3PO_4 at 303 and 333 K. - - - - - - 146

5.32. Temkin isotherm for the adsorption of xanthine (XN) on mild steel surface in 0.1 M solutions of HCl, H_2SO_4 and H_3PO_4 at 303 and 333 K. - - - - - - - 147

5.33. Temkin isotherm for the adsorption of adenine (AD), guanine (GU) and xanthine (XN) on aluminium surface in 0.1 M solutions of HCl at 303 and 333 K. - - - - - - 148

5.34. Temkin isotherm for the adsorption of hypoxanthine (HYP) on aluminium surface in 0.1 M solutions of HCl and H_2SO_4 at 303 and 333 K. - - - - - - - 149

5.35. Flory Huggins isotherm for the adsorption of adenine (AD) on mild steel surface in 0.1 M solutions of HCl, H_2SO_4 and H_3PO_4 at 303 and 333 K. - - - - - - - 150

5.36. Flory Huggins isotherm for the adsorption of guanine (GU) on mild steel surface in 0.1 M solutions of HCl, H_2SO_4 and H_3PO_4 at 303 and 333 K. - - - - - - - 151

5.37. Flory Huggins isotherm for the adsorption of hypoxanthine (HYP) on mild steel surface in 0.1 M solutions of HCl, H_2SO_4 and H_3PO_4 at 303 and 333 K. - - - - - - - 152

5.38. Flory Huggins isotherm for the adsorption of xanthine (XN) on mild steel surface in 0.1 M solutions of HCl, H_2SO_4 and H_3PO_4 at 303 and 333 K. - - - - - - 153

5.39. Flory Huggins isotherm for the adsorption of adenine (AD), guanine (GU) and xanthine (XN) on aluminium surface in 0.1 M solutions of HCl at 303 and 333 K. - - - - 154

5.40. Flory Huggins isotherm for the adsorption of hypoxanthine (HYP) on aluminium surface in 0.1 M solutions of HCl and H_2SO_4 at 303 and 333 K. - - - - - - - 155

5.41. El-Awardy isotherm for the adsorption of adenine (AD) on mild steel surface in 0.1 M solutions of HCl, H_2SO_4 and H_3PO_4 at 303 and 333 K. - - - - - - - 156

5.42. El-Awardy isotherm for the adsorption of guanine (GU) on mild steel surface in 0.1 M solutions of HCl, H_2SO_4 and H_3PO_4 at 303 and 333 K. - - - - - - - 157

5.43. El-Awardy isotherm for the adsorption of hypoxanthine (HYP) on mild steel surface in 0.1 M solutions of HCl, H_2SO_4 and H_3PO_4 at 303 and 333 K. - - - - - - - 158

5.44. El-Awardy isotherm for the adsorption of xanthine (XN) on mild steel surface in 0.1 M solutions of HCl, H_2SO_4 and H_3PO_4 at 303 and 333 K. - - - - - - - 159

5.45. El-Awardy isotherm for the adsorption of adenine (AD), guanine (GU) and xanthine (XN) on aluminium surface in 0.1 M solutions of HCl at 303 and 333 K. - - - - - - 160

5.46. El-Awardy isotherm for the adsorption of hypoxanthine (HYP) on aluminium surface in 0.1 M solutions of HCl and H_2SO_4 at 303 and 333 K. - - - - - - - 161

5.47. Frumkin isotherm for the adsorption of adenine (AD) on mild steel surface in 0.1 M solutions of HCl, H_2SO_4 and H_3PO_4 at 303 and 333 K. - - - - - - - 162

5.48. Frumkin isotherm for the adsorption of guanine (GU) on mild steel surface in 0.1 M solutions of HCl, H_2SO_4 and H_3PO_4 at 303 and 333 K. - - - - - - - 163

5.49. Frumkin isotherm for the adsorption of hypoxanthine (HYP) on mild steel surface in 0.1 M solutions of HCl, H_2SO_4 and H_3PO_4 at 303 and 333 K. - - - - - - - 164

5.50. Frumkin isotherm for the adsorption of xanthine (XN) on mild steel surface in 0.1 M solutions of HCl, H_2SO_4 and H_3PO_4 at 303 and 333 K. - - - - - - - 165

5.51. Frumkin isotherm for the adsorption of adenine (AD), guanine (GU) and xanthine (XN) on aluminium surface in 0.1 M solutions of HCl at 303 and 333 K. - - - - - - 166

5.52. Frumkin isotherm for the adsorption of hypoxanthine (HYP) on aluminium surface in 0.1 M solutions of HCl and H_2SO_4 at 303 and 333 K. - - - - - - - 167

LIST OF TABLES

Table(s) **Page**

4.1: Corrosion rates of mild steel in the absence and presence of various concentrations of adenine (AD), guanine (GU), hypoxanthine (HYP) and xanthine (XN) in 0.1 M HCl, H_2SO_4 and H_3PO_4 at 303 and 333 K. - - - - - - - - 59

4.2: Inhibition efficiencies (IE%) of various concentrations of adenine (AD), guanine (GU), hypoxanthine (HYP) and xanthine (XN) on the corrosion of mild steel in 0.1 M HCl, H_2SO_4 and H_3PO_4 at 303 and 333 K. - 60

4.3: Corrosion rates of aluminiumin the absence and presence of various concentrations of adenine (AD), guanine (GU), hypoxanthine (HYP) and xanthine (XN) in 0.1 M HCl, H_2SO_4 and H_3PO_4 at 303 and 333 K - - - - - - - - 61

4.4: Inhibition efficiencies (IE%) of various concentrations of adenine (AD), guanine (GU), hypoxanthine (HYP) and xanthine (XN) on the corrosion of aluminium in 0.1 M HCl, H_2SO_4 and H_3PO_4 at 303 and 333 K. - 62

4.5: Kinetic parameters of the corrosion of mild steel at 303 K in the absence and presence of various concentrations of adenine (AD), guanine (GU), hypoxanthine (HYP) and xanthine (XN) in 0.1 M HCl, H_2SO_4 and H_3PO_4. - - - - - - - - 64

4.6: Kinetic parameters of the corrosion of aluminium at 303 K in the absence and presence of various concentrations of adenine (AD), guanine (GU), hypoxanthine (HYP) and xanthine (XN) in 0.1 M HCl, H_2SO_4 and H_3PO_4.- - - - - - - - - 65

4.7: Kinetic parameters of the corrosion of mild steel at 333 K in the absence and presence of various concentrations of adenine (AD), guanine (GU), hypoxanthine (HYP) and xanthine (XN) in 0.1 M HCl, H_2SO_4 and H_3PO_4. - - - - - - - - 66

4.8: Kinetic parameters of the corrosion of aluminium at 333 K in the absence and presence of various concentrations of adenine (AD), guanine (GU), hypoxanthine (HYP) and xanthine (XN) in 0.1 M HCl, H_2SO_4 and H_3PO_4 - - - - - - - - 67

4.9: Impedance data for the corrosion of mild steel in 0.1 M HCl, H_2SO_4 and H_3PO_4 in the absence and presence of 0.01 M adenine (AD), guanine (GU), hypoxanthine (HYP) and xanthine (XN) at 303 K. - - 73

4.10: Impedance data for the corrosion of aluminium in 0.1 M HCl, H_2SO_4 and H_3PO_4 in the absence and presence of 0.01 M adenine (AD), guanine (GU), hypoxanthine (HYP) and xanthine (XN) at 303 K.- 74

4.11: Polarization data for the corrosion of mild steel in 0.1 M HCl, H_2SO_4 and H_3PO_4 in the absence and presence of 0.01 M adenine (AD), guanine (GU), hypoxanthine (HYP) and xanthine (XN) at 303 K. 75

4.12: Polarisation data for the corrosion of aluminium in 0.1 M HCl, H_2SO_4 and H_3PO_4 in the absence and presence of 0.01 M adenine (AD), guanine (GU), hypoxanthine (HYP) and xanthine (XN) at 303 K. 76

4.13: The effect of 0.005 M potassium iodide (KI) on inhibition efficiency for mild steel corrosion in 0.1 M HCl, H_2SO_4 and H_3PO_4 in the absence and presence of 0.01 M adenine (AD), guanine (GU), hypoxanthine (HYP)and xanthine (XN) at 303 K using weight loss, impedance and polarization techniques. - - - - - - 80

4.14: The effect of 0.005 M potassium iodide (KI) on inhibition efficiency for aluminium corrosion in 0.1 M HCl, H_2SO_4 and H_3PO_4 in the absence and presence of 0.01 M adenine (AD), guanine (GU), hypoxanthine (HYP) and xanthine (XN) at 303 K using weight loss, impedance and polarization techniques. - - - - 81

4.15. Computed quantum chemical parameters of the studied compounds. 96

4.16 Fukui indices calculated with PBR/DND - - - - 96

4.17. Caculated binding energies of the adsorption of adenine (AD), guanine (GU), hypoxanthine (HYP) and xanthine (XN) molecules on Fe (110) using Forcite quench molecular dynamics. - - - - 101

4.18 Calculated binding energies of the adsorption of adenine (AD), guanine (GU), hypoxanthine (HYP) and xanthine (XN) molecules on Al (110) using Forcite quench molecular dynamics. - - - - 101

5.1: Calculated activation energies (E_a) and heats of adsorption (Q_{ads}) for the corrosion of mild steel in 0.1M HCl, H_2SO_4 and H_3PO_4 in the absence and presence of various concentrations of adenine (AD), guanine (GU), hypoxanthine (HYP) and xanthine (XN). - - 127

5.2: Calculated activation energies (E_a) and heats of adsorption (Q_{ads}) for the corrosion of aluminium in 0.1M HCl, H_2SO_4 and H_3PO_4 in the absence and presence of various concentrations of adenine (AD), guanine (GU), hypoxanthine (HYP) and xanthine (XN). 128

LIST OF APPENDICES

Appendix **Page**

I: Data for average weight loss as a function of time (hrs) for the corrosion of mild steel in 0.1 M HCl, H_2SO_4 and H_3PO_4 in the absence and presence of various concentrations of adenine (AD) at 303 and 333 K respectively. - - - - - 202

II: Data for average weight loss as a function of time (hrs) for the corrosion of mild steel in 0.1 M HCl, H_2SO_4 and H_3PO_4 in the absence and presence of various concentrations of guanine (GU) at 303 and 333 K respectively. - - - - - 203

III: Data for average weight loss as a function of time (hrs) for the corrosion of mild steel in 0.1 M HCl, H_2SO_4 and H_3PO_4 in the absence and presence of various concentrations of hypoxanthine (HYP) at 303 and 333 K respectively. - - - - 204

IV: Data for average weight loss as a function of time (hrs) for the corrosion of mild steel in 0.1 M HCl, H_2SO_4 and H_3PO_4 in the absence and presence of various concentrations of xanthine (XN) at 303 and 333 K respectively. - - - - - 205

V: Data for average weight loss as a function of time (hrs) for the corrosion of aluminium in 0.1 M HCl, H_2SO_4 and H_3PO_4 in the absence and presence of various concentrations of adenine (AD) at 303 and 333 K respectively. - - - - - - 206

VI: Data for average weight loss as a function of time (hrs) for the corrosion of aluminium in 0.1 M HCl, H_2SO_4 and H_3PO_4 in the absence and presence of various concentrations of guanine (GU) at 303 and 333 K respectively. - - - - - 207

VII: Data for average weight loss as a function of time (hrs) for the corrosion of aluminium in 0.1 M HCl, H_2SO_4 and H_3PO_4 in the absence and presence of various concentrations of hypoxanthine (HYP) at 303 and 333 K respectively. - - - - 208

VIII: Data for average weight loss as a function of time (hrs) for the corrosion of aluminium in 0.1 M HCl, H_2SO_4 and H_3PO_4 in the absence and presence of various concentrations of xanthine (XN) at 303 and 333 K respectively. - - - - - 209

IX: Corrosion Potentials in Flowing Seawater (8-13 ft/s), Temperature Range 10-27 °C. - - - - - - - 210

X: Functional and linear forms of adsorption isotherm equations tested 211

XI: Adsorption isotherm parameters obtained from the corrosion data for mild steel in 0.1 M HCl containing various concentrations of adenine (AD), guanine (GU), hypoxanthine (HYP) and xanthine (XN). 212

XII: Adsorption isotherm parameters obtained from the corrosion data for mild steel in 0.1 M H_2SO_4 containing various concentrations of adenine (AD), guanine (GU), hypoxanthine (HYP) and xanthine (XN). - 213

XIII: Adsorption isotherm parameters obtained from the corrosion data for mild steel in 0.1 M H_3PO_4 containing various concentrations of adenine (AD), guanine (GU), hypoxanthine (HYP) and xanthine (XN). - 214

XIV: Adsorption isotherm parameters obtained from the corrosion data for aluminium in 0.1 M HCl containing various concentrations of adenine (AD), guanine (GU), hypoxanthine (HYP) and xanthine (XN). - 215

XV: Adsorption isotherm parameters obtained from the corrosion data for mild steel in 0.1 M H_2SO_4 containing various concentrations of hypoxanthine (HYP). - - - - - - 216

XVI: Frequencies, intensities and functional groups associated with adsorption of IR by adenine (AD) powder. - - - - 217

XVII: Frequencies, intensities and functional groups associated with adsorption of IR by the corrosion product of mild steel in the presence of adenine (AD) as an inhibitor. - - - - 218

XVIII: Frequencies, intensities and functional groups associated with adsorption of IR by the corrosion product of aluminium in the presence of adenine (AD) as an inhibitor. - - - - 219

XIX: Frequencies, intensities and functional groups associated with adsorption of IR by guanine (GU). - - - - - 220

XX: Frequencies, intensities and functional groups associated with adsorption of IR by the corrosion product of mild steel in the presence of guanine (GU) as an inhibitor. - - - - 221

XXI: Frequencies, intensities and functional groups associated with adsorption of IR by the corrosion product of aluminium in the presence of guanine (GU) as an inhibitor. - - - - 222

XXII: Frequencies, intensities and functional groups associated with adsorption of IR by hypoxanthine (HYP) powder - - - 223

XXIII: Frequencies, intensities and functional groups associated with adsorption of IR by the corrosion product of mild steel in the presence of hypoxanthine (HYP) as an inhibitor. - - - 224

XXIV: Frequencies, intensities and functional groups associated with adsorption of IR by the corrosion product of aluminium in the presence of hypoxanthine (HYP) as an inhibitor - - - 225

XXV: Frequencies, intensities and functional groups associated with adsorption of IR by xanthine (XN) powder - - - - 226

XXVI: Frequencies, intensities and functional groups associated with adsorption of IR by the corrosion product of mild steel in the presence of xanthine (XN) as an inhibitor - - - - 227

XXVII: Frequencies, intensities and functional groups associated with adsorption of IR by the corrosion product of aluminium in the presence of xanthine (XN) as an inhibitor - - - - 228

ABBREVIATIONS AND SYMBOLS

mv	millivolts
mv/s	millivolts per sec
$moldm^{-3}$	mol per decimetre cube
ps	pico second
fs	femto second
E_{corr}	Corrosion potential
I_{corr}	Corrosion current density
Inh	Inhibitor
Z_{re}	Real impedance
Z_{im}	Imaginary Impedance
$Z_{(w)}$	A combination Real and Imaginary Impedance
R_s	Solution resistance
R_{ct}	Charge transfer resistance
CPE	Constant Phase Element
C_{dl}	Double layer capacitance
IE%	Inhibition efficiency in percentage
R^2	Regression coefficient
$t_{1/2}$	Half life
A/cm^2	Ampere per centimetre square
SCE	Saturated Calomel Electrode
ASTM	American Society for Testing Materials
NACE	National Association of Corrosion Engineers
$DMOl^3$	A unification of density functional calculations on molecules (DMol) and DSolid

DFT	Density Functional Theory
DND	Double-Numerical + d-orbital
COMPASS	Condensed-phase Optimised Molecular Potentials for atomistic Simulation Studies
NVE	Microcanonical Essemble
Å	Angstrom
Fe (1 1 0)	A plane in the Fe lattice that intersects the x-axis at a distance **'a'** from the origin, the y-axis at a distance **'b'**, and the z-axis at **infinity**.
Al (1 1 0)	A plane in the Al lattice that intersects the x-axis at a distance **'a'** from the origin, the y-axis at a distance **'b'**, and the z-axis at **infinity**.
Fe (1 1 1)	A plane in the Fe lattice that intersects the x-axis at a distance **'a'** from the origin, the y-axis at a distance **'b'**, and the z-axis at a distance **'c'**.
Fe (1 0 0)	A plane in the Fe lattice that intersects the x-axis at a distance **'a'** from the origin, the y- and z- axis at **infinity**.

CHAPTER ONE

INTRODUCTION

1.1 Background to the Study

Corrosion of metals is an electrochemical process that occurs whenever a metal is in contact with an aggressive medium such as acids, bases and salts.The susceptibility of a metal to corrosion depends on the nature of the metal and the environment.

Despite the invention and over-usage of plastics in most industrial applications, metals still rule manufacturing industries. Metals like steel (iron), aluminium, copper, zinc and tin are commonly used in most industries. Mild steel is one of the best preferred materials for industries due to its easy availability and excellent structural properties. Aluminium on the other hand, is the most abundant metal in the earth's crust (8.1%), although it is not found free in nature. The versatility of aluminium makes it the most widely used metal after steel. Most often, during industrial processes such as pickling and etching, these metals come in contact with aggressive media such as acids, bases and salts thereby exposing them to corrosion attack.

Corrosion can cause dangerous and costly damages to oil, gas and water pipelines, bridges, public buildings, vehicles, water and waste water systems and even home appliances. The effects of corrosion include large loss of products and resources, and ecological damages (Günter, 2009).

Corrosion of metals costs the United States excess of $276 billion per year (Denny, 2004).This loss to the economy is more than the Gross National Product of many countries around the world. It has been estimated that 40% of U.S. steel production goes

to the replacement of corroded parts and products (Jorge and Leandro, 2005). Analysis of oil pipeline failures in oil and gas industries in the Niger Delta area of Nigeria showed corrosion as one of the major causes of failure (Achebe *et al.,* 2012). SPE (2008) stated in their report that Nigeria oil and gas industry suffered greatly between 2000 and 2004.The total pipeline breakage loss figure due to corrosion in 2004 alone was 396,000 metric tons (about four super tankers) while the financial losses were estimated to be #19.66 billions (US $154.4).

This menace of corrosion of metals in the oil, metallurgical and other industries has been widely acknowledged and several researches have been carried out on the protection of metals against corrosion. The results obtained revealed that one of the best methods involves the use of inhibitors. However, owing to stringent environmental regulations, organic compounds are preferred to inorganic compounds especially heavy metals derivatives, as corrosion inhibitors. Organic compounds containing hetero atoms such as N, S, P or O in conjugated or aromatic systems have been reported to be effective corrosion inhibitors (Abdallah, 2004; Ashassi-Sorkhabi *et al.*, 2006; Umoren and Ebenso, 2008). The presence of polar functional groups (such as $–NH_2$, -COOH and –OH) as well as π-electrons facilitates the adsorption of the inhibitor on the surface of the metal (Ebenso *et al.*, 2008; Eddy, 2008; Obot *et al,* 2009a).

In the absence of adequate information on corrosion rate (metal weight loss/unit area/unit time) and various methods of protecting a metal, overdesign (e.g. thicker tube wall, leading to greater power requirements for moving parts), lower efficiency of equipment, contaminations, plants shut down, loss of production and loss of equipment will be inevitable.

1.2 Forms of Corrosion

Based on the appearance of the corroded metal, eight forms of corrosion have been identified and are discussed below.

1.2.1 Uniform corrosion

Uniform corrosion is the attack of a metal at essentially the same rate at all exposed areas of its surface. It is characterized by laterally constant speed of corrosion. For example, in the atmospheric corrosion of galvanized steel, the speed of corrosion depends on the thickness of the steel, as such, the thicker the steel coating, the longer the service life of the metal. Uniform attack is the most common type of corrosion and causes the greatest destruction of metals on a weight basis (Moore, 1996).

1.2.2 Galvanic corrosion

Galvanic corrosion is a type of corrosion by which metals are preferentially corroded. This form of corrosion has the potential to attack junctions of metals, or regions where one construction metal is changed to another. The extent of galvanic corrosion increases with the potential difference of the metal. The relative size of the anode or cathode significantly affects the relationship between the active and inert metals. Galvanic corrosion can be prevented by keeping dissimilar metals apart or by the provision of insulating materials between the metals in order to interrupt current flow (Oldfield, 1988; Baboian *et al.*, 1990; Eddy, 2008).

1.2.3 Pitting corrosion

Pitting corrosion results from galvanic action, where the metal surface appears to have pinholes. The pit is the anode while the surrounding surface is the cathode (Jones, 1982). Pitting may occur as a result of one of the following.

i. A change in the acidity of the pit area

ii. Differential aeration may also be a contributing factor to the occurrence of pitting corrosion because most solutions are in contact with air and because of convection, transportation of oxygen through the solution leads to areas of high or low oxygen concentration. Therefore, where the metal surface contains the solutions, the variation may cause the area with the higher oxygen concentration to become a cathode while an area of lower oxygen concentration becomes an anode resulting in localized attacks (Moniz, 1986; Szklarska-Smialowska, 1986).

1.2.4 Crevice corrosion

Crevices are present in some equipment. They occur naturally around bolts, rivets etc. They are also created by scratches on metal surfaces. Crevice corrosion absorbs and draws solution toward the reactive area. Crevice corrosion is influenced by the same factors that affect pitting corrosion and is indeed a specific form of pitting corrosion (Fontana, 1986).

1.2.5 Intergranular corrosion

Intergranular corrosion occurs by localized attack at grain boundaries, which behave as anode to the larger surrounding cathode grains (Moore, 1996). Metals usually are not homogeneous. Impurities or alloying elements may segregate into grain boundaries. Heat treatment or localized heating by welding may provoke change in composition localized in or near grain boundaries.

1.2.6 Erosion corrosion

Almost all corrosive media can bring about erosion corrosion and nearly all metals and alloys are susceptible to this except those metals or alloys that are capable of forming hard, dense, adherent and continuous surface film (Staehle, 1989; Moore, 1996). The extent of erosion corrosion increases as the velocity of the corroding medium increases.

In some cases, the high velocity increases the supply of oxygen or other gases at the metal surface, which may depolarize the cathodic reaction and consequently increase the corrosion rate (Roberge, 1999; Sastri, 2011).

1.2.7 Cavitation corrosion

Formation and collapse of tiny gas bubbles in a liquid stream called cavitation may mechanically destroy any protective layer, causing localized corrosion called cavitation corrosion (Moore, 1996). Similarly when an object such as a propeller rotates in water, the pressure on the trailing surface of the blade fluctuates continually. At some point, very low pressures are produced which create tensile forces high enough to exceed the interatomic binding forces of the liquid.

1.2.8 Interfilm corrosion

Coatings such as paints, conversion coating or metallic coating may lose their adhesion with substrate due to diffusion through the actual coating or to a reaction starting from defects like pinholes or scratches (Morgan, 1984). When this happens, residues of soluble salts, acids or bases will attract water through a paint film because of osmotic effect. The blister filled with water will be formed. Fill-form corrosion is a wormlike delamination of a paint film driven by salt residue and high humidity.

1.2.9 Fretting corrosion

Fretting corrosion is a combination of mechanical wear and atmospheric oxidation which frequently occurs between close fitting metal components (Moore, 1996 and Roberge, 1999). For fretting corrosion to occur, the surface is usually under load and subject to slight relative movement resulting in damage to the contact surface and formation of an oxide debris such as Fe_3O_4 for iron.

In theory, the eight forms of corrosion are clearly distinct, in practice however, there are corrosion cases that fit into more than one category.

1.3 Corrosion Monitoring Techniques

Corrosion measurement is the quantitative way by which the effectiveness of corrosion control and prevention techniques can be evaluated and provides the feedback to enable corrosion control and prevention methods to be optimized. In any corrosion monitoring system, it is common to find two or more of the techniques combined to provide a wide base for data gathering. The exact techniques which can be used depend on the actual process fluid, alloy system, and operating parameters. Some of these techniques are discussed below:

1.3.1 Gravimetric technique

The weight loss technique is the simplest, and longest-established, method of estimating corrosion losses in plants and equipment. A weighed sample (coupon) of the metal or alloy under consideration is introduced into a medium, and later removed after a reasonable time interval. The coupon is then cleaned of all corrosion products and weighed. The weight loss is converted to an average corrosion rate using proper conversion equations. The basic measurement which is determined from corrosion coupons is weight loss; the weight loss over the period of exposure being expressed as corrosion rate (Oguzie, 2005; Eddy *et al*., 2010; Olasehinde *et al*., 2012; Adejo *et al*., 2012).

The technique is extremely versatile, since weight loss coupons can be fabricated from any commercially available alloy. Also, using appropriate geometric designs, a wide variety of corrosion phenomena may be studied. These include, but is not limited to the following:

a) Stress-assisted corrosion
b) Bimetallic (galvanic) attack

c) Differential aeration

d) Heat-affected zones

Advantages of weight loss coupons are as follows:

i. The technique is applicable to all environments - gases, liquids, solids/particulate flow.

ii. Visual inspection can be undertaken.

iii. Corrosion deposits can be observed and analyzed.

iv. Weight loss can be readily determined and corrosion rate easily calculated.

v. Localized corrosion can be identified.

vi. Inhibitor performance can be easily assessed.

The disadvantage of the coupon technique is that, if a corrosion upset occurs during the period of exposure, the coupon alone will not be able to identify the time of occurrence of the upset, and depending upon the peak value of the upset and its duration, may not even register a statistically significant increased weight loss (NACE, 1999; Dean, 2003). Therefore, coupon monitoring is most useful in environments where corrosion rates do not significantly change over long time periods. However, they can provide a useful correlation with other techniques such as potentiodynamic polarisation technique (Oguzie *et al.*, 2012a, 2012b).

1.3.2 Gasometric technique

The gasometric assembly is essentially an apparatus which measures the rate of gas evolution during a corrosion reaction. In an acid medium, the volume of hydrogen gas evolved is directly proportional to the rate of corrosion of the metal (Umoren *et al.*, 2009). It consists of a graduated gas burette which is connected to a flask containing paraffin oil. The burette is surrounded with a glass jacket with a water inlet and outlet to

regulate the temperature of the gas evolved. A reaction vessel is connected to the gas burette through a delivery tube with a tap for incoming gas and another to expel the gas when the burette is full or at the end of the reaction. The reaction vessel is a three-necked flask consisting of an inlet for the metallic coupon, another one for the thermometer and the last leading to the gas burette (Umoren *et al*., 2009).

1.3.3 Thermometric technique

The reaction vessel is a well lagged, three-necked round bottom flask consisting of an inlet for the metallic coupon, another one for the thermometer and the last for introducing the test solution.

The flask is well lagged to prevent heat losses. In the thermometric technique, the progress of the corrosion reaction is monitored by determining changes in temperature with time using a thermometer (0 - 100°C) (Eddy and Ebenso, 2008; Obot *et al*., 2009b).

1.3.4 Potentiodynamic polarisation techniques

Polarisation techniques such as potentiodynamic polarisation, potentiostaircase and cyclic voltammetry are often used for laboratory corrosion testing. These techniques can provide significant useful information regarding the corrosion mechanisms, corrosion rate and susceptibility of specific materials to corrosion in designated environments. Polarisation methods involve changing the potential of the working electrode and monitoring the current which is produced as a function of time or potential. It is probably the most commonly used polarisation testing method for measuring corrosion resistance and is used for a wide variety of functions (Van, 1998; Khaled, 2010a, 2010b).

1.3.5 Linear polarisation resistance (LPR)

The polarisation resistance of a material is defined as the slope of the potential-current density ($\Delta E_{corr}/\Delta i_{corr}$) curve at the free corrosion potential, yielding the polarisation resistance R_p that can be related (for reactions under activation control) to the corrosion current by the Stern-Geary equation (ASTM, 2001; Dean, 2003) .

1.3.6 Electochemical noise

The non-intrusive use of electrochemical noise (EN) for corrosion monitoring is very attractive; examples are found in aircraft corrosion and gas scrubbing tower monitoring. Fluctuations of potential or current of a corroding metallic specimen are a well known and easily observable phenomenon. The extensive development in the sensitivity of the equipment for studying electrochemical systems has rendered the study of oscillations in electrochemical processes, that translate into measurable electrochemical noise, EN, increasingly accesible. No other technique, electrochemical or otherwise is remotely as sensitive as EN to system changes and upsets (Sastri, 2011) .

1.3.7 Electrochemical impedance spectroscopy (EIS)

Impedance spectroscopy is also called AC impedance or just impedance spectroscopy. Electrochemical impedance is usually measured by applying an AC potential to an electrochemical cell and measuring the current through the cell. A small amplitude signal, usually a voltage between 5 to 50mV, is applied to a specimen over a range of frequencies of 0.001 Hz to 100,000Hz. The EIS instrument records the real and imaginary components of the impedance response of the system. Depending upon the shape of the EIS spectrum, a circuit model or circuit description code and initial circuit parameters are assumed and analysed (Oguzie *et al.,* 2012a, 2012b).

An important advantage of EIS over other laboratory techniques is the possibility of using very small amplitude signals without significantly disturbing the properties being measured. It is a non-destructive technique and so can provide time dependent information about the properties but also about ongoing processes such as corrosion. It is however, expensive and complex data analysis is required for quantification (NACE, 1999; Sastri, 2011).

1.3.8 Galvanic/potential monitoring

The galvanic monitoring technique, also known as Zero Resistance Ammetry (ZRA) is another electrochemical measuring technique. With ZRA probes, two electrodes of dissimilar metals are exposed to the process fluid. When immersed in solution, a natural voltage (potential) difference exits between the electrodes. The current generated due to this potential difference relates to the rate of corrosion occurring on the more active of the electrode couple. Galvanic/potential monitoring is applicable to the following:

i. Bimetallic corrosion
ii. Crevice and pitting attack
iii. Corrosion assisted cracking
iv. Corrosion by highly oxidizing species
v. Weld decay

Galvanic current measurement has found widest applications in water injection systems where dissolved oxygen concentrations are a primary concern. Oxygen leaking into such systems greatly increases galvanic currents and thus the rate of corrosion of steel process components. Galvanic monitoring systems are used to provide an indication that oxygen may be invading injection waters through leaking gaskets or deaeration systems.

In any corrosion monitoring system, it is common to find two or more techniques combined to provide a wide base for data gathering. The exact techniques which can be used depend on the actual process fluid, alloy system, and operating parameters. Corrosion monitoring offers an answer to the question of whether more corrosion is occurring today compared to yesterday. Using this information, it is possible to identify the cause of corrosion and quantify its effect. Corrosion monitoring remains a valuable weapon in the fight against corrosion, thereby providing substantial economic benefit to the user (ASTM, 2001) .

1.4 Common Methods of Corrosion Prevention

In most industrial situations, it is virtually impossible to prevent corrosion. The general strategy is to use measures that reduce the corrosion rate to an economically sustainable level. The most important corrosion mitigation procedures are as follows (Sastri, 1998; 2011):

(i). Selection of materials and design against corrosion

(ii). Cathodic protection

(iii) Protective coatings

(iv). Chang of the environment

(v). Addition of inhibitors

1.4.1 Selection of materials and design against corrosion

Materials for a particular working environment (composition, temperature, velocity) are selected taking into account mechanical and physical properties, availability, method of fabrication and overall cost of component or structure. Geometrical configurations that facilitate corrosive conditions should be avoided. These include the following:

a. Features that trap dust, air and water

b. Designs with inaccessible areas that cannot be re-protected, e.g., by maintenance painting
c. Designs that lead to heterogeneity in the metal or in the environment

Also, metal-metal or metal-non metallic contacting materials that facilitate corrosion such as bimetallic couples, a metal in contact with absorbent materials that maintain constantly wet conditions and contact with substances that give off corrosive vapours, should be avoided.

1.4.2 Cathodic protection

Metals can be protected cathodically by making the interfacial (metal/solution) potential sufficiently negative by means of either sacrificial anode or impressed current or by making the interfacial potential sufficiently positive to cause passivation (formation of a protective film on the metal). This method is used for metals that passivate in the corrodent under consideration.

1.4.3 Protective coatings

Ideally, a protective coating should provide a complete barrier and exclude the corrosive environment from having contact with the metal which it is designed to protect. This can be achieved by the following techniques:

a. Using inorganic coatings , e.g., vitreous enamel, glasses, ceramics
b. Application of organic coatings, e.g., paints, plastics, greases.
c. Generating metallic coatings that form protective barriers (Ni, Cr) or protect the substrate by sacrificial action (Zn, Al, Cd on steel).

1.4.4 Environment modification and addition of inhibitors

For aqueous corrosion, the environment can be made less agressive by removing constituents or modifying conditions that facilitate corrosion: decrease temperature,

decrease velocity, prevent access of water and moisture, remove dissolved O_2 , increase pH (for steel) while for atmospheric corrosion, the air is dehumidified and solid particles removed (Roberge, 1999).

Where these methods are not applicable, then chemicals may be added to the environment to interfere with the corrosion process, usually by forming a film of some kind. These chemicals called corrosion inhibitors are substances which, when added in small quantities to a normally corrosive environment, reduce the corrosion rate of the metal, without significantly changing the concentration of corrosive species (Umoren *et al*., 2009; Eddy *et al.,* 2010; Akalezi *et al.,* 2012).

1.5 Inhibitors

Inhibitors are chemicals that react with a metallic surface giving the surface a certain level of protection. Inhibitors often work by being adsorbed on the metallic surface, protecting the metallic surface by forming a film (Sastri, 2011). Inhibitors are normally distributed from a solution or dispersion. Some are included in a protective coating formulation. Inhibitors slow corrosion processes as follows:

I. Increasing the anodic or cathodic polarization behaviour (Tafel slopes)
II. Reducing the movement or diffusion of ions to the metallic surface
III. Increasing the electrical resistance of the metallic surface

1.5.1 Classification of inhibitors

Inhibitors have been classified differently by various authors. Some authors prefer to group inhibitors by their chemical functionality as follows (Jones, 1988):

a) ***Inorganic inhibitors.*** These are usually crystalline salts such as sodium chromate, phosphate, or molybdate. Only the anions of these compounds are involved in reducing metal corrosion. When zinc is used instead of sodium, the

zinc cation can add some beneficial effect. These zinc-added compounds are called mixed-charge inhibitors.

b) ***Organic anionic.*** Sodium sulfonates, phosphonates, or mercaptobenzotriazole (MBT) are used commonly in cooling waters and anti-freeze solutions.

c) ***Organic cationic.*** In their concentrated forms, these are either liquids or wax-like solids. Their active portions are generally large aliphatic or aromatic compounds with positively charged amine groups.

However, by far the most popular organization scheme consists of regrouping corrosion inhibitors as follows (Hackerman and Snaveley, 1984):

(I). **Passivating (anodic) inhibitors**

Passivating inhibitors cause a large anodic shift of the corrosion potential, forcing the metallic surface into the passivation range (Enenebeaku, 2011). There are two types of passivating inhibitors viz: (a) oxidizing anions, such as chromate, nitrite, and nitrate, that can passivate steel in the absence of oxygen and (b) the nonoxidizing ions, such as phosphate, tungstate, and molybdate, that require the presence of oxygen to passivate steel. These inhibitors are the most effective and consequently the most widely used (Thomas, 1994).

Chromate-based inhibitors are the least-expensive inhibitors and were used until recently in a variety of applications (e.g., recirculation-cooling systems of internal combustion engines, rectifiers, refrigeration units, and cooling towers). Sodium chromate, typically in concentrations of 0.04 to 0.1%, was used for these applications. At higher temperatures or in fresh water with chloride concentrations above 10 ppm higher concentrations are required. If necessary,

sodium hydroxide is added to adjust the pH to a range of 7.5 to 9.5. If the concentration of chromate falls below a concentration of 0.016%, corrosion will be accelerated. Therefore, it is essential that periodic colorimetric analysis be conducted to prevent this from occurring (Roberge, 1999).

In general, passivation inhibitors can actually cause pitting and accelerate corrosion when concentrations fall below minimum limits. For this reason it is essential to monitor the inhibitor concentration.

(II). **Cathodic inhibitors**

Cathodic inhibitors either slow the cathodic reaction itself or selectively precipitate on cathodic areas to increase the surface impedance and limit the diffusion of reducible species to these areas (Oguzie *et al.*, 2012a). Cathodic inhibitors can provide inhibition by three different mechanisms viz: (a) as cathodic poisons, (b) as cathodic precipitates, and (c) as oxygen scavengers. Some cathodic inhibitors, such as compounds of arsenic and antimony, work by making the recombination and discharge of hydrogen more difficult.

Other cathodic inhibitors such as calcium, zinc, or magnesium ions may be precipitated as oxides to form a protective layer on the metal. Oxygen scavengers help to inhibit corrosion by preventing the cathodic depolarization caused by oxygen. The most commonly used oxygen scavenger at ambient temperature is probably sodium sulphite (Na_2SO_3).

(III). **Organic inhibitors**

Both anodic and cathodic effects are sometimes observed in the presence of organic inhibitors, but as a general rule, organic inhibitors affect the entire surface of a corroding metal when present in sufficient concentration. Organic

inhibitors, usually designated as *film-forming*, protect the metal by forming a hydrophobic film on the metal surface.Their effectiveness depends on their chemical composition, molecular structure, and affinities for the metal surface. Since film formation is an adsorption process, the temperature and pressure in the system are important factors. Organic inhibitors will be adsorbed according to the ionic charge of the inhibitor and the charge on the surface. Cationic inhibitors, such as amines, or anionic inhibitors, such as sulphonates, will be adsorbed preferentially depending on whether the metal is charged negatively or positively. The strength of the adsorption bond is the dominant factor for soluble organic inhibitors. These materials build up a protective film of adsorbed molecules on the metal surface, which provides a barrier to the dissolution of the metal in the electrolyte. Because the metal surface covered is proportional to the inhibitor concentrations, the concentration of the inhibitor in the medium is critical (Enenebeaku, 2011; Olasehinde *et al.*, 2012; Adejo *et al*., 2012).

For any specific inhibitor in any given medium there is an optimal concentration. For example, a concentration of 0.05% sodium benzoate or 0.2% sodium cinnamate is effective in water at a pH of 7.5 containing either 17 ppm sodium chloride or 0.5% by weight of ethyl octanol. The corrosion due to ethylene glycol cooling water systems can be controlled by the use of ethanolamine as an inhibitor (Mercer, 1994; Roberge, 1999).

(IV). **Precipitation inhibitors**

Precipitation-inducing inhibitors are film-forming compounds that have a general action over the metal surface, blocking both anodic and cathodic sites indirectly. Precipitation inhibitors are compounds that cause the formation of

precipitates on the surface of the metal, therebyproviding a protective film. Hard water that is high in calcium and magnesium is less corrosive than soft water because of the tendency of the salts in the hard water to precipitate on the surface of the metal and form a protective film.The most common inhibitors of this category are the silicates and the phosphates. Sodium silicate, for example, is used in many domestic water softeners to prevent the occurrence of *brownish water*. In aerated hotwater systems, sodium silicate protects steel, copper, and brass. However, protection is not always reliable and depends heavily on pH and a saturation index that depends on water composition and temperature. Phosphates also require oxygen for effective inhibition. Silicates and phosphates do not afford the degree of protection provided by chromates and nitrites; however, they are very useful in situations where non toxic additives are required (Mercer, 1994; Roberge, 1999; Sastri, 2011).

(V). Volatile corrosion inhibitors

Volatile corrosion inhibitors (VCIs), also called vapour phase inhibitors(VPIs), are compounds transported in a closed environment to the site of corrosion by volatilization from a source. In boilers, volatile basic compounds, such as morpholine or hydrazine, are transported with steam to prevent corrosion in condenser tubes by neutralizing acidic carbon dioxide or by shifting surface pH toward less acidic and corrosive values. In closed vapour spaces, such as shipping containers, volatile solids such as salts of dicyclohexylamine, cyclohexylamine,and hexamethylene-amine are used. On contact with the metal surface,the vapour of these salts condenses and is hydrolyzed by any moistureto liberate protective ions. It is desirable, for an efficient VCI, to provide inhibition rapidly and to last for long periods. Both qualities depend on the volatility of

these compounds and fast action requiring high volatility, whereas enduring protection requires low volatility (Miksic, 1993; Fiaud, 1994; Roberge, 1999).

1.6 Adsorption Isotherms

Adsorption isotherms are very important in understanding the mechanism of inhibition of corrosion of metals and alloys. The most frequently used adsorption isotherms are Langmuir, Freundlich, Temkin, Flory-Huggins and Frumkin isotherms. All these isotherms can be represented as follows (Oguzie *et al.,* 2012b):

$$f(\theta, x)\exp(-2a\theta) = kC \qquad 1.1$$

where $f(\theta, x)$ is the configuration factor which depends upon the physical model and the assumptions underlying the derivation of the isotherm, θ is the degree of surface coverage, C is the inhibitor concentration in the electrolyte, x is the size ratio, a is the molecular interaction parameter and k is the equilibrium constant of the adsorption process (Ebenso *et al*., 2008; Oguzie *et al*., 2012b).

The heat of adsorption (Q_{ads}) of the inhibitor on the surface of the metal can be calculated using equation 1.2

$$Q_{ads} = 2.303R\left[\log\left(\frac{\theta_2}{1-\theta_2}\right) - \log\left(\frac{\theta_1}{1-\theta_1}\right)\right]\left(\frac{T_1 \times T_2}{T_2 - T_1}\right) kJmol^{-1} \qquad 1.2$$

where θ_1 and θ_2 are the degrees of surface coverage at the temperatures T_1 and T_2 respectively (Ogoko *et al.,* 2009). At constant pressure, the values of Q_{ads} approximate enthalpy of adsorption (ΔH_{ads}) .

1.6.1 Langmuir adsorption isotherm

The Langmuir adsorption isotherm assumes monolayer adsorption onto a surface containing a finite number of identical sites and absence of lateral interactions between the adsorbed species. It can be written as follows

_____

where *k* is the adsorption equilibrium constant and θ is the degree of surface coverage of the inhibitor. By plotting values of C/θ versus values of *C*, straight line graphs are obtained (Eddy and Ebenso, 2010; Akalezi *et al.*, 2012).

1.6.2 Freundlich isotherm

Freundlich suggested an empirical equation which describes adsorption on heterogenous surfaces. His isotherm is based on the assumption that adsorption sites are distributed exponentially with respect to energy of adsorption and that the surface sites are subdivided into several types, each possessing a characteristic heat of adsorption (Odoemelam *et al*., 2009). Freundlich equation is presented as equation 1.5,

where θ = surface coverage.

C = concentration of inhibitor in solution, M.

k = adsorption equilibrium constant.

n = Freundlich isotherm constant (with $0 < n < 1$)

1.6.3 Temkin adsorption isotherm

According to Temkin adsorption isotherm, the degree of surface coverage (θ) is related to the inhibitor's concentration *(C)* in the bulk electrolyte according to equation 1.6:

where k is the equilibrium constant of adsorption, θ and 'α' is the molecular interaction parameter. Rearranging and taking logarithm of both sides gives equations 1.7 and 1.8

$$\theta = \frac{-2.303\log k}{2\alpha} - \frac{2.303\log C}{2\alpha} \quad 1.7$$

or $-2\alpha\theta = 2.303(\log k + \log C)$ 1.8

a plot of θ versus *log C* gives a linear plot provided the assumptions of Temkin isotherm are valid (Eddy and Ebenso, 2010; Adejo *et al.*, 2012).

1.6.4 Flory-Huggins adsorption isotherm

The assumptions of Flory-Huggins adsorption isotherm can be expressed as equation 1.9:

$$\log\left(\frac{\theta}{C}\right) = \log k + x\log(-\theta) \quad 1.9$$

where 'x' is the number of inhibitor molecules occupying one site (or the number of water molecules replaced by one molecule of the inhibitor). A plot of *log(θ/C)* versus *log(1- θ)* is linear confirming the application of Flory-Huggins (Eddy and Ita, 2010).

1.6.5 El-Awady *et al.* kinetic-thermodynamic adsorption isotherm

The kinetic-thermodynamic model can be expressed as equation 1.10:

where K is a constant which is related to the adsorption equilibrium constant, k expressed as equation 1.11:

where *y* is the number of the inhibitor molecules occupying one active site and *1/y = x* which is the number of active sites of the surface occupied by one molecule of the inhibitor. It has been found that values of *x* greater than unity indicate that a given inhibitor molecule will occupy more than one active site. Also, values of *y > 1* imply the formation of multilayers of inhibitor on the surface of the metal, while *y < 1* indicates that a given inhibitor molecule will occupy more than one active site (Noor, 2009; Li *et al.,* 2010; Adejo *et al.,* 2012).

1.6.6 Frumkin adsorption isotherm

The assumptions of Frumkin isotherm can be expressed as equation 1.12:

____

where *k* is the adsorption equilibrium constant and α is the lateral interaction term describing the molecular interaction in the adsorbed layer. When α is positive, it indicates the attractive behaviour of the surface of the metal (Eddy and Odiongenyi, 2010).

The equilibrium constant of adsorption *k*, of an inhibitor on the surface of a metal is related to the free energy of adsorption ΔG_{ads}° as according to equation 1.13:

____ _____

where R is the molar gas constant, T is the absolute temperature and 55.5 is the concentration of water in solution expressed in M.

Generally, ΔG_{ads} values with magnitude much less than 40 kJ mol^{-1} have typically been correlated with the electrostatic interactions between organic molecules and charged

metal surface (physisorption), whilst those of magnitude in the order of 40 kJ mol^{-1} and above are associated with charge sharing or transfer from the organic molecules to the metal surface (chemisorption) (Popova *et al.*, 2003; Eddy and Ita, 2010; Oguzie *et al.*, 2012b).

1.7 Purines

A purine is a heterocyclic aromatic organic compound, consisting of a pyrimidine ring fused to an imidazole ring. They are kinds of nitrogen-containing bases (nucleotides) which form the building blocks of nucleic acids. Purines, including substituted purines and their tautomers, are the most widely distributed kind of nitrogen-containing heterocycles in nature. The following purines have been chosen for the present study:

i. Adenine
ii. Guanine
iii. Hypoxanthine
iv. Xanthine

Their chemical structures are presented in Figure 1.1.

1.7.1 Adenine

In older literatures, adenine is called vitamin B_4 . It is no longer considered a true vitamin or part of the Vitamin B complex. However, two B vitamins, niacin and riboflavin, bind with adenine to form the essential cofactors nicotinamide adenine dinucleotide (NAD) and flavin adenine dinucleotide (FAD), respectively. Numerous references to its use occur in biochemical literature (Parker *et al.*, 2010). Adenine has been tested for use in cell cultures. Natural sources of adenine include raw unadulterated honey, bee pollen, royal jelly, propolis, most fresh vegetables and fruits. It is believed that all complex carbohydrates contain varying amounts of adenine.

1.7.2 Guanine

Guanine is a derivative of purine, consisting of a fused pyrimidine-imidazole ring system with conjugated double bonds. Guanine is found in integumentary system of many fish such as sturgeon. It is also present in the reflective deposits of the eyes of deep-sea fish and some reptiles such as crocodiles (Fox, 1979; Wilson et al., 1982). In the cosmetics industry, crystalline guanine is used as an additive to various products (e.g., shampoos), where it provides a pearly iridescent effect. It is also used in metallic paints and simulated pearls and plastics. It provides shimmering luster to eye shadow and nail polish.

1.7.3 Hypoxanthine

Hypoxanthine is a naturally occurring purine derivative. It is occasionally found as a constituent of nucleic acids, where it is present in the anticodon of tRNA in the form of its nucleoside inosine. Hypoxanthine is a necessary additive in certain cell, bacteria, and parasite cultures as a substrate and nitrogen source (WWARN, 2012).

1.7.4 Xanthine

Xanthine is a purinebase found in most human body tissues and fluids and in other organisms. A number of stimulants are derived from xanthine, including caffeine and theobromine (Spiller, 1998).

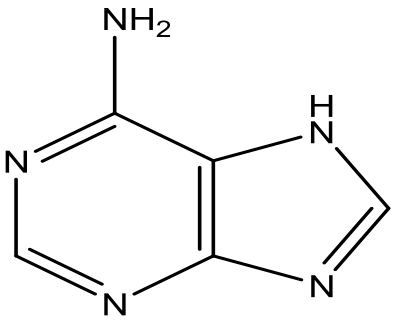
1.8 Statement of the Problem

Due to strict environmental regulations, the continued usage of non environmentally friendly chemical compounds as corrosion inhibitors has faced relentless condemnation. Consequently, large numbers of organic compounds, principally those containing heteroatoms like oxygen, nitrogen or sulphur groups in conjugated systems are being investigated as corrosion inhibitors for the corrosion of different metals in various aggressive media.

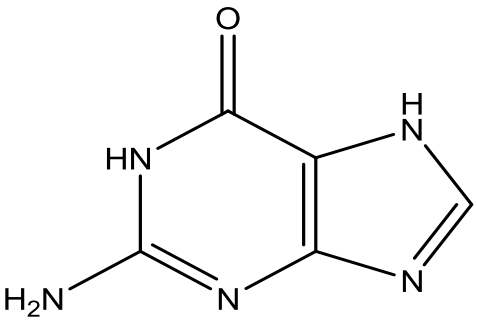
Although some plants extracts have been found to be useful as eco-friendly inhibitors (Oguzie, 2005; Eddy *et al.*, 2009), the actual constituents of the extracts that are responsible for inhibition have been difficult to determine making it difficult to elucidate the specific mechanism for corrosion inhibition. Hence, the challenge for search of corrosion inhibitors, whose actual chemical structures and eco-friendliness have been established are on the increase. Purines are organic compounds with hetero atoms like O and N in their aromatic rings. They are non toxic and can therefore be used as eco-friendly inhibitors against the corrosion of metals in various aggressive media.

1.9 Justification for the Choice of Purines as Corrosion Inhibitors

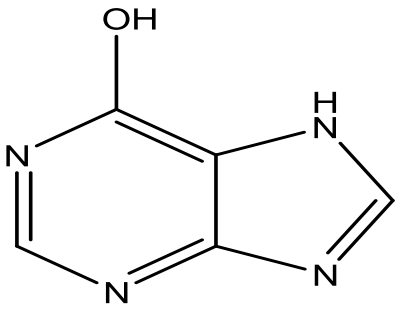
Organic compounds containing C, N , S and or O in a conjugated system are known to be effective corrosion inhibitors (Eddy, 2008). Purines have hetero atoms like O and N in their aromatic rings. Therefore, they are expected to be good corrosion inhibitors. They are relatively cheap and commercially available. They are non- toxic and can therefore compete with eco-friendly inhibitors. The molecular and electronic structures of the selected purine derivatives have close similarities with those of conventional organic inhibitor molecules hence, they can be investigated as corrosion inhibitors.



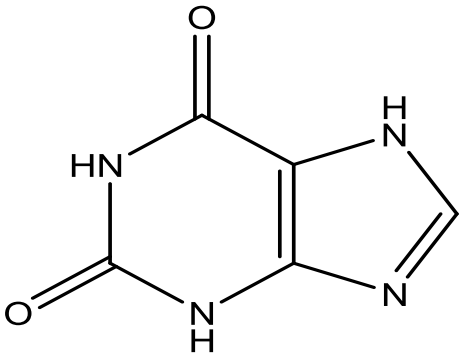
(a) Adenine



(b) Guanine



(c) Hypoxanthine



(d) Xanthine

Figure 1.1 Chemical structures of (a) Adenine (b) Guanine (c) Hypoxanthine and (d) Xanthine

1.10 Aims of the Research

This research aims at investigating some selected purines as eco-friendly inhibitors for the corrosion of mild steel and aluminium in 0.1 M HCl, H_2SO_4 and H_3PO_4 (a low acid concentration) at 303 and 333 K respectively.

1.11 Objectivesof the Research

The objectives of the research are as follows:

a. To carry out a comparative study of the effect of adenine (AD), guanine (GU), hypoxanthine (HYP) and xanthine (XN) on the corrosion of mild steel and aluminium in 0.1 M HCl, H_2SO_4 and H_3PO_4 using gravimetric technique at 303 and 333 K respectively.

b. To investigate the adsorptive properties, thermodynamics and kinetic parameters of the purines from weight loss measurements.

c. To establish the effect of each purine derivative at 303 K on the current density and corrosion potentials of mild steel and aluminium in HCl, H_2SO_4 and H_3PO_4 at 303 K, using potentiodynamic polarisation measurements.

d. To evaluate the interaction of each purine derivative with the mild steel and aluminium surfaces in HCl, H_2SO_4 and H_3PO_4 at 303 K, by electrochemical impedance spectroscopy.

e. To investigate the synergistic effects of iodide ions (using [KI]= 0.005 M) on the adsorptive behaviour of the selected purines on mild steel and aluminium in the different acid media at 303 K.

f. To carry out quantum chemical calculations in order to get useful theoretical information about the selected purines. Molecular dynamics simulations will be

employed to understand the interactions of the inhibitors with the Fe (1 1 0) and Al (1 1 0) surfaces.

CHAPTER TWO

LITERATURE REVIEW

2.1 Corrosion Inhibitors

Corrosion inhibitors are compounds that can reduce the rate of corrosion of a metal through the mechanism of adsorption, which may be physical (i.e, involving the transfer of charges from charged inhibitor to a charged metal surface) or chemical adsorption (which involves the transfer of electrons from the inhibitor to the vacant d-orbital of the metal).

Most corrosion inhibitors have been observed to posses one or more of the following properties (Eddy *et al*, 2010):

(i). Possession of hetero atoms in aromatic rings or long carbon chain

(ii). Possession of polar functional groups such as –COOH, -NH_2, etc as well as π-electrons.

Based on the above criteria, several organic inhibitors have been investigated including triazoles, benzotriazoles, organic dyes, amino acids, schiff bases, imidazoles and purines.

2.1.1 Triazoles and benzotriazoles derivativesas corrosion inhibitors

Li *et al*. (2011) synthesized two triazole derivatives [1-phenyl-2-(5-(1,2,4) triazol-1-ylmethyl-(1,3,4) oxadizaol-2-ylsulphanyl)-ethanone (PTOE) and 2-(4-tert-butyl-benzylsulphanyl)-5-(1,2,4) triazol-1-ylmethyl-(1,3,4) oxadiazole (TBTO)] as new corrosion inhibitors for the corrosion of mild steel in 1 M hydrochloric acid. The inhibition efficiencies of the different inhibitors were evaluated using weight loss and electrochemical techniques such as electrochemical impedance spectroscopy (EIS) and polarization curves. The results obtained from electrochemical investigation revealed

that these compounds acted as mixed-type inhibitors retarding the anodic and cathodic corrosion reactions and did not change the mechanism of either hydrogen evolution reaction or mild steel dissolution. The adsorption of the inhibitors obeyed the Langmuir adsorption model.The effect of molecular structure on the inhibition efficiency of the inhibitors was investigated using ab initio calculations while electronic properties such as the energy of the highest occupied molecular orbital (HOMO), the energy of the lowest unoccupied molecular orbital (LUMO), dipole moment (μ) and molecular orbital densities were also calculated.

Khadom *et al*. (2009) investigated the adsorption of 4-amino-5-phenyl-4H-1, 2, 4-triazole-3-thiol (APTT) as a corrosion inhibitor for mild steel in hydrochloric acid (HCl) solution using the weight loss technique. The degree of surface coverage by APTT was used to calculate the free energy of adsorption, using Bockris-Swinkels isotherm. The dependence of free energy of adsorption, on the surface coverage, was ascribed to the surface heterogeneity of the adsorbent. The adsorption of APTT molecules on the surface occurred without modifying the kinetics of the corrosion process.

Gopi *et al.*(2007) studied the corrosion inhibition of mild steel by means of newly synthesized triazole phosphonates 3-vanilidene amino 1,2,4-triazole phosphonate (VATP), 3-anisalidene amino 1,2,4-triazole phosphonate (AATP) and 3-paranitro benzylidene amino 1,2,4-triazole phosphonate (PBATP) together with cetyl trimethyl ammonium bromide (CTAB) in natural aqueous environment using weight loss, potentiodynamic polarisation and AC impedance measurements. Addition of molybdate was noticed to increase the inhibition efficiency of triazole in a synergistic manner. Results from experimental observations indicated VATP as a better corrosion inhibitor

for mild steel in aqueous solution. Additionally the formulation consisting of VATP, sodium molybdate and CTAB offered good corrosion inhibition efficiency.

Matheswaran and Ramasamy (2010) studied benzotriazole as an inhibitor for the corrosion inhibition of mild steel in 1 N citric acid using weight loss method. The results obtained indicated that the corrosion inhibition efficiency of the benzotriazole varied with the temperature and acid concentrations. Also, it was found that the corrosion inhibition behaviour of benzotriazole was better when the concentration of inhibitor was increased. Kinetic treatment of the results showed first order kinetics.

Selvi *et al*. (2003) also synthesized some benzotriazole derivatives (namely, N-[1-(benzotriazolo-1-yl)alkyl] aryl amine (BTMA), N-[1-(benzotriazolo-1-yl)aryl] aryl amine (BTBA), and 1-hydroxy methyl benzotriazole (HBTA) and found that these compounds possess excellent inhibition properties for corrosion of mild steel in 0.5 M H_2SO_4 at room temperature. Potentiodynamic polarization and AC impedance studies were used to investigate the inhibition mechanism. Benzotriazole derivatives were found to act as mixed type inhibitors. Among the compounds studied, HBTA exhibited the best inhibiting performance giving more than 95% IE. They also found that R_{ct} values increased while C_{dl} values tend to decrease with increase in the concentration of benzotriazole. The observed trend was attributed to the adsorption of benzotriazole on the metal surface.

2.1.2 Dyes as corrosion inhibitors

The inhibitive properties of some organic dyes have been investigated by some researchers. For instance, Abdeli *et al.* (2009) studied the inhibiting behaviour of nile blue and indigo carmine organic dyes on corrosion of mild steel in 1 M HCl, using

weight loss, potentiodynamic polarization and electrochemical impedance spectroscopy techniques. Polarization curves indicated that both inhibitors are mixed anodic–cathodic in nature, and Langmuir isotherm was found to be the best isotherm that described the adsorption behaviour.

Gravimetric method was used by Oguzie *et al*. (2004) to study the inhibitory properties of congo red (CR) dye for the corrosion of mild steel in aerated sulphuric acid solution between 30-60°C. The effect of addition of halide salts viz KCl, KBr and KI was also investigated. Inhibition efficiency was found to increase with increase in the concentration of CR but decreased with increase in temperature. Corrosion activation energies of 82.98 and 96.92 kJ mol^{-1} were observed in the absence and presence of CR, respectively. The observed corrosion data suggested that inhibition of mild steel corrosion is due to physical adsorption of the CR molecules on the metal surface. The adsorption of CR obeyed the follow Flory–Huggins isotherm. Inhibition antagonism and synergism (KCl < KBr <KI) were observed at 30 and 60°C respectively on addition of halide salts to inhibited systems containing CR. The inhibition efficiency of CR in the presence of halides increased with rise in temperature and corrosion activation energy in these systems decreased to 40.63 kJ mol^{-1}. These observations indicate a chemical adsorption mechanism, thus suggesting that the halide ions reversed the mechanism of CR adsorption within the concentration range studied. The calculated values of heat of adsorption confirm physisorption and chemisorption mechanisms respectively for CR adsorption in the absence and presence of halides.

2.1.3 Amino acids as corrosion inhibitors

Some amino acids have been found to be good inhibitors for the corrosion of mild steel in HCl (Silva *et al.*, 2006; El-Rabiee *et al*., 2008). Amino acids are molecules that contain both amino and carboxylic acid functional groups. These acids are non toxic, natural and contain $–NH_2$ and -COOH functional groups. Amino acids are completely soluble in aqueous media and can be produced with high purity at reduced costs (Eddy, 2010). They are therefore expected to be good inhibitors for the corrosion of mild steel in acid solutions.

Olivares-Xometl *et al*. (2006) investigated the potentials of new compounds of alkylamides derived from amino acids as corrosion inhibitors for carbon steel in an aqueous solution of hydrochloric acid. Electrochemical testing was carried out using polarization scans and weight loss measurements. Polarization scans indicated that the compounds acted as mixed corrosion inhibitors with an efficiency of 80–90% which was similar to the results obtained from gravimetric measurements, when dissolved in the test solution ($\geq$50 ppm).

Zhang *et al*. (2008) investigated the inhibition effect of four amino acids (aspartic acid, glutamic acid, asparagines and glutamine) for the corrosion of copper in 0.5 M hydrochloric acid using potentiodynamic polarization and electrochemical impedance spectroscopy (EIS). Both potentiodynamic and EIS measurements indicated that the amino acids have some protective effect against copper corrosion in 0.5 M HCl solution. The inhibition efficiency of these compounds was found to increase in the order Gln > Asn > Glu > Asp and tends to increase with increase in the concentration of the inhibitors. Addition of iodide ions into 10 mM glutamine solution gave an

improvement of the protection efficiency, up to a maximum value of 93.74 % for 5 mM KI. Physical adsorption mechanism was proposed for the studied amino acids and the adsorption was consistent with the Langmuir adsorption model.

2.1.4 Schiff bases as corrosion inhibitors

Weight loss and thermometric methods were used by Upadhyay *et al.* (2007) to study the inhibitory effect of synthesised Schiff's bases (including:N-(furfurilidine) – 4-methoxy aniline (SB1), N-(furfurilidine) – 4- methylaniline (SB2), N- (salicylidine) – 4-methoxy aniline (SB3), N-(cinnamalidine) – 4 –methoxy aniline (SB4) and N-(cinnamalidine) - 2-methylaniline (SB5)) for the corrosion of mild steel in sulphuric acid solutions. The results obtained by both methods were in good agreement with each other and that the inhibition efficiency depended upon the concentration of inhibitor and that of the acid. Maximum inhibition efficiency was shown at highest concentration of Schiff's bases at the highest concentration of acid.

The corrosion inhibition of mild steel in 0.5 M sulphuric acid by two newly synthesized Schiff bases namely 4-X-2-{[2-(2-pyridin-2-yl-ethylsulfanyl) ethylimino] and methyl}-phenol [X = $–NO_2$ and –OMe] have been investigated in the temperature range 298–318 K using Tafel polarization and electrochemical impedance spectroscopy (EIS) methods (Hosseini *et al.,* 2009). The Temkin isotherm was found to provide an accurate description of the adsorption behaviour of the Schiff bases.

2.1.5 Imidazoles as corrosion inhibitors

Gasparac *et al.* (2000a) investigated the efficiency of imidazole derivatives for corrosion inhibition of copper in 0.5 M hydrochloric acid using impedance spectroscopy. Imidazole and its derivatives 4-methylimidazole, 4-methyl-5-hydroxymethylimidazole, 1-phenyl-4-methylimidazole, 1-(*p*-tolyl)-4-methylimidazole

were investigated. The study showed that 1-(*p*-tolyl)-4-methylimidazole was the best inhibitor in the series and that it acted as a mixed inhibitor. Similar studies using potentiodynamic methods have shown that 1-(*p*-tolyl)-4- methylimidazole has the best inhibitory efficiency (Gasparac *et al., 2000b*).

2.1.6 Purines as Corrosion Inhibitors

The non-toxic and biodegradable nature of purine derivatives like adenine, guanine, hypoxanthine and xanthine make the investigation of their inhibiting properties significant in the context of the current priority to produce 'green' or environmentally friendly inhibitors.

Scendo (2007a, 200b; 2008) investigated the inhibitive actions of purine and adenine on copper corrosion in 0.5 M Na_2SO_4 (pH 6.8), 0.5 M $NaNO_3$ (pH 1.0) and 1.0 M NaCl at pH 6.8. It was found that purine and adenine were adsorbed chemically on the surface of copper thereby inhibiting the corrosion of copper in these aqueous media.

Sayed *et al*. (2008) studied the effect of various concentrations of adenine (AD) on the corrosion of low carbon steel (LCS) in aerated 4.0 M H_2SO_4 using weight loss, potentiodynamic polarization, impedance and electrochemical frequency modulation (EFM) methods. Variation of open- circuit potential (OCP) as a function of time was also investigated. Results obtained revealed that AD alone did not exhibit very good inhibition performance but together with iodide ion, AD was an effective corrosion inhibitor for LCS corrosion in H_2SO_4 solutions. Synergism between iodide ions and AD was therefore proposed. Moreover, potentiodynamic polarization studies showed that AD alone and the mixture of AD and iodide ions acted as mixed-type inhibitors for the corrosion of LCS in 4.0 M H_2SO_4 solution. The inhibition mechanism involved the

electrostatic adsorption of protonated AD molecules on the LCS surface charged with a negative layer of chemisorbed I^- ions. The results obtained from chemical and electrochemical measurements were in good agreement.

Amin *et al.* (2008) investigated the synergistic effect of I^- ions and purine on the corrosion of aluminium in 1.0 M phosphoric acid using polarization and impedance measurements, complemented with EDX examinations of the electrode surface. Their results indicated that purine alone showed a poor inhibition effect but due to synergistic interaction with I^-ions, better inhibition efficiencies were obtained. The synergistic effect was attributed to enhanced adsorption of purine by the adsorbed I^-ions. Potentiodynamic polarization studies showed that purine and the mixture of purine and I^-ions acted as mixed-type inhibitors for the corrosion of Al in 1.0 M H_3PO_4.

Yan *et al.* (2008) also carried out studies on corrosion inhibition properties of some purines for the corrosion of mild steel in 1M HCl acid using weight loss measurements, electrochemical tests and quantum studies. The compounds studied were guanine, adenine, 2,6-diamiopurine, 6-thioguanine and 2,6-dithiopurine. Increase in inhibition efficiency was in the following order 2,6 dithiopurine > 6 thioguanine > 2,6-diaminopurine > adenine> guanine,with the highest efficiency of 80% for 10^{-3} M 2,6-dithiopurine. Results obtained from quantum chemical calculation indicated that the adsorption of the purines is physical in nature which might arise from the π- stacking between the π-electrons of the purines and the metal surface.

Li *et al.* (2009a, 2009b, 2009c, 2009d) studied the inhibition effect of 6 benzylamino purine (BAP) on the corrosion of cold rolled steel in 1.0-7.0 M H_2SO_4 solution and in

1.0 M HCl solution at 25-50 ^{0}C using weight loss and potentiodynamic methods. Polarisation curves obtained from the studies showed that BAP acted as a mixed-type inhibitor in both sulphuric acid and hydrochloric acid solutions. They also investigated the synergistic inhibition effect of red tetrazolium (RT) and uracil (Ur) on the corrosion of cold rolled steel in 1.0-10 M H_3PO_4 solution and in 1.0-5.0 M H_2SO_4 using weight loss, electrochemical and atomic force microscopy (AFM) approaches at 20-50 ^{0}C. The results obtained revealed that RT had a moderate inhibitive effect, and that the adsorption of RT obeyed the Freundlich adsorption isotherm. Polarisation curves showed that RT was a mixed type inhibitor in both acidic media. Ur was found to have a poor inhibition effect, and acted as a cathodic inhibitor in both acidic media. However, synergistic combination of RT with Ur resulted in enhancement of inhibition efficiency.

CHAPTER THREE

MATERIALS AND METHODS

3.1 Material Preparation

Mild steel sheet of composition {wt.%: Mn (0.6), P (0.36), C (0.15), Si (0.03) and Fe (98.86)} and aluminium sheet (AA 1060 type) of purity 98.5%, were mechanically press-cut to form coupons, each of dimensions, 5 cm x 4cm x 0.15 cm for gravimetric studies and 2 cm x 2 cm x 0.15 cm for electrochemical studies. The coupons were wet polished with different grades of SiC abrasive paper (#400 to #1200), washed with distilled water, rinsed with absolute ethanol, cleaned in acetone and allowed to dry in the air before being preserved in a desiccator prior to corrosion testing. The reagents HCl, H_2SO_4, H_3PO_4 and KI used in the study were analar grades. Distilled water was used for their preparations. Acid concentrations of 0.1 M HCl, H_2SO_4 and H_3PO_4 were used for gravimetric (weight loss) and electrochemical studies respectively. The concentration of the halide (KI) used for inhibitive synergistic studies was 0.005 M while the concentration range for the inhibitors was 2×10^{-3} to 1×10^{-2}M respectively.

3.2 Gravimetric Method

Previously weighed mild steel and aluminium metal coupons were completely immersed in 150 cm^3 of the test solutions (0.1 M HCl, H_2SO_4 and H_3PO_4) in an open beaker placed in a water bath maintained at 303 and 333 K respectively. After every 24 hours, the corrosion products were removed by washing each coupon (withdrawn from the test solutions) in a solution containing 40% NaOH and 100 g/L of zinc dust for mild steel coupons while aluminium coupons were dipped in 70% nitric acid for 2 mins and later washed with distilled water using bristle brush and rinsed with distilled water. The washed coupons were rinsed in acetone and dried in air before re-weighing. The difference in weights for a period of 120 hours was taken as the total weight loss. From

the weight loss results, the inhibition efficiency (IE_{exp}) of the inhibitor, the degree of surface coverage (θ) and the corrosion rate (CR) of mild steel and aluminium were calculated using equations 3.1 to 3.3 respectively (Eddy and Ebenso, 2010).

$$IE_{\exp} = \left(1 - \frac{W_1}{W_2}\right) x100 \qquad 3.1$$

$$\theta = 1 - \frac{W_1}{W_2} \qquad 3.2$$

$$CR\left(gh^{-1}cm^{-2}\right) = \frac{\Delta W}{At} \qquad 3.3$$

where W_1 and W_2 are the weight losses (g) for metal in the presence and absence of the inhibitor respectively, θ is the degree of surface coverage of the inhibitor, A is the area of the metal coupon (in cm^2), t is the period of immersion (in hours) and $\Delta W = W_2 - W_1$ is the weight loss of metal after time, t.

3.3 Electrochemical Impedance Spectroscopy (EIS)

EIS tests were performed at 303 ± 1K in a three electrode cell using a VERSASTAT 400 complete DC voltammetry and corrosion system, with V3 Studio software over a frequency range of 100 kHz - 10 mHz, with a signal amplitude of 5 mV. A graphite rod was used as counter electrode and saturated calomel electrode (SCE) was used as the reference electrode. The latter was connected via a Luggin's capillary. Measurements were performed in aerated and unstirred solutions after 30 minutes immersion in the test solutions. All potentials were reported vs. SCE. The working electrodes were prepared from square sheets of mild steel and aluminium respectively with $1cm^2$ of the area exposed to the test solution.

The charge transfer resistance values were obtained from the diameter of the semi circles of the Nyquist plots. The inhibition efficiencies of the inhibitors were calculated from the charge transfer resistance values using equation 3.4

———— 3.4

where R_{ct} and $R_{ct(inh)}$ are the charge transfer resistance in absence and in presence of the inhibitor, respectively (Oguzie *et al*, 2010; Khaled, 2010a and 2010b).

3.4 Potentiodynamic Polarisation

Potentiodynamic polarization studies were carried out at a potential range of ± 250 mV for mild steel and in the potential range of -1000 to 2000 mV for aluminium, versus corrosion potential at a scan rate of 0.33 mV/s at 303 K . Each test was run in triplicate. Measurements were performed in 0.1 M acid solutions containing 0.01 M concentration of the test inhibitors. The inhibition efficiencies were calculated using equation 3.5

—— 3.5

where i_{corr} and i_{inh} are the corrosion currents in the absence and presence of the inhibitor respectively (Oguzie *et al*, 2010; Quraishi and Singh, 2010).

3.5 Synergistic Effects

Synergistic studies were carried out with the combination of each of the inhibitors (within the range of concentrations stated earlier) with0.005M potassium iodide (KI) respectively. Ion-pair interactions between the organic cations and the halide ions will result in increased surface coverage (Oguzie *et al.*, 2007; Umoren, 2007; Eddy *et al.*, 2010).

3.6 Fourier Transform Infrared Spectrophotometery(FTIR)

IR analyses of the inhibitor and that of the corrosion products (in the presence and absence of the respective inhibitors) were carried out using a SHIMADZU, FTIR-8400S

Fourier Transform Infrared Spectrophotometer. Two coupons were separately dipped in 250 mL of 0.01 M inhibitor concentration for 2 days to form an adsorbed layer after which they were retrieved, dried and scraped with a sharp blade. The scrappings were collected for analysis. The samples were prepared using KBr and the analysis was done by scanning the sample through a wave number range of 400-4000 cm^{-1} (Eddy and Odoemelam, 2008; Eddy *et al.,* 2009; Enenebeaku, 2011).

3.7 Scanning Electron Microscopy (SEM)

Surface morphologies of the mild steel and aluminium coupons before and after inhibition were studied using a JSM-5600 LV scanning electron microscope of JEOL, TOKYO, Japan. 1 cm x 1 cm coupons were dipped in blank solutions and 0.01 M inhibitor solutions for 2 days. The coupons were retrieved, rinsed with distilled water and dried in the air. Each sample was mounted on a metal stub and sputtered with gold in order to make the sample conductive. Scanned images were taken at an accelerating voltage of 2.00 and 15.00 kV (Enenebeaku, 2011).

3.8 Computational and Theoretical Considerations

3.8.1 Quantum chemical calculations

The electronic structure of the purines, including the distribution of frontier molecular orbitals E_{HOMO} and E_{LUMO}, Fukui indices were assessed, with a view to establishing the active sites as well as local reactivity of the molecule. The simulations were performed by means of the Density Functional Theory (DFT) electronic program $DMol^3$ using the Mulliken population analysis in the Material Studio 4.0 software. $DMol^3$ permits analysis of the electronic structures and energetics of molecules, solids and surfaces using DFT. Electronic parameters for the simulations include restricted spin polarization using the DND basis set and the Perdew Wang local correlation density functional. Local reactivity of the studied compounds was analysed by means of the Fukui indices

(FI) to assess regions of nucleophilic and electrophilic behaviour (Khaled, 2009; Eddy, 2010; Enenebeaku, 2011; Oguzie, 2011).

3.8.2 Molecular dynamics simulation

In order to sample many different low energy configurations and identify the low energy minima, molecular dynamics (MD) simulation of the interactions between a single molecule of interest and Fe/Al surface was performed using Forcite quench molecular dynamics in the Material Studio (MS) modelling 4.0 software. Calculations were carried out using COMPASS forcefield and Smart algorithm in a simulation box 17Å x 12 Å x 28 Å with a periodic boundary condition, to model a representative part of the Fe/Al slab and a vacuum layer of 20 Å height. The Fe/Al crystal was cleaved along the (110) plane with a fractional depth of 3.0 Å. The (110) plane was chosen because it is more densely packed and has the most stabilisation compared to Fe/Al (111) and Fe/Al (100) surfaces with relatively open structures.

The geometry of the bottom layers were constrained before optimizing the Fe/Al (110) surface which was subsequently enlarged into a 9 x 7 supercell to avoid edge effects. Temperature was fixed at 350 K which represents a trade off between a system with too much kinetic energy where the molecule desorbs from the surface and a system with not enough kinetic energy for the molecule to move around the surface. Temperature was fixed with the NVE (microcanonical) ensemble with a time step of 1 fs and simulation time 5 ps. The system is quenched every 250 steps. Forcite optimised structures of the purine compounds and the Fe/Al surfaces were used to sample the different interactions of the molecule with the surfaces. The slab of iron and aluminium constructed for the docking were significantly bigger than the purin molecules docked in order to avoid edge effects (Oguzie, 2011; Enenebeaku, 2011).

CHAPTER FOUR

RESULTS

4.1 Gravimetric Measurements

Figures 4.1 - 4.16 show the variation of weight loss (g) with time (hrs) at 303 and 333 K for the corrosion of mild steel and aluminium in 0.1 M HCl, H_2SO_4 and H_3PO_4 acids in the presence of various concentrations of adenine (AD), guanine (GU), hypoxanthine (HYP) and xanthine (XN). The plots on Figures 4.1 – 4.16 were obtained from the data on Appendices I –VIII. From the plots (Figures 4.1 – 4.8), it is evident that weight loss of mild steel in the different acid media decreased in the presence of AD, GU, HYP and XN indicating that the purines retarded the corrosion of mild steel in HCl, H_2SO_4 and H_3PO_4. It can also be deduced from the plots that although the weight loss of mild steel increased over time, the corrosion rates of mild steel coupons in the presence of the inhibitors decreased with increasing inhibitor concentrations.

Figures 4.2, 4.4, 4.6 and 4.8 show that the weight loss of mild steel in the test solutions both in the absence and presence of the inhibitors increased with time at 333 K compared to that at 303 K. Corresponding values of corrosion rates of mild steel and inhibition efficiencies, IE%, of the inhibitors in the various media which were derived from the plots are presented on Tables 4.1 and 4.2 respectively.

Figures 4.9-16 show the variation of weight loss with time at 303 and 333 K for the corrosion of aluminium in 0.1 M HCl, H_2SO_4 and H_3PO_4 in the absence and presence of various concentrations of AD, GU, HYP and XN while Tables 4.3 and 4.4 present calculated rates of corrosion of aluminium and inhibition efficiencies of the purines in the various media at 303 and 333 K respectively.

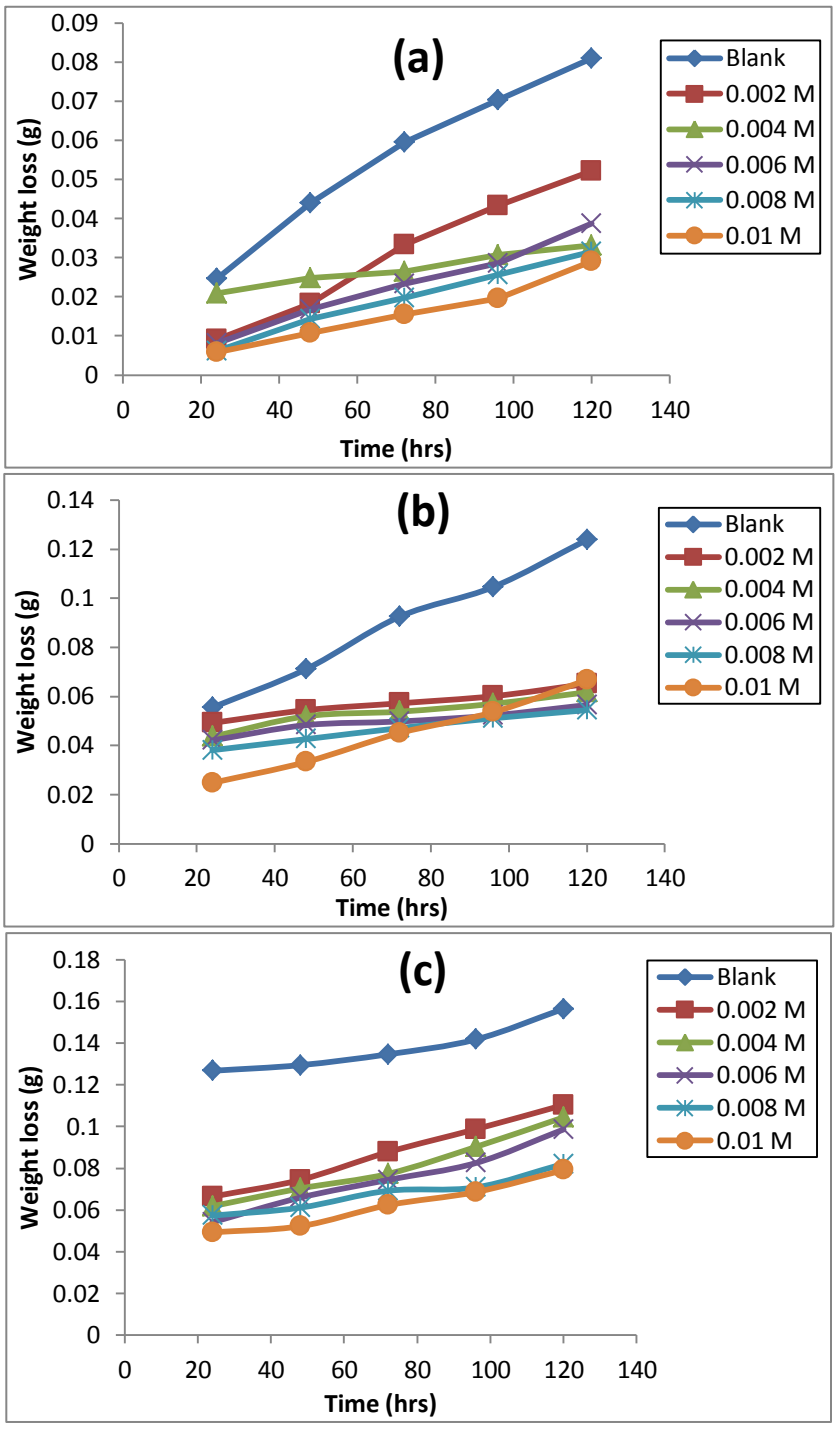


Figure 4.1. Variation of weight loss with time (hrs) for the corrosion of mild steel in 0.1 M (a). HCl (b). H_2SO_4 and (c) H_3PO_4 containing various concentrations of adenine (AD) at 303 K

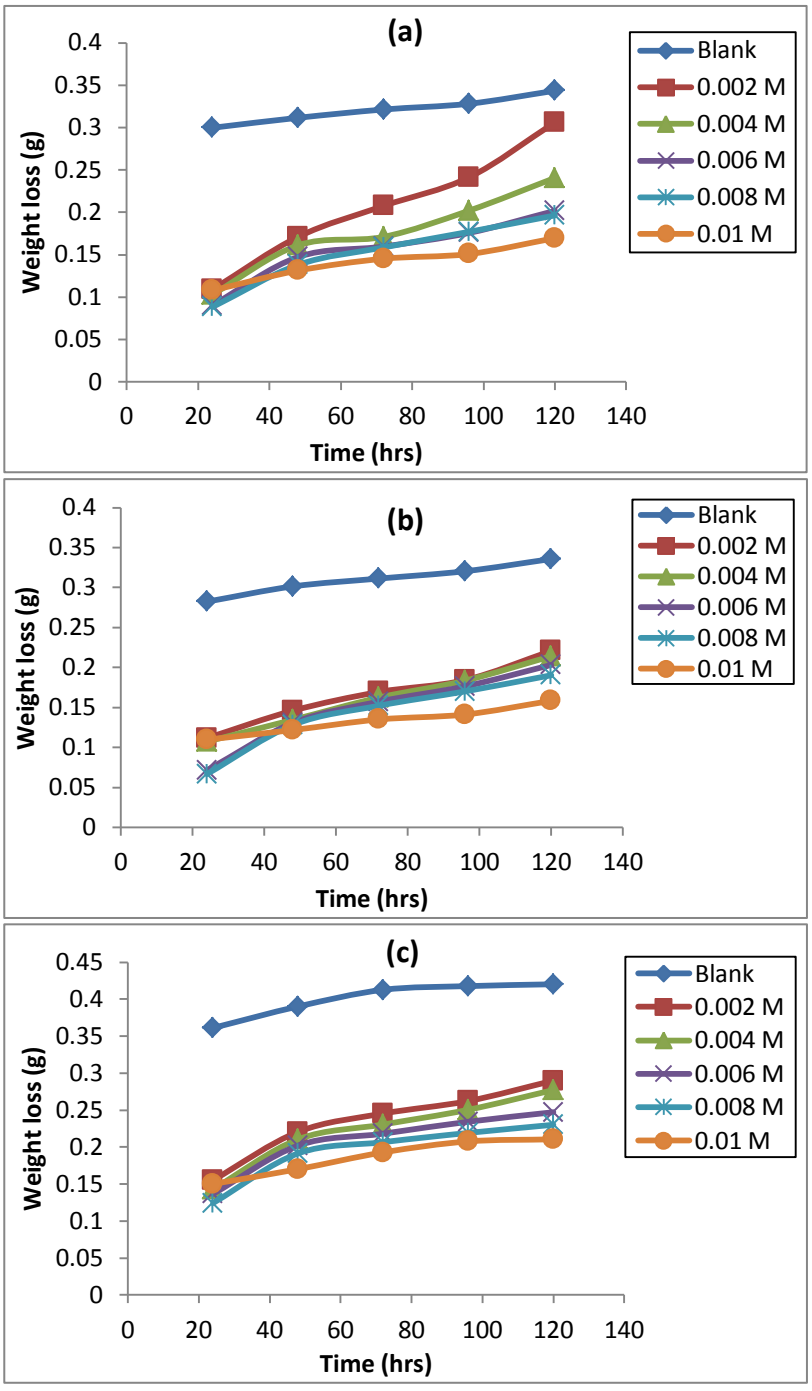


Figure 4.2. Variation of weight loss with time (hrs) for the corrosion of mild steel in 0.1 M (a). HCl (b). H_2SO_4 and (c). H_3PO_4 containing various concentrations of adenine (AD) at 333 K.

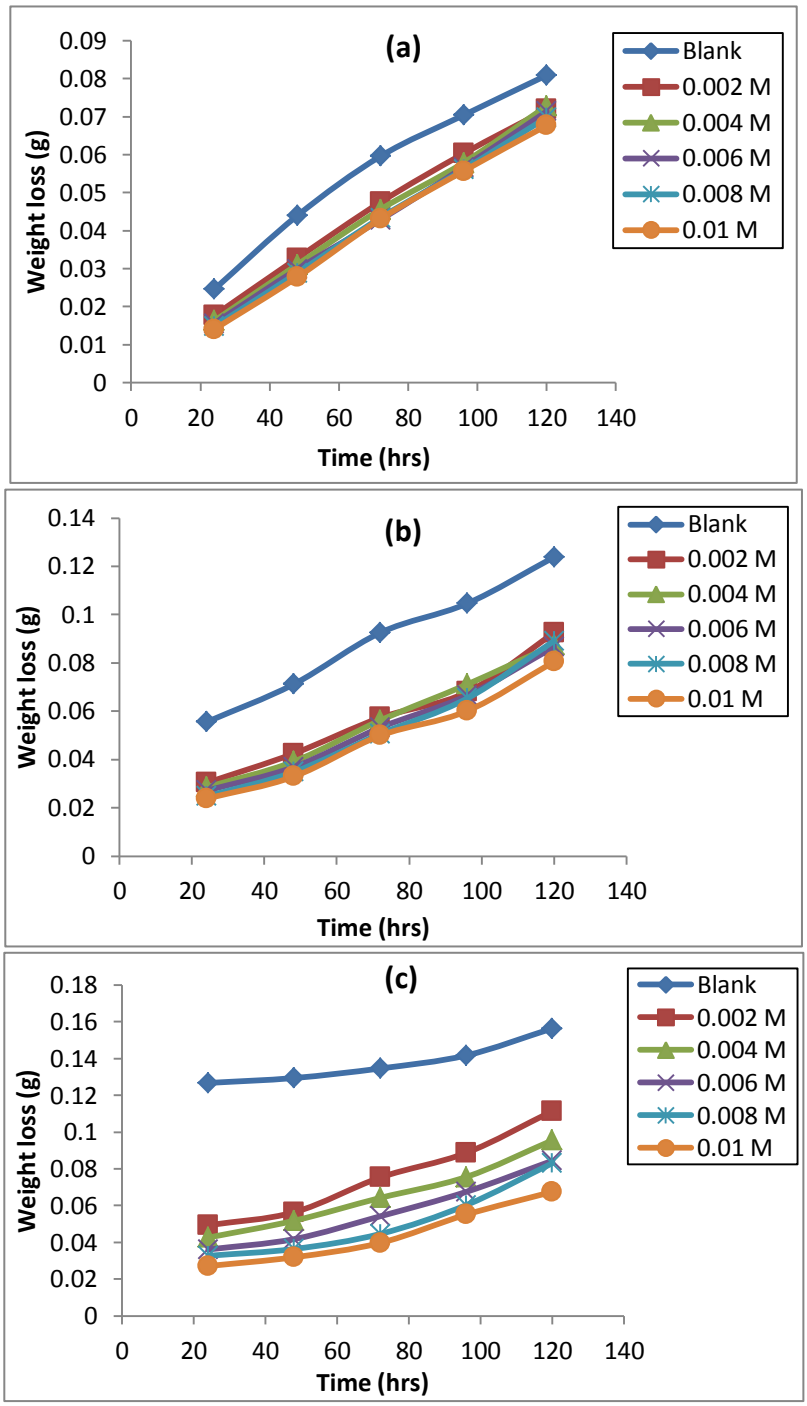


Figure 4.3. Variation of weight loss with time (hrs) for the corrosion of mild steel in 0.1 M (a). HCl (b). H_2SO_4 and (c). H_3PO_4 containing various concentrations of guanine (GU) at 303 K.

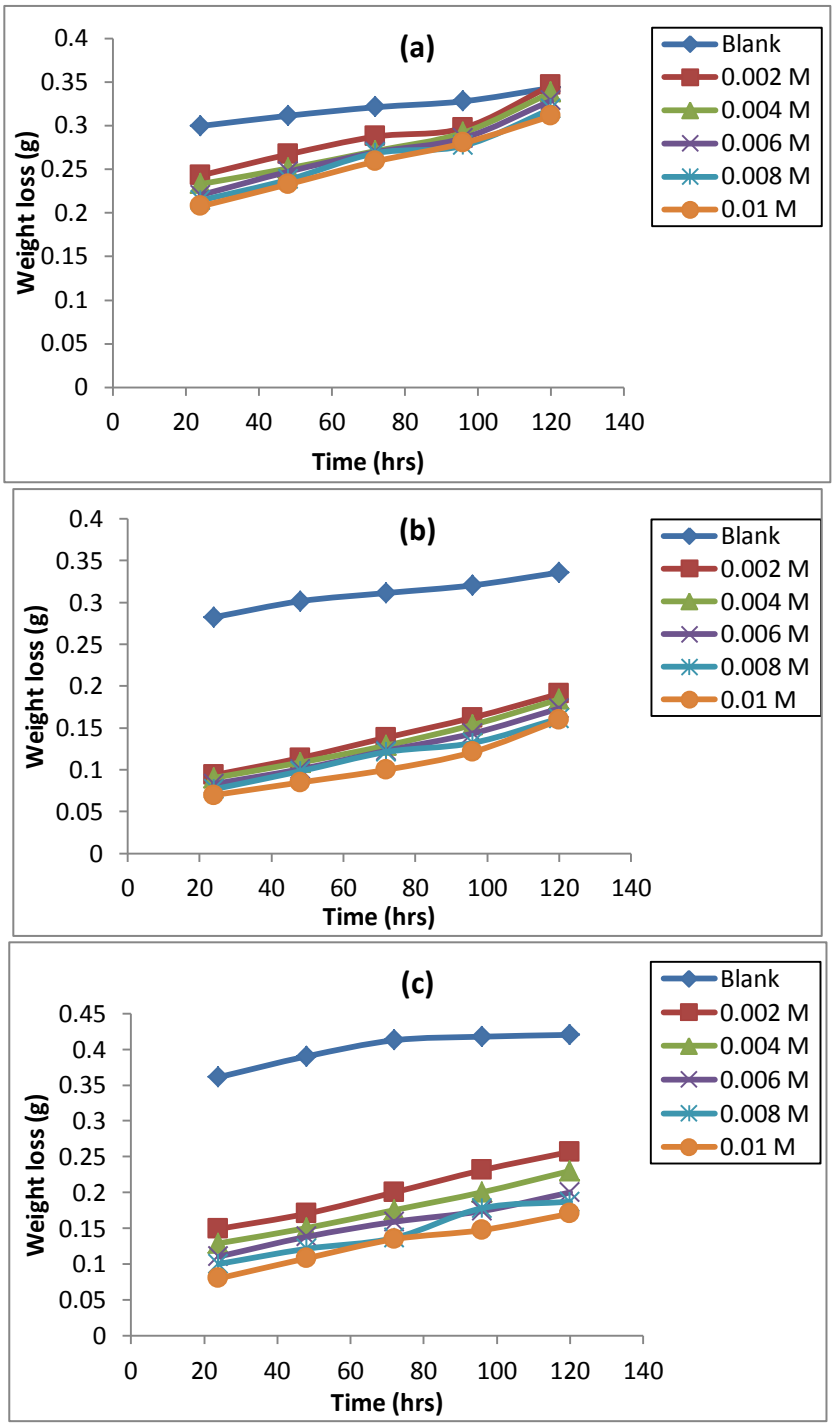


Figure 4.4. Variation of weight loss with time (hrs) for the corrosion of mild steel in 0.1 M (a). HCl (b). H_2SO_4 and (c). H_3PO_4 containing various concentrations of guanine (GU) at 333 K.

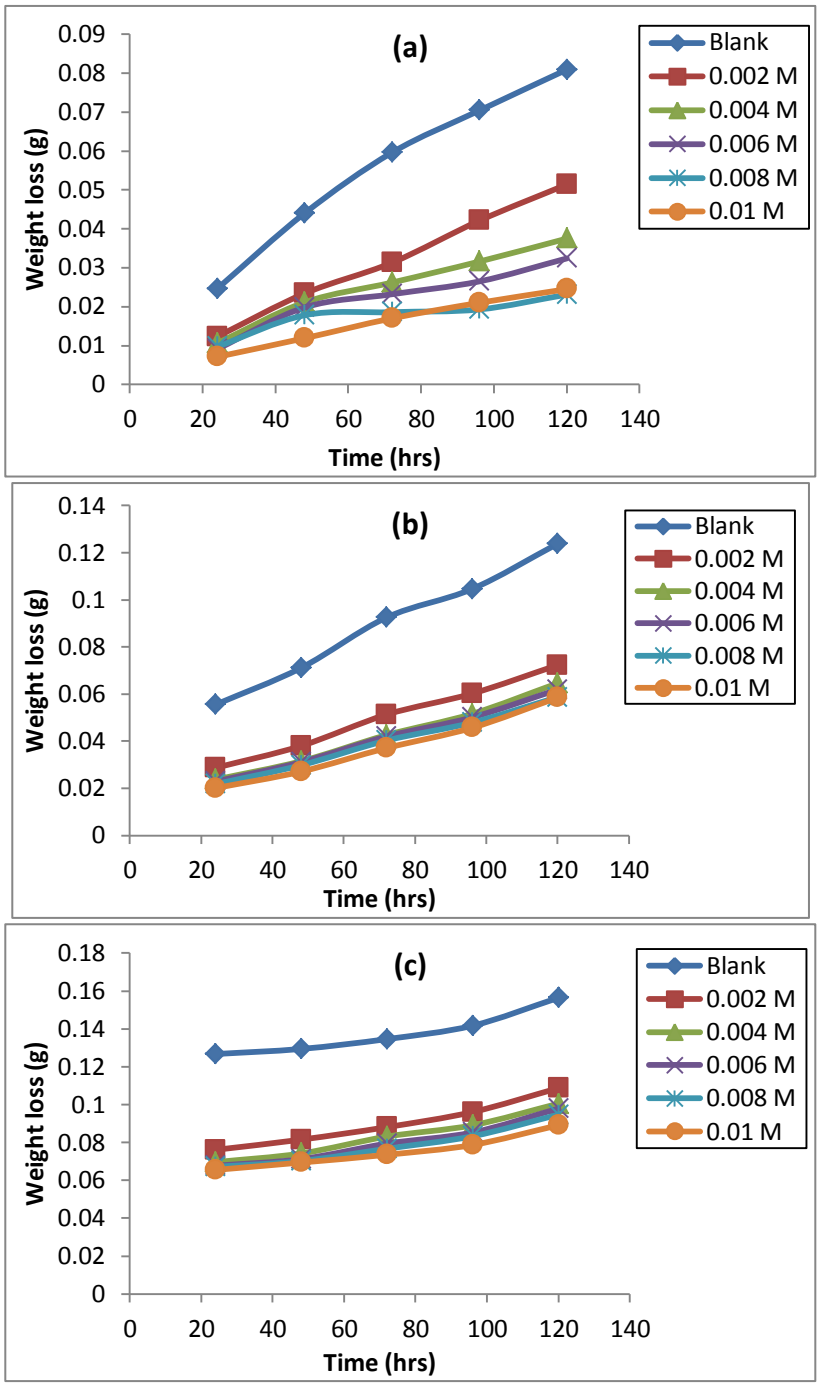


Figure 4.5. Variation of weight loss with time (hrs) for the corrosion of mild steel in 0.1 M (a). HCl (b). H_2SO_4 and (c). H_3PO_4 containing various concentrations of hypoxanthine (HYP) at 303 K.

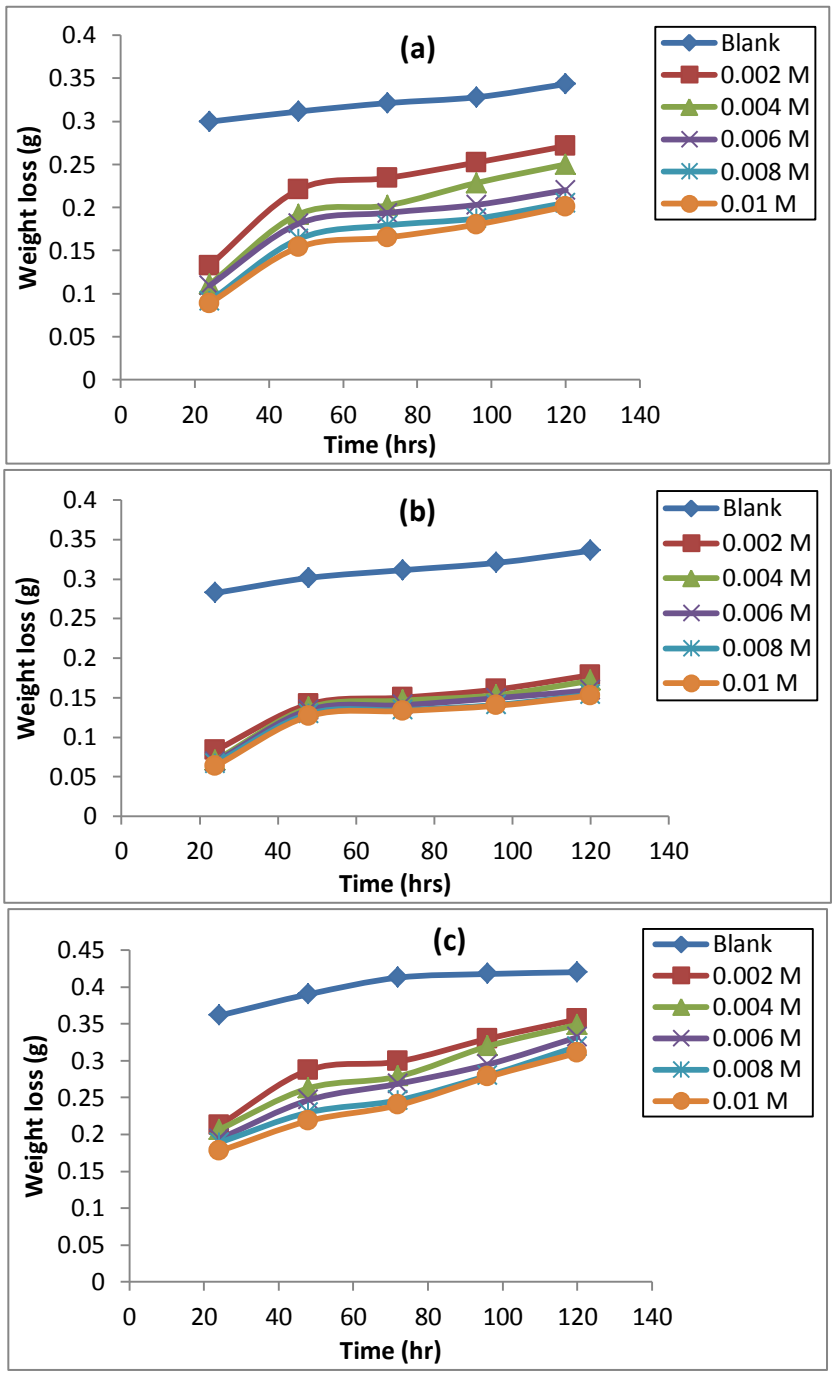


Figure 4.6. Variation of weight loss with time (hrs) for the corrosion of mild steel in 0.1 M (a). HCl (b). H_2SO_4 and (c). H_3PO_4 containing various concentrations of hypoxanthine (HYP) at 333 K.

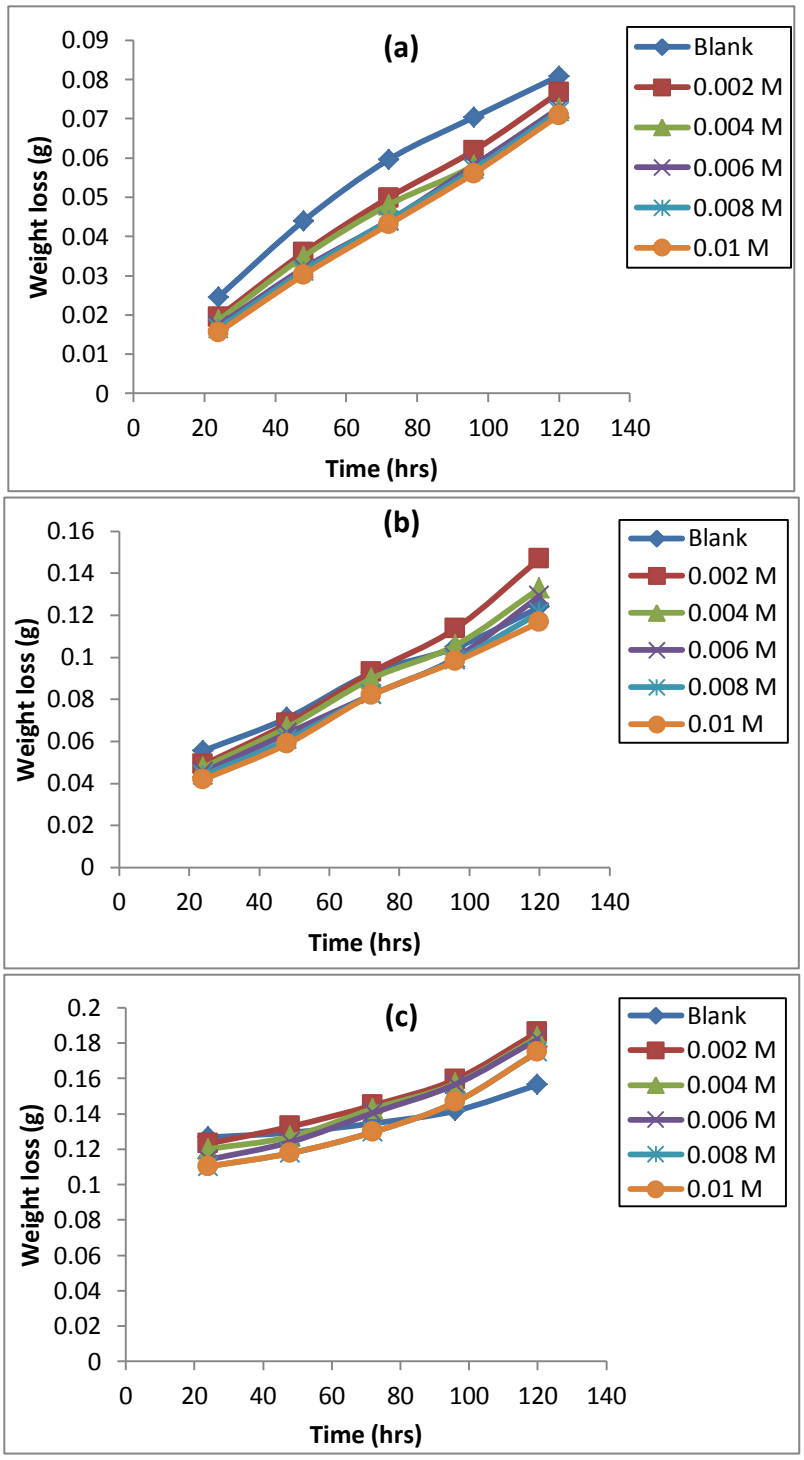


Figure 4.7. Variation of weight loss with time (hrs) for the corrosion of mild steel in 0.1 M (a). HCl (b). H_2SO_4 and (c). H_3PO_4 containing various concentrations of xanthine (XN) at 303 K.

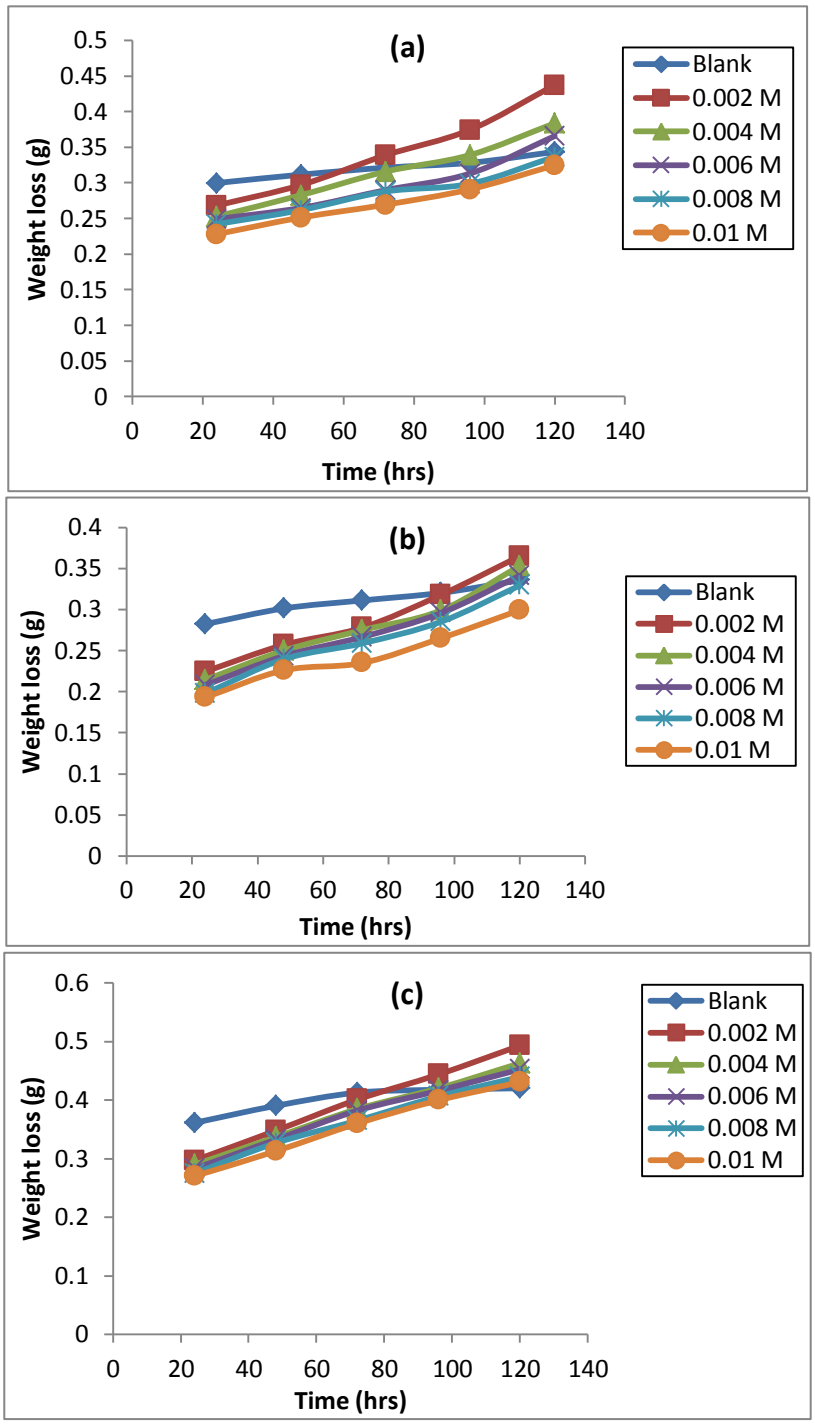


Figure 4.8. Variation of weight loss with time (hrs) for the corrosion of mild steel in 0.1 M (a). HCl (b). H_2SO_4 (c). H_3PO_4 containing various concentrations of xanthine (XN) at 333 K.

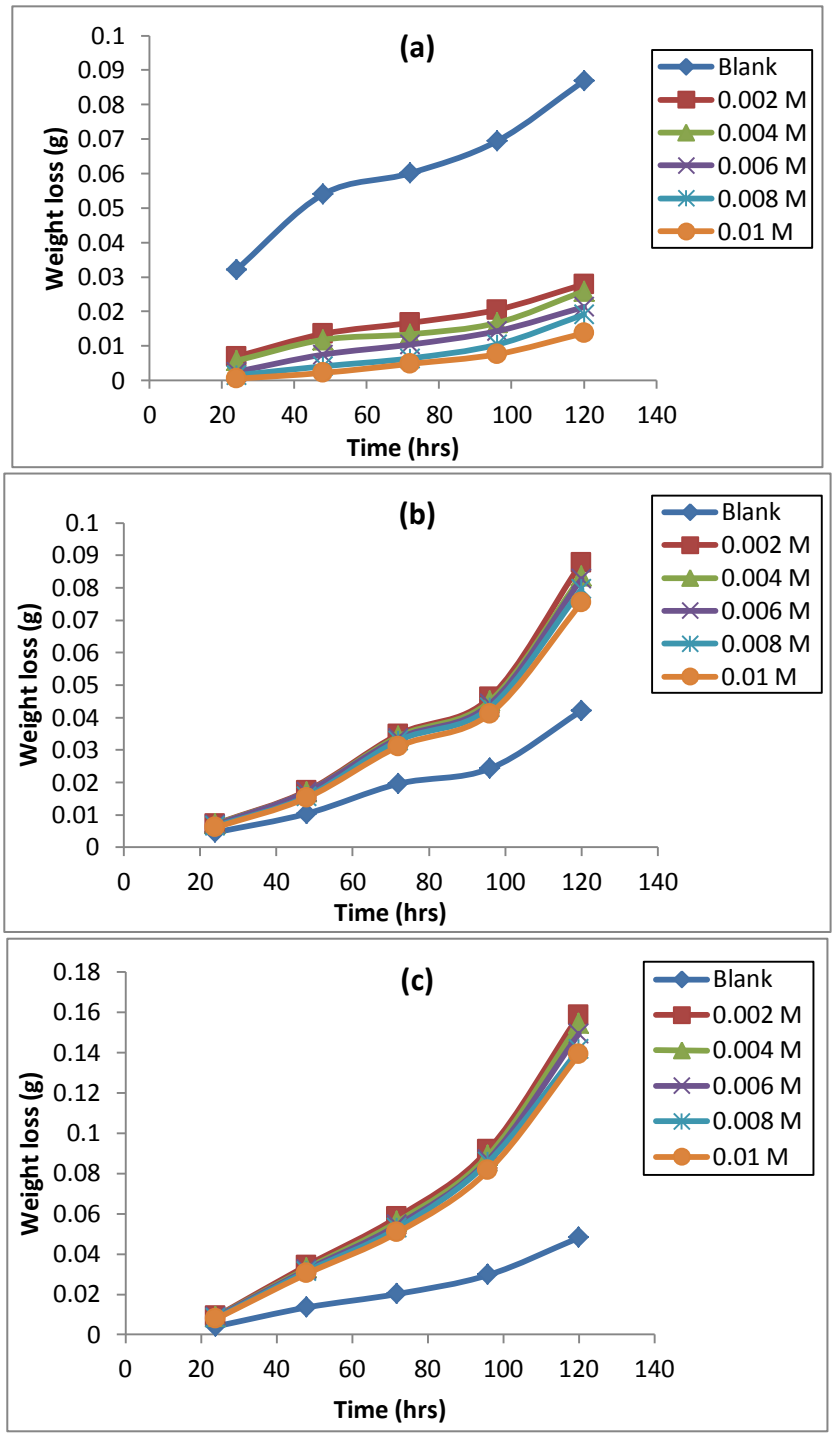


Figure 4.9. Variation of weight loss with time (hrs) for the corrosion of aluminium in 0.1 M (a). HCl (b). H_2SO_4 and (c). H_3PO_4 containing various concentrations of adenine (AD) at 303 K.

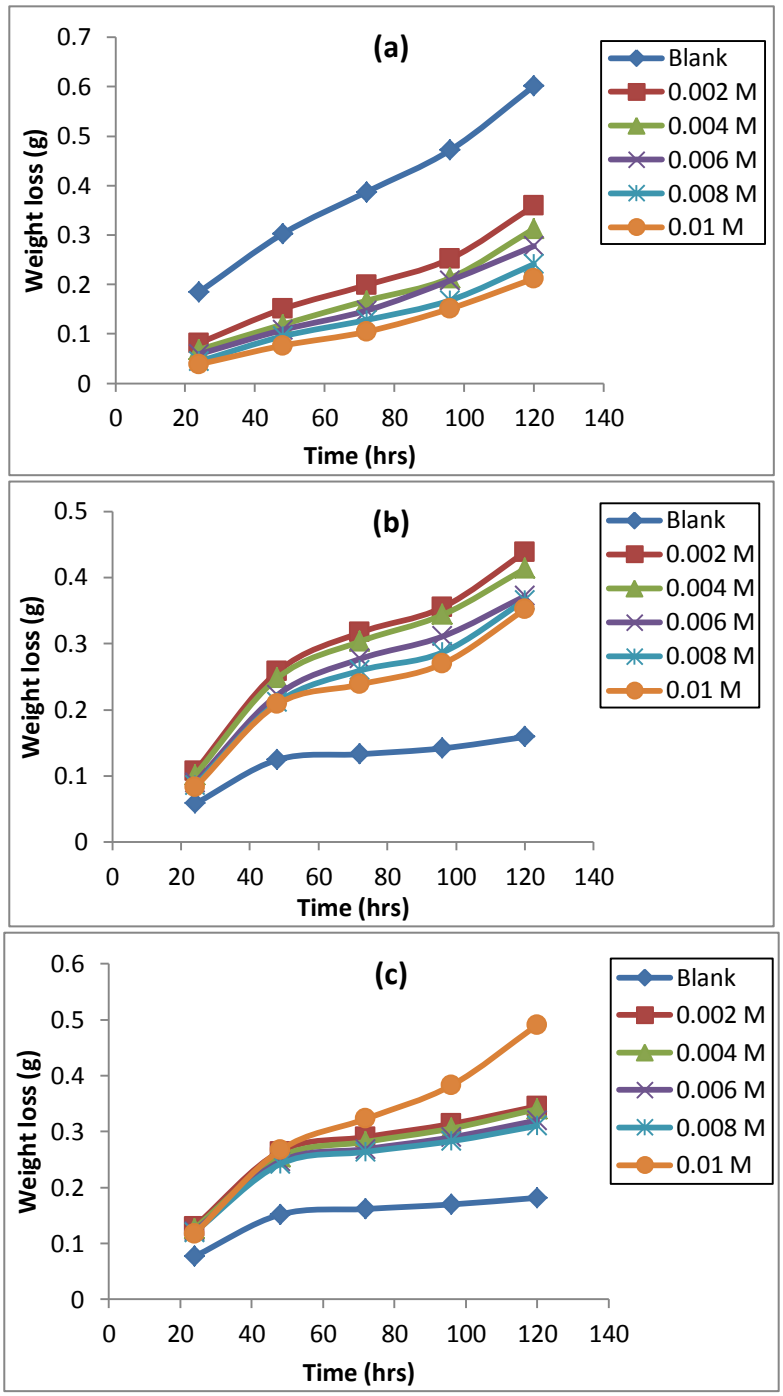


Figure 4.10. Variation of weight loss with time (hrs) for the corrosion of aluminiumin 0.1 M (a). HCl (b). H_2SO_4 and (c). H_3PO_4 containing various concentrations of adenine (AD) at 333 K.

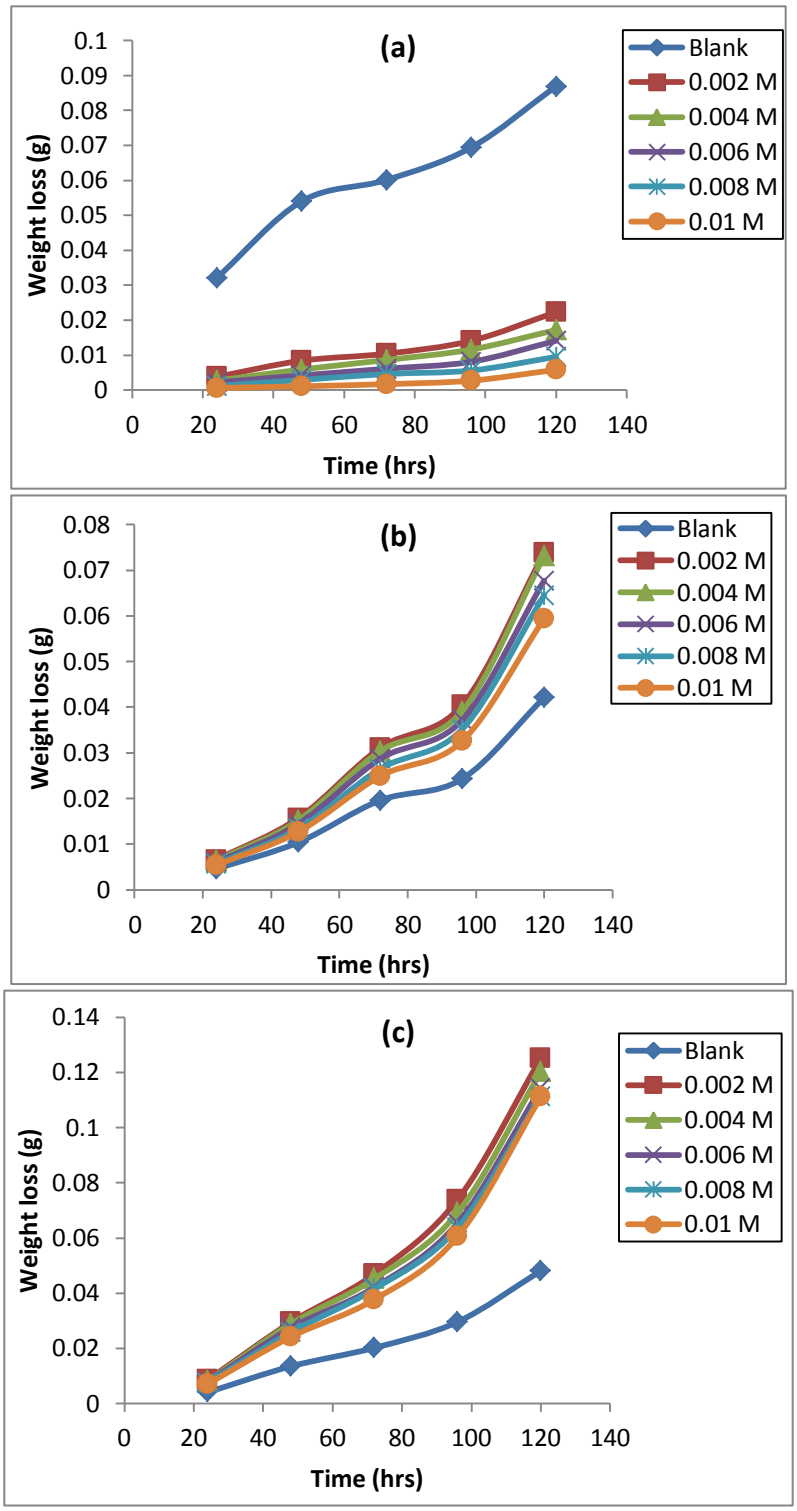


Figure 4.11. Variation of weight loss with time (hrs) for the corrosion of aluminium in 0.1 M (a). HCl (b). H_2SO_4 and (c). H_3PO_4 containing various concentrations of guanine (GU) at 303 K.

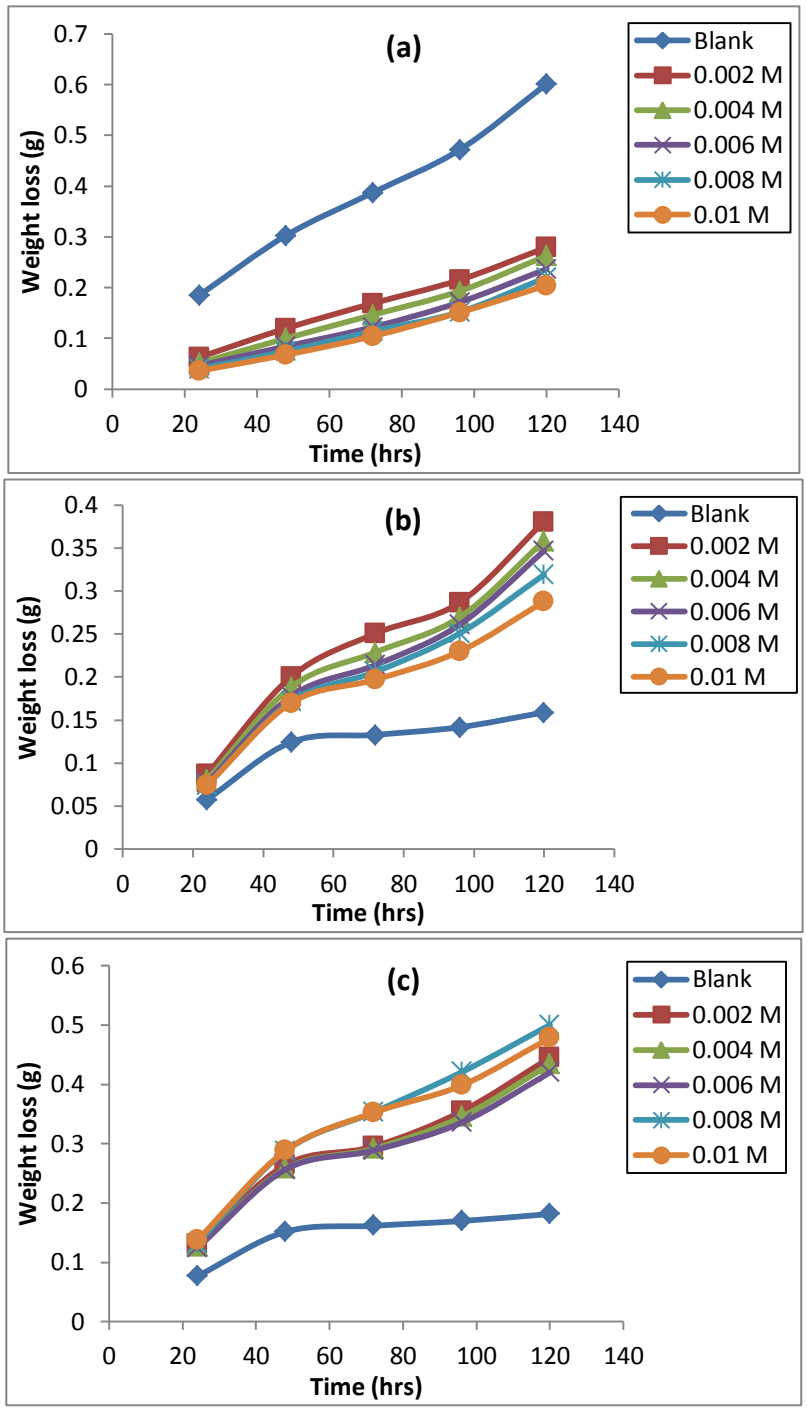


Figure 4.12. Variation of weight loss with time (hrs) for the corrosion of aluminium in 0.1 M (a). HCl (b). H_2SO_4 and (c). H_3PO_4 containing various concentrations of guanine (GU) at 333 K.

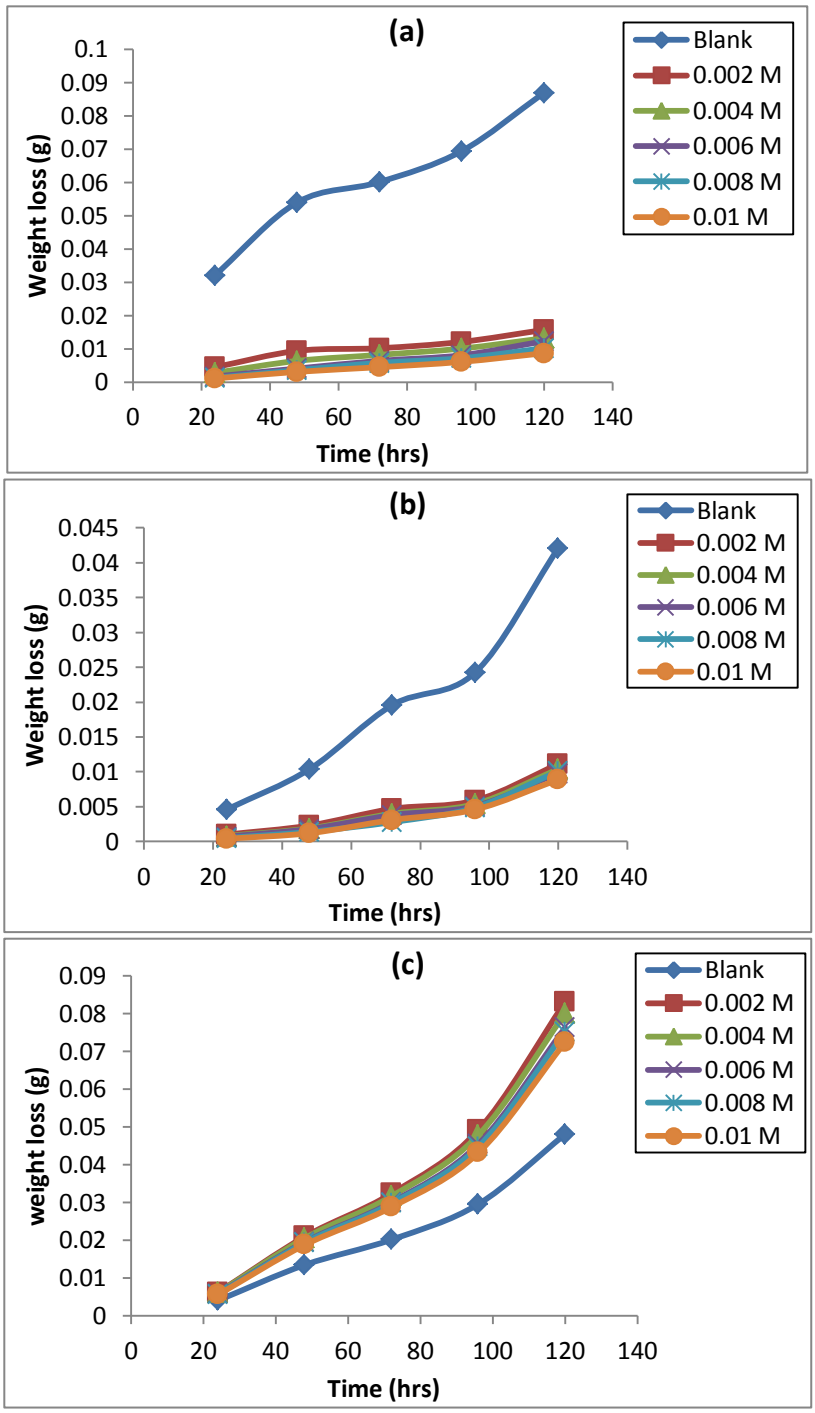


Figure 4.13. Variation of weight loss with time (hrs) for the corrosion of aluminium in 0.1 M (a). HCl (b). H_2SO_4 and (c). H_3PO_4 containing various concentrations of hypoxanthine (HYP) at 303 K.

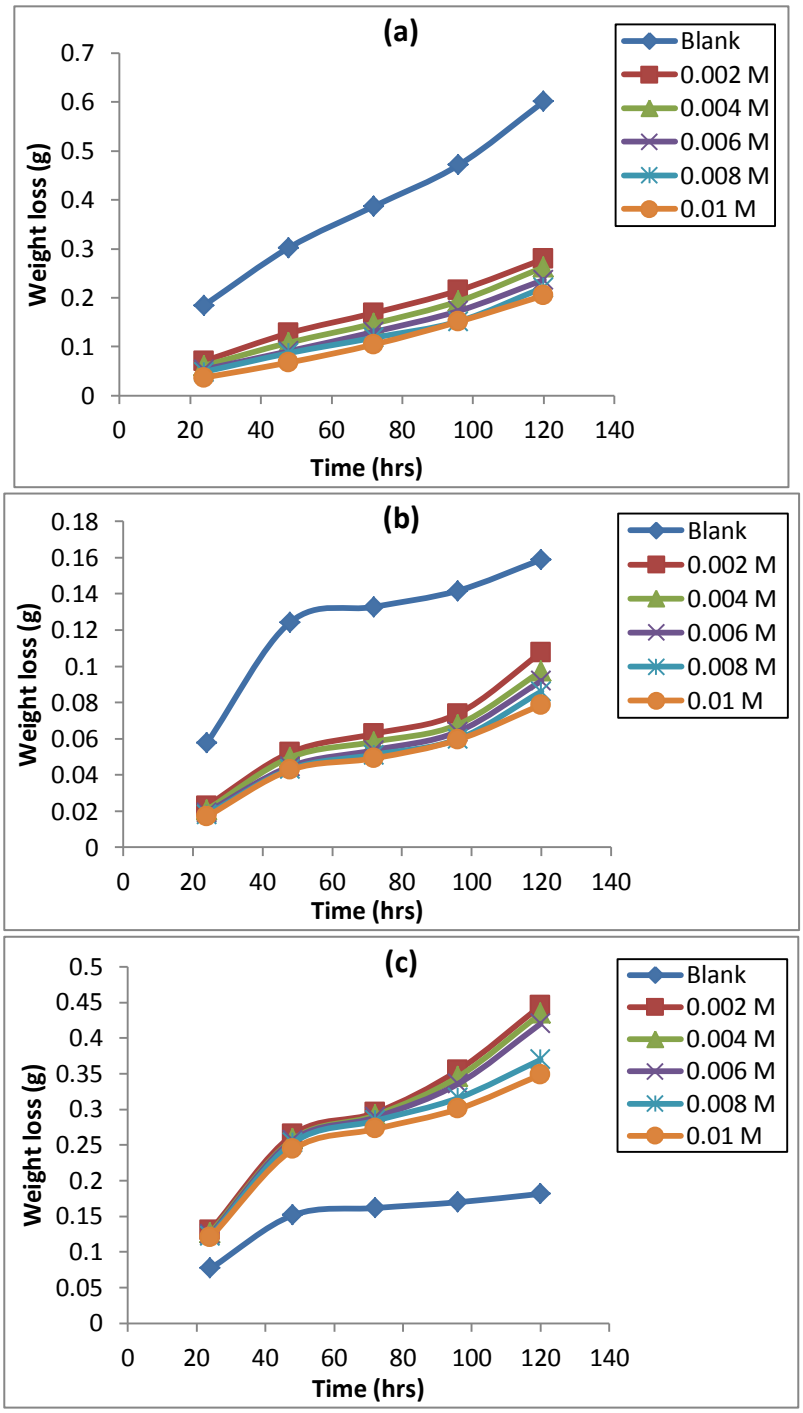


Figure 4.14. Variation of weight loss with time (hrs) for the corrosion of aluminium in 0.1 M (a). HCl (b). H_2SO_4 and (c). H_3PO_4 containing various concentrations of hypoxanthine (HYP) at 333 K.

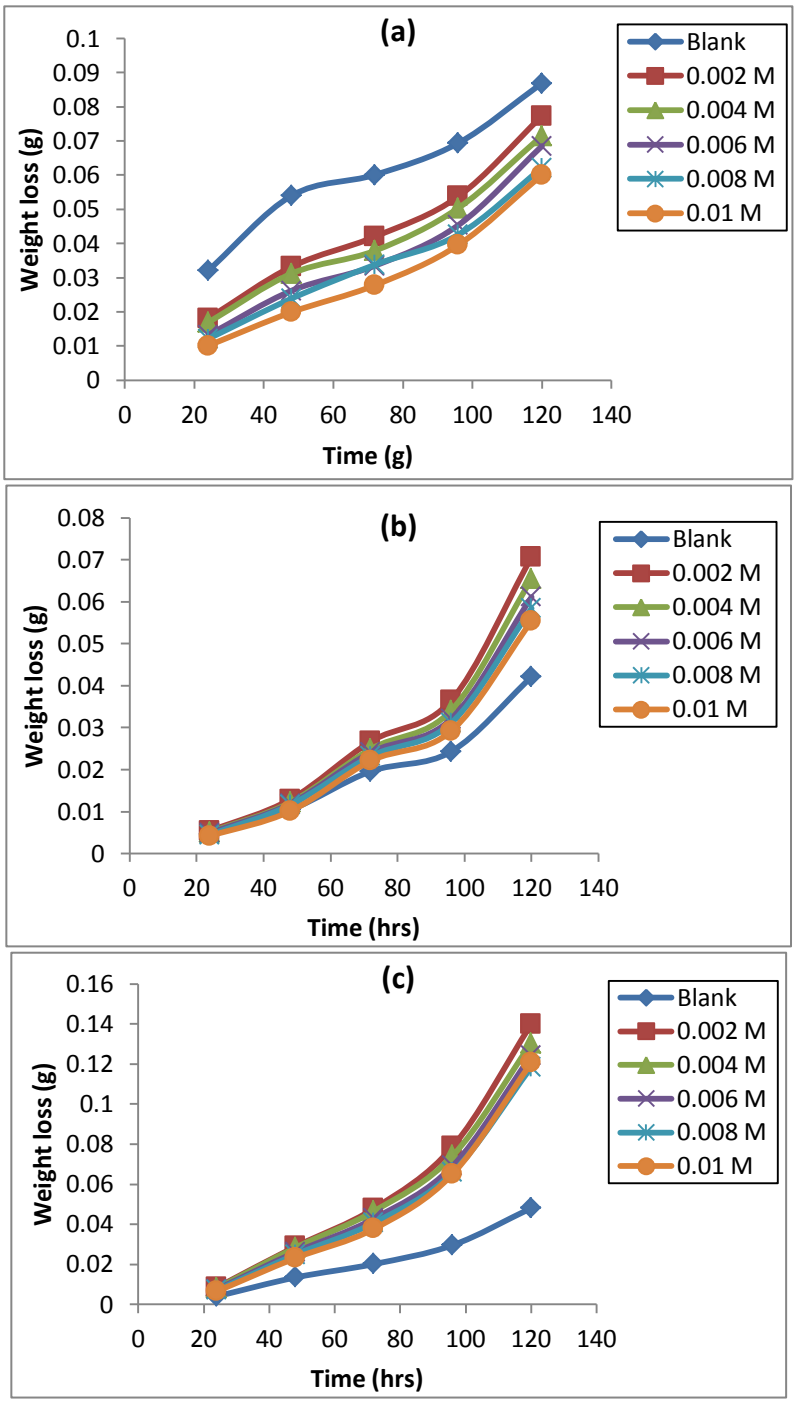


Figure 4.15. Variation of weight loss with time (hrs) for the corrosion of aluminium in 0.1 M (a). HCl (b). H_2SO_4 and (c). H_3PO_4 containing various concentrations of xanthine (XN) at 303 K.

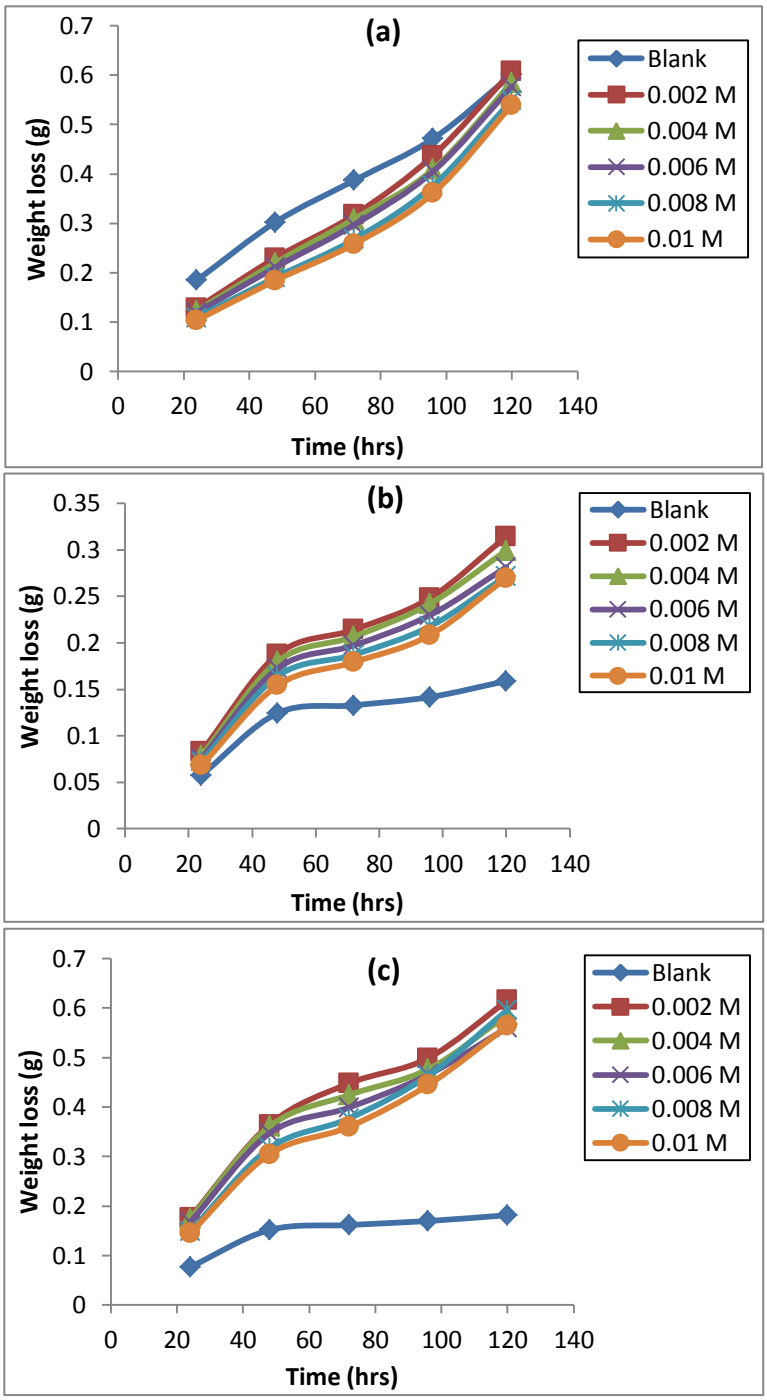


Figure 4.16: Variation of weight loss with time (hrs) for the corrosion of aluminium in 0.1 M (a). HCl (b). H_2SO_4 and (c). H_3PO_4 containing various concentrations of xanthine (XN) at 333 K.

Table 4.1: Corrosion rates of mild steel in the absence and presence of various concentrations of adenine (AD), guanine (GU), hypoxanthine (HYP) and xanthine (XN) in 0.1 M HCl, H_2SO_4 and H_3PO_4 at 303 and 333 K.

Inhibitor	Concentration (M)	Corrosion rate X 10^{-4} ($gh^{-1}cm^2$)					
		HCl		H_2SO_4		H_3PO_4	
		303 K	333 K	303 K	333 K	303 K	333 K
	Blank	1.16	6.68	1.86	6.46	2.87	8.34
AD	0.002	0.65	4.31	1.19	3.47	1.82	4.89
	0.004	0.57	3.66	1.12	3.34	1.68	4.63
	0.006	0.481	3.23	1.04	3.08	1.56	4.33
	0.008	0.41	3.16	0.97	2.94	1.42	4.05
	0.01	0.34	2.94	0.93	2.78	1.30	3.88
GU	0.002	0.93	5.85	1.14	2.89	1.56	11.18
	0.004	0.90	5.79	1.11	2.78	1.36	9.88
	0.006	0.87	5.61	1.09	2.41	1.16	8.57
	0.008	0.85	5.46	1.05	2.25	1.05	7.84
	0.01	0.83	5.36	1.02	2.01	0.91	6.88
HYP	0.002	0.67	4.63	1.04	2.98	1.88	5.56
	0.004	0.53	4.10	0.89	2.66	1.74	5.11
	0.006	0.46	3.78	0.87	2.64	1.67	4.96
	0.008	0.37	3.44	0.83	2.59	1.63	4.85
	0.01	0.34	3.29	0.79	2.46	1.57	4.74
XN	0.002	1.00	6.67	1.86	5.99	3.02	8.13
	0.004	0.95	6.63	1.78	5.78	3.00	7.86
	0.006	0.90	6.25	1.69	5.73	2.94	7.71
	0.008	0.88	6.01	1.67	5.59	2.83	7.54
	0.01	0.87	5.64	1.63	5.07	2.72	7.34

Table 4.2: Inhibition efficiencies (IE%) of various concentrations of adenine (AD), guanine (GU), hypoxanthine (HYP) and xanthine (XN) on the corrosion of mild steel in 0.1 M HCl, H_2SO_4 and H_3PO_4 at 303 and 333 K.

Inhibitor	Concentration (M)	Inhibition Efficiency (IE%)					
		HCl		H_2SO_4		H_3PO_4	
		303 K	333 K	303 K	333 K	303 K	333 K
AD	0.002	44.17	35.47	36.09	46.34	36.48	41.40
	0.004	51.34	45.26	40.11	48.28	41.35	44.47
	0.006	58.68	51.68	44.36	52.34	45.48	48.14
	0.008	65.12	52.71	47.82	54.37	50.57	51.46
	0.01	71.20	56.05	50.06	57.04	54.78	53.49
GU	0.002	19.86	12.50	38.77	55.33	45.48	49.41
	0.004	22.54	13.43	40.33	57.01	52.53	55.31
	0.006	25.76	16.05	41.56	62.78	59.49	61.23
	0.008	27.01	18.27	43.46	65.26	63.34	64.51
	0.01	28.80	19.86	45.14	68.90	68.35	68.88
HYP	0.002	42.58	30.70	44.02	53.98	34.60	33.35
	0.004	54.56	38.65	52.18	58.81	39.53	38.75
	0.006	60.29	43.42	53.52	59.23	41.71	40.52
	0.008	68.33	48.47	55.64	60.00	43.09	41.84
	0.01	70.84	50.81	57.88	61.94	45.38	43.22
XN	0.002	13.77	0.19	0.22	7.41	-5.33	2.52
	0.004	18.60	4.86	4.80	10.67	-4.67	5.80
	0.006	22.90	6.45	9.27	11.44	-2.42	7.54
	0.008	24.15	10.07	10.50	13.47	1.28	9.62
	0.01	25.76	15.65	12.74	21.56	5.34	11.94

Table 4.3: Corrosion rates of aluminium in the absence and presence of various concentrations of adenine (AD), guanine (GU), hypoxanthine (HYP) and xanthine (XN) in 0.1 M HCl, H_2SO_4 and H_3PO_4 at 303 and 333 K

Inhibitor	Concentration (M)	Corrosion rate X 10^{-4} ($gh^{-1}cm^2$)					
		HCl		H_2SO_4		H_3PO_4	
		303 K	333 K	303 K	333 K	303 K	333 K
	Blank	1.26	8.11	0.42	2.56	0.48	3.09
AD	0.002	0.35	4.20	0.78	6.00	1.36	9.97
	0.004	0.31	3.51	0.76	5.67	1.33	9.62
	0.006	0.23	3.21	0.74	5.15	1.28	9.36
	0.008	0.17	2.49	0.73	4.91	1.24	9.12
	0.01	0.12	2.23	0.72	4.64	1.21	8.90
GU	0.002	0.23	3.06	0.68	4.82	1.13	7.98
	0.004	0.18	2.74	0.66	4.51	1.08	7.71
	0.006	0.13	2.52	0.64	4.32	1.02	7.39
	0.008	0.09	2.43	0.60	4.11	0.99	7.05
	0.01	0.04	2.15	0.56	3.89	0.94	6.73
HYP	0.002	0.22	3.59	0.10	1.26	0.75	5.56
	0.004	0.17	3.22	0.09	1.16	0.75	5.41
	0.006	0.14	2.85	0.09	1.09	0.73	5.30
	0.008	0.12	2.61	0.08	1.03	0.69	5.14
	0.01	0.10	2.35	0.08	0.99	0.68	4.99
XN	0.002	0.90	6.73	0.59	4.24	1.17	8.53
	0.004	0.84	6.53	0.55	4.09	1.12	8.22
	0.006	0.74	6.41	0.52	3.89	1.05	7.89
	0.008	0.69	5.92	0.50	3.70	0.99	7.64
	0.01	0.63	5.66	0.47	3.43	0.96	7.32

Table 4.4: Inhibition efficiencies (IE%) of various concentrations of adenine (AD), guanine (GU), hypoxanthine (HYP) and xanthine (XN) on the corrosion of aluminium in 0.1 M HCl, H_2SO_4 and H_3PO_4 at 303 and 333 K.

Inhibitor	Concentration (M)	Inhibition Efficiency (IE%)					
		HCl		H_2SO_4		H_3PO_4	
		303 K	333 K	303 K	333 K	303 K	333 K
	0.002	71.73	48.27	-85.64	-133.79	-181.82	-222.81
AD	0.004	75.70	56.74	-80.69	-121.04	-176.19	-211.61
	0.006	81.49	60.41	-76.24	-100.65	-166.67	-203.04
	0.008	86.28	69.29	-73.27	-91.06	-158.01	-195.34
	0.01	90.58	72.58	-69.80	-82.12	-151.52	-188.26
GU	0.002	81.65	62.28	-60.40	-87.81	-135.50	-158.50
	0.004	85.95	66.26	-57.43	-75.79	-123.38	-149.80
	0.006	89.92	68.91	-52.48	-68.40	-112.55	-139.34
	0.008	92.89	70.06	-44.06	-60.11	-105.63	-128.27
	0.01	96.53	73.50	-33.17	-51.75	-95.67	-117.88
HYP	0.002	82.84	55.79	76.23	50.69	-56.28	-80.03
	0.004	86.54	60.36	78.21	54.91	-54.98	-75.10
	0.006	89.22	64.88	79.70	57.35	-52.81	-71.66
	0.008	90.72	67.83	80.69	59.79	-43.29	-66.53
	0.01	92.23	71.01	82.18	61.49	-41.56	-61.74
	0.002	28.76	17.12	-39.11	-65.15	-143.72	-176.25
XN	0.004	33.06	19.51	-30.69	-59.62	-132.03	-166.19
	0.006	40.99	21.00	-24.26	-51.75	-117.32	-155.53
	0.008	45.12	27.01	-18.32	-44.27	-106.49	-147.37
	0.01	50.08	30.27	-11.88	-33.71	-98.70	-137.04

4.2 Half Lives ($t_{1/2}$) of Mild Steel and Aluminium in the Test Solutions

The kinetics of corrosion of mild steel and aluminium in 0.1 M HCl, H_2SO_4 and H_3PO_4 solutions was studied at 303 and 333 K by fitting data obtained from weight loss measurements into different equations. The test revealed that the corrosion of mild steel and aluminium in solutions of HCl, H_2SO_4 and H_3PO_4 is consistent with a first order kinetics presented in an earlier report (James *et al.*, 2006),

——— 4.1

where ΔW = weight loss after time (t) = $(W_0 - W_t)$. W_0 Initial weight of the metal, W_t = weight of metal left after time(t) and k_1 = is the first order reaction rate constant. Re-arrangement of equation 4.2 and its integration yields equation 4.3,

—— 4.2

4.3

where C = constant of integration. At time (t) = 0, $\Delta W = W_0$ = initial/original weight of metal.

4.4

—— 4.5

Half lives values of mild steel and aluminium deduced from the plots at 303 and 333 K are presented on Tables 4.5-4.8 respectively.

Table 4.5: Kinetic parameters of the corrosion of mild steel at 303 K in the absence and presence of various concentrations of adenine (AD), guanine (GU), hypoxanthine (HYP) and xanthine (XN) in 0.1 M HCl, H_2SO_4 and H_3PO_4.

Inhibitor	Concentration (M)	HCl		H_2SO_4		H_3PO_4	
		R^2	$t_{1/2}$	R^2	$t_{1/2}$	R^2	$t_{1/2}$
	Blank	0.909	47	0.979	42	0.925	38
AD	0.002	0.933	85	0.982	64	0.995	65
	0.004	0.981	89	0.926	68	0.993	76
	0.006	0.934	98	0.941	72	0.987	81
	0.008	0.902	121	0.987	78	0.962	81
	0.01	0.972	125	0.988	80	0.982	83
GU	0.002	0.938	47	0.989	51	0.990	91
	0.004	0.954	50	0.987	55	0.997	98
	0.006	0.951	57	0.993	57	0.994	98
	0.008	0.948	61	0.996	63	0.964	99
	0.01	0.954	69	0.986	69	0.987	125
HYP	0.002	0.948	82	0.979	63	0.986	65
	0.004	0.891	82	0.992	67	0.990	73
	0.006	0.842	95	0.986	67	0.977	73
	0.008	0.758	112	0.983	89	0.973	77
	0.01	0.943	119	0.994	92	0.968	77
XN	0.002	0.941	41	0.985	30	0.995	37
	0.004	0.933	45	0.991	30	0.993	37
	0.006	0.956	47	0.992	33	0.987	38
	0.008	0.951	47	0.985	41	0.962	38
	0.01	0.948	53	0.984	47	0.982	41

Table 4.6: Kinetic parameters of the corrosion of aluminium at 303 K in the absence and presence of various concentrations of adenine (AD), guanine (GU), hypoxanthine (HYP) and xanthine (XN) in 0.1 M HCl, H_2SO_4 and H_3PO_4.

Inhibitor	Concentration (M)	HCl		H_2SO_4		H_3PO_4	
		R^2	$t_{1/2}$	R^2	$t_{1/2}$	R^2	$t_{1/2}$
	Blank	0.911	26	0.963	48	0.933	32
AD	0.002	0.935	189	0.972	30	0.941	17
	0.004	0.927	189	0.966	10	0.944	18
	0.006	0.916	191	0.968	11	0.943	18
	0.008	0.941	191	0.969	12	0.938	19
	0.01	0.975	193	0.967	12	0.940	19
GU	0.002	0.952	198	0.963	12	0.946	19
	0.004	0.961	210	0.969	14	0.940	20
	0.006	0.981	211	0.967	14	0.943	21
	0.008	0.947	211	0.972	16	0.946	21
	0.01	0.989	231	0.970	16	0.954	21
HYP	0.002	0.933	198	0.968	159	0.941	21
	0.004	0.900	198	0.976	161	0.939	21
	0.006	0.942	202	0.969	163	0.940	21
	0.008	0.910	202	0.987	175	0.938	22
	0.01	0.920	229	0.968	177	0.939	22
XN	0.002	0.965	65	0.977	12	0.958	18
	0.004	0.965	65	0.976	14	0.950	18
	0.006	0.967	71	0.972	14	0.955	19
	0.008	0.960	71	0.968	18	0.953	19
	0.01	0.980	77	0.972	19	0.961	19

Table 4.7: Kinetic parameters of the corrosion of mild steel at 333 K in the absence and presence of various concentrations of adenine (AD), guanine (GU), hypoxanthine (HYP) and xanthine (XN) in 0.1 M HCl, H_2SO_4 and H_3PO_4.

Inhibitor	Concentration (M)	HCl		H_2SO_4		H_3PO_4	
		R^2	$t_{1/2}$	R^2	$t_{1/2}$	R^2	$t_{1/2}$
	Blank	0.988	18	0.977	24	0.842	17
AD	0.002	0.954	58	0.966	48	0.874	29
	0.004	0.915	58	0.986	51	0.866	33
	0.006	0.850	63	0.861	53	0.803	36
	0.008	0.879	67	0.827	60	0.765	39
	0.01	0.941	68	0.986	60	0.929	39
GU	0.002	0.960	20	0.997	54	0.995	38
	0.004	0.975	20	0.999	56	0.998	40
	0.006	0.984	20	0.998	61	0.975	41
	0.008	0.975	21	0.977	61	0.970	43
	0.01	0.996	21	0.991	63	0.952	44
HYP	0.002	0.994	56	0.773	54	0.877	29
	0.004	0.994	57	0.719	58	0.953	33
	0.006	0.970	57	0.681	60	0.953	33
	0.008	0.982	59	0.682	60	0.981	35
	0.01	0.993	63	0.687	61	0.984	37
XN	0.002	0.763	19	0.992	28	0.989	25
	0.004	0.802	19	0.985	28	0.986	25
	0.006	0.745	20	0.991	30	0.976	28
	0.008	0.744	20	0.978	34	0.979	28
	0.01	0.797	21	0.976	34	0.983	31

Table 4.8: Kinetic parameters of the corrosion of aluminium at 333 K in the absence and presence of various concentrations of adenine (AD), guanine (GU), hypoxanthine (HYP) and xanthine (XN) in 0.1 M HCl, H_2SO_4 and H_3PO_4.

Inhibitor	Concentration (M)	HCl		H_2SO_4		H_3PO_4	
		R^2	$t_{1/2}$	R^2	$t_{1/2}$	R^2	$t_{1/2}$
	Blank	0.962	15	0.715	31	0.684	28
AD	0.002	0.965	29	0.826	18	0.743	11
	0.004	0.979	35	0.816	18	0.761	11
	0.006	0.976	35	0.811	18	0.742	11
	0.008	0.951	41	0.825	21	0.866	12
	0.01	0.974	43	0.819	25	0.872	13
GU	0.002	0.951	49	0.872	21	0.878	14
	0.004	0.963	49	0.874	21	0.875	14
	0.006	0.981	51	0.889	23	0.860	16
	0.008	0.978	55	0.875	23	0.863	17
	0.01	0.979	58	0.845	25	0.850	17
HYP	0.002	0.958	49	0.896	25	0.878	15
	0.004	0.974	54	0.875	51	0.875	15
	0.006	0.988	54	0.896	54	0.860	16
	0.008	0.976	57	0.879	54	0.805	17
	0.01	0.981	58	0.856	57	0.799	17
XN	0.002	0.981	38	0.845	21	0.859	12
	0.004	0.979	41	0.841	22	0.850	12
	0.006	0.984	41	0.834	22	0.854	12
	0.008	0.989	44	0.840	23	0.899	12
	0.01	0.988	48	0.859	25	0.898	14

4.3 Electrochemical Tests at 303 K

The features of mild steel and aluminium dissolutions in HCl, H_2SO_4 and H_3PO_4 and in the presence of the purines were also confirmed by electrochemical studies at 303 K.

Figures 4.17 and 4.18 depict the characteristic impedance responses at the metal/acid interfaces for the corrosion of mild steel and aluminium in the absence and in the presence of 0.01 M inhibitors in 0.1 M HCl, H_2SO_4 and H_3PO_4 solutions. The impedance spectra for the Nyquist plots of mild steel and aluminium in the different acid solutions in the absence and presence of the purines were appropriately analyzed by fitting to the equivalent circuit model $R_s(C_{dl}R_{ct})$, which has been previously used to model the metal/acid interface (Zucchi and Omar, 1985; Mu and Li, 2005). The corresponding electrochemical parameters are shown on Tables 4.9 and 4.10.

Typical potentiodynamic polarization (anodic and cathodic) curves for the corrosion of mild steel and aluminium in 0.1 M solutions of HCl, H_2SO_4 and H_3PO_4 in the absence and presence of 0.01 M of AD, GU, HYP and XN are shown in Figures 4.19 and 4.20. Electrochemical parameters derived from the polarization curves are summarized on Tables 4.11 and 4.12.

The IE % values obtained from electrochemical measurements (Tables 4.9- 4.12), follow the same trend as the gravimetric data indicating the corrosion inhibiting efficacy of the purines.

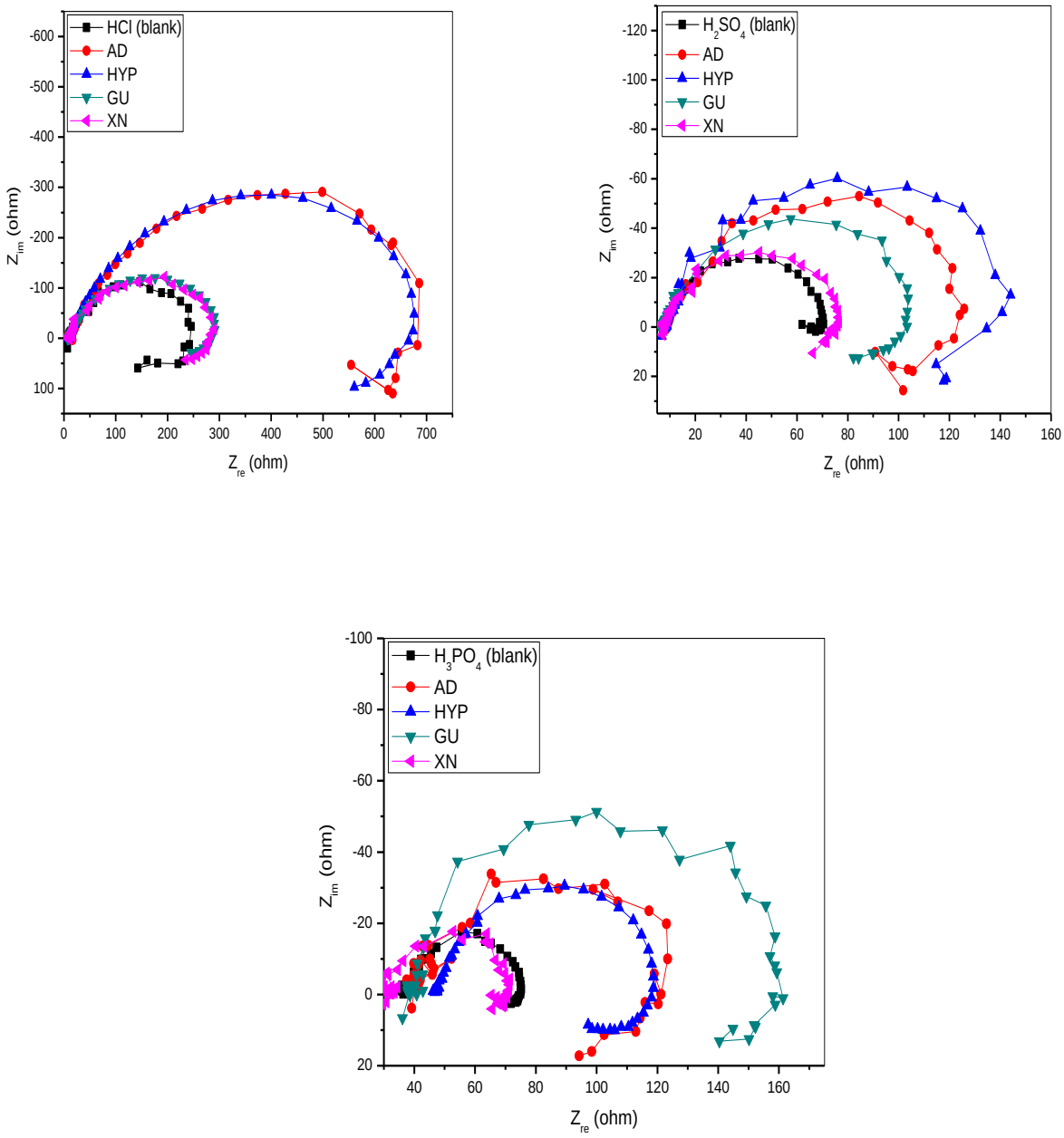


Figure 4.17. Impedance spectra of the corrosion of mild steel in 0.1 M HCl, H_2SO_4 and H_3PO_4 in the absence and presence of 0.01 M adenine (AD), guanine (GU), hypoxanthine (HYP) and xanthine (XN) at 303 K.

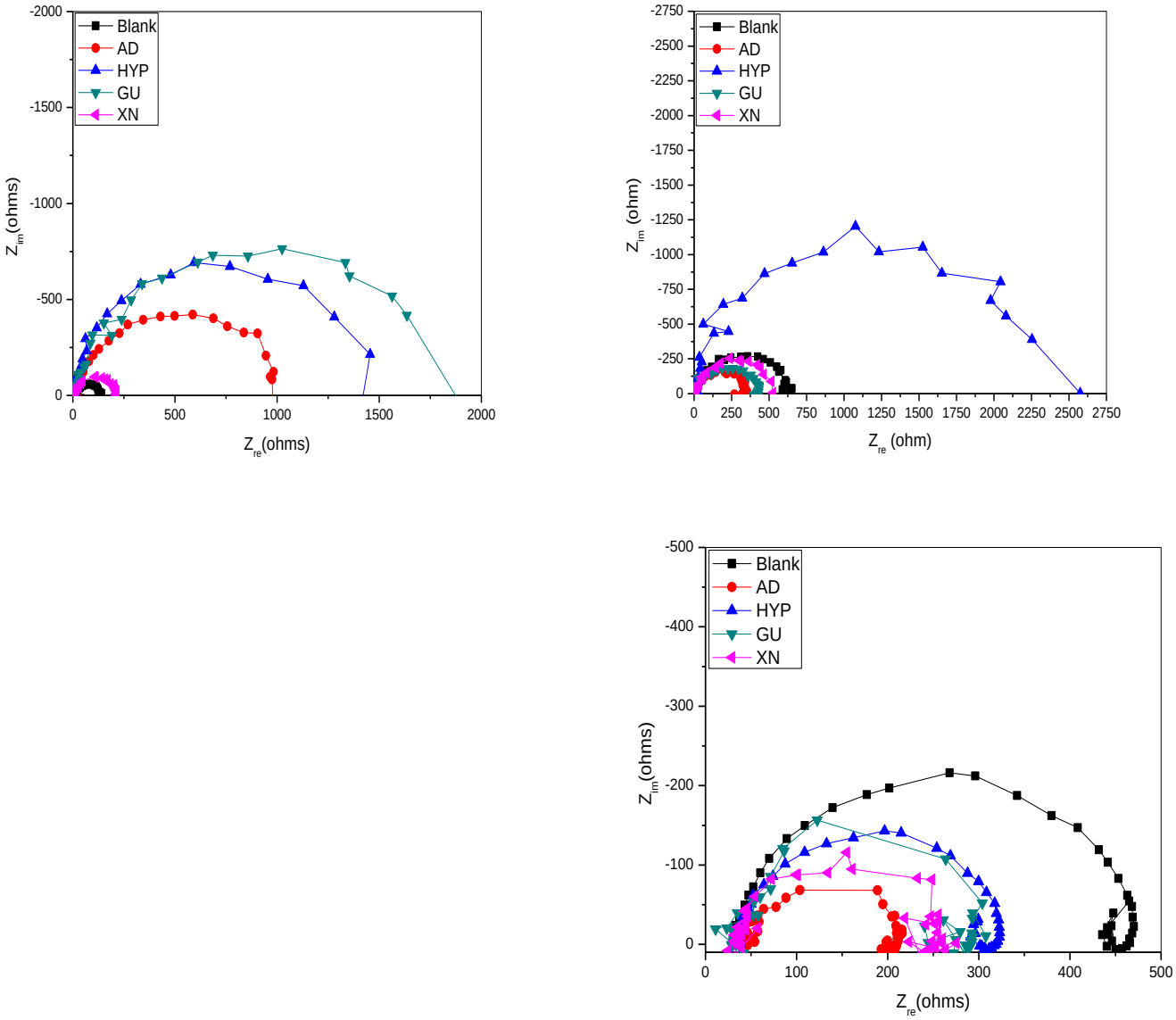


Figure 4.18. Impedance spectra of the corrosion of aluminium in 0.1 M HCl, H_2SO_4 and H_3PO_4 in the absence and presence of 0.01 M adenine (AD), guanine (GU), hypoxanthine (HYP) and xanthine (XN) at 303 K.

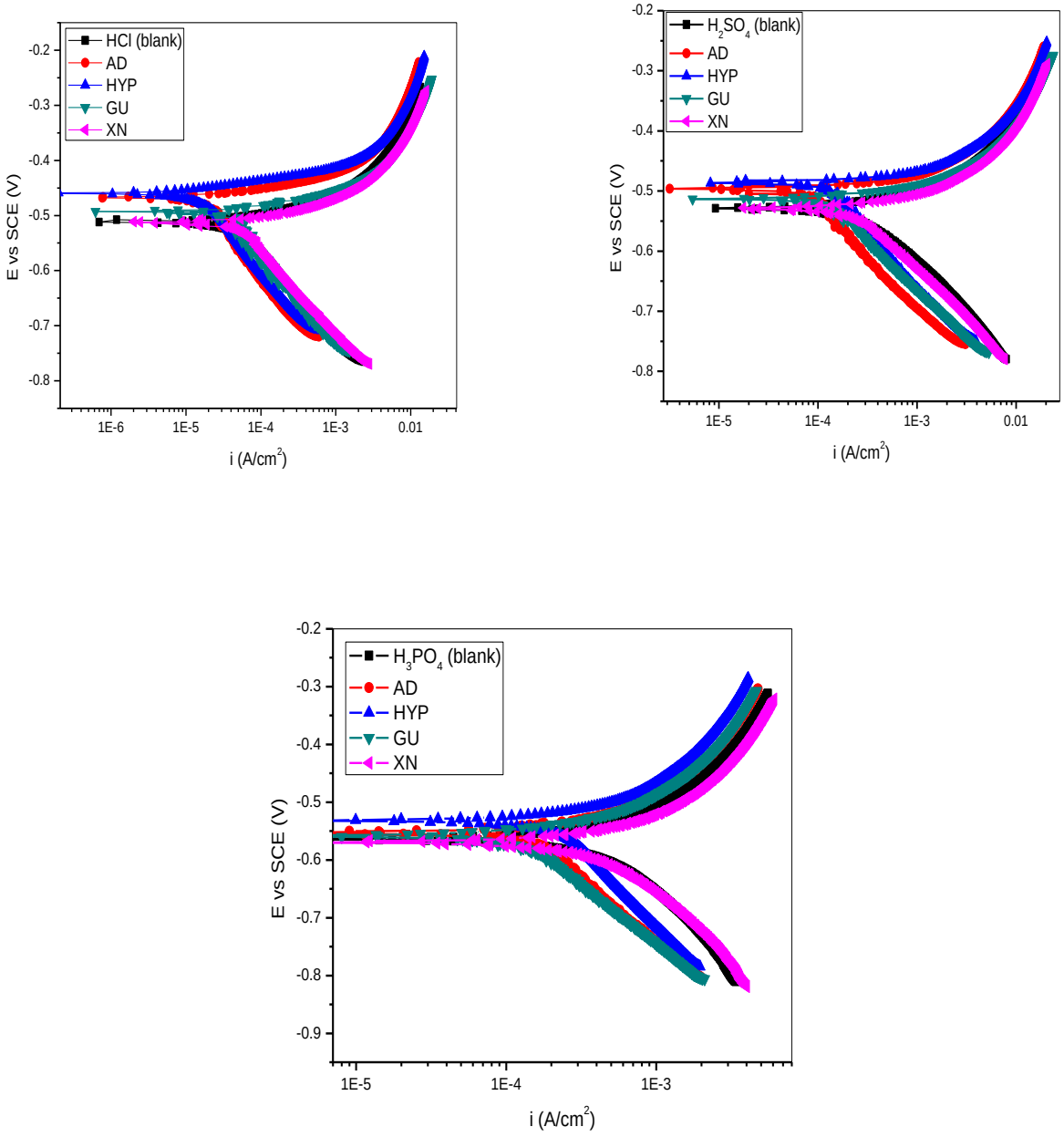


Figure 4.19. Polarisation curves of the corrosion of mild steel in 0.1 M HCl, H_2SO_4 and H_3PO_4 in the absence and presence of 0.01 M adenine (AD), guanine (GU), hypoxanthine (HYP) and xanthine (XN) at 303 K.

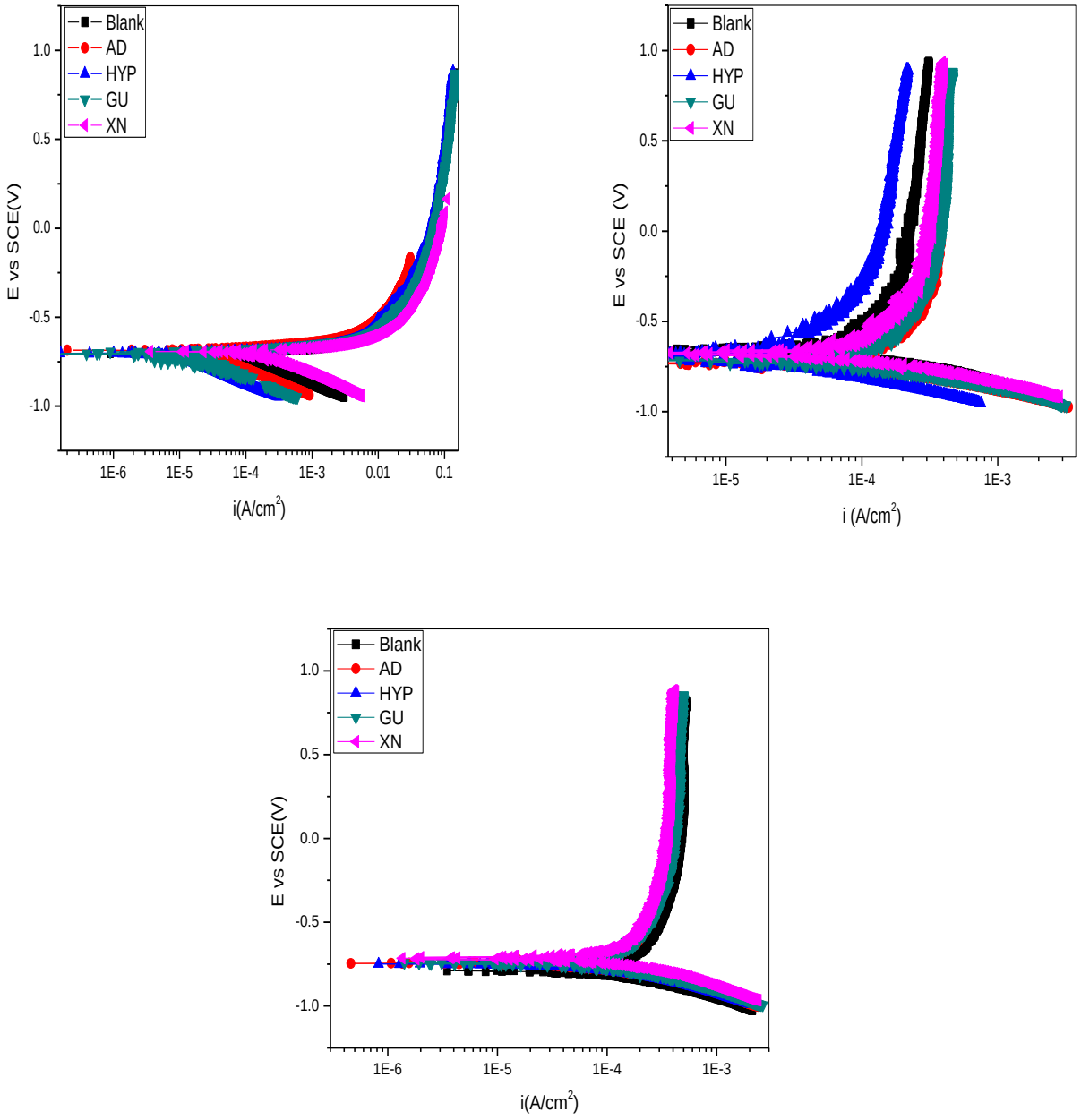


Figure 4.20. Polarisation curves of the corrosion of aluminium in 0.1 M solution of HCl, H_2SO_4 and H_3PO_4 in the absence and presence of 0.01 M adenine (AD), guanine (GU), hypoxanthine (HYP) and xanthine (XN) at 303 K.

Table 4.9: Impedance data for the corrosion of mild steel in 0.1 M HCl, H_2SO_4 and H_3PO_4 in the absence and presence of 0.01 M adenine (AD), guanine (GU), hypoxanthine (HYP) and xanthine (XN) at 303 K.

System	R_{ct} (Ω cm^2)	C_{dl} ($\mu\Omega^{-1}S^n cm^{-2}$)	N	IE%
HCl (Blank)	231.4	3.50	0.87	
AD	698.67	0.39	0.82	66.88
GU	292.5	1.25	0.87	20.88
HYP	689.8	0.39	0.82	66.45
XN	283	1.51	0.92	18.23
H_2SO_4 (Blank)	62.56	5.90	0.88	
AD	115.4	2.70	0.84	45.79
GU	96.36	2.50	0.86	35.08
HYP	137	2.00	0.85	54.33
XN	69.45	4.70	0.85	9.92
H_3PO_4	37.28	23.80	0.89	
AD	76.70	7.30	0.82	48.60
GU	119.4	7.31	0.87	68.78
HYP	65.13	9.80	0.94	42.76
XN	38.42	19.31	0.92	2.97

Table 4.10: Impedance data for the corrosion of aluminium in 0.1 M HCl, H_2SO_4 and H_3PO_4 in the absence and presence of 0.01 M adenine (AD), guanine (GU), hypoxanthine (HYP) and xanthine (XN) at 303 K.

System	R_{ct} (Ω cm^2)	C_{dl}($\mu\Omega^{-1}S^n cm^{-2}$)	N	IE%
HCl (Blank)	101	21.89	0.99	
AD	907	3.72	0.92	88.87
GU	1756.52	2.51	0.91	94.25
HYP	1175.80	2.68	0.98	91.41
XN	187.6	7.51	0.96	46.16
H_2SO_4 (Blank)	591.7	14.90	0.96	
AD	337.2	9.70	0.94	-75.47
GU	423	5.50	0.92	-39.88
HYP	2301	3.00	0.93	74.29
XN	505.50	4.88	0.98	-17.05
H_3PO_4	432.1	21.22	0.95	
AD	163.7	8.11	0.94	-163.95
GU	230.1	6.90	0.92	-87.79
HYP	280.2	5.41	0.96	-54.21
XN	211.4	7.33	0.98	-104.40

Table 4.11: Polarization data for the corrosion of mild steel in 0.1 M HCl, H_2SO_4 and H_3PO_4 in the absence and presence of 0.01 M adenine (AD), guanine (GU), hypoxanthine (HYP) and xanthine (XN) 303 K.

System	E_{corr} (mV vs SCE)	i_{corr} (μA cm^{-2})	IE%
HCl (Blank)	-512.13	173.1	
AD	-468.23	52.10	69.90
GU	-493.58	129.82	25.0
HYP	-459.78	57.59	66.73
XN	-529.74	141.54	18.23
H_2SO_4 (Blank)	-528.64	212.35	
AD	-499.10	114.39	46.13
GU	-492.30	132.17	37.76
HYP	-482.4	97.45	54.11
XN	-529.74	195.7	7.84
H_3PO_4 (Blank)	-568.31	229.27	
AD	-550	124.38	45.75
GU	-560.1	73.80	67.81
HYP	-528.38	134.53	41.32
XN	-568.57	222.12	3.12

Table 4.12: Polarisation data for the corrosion of aluminium in 0.1 M HCl, H_2SO_4 and H_3PO_4 in the absence and presence of 0.01 M adenine (AD), guanine (GU), hypoxanthine (HYP) and xanthine (XN) at 303 K.

System	E_{corr} (mV vs SCE)	i_{corr} (μA cm^{-2})	IE%
HCl (Blank)	-703	265.12	
AD	-685.93	29.56	88.85
GU	-707.72	14.93	94.37
HYP	-703.05	23.28	91.22
XN	-702.16	145.74	45.03
H_2SO_4 (Blank)	-661.12	109.13	
AD	-747.48	191.96	-75.61
GU	-716.50	152.92	-40.13
HYP	-703.11	27.42	74.87
XN	-679.02	127.79	-17.10
H_3PO_4 (Blank)	-837.33	157.35	
AD	-750.15	182.70	-161.09
GU	-745.58	295.93	-88.07
HYP	-739.16	243.98	-55.06
XN	-716.43	173.45	-102.33

4.4 Synergistic Considerations

The influence of 0.005 M KI on the corrosion of mild steel and aluminium in 0.1 M HCl, H_2SO_4 and H_3PO_4 containing 0.01 M AD, GU, HYP and XN, corresponding to [KI]/[INH] ratio of 1.2, is depicted on Tables 4.13 and 4.14 by weight loss, polarization and impedance measurements.

The inhibition efficiencies obtained from the different techniques are again, closely similar.

4.5 Infrared Spectroscopy Analysis

The FTIR spectra of AD, GU, HYP and XN powder as well as scrapings from the inhibitor films on the surface of mild steel specimens immersed for 2 days in 0.1 M HCl, H_2SO_4 and H_3PO_4 containing 0.1 M AD, GU, HYP and XN are presented in Figures 4.21-4.28. The Appendices XVI – XXVII present the various peaks intensities and the corresponding functional groups responsible.

4.6 Scanning Electron Microscopy

The surface morphologies of mild steel and aluminium in solutions of HCl were studied using scanning electron microscopy. Figures 4.29-4.30 show the micrographs of the corroded mild steel and aluminium at x5000 magnification in the absence and presence of adenine (AD), guanine (GU) and hypoxanthine (HYP) respectively.

4.7 Quantum Chemical Calculations

Quantum chemical calculations were performed in order to gain insights at the molecular level, electron distribution of the different purine molecules as well as to understudy the nature of their interactions with the metal surfaces. The first consideration was to assess the electronic structures of the molecules, including the distribution of frontier molecular orbitals and Fukui indices, with a view to establish the

active sites as well as local reactivity of the molecules. The simulations were performed by means of the density functional theory (DFT) electronic structure program DMol^3 available in Material Studio 4.0 (Accelrys Inc., San Diego, CA, USA) (Delley, 1990, 2000; Xia et al., 2008; Khaled, 2010a, 2010b). Electronic structures parameters for the simulation include restricted spin polarization using the DND basis set and the Perdew-Wang local-correlation density functional. The molecular structures were initially subjected to geometry optimization using the COMPASS force field.

Figures 4.31 – 4.34 illustrate the total electron density, the highest occupied molecular orbital (HOMO), lowest unoccupied molecular orbital (LUMO), as well as the optimised structures of adenine (AD), guanine (GU), hypoxanthine (HYP) and xanthine (XN) respectively. The corresponding quantum chemical parameters are presented on Tables 4.15 and 4.16.

4.8 Molecular Dynamics

Figure 4.35 shows representative snapshots of the crosssection of the lowest energy adsorption configurations for the single molecules on the Fe (110) surface while Figure 4.36 shows the representative snapshots for the single molecules on the Al (110) surface. A detailed analysis of the on-top view of the adsorbed molecules on Fe (110) and Al (110), are presented in Figures 4.37 and 4.38 respectively.

The binding energy (E_{bind}) between the metal surface and the inhibitor molecules was calculated using equation 4.35 (Casewit *et al.,* 1992a and 1992b);

where E_{mol}, E_{metal} and E_{total} correspond to the total energies of the molecule, metal (110) slab and the adsorbed molecule/metal (110) couple respectively. (metal = Fe/Al).

The obtained values are given on Tables 4.17 and 4.18.

Table 4.13: The effect of 0.005 M potassium iodide (KI) on inhibition efficiency for mild steel corrosion in 0.1 M HCl, H_2SO_4 and H_3PO_4 in the absence and presence of 0.01 M adenine (AD), guanine (GU), hypoxanthine (HYP) and xanthine (XN) at 303 K using weight loss, impedance and polarization techniques.

SYSTEM	INHIBITION EFFICIENCY (IE%)		
	WEIGHT LOSS	POLARISATION	IMPEDANCE
HCl			
KI	81.36	75.41	77.15
AD	71.20	69.90	66.88
AD + KI	80.40	79.50	79.20
GU	28.80	25.00	20.88
GU + KI	90.52	90.11	88.89
HYP	70.84	66.73	66.45
HYP + KI	79.25	80.21	77.18
XN	25.76	18.23	18.23
XN + KI	91.41	86.11	87.78
H_2SO_4			
KI	92.84	94.63	95.87
AD	50.06	46.13	45.79
AD + KI	87.50	88.68	88.35
GU	45.14	37.76	35.08
GU + KI	90.52	93.81	94.34
HYP	57.88	54.11	54.33
HYP + KI	92.79	94.52	94.25
XN	12.74	7.84	9.92
XN + KI	90.17	93.31	92.11
H_3PO_4			
KI	60.38	63.50	63.52
AD	54.78	45.75	48.60
AD + KI	57.32	56.70	56.27
GU	68.35	67.81	68.78
GU + KI	78.01	74.05	74.64
HYP	45.38	41.32	42.76
HYP + KI	50.13	48.21	46.46
XN	5.34	3.12	2.97
XN + KI	89.76	84.25	84.08

Table 4.14: The effect of 0.005 M potassium iodide (KI) on inhibition efficiency for aluminium corrosion in 0.1 M HCl, H_2SO_4 and H_3PO_4 in the absence and presence of 0.01 M adenine (AD), guanine (GU), hypoxanthine (HYP) and xanthine (XN) at 303 K using weight loss, impedance and polarization techniques.

SYSTEM	INHIBITION EFFICIENCY (IE%)		
	WEIGHT LOSS	POLARISATION	IMPEDANCE
HCl			
KI	93.55	92.78	92.14
AD	90.58	88.85	88.87
AD + KI	92.73	90.13	90.69
GU	96.53	94.37	94.25
GU + KI	93.06	92.04	91.98
HYP	92.23	91.22	91.41
HYP + KI	96.53	94.77	94.96
XN	50.08	45.03	46.16
XN + KI	89.15	88.61	88.10
H_2SO_4			
KI	1.05	-0.38	-0.30
AD	-69.80	-75.61	-75.47
AD + KI	45	43.51	43.00
GU	-33.17	-40.13	-39.88
GU + KI	58	53.21	53.45
HYP	82.18	74.87	74.29
HYP + KI	37	30.54	30.43
XN	-11.88	-17.10	-17.05
XN + KI	72	76.11	76.15

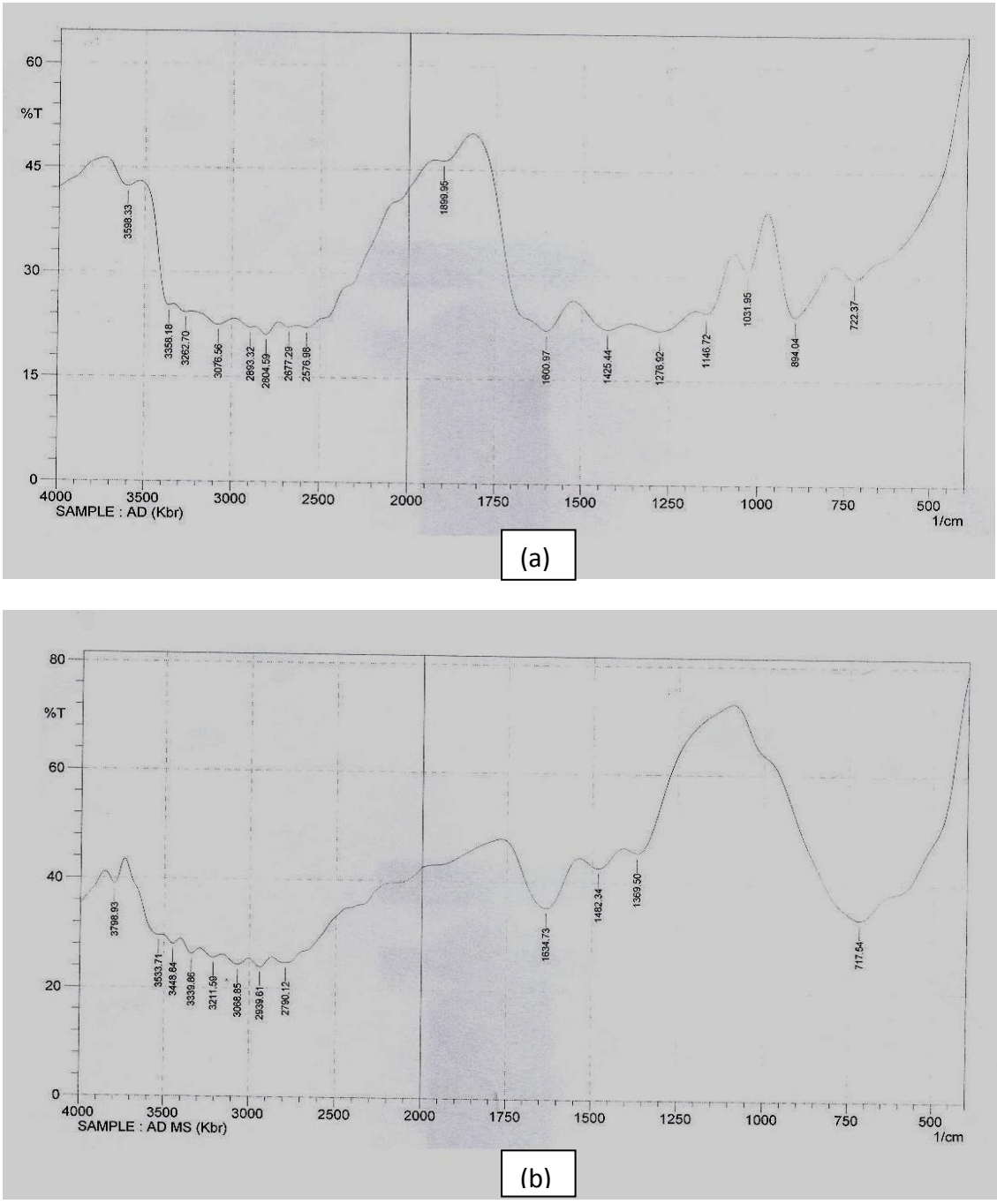
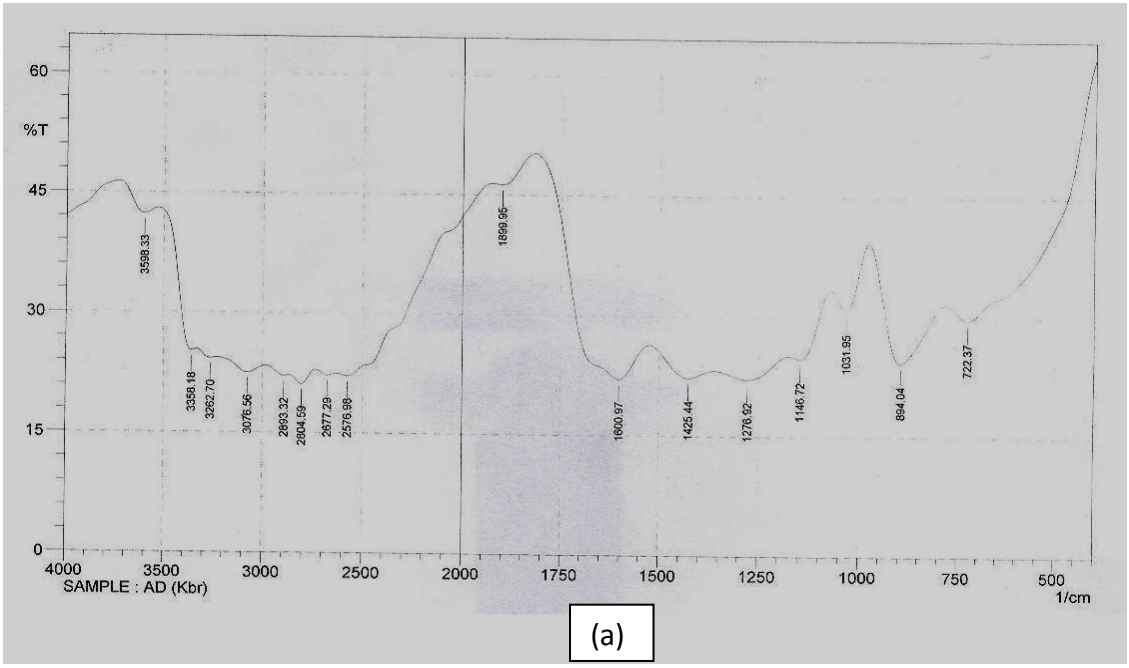
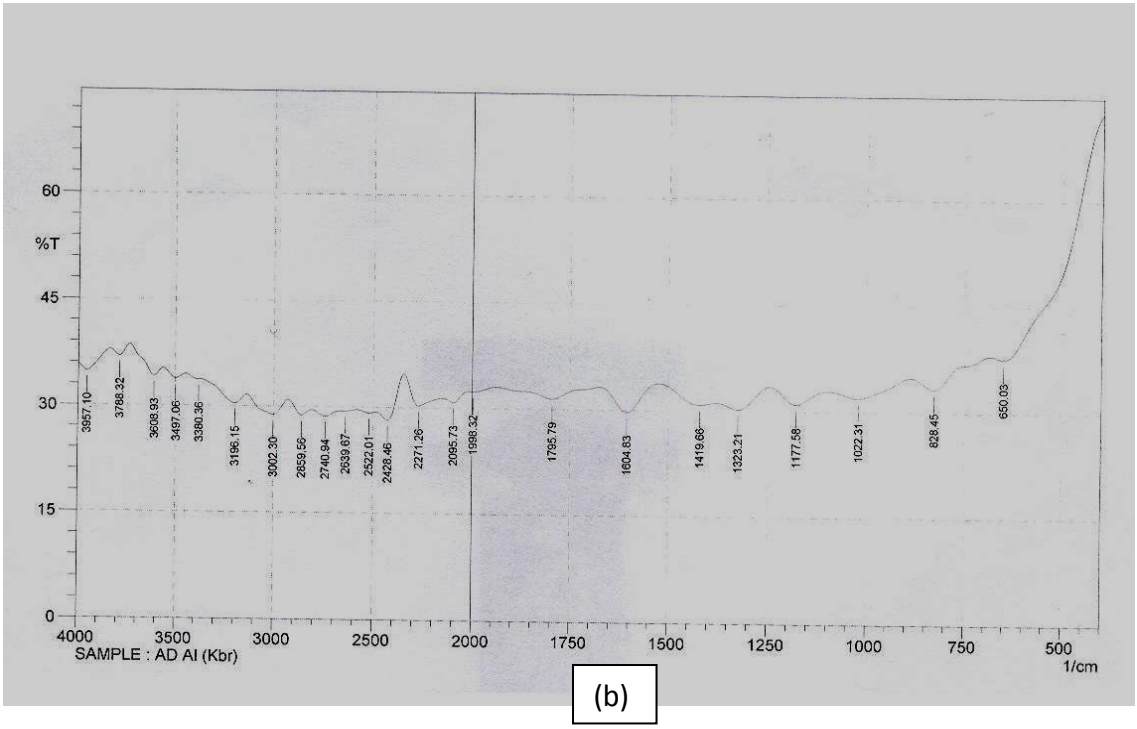


Figure 4.21. FTIR spectra of (a). adenine (AD) powder alone and (b). corrosion product of mild steel obtained in the presence of adenine (AD) in 0.1 M HCl solution.



(a)



(b)

Figure 4.22. FTIR spectra of (a). adenine (AD) powder alone and (b). corrosion product of aluminium obtained in the presence of adenine (AD) in 0.1 M HCl solution.

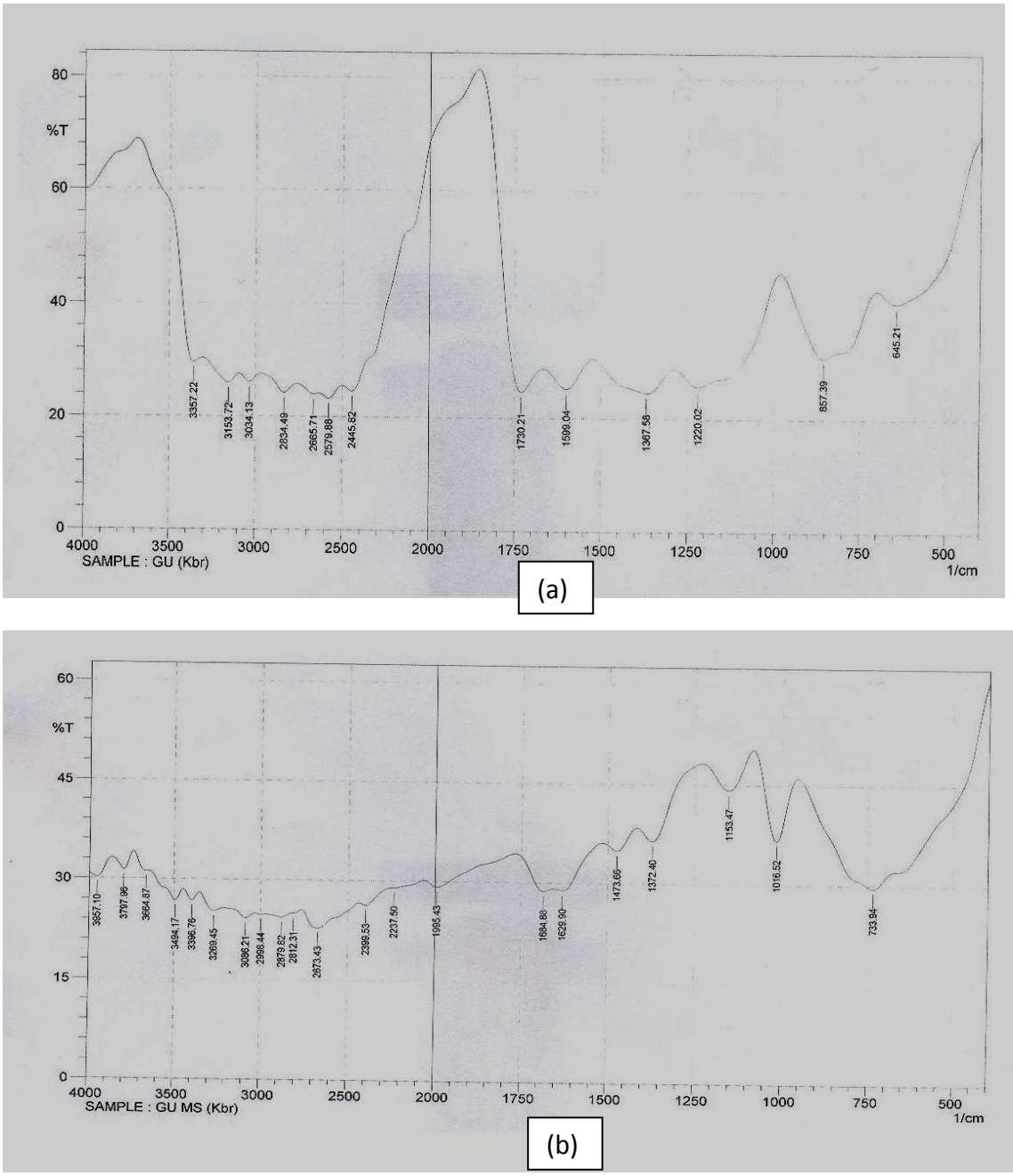


Figure 4.23. FTIR spectra of (a). guanine (GU) powder alone and (b). corrosion product of mild steel obtained in the presence of guanine (GU) in 0.1 M HCl solution.

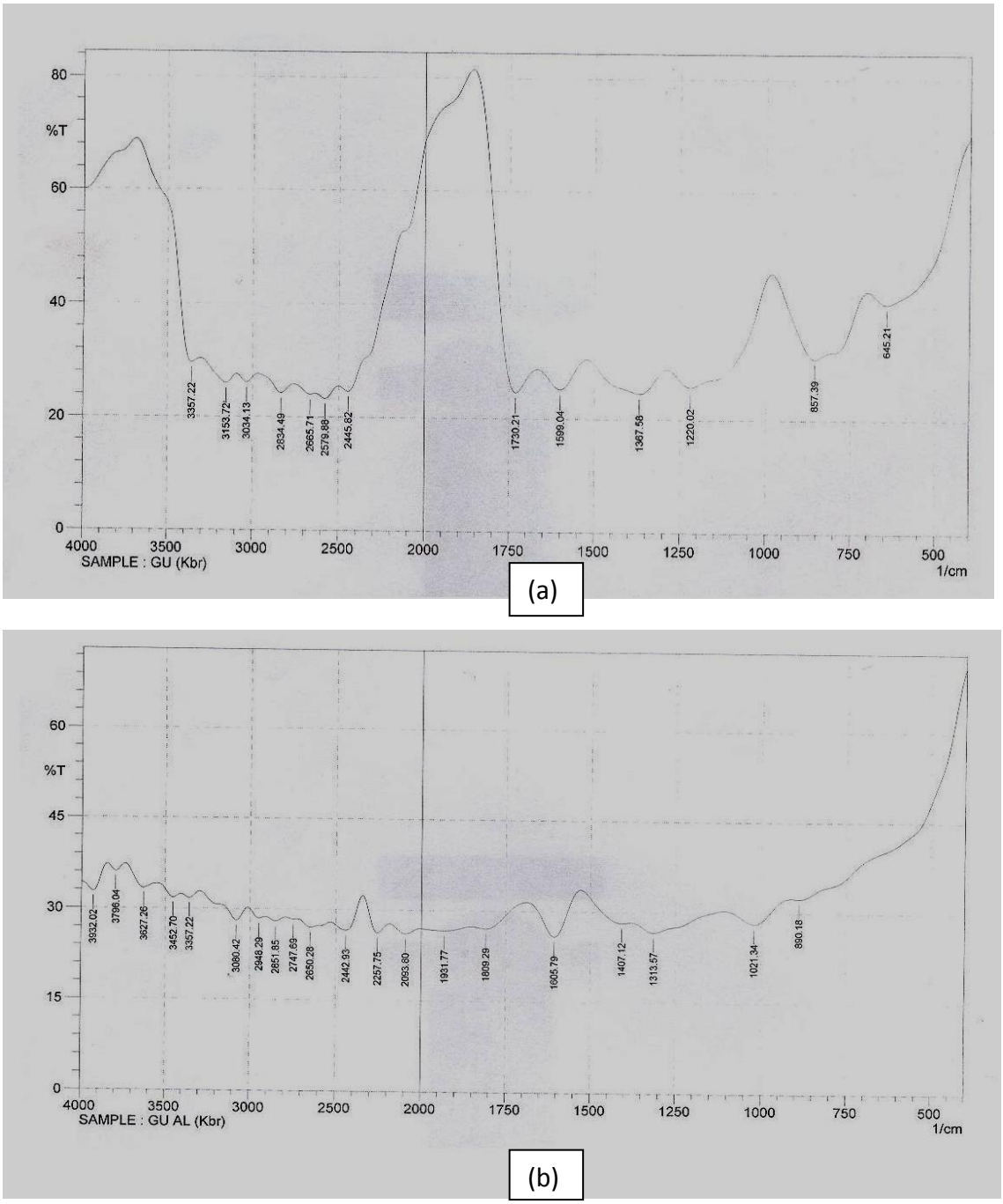


Figure 4.24. FTIR spectra of (a). guanine (GU) powder alone and (b). corrosion product of aluminium obtained in the presence of guanine (GU) in 0.1 M HCl.

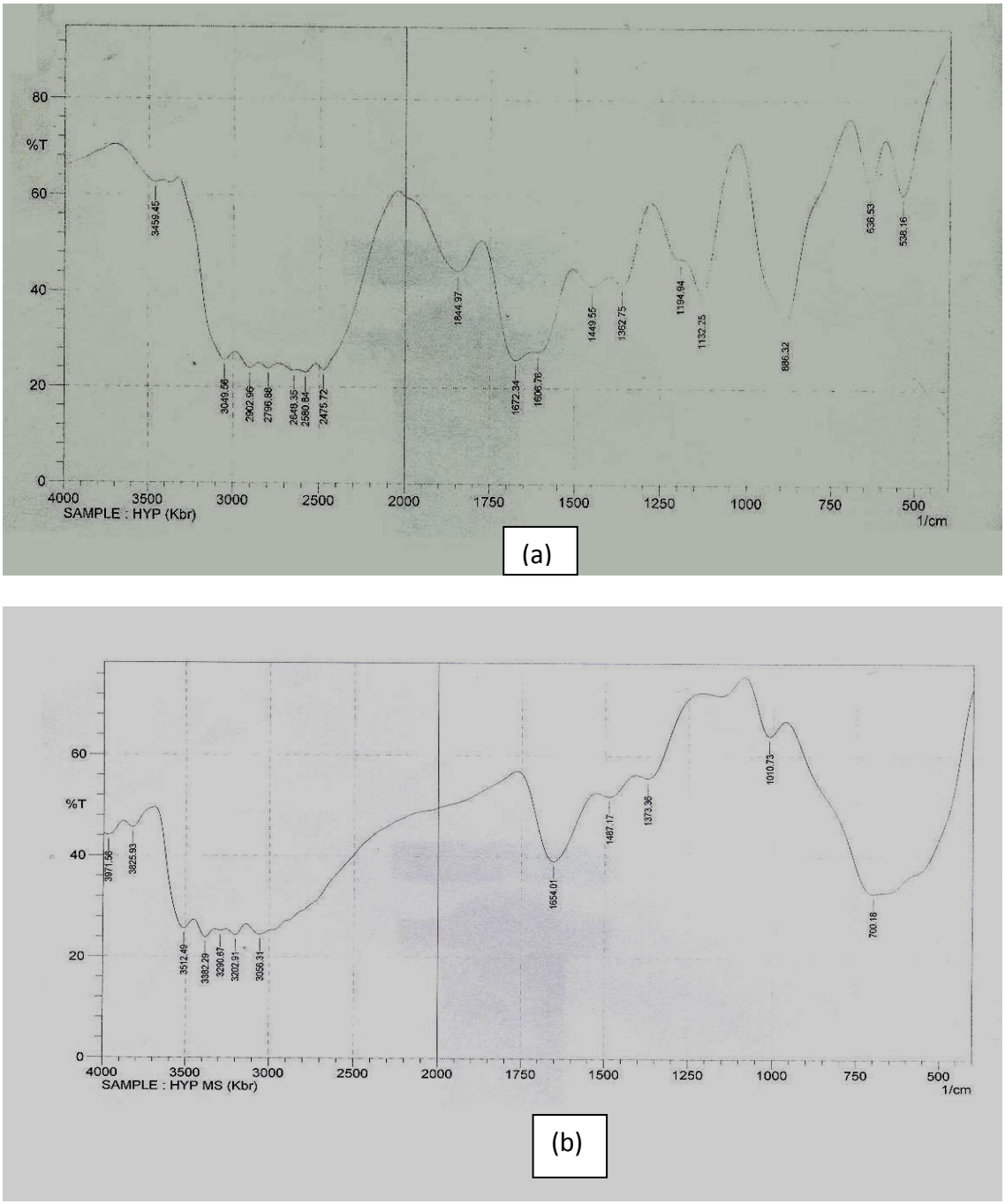


Figure 4.25. FTIR spectra of (a). hypoxanthine (HYP) powder alone and (b). corrosion product of mild steel obtained in the presence of hypoxanthine (HYP) in 0.1 M HCl solution.

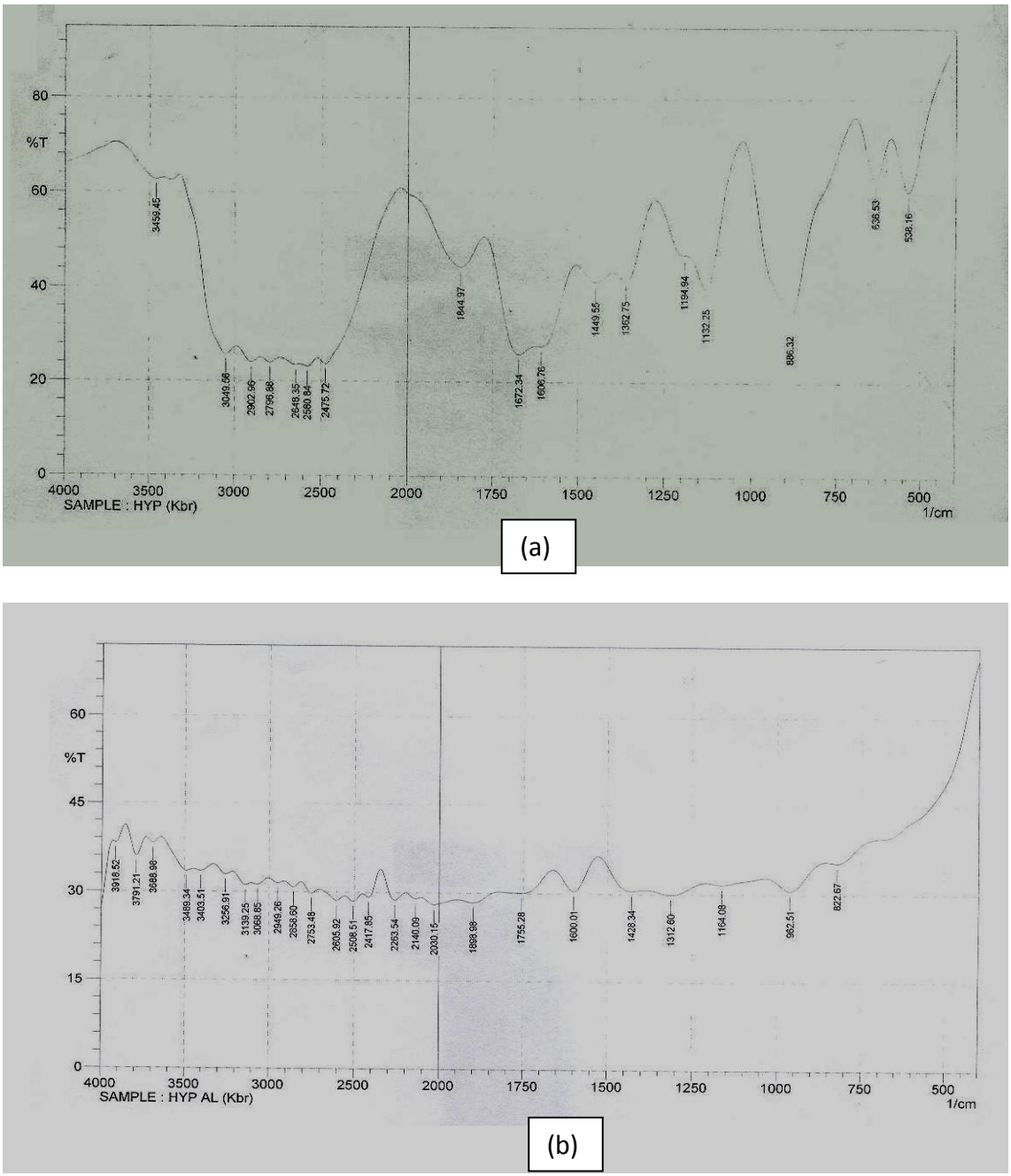


Figure 4.26. FTIR spectra of (a). hypoxanthine (HYP) powder alone and (b). corrosion product of aluminium obtained in the presence of hypoxanthine (HYP) in 0.1 M HCl.

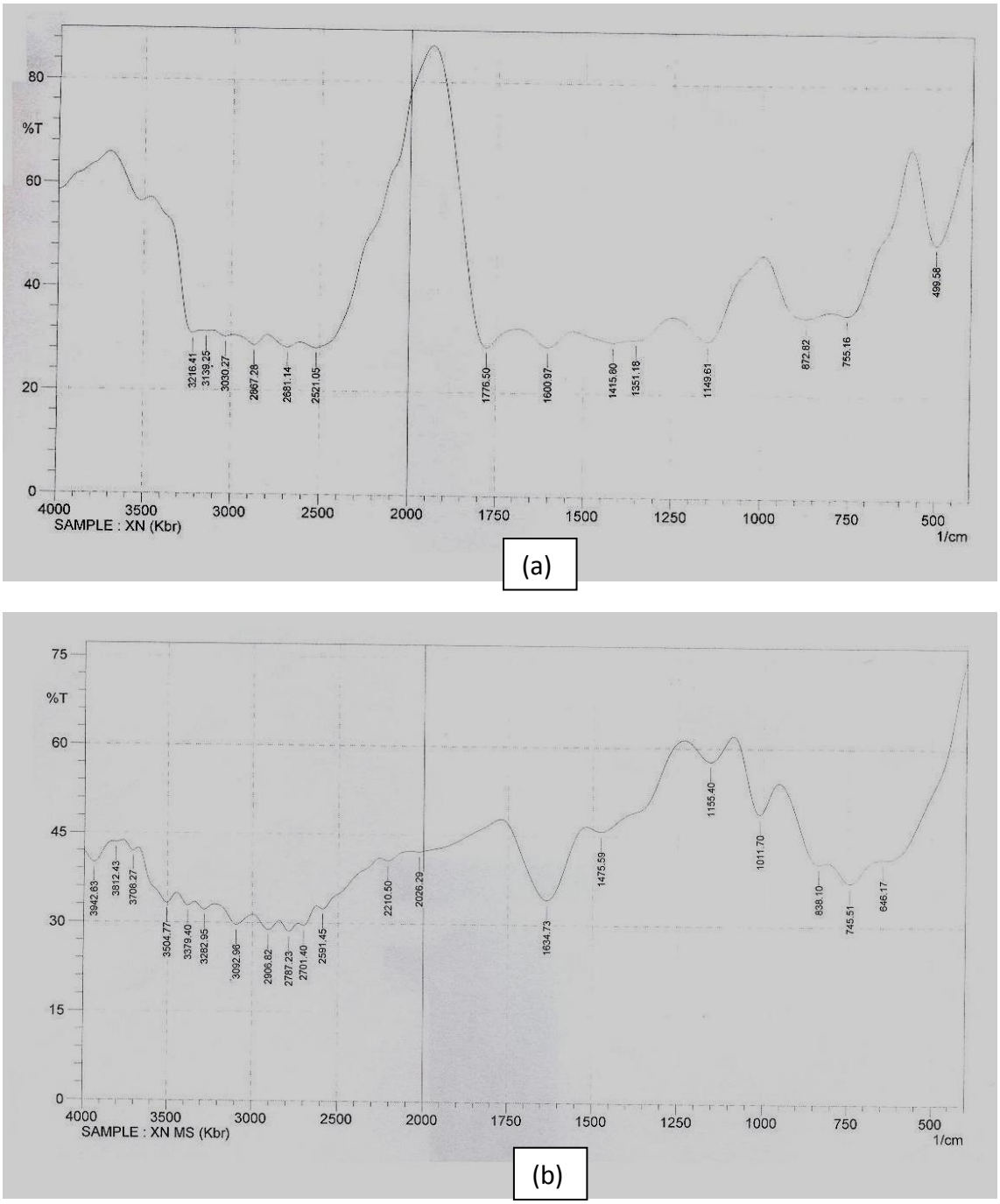


Figure 4.27. FTIR spectra of (a). xanthine (XN) powder alone and (b). corrosion product of mild steel obtained in the presence of xanthine (XN) in 0.1 M HCl.

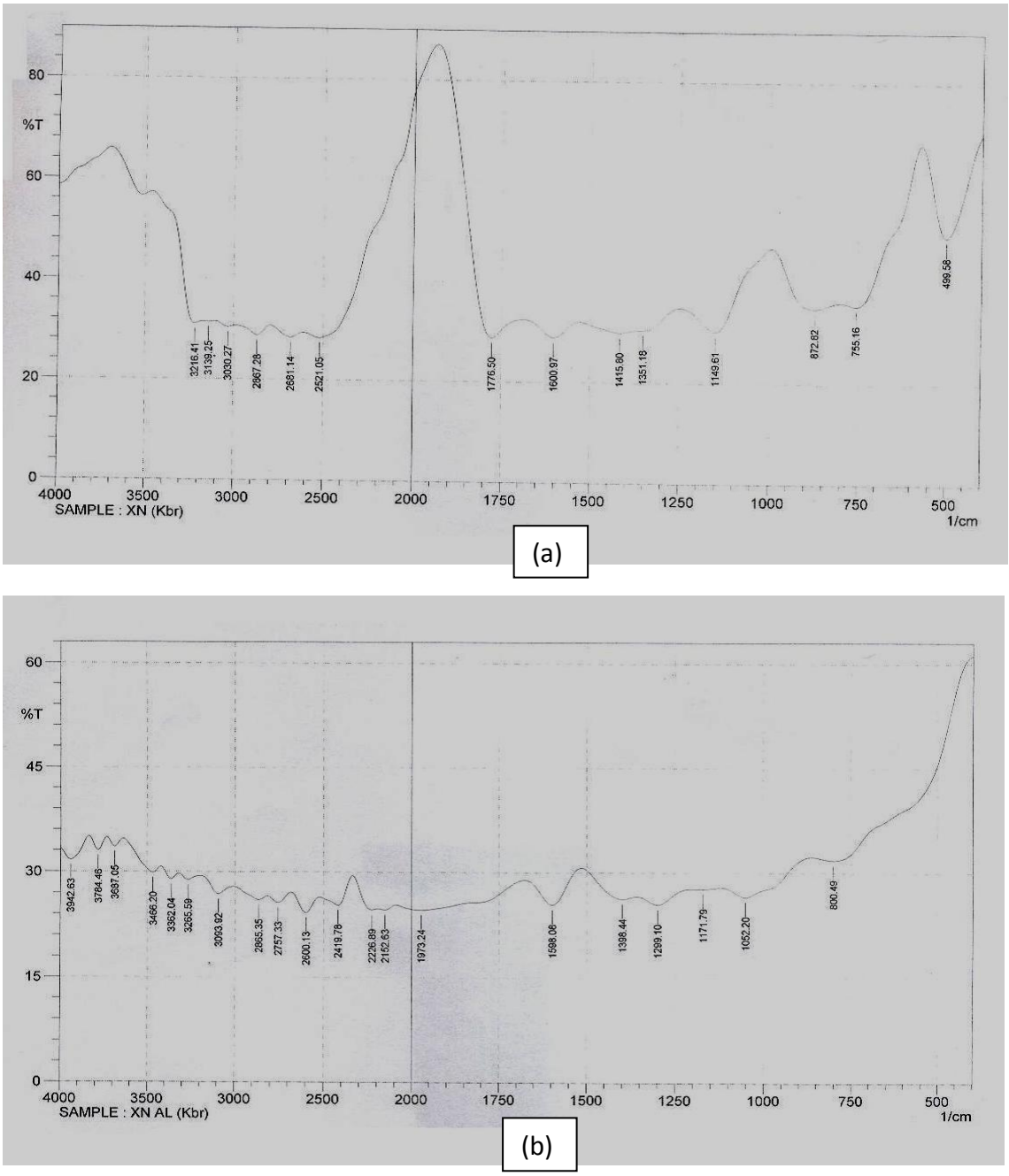


Figure 4.28. FTIR spectra of (a). xanthine (XN) powder alone and (b). corrosion product of aluminium obtained in the presence of xanthine (XN) in 0.1 M HCl.

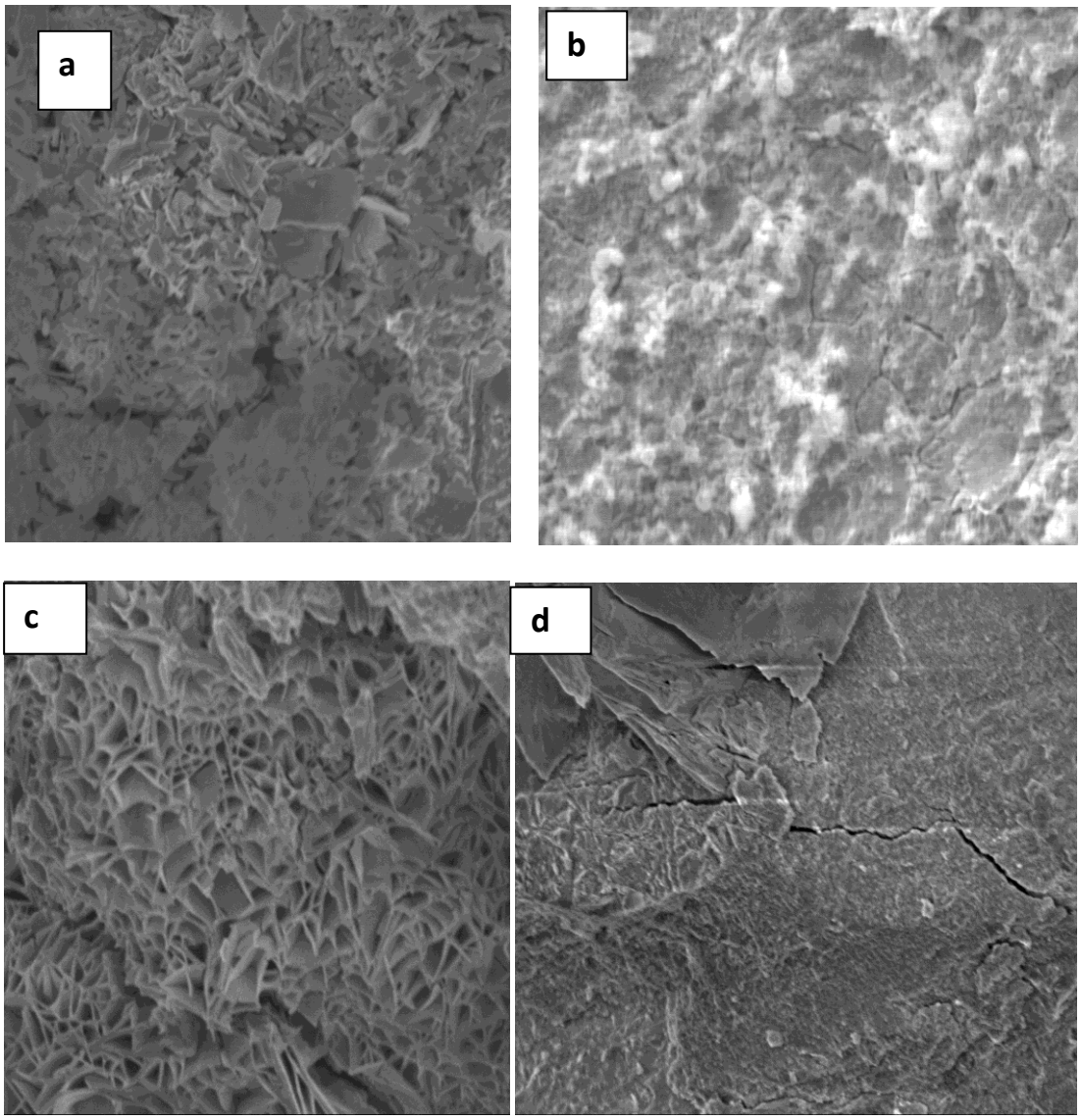


Figure 4.29. Micrographs of mild steel after dipping in 0.1 M HCl solution for 2 days at x 5,000 magnification (a). mild steel alone and in the presence of (b). adenine (AD) (c). guanine (GU) and (d). hypoxanthine (HYP).

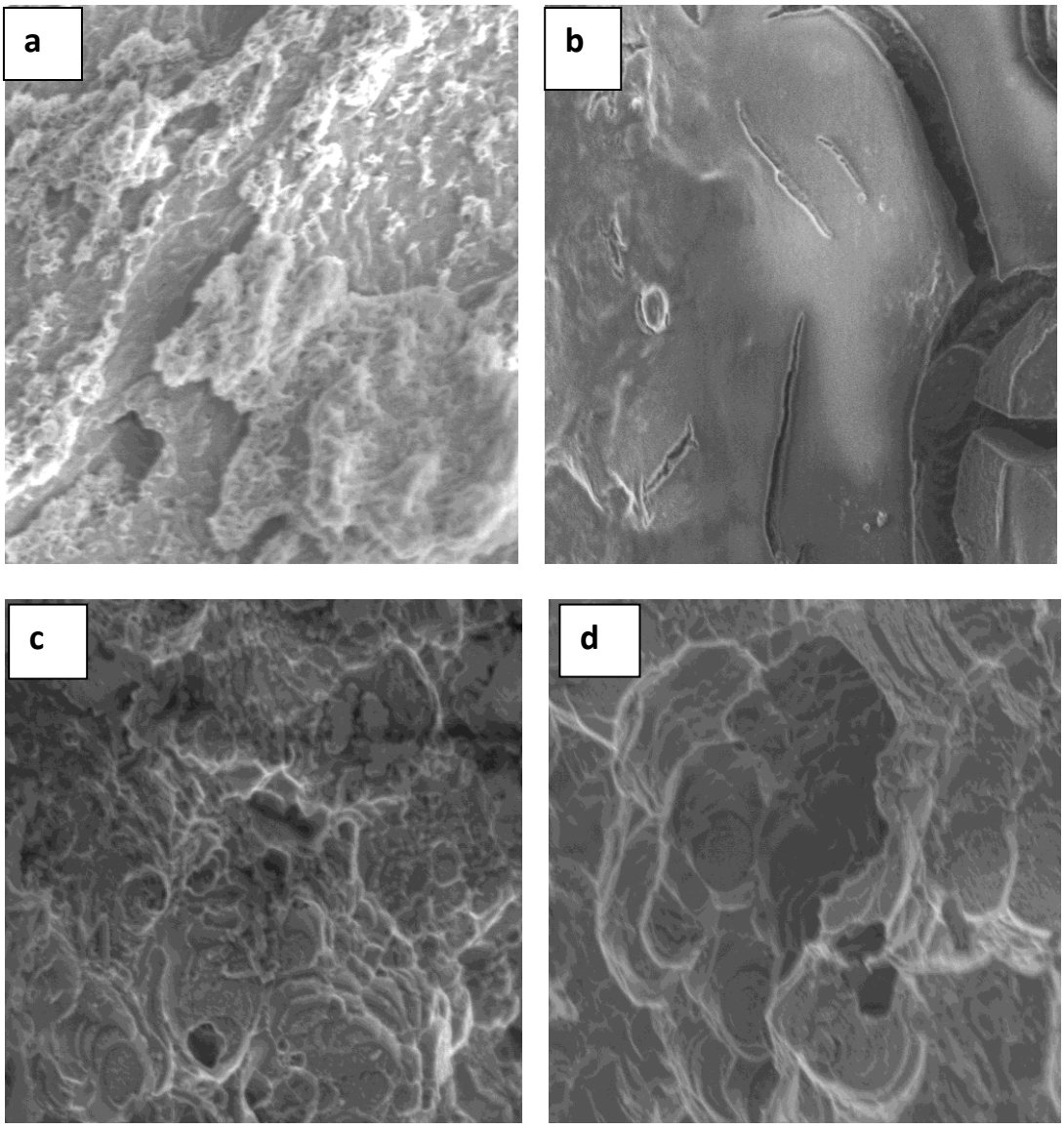
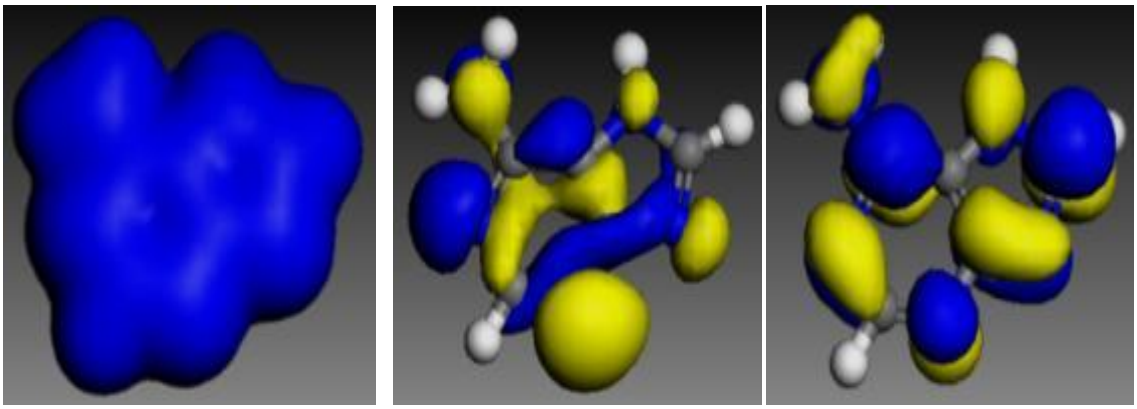
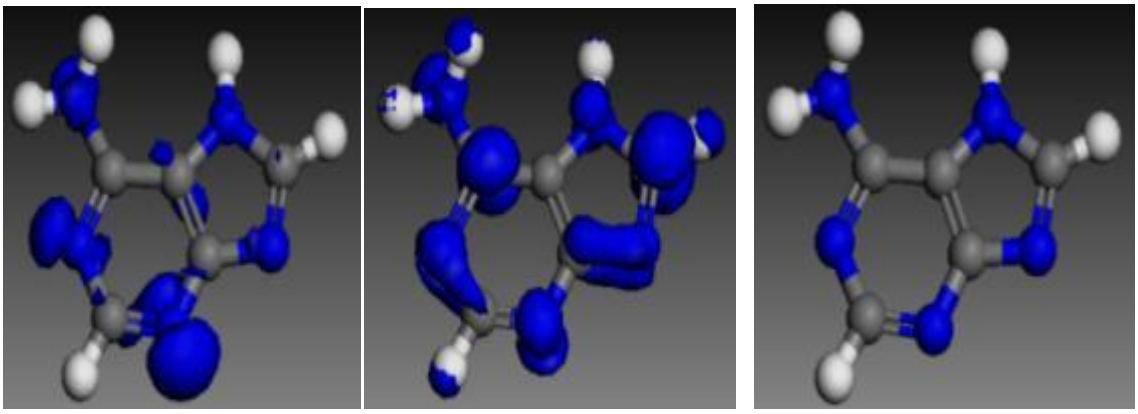


Figure 4.30. Micrographs of aluminium after dipping in 0.1 M HCl solution for 2 days at x 5,000 magnification (a). aluminium alone and in the presence of (b). adenine (AD) (c). guanine (GU) and (d). hypoxanthine (HYP).

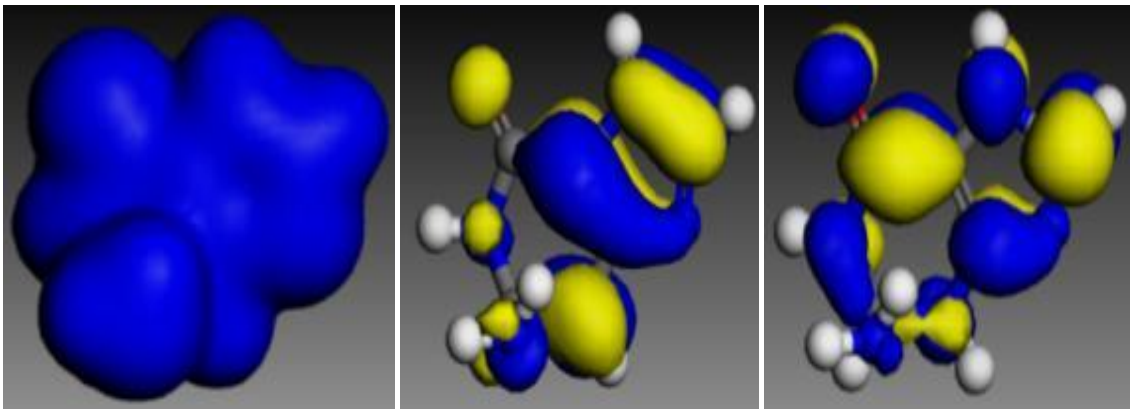


(i) Electron density (ii) HOMO (iii)LUMO

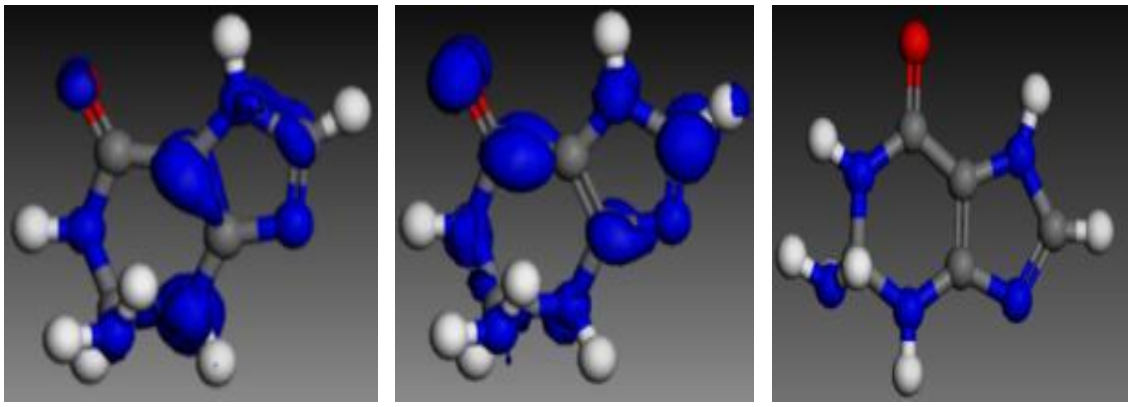


(iv) Electrophilic (f-) (v) Nucleophilic (f+) (vi) Geometry optimized

Figure 4.31. Electronic structure properties of adenine (AD).

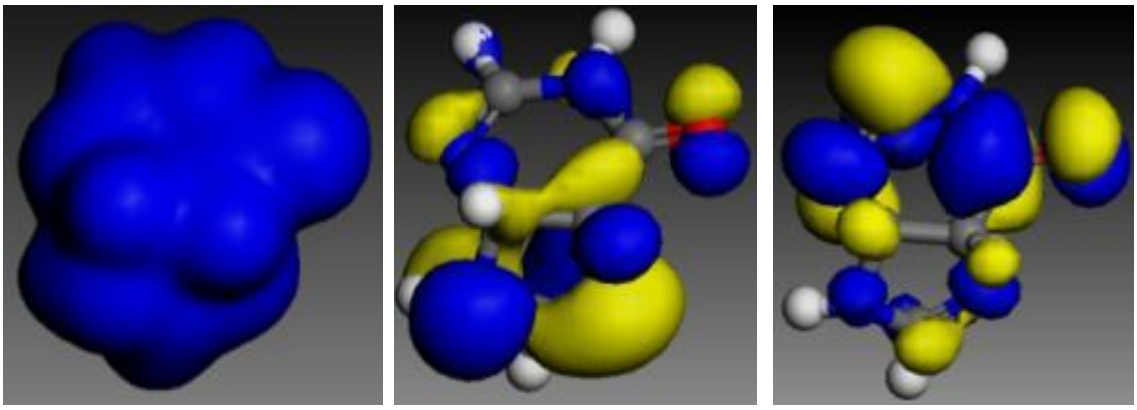


(i) Electron density (ii) HOMO (iii) LUMO

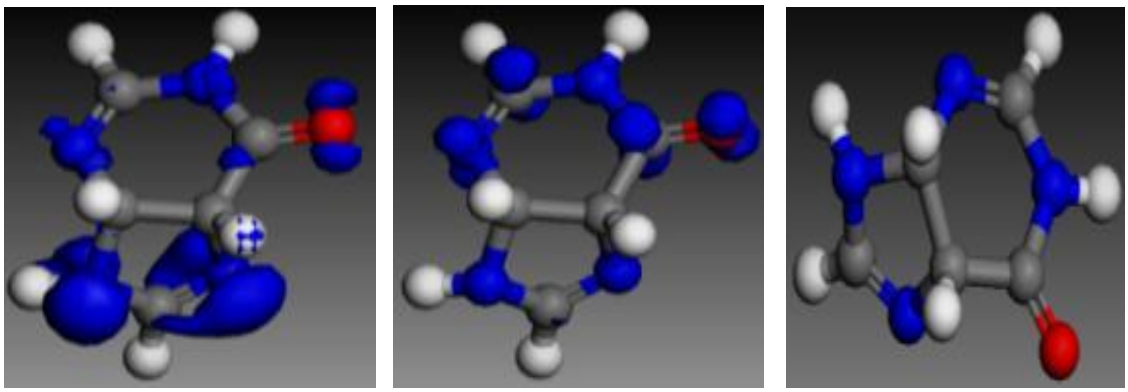


(iv) Electrophilic (f-) (v) Nucleophilic (f+) (vi) Geometry optimised

Figure 4.32. Electronic structure properties of guanine (GU).

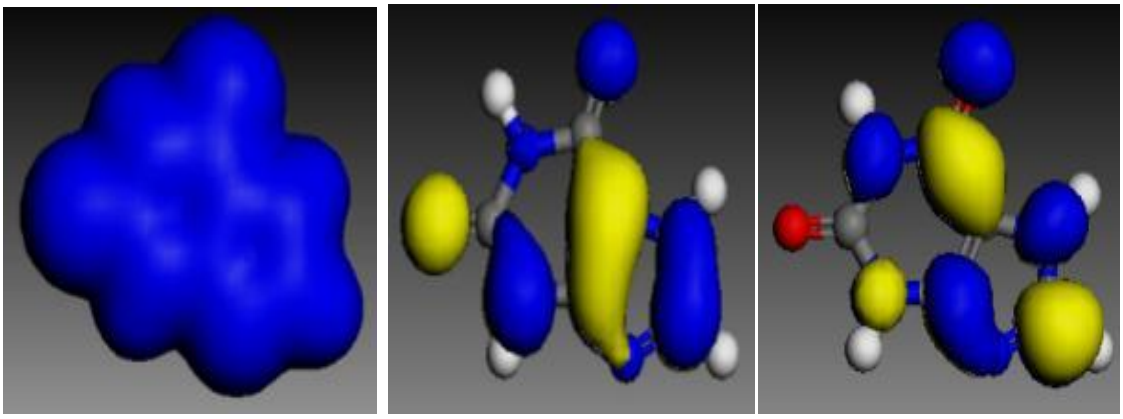


(i) Electron density (ii) HOMO (iii) LUMO

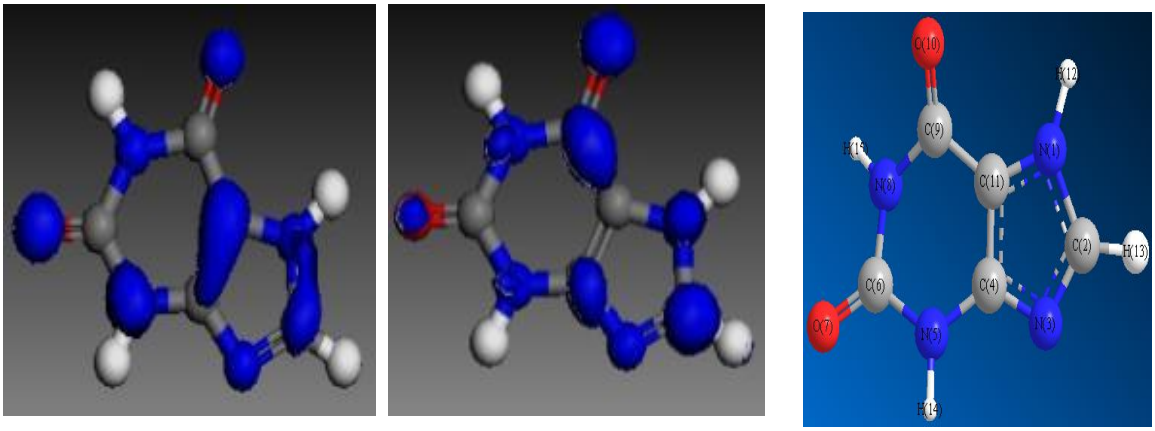


(iv) Electrophilic (f-) (v) Nucleophilic (f+) (vi) Geometry optimized

Figure 4.33. Electronic structure properties of hypoxanthine (HYP).



(i) Electron density (ii) HOMO (iii) LUMO



(iv) Electrophilic (f-) (v) Nucleophilic (f+) (iv) Geometry optimized

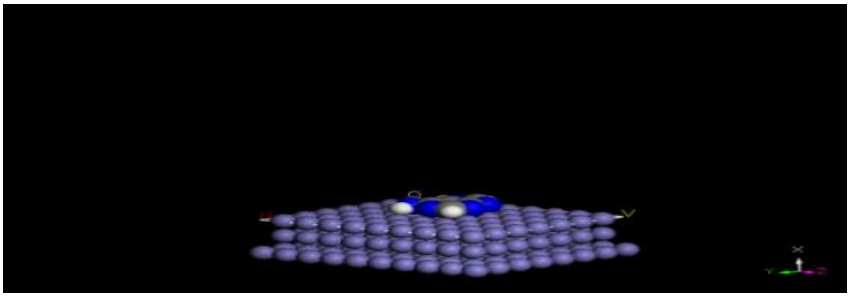
Figure 4.34. Electronic structure properties of xanthine (XN).

Table 4.15. Computed quantum chemical parameters of the studied compounds.

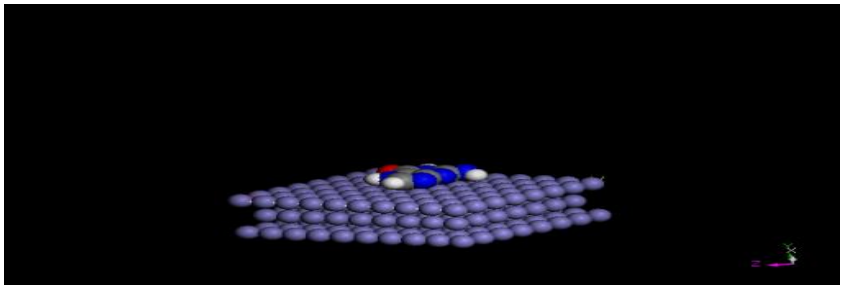
Molecule	E_{HOMO} (eV)	E_{LUMO} (eV)	Δ E	Dipole moment(Debye)
AD	-9.107	-4.506	4.601	7.003
GU	-9.300	-4.109	5.191	2.387
HYP	-9.237	-4.604	4.633	3.980
XN	-8.780	-4.139	4.641	4.201

Table 4.16 Fukui indices calculated with PBR/DND

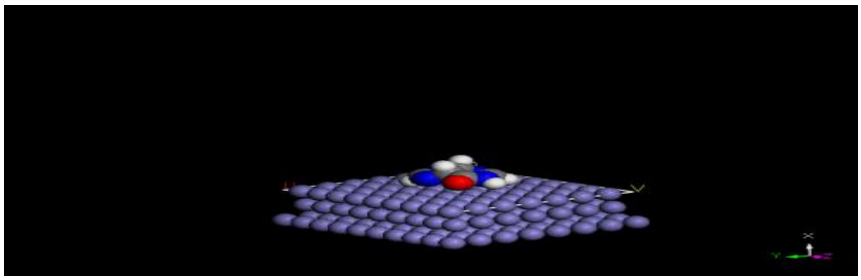
Molecules	Nucleophilic (F^+)				Electrophilic (F^-)			
	Mulliken		Hirshfeld		Mulliken		Hirshfeld	
	Atom	Value	Atom	Value	Atom	Value	Atom	Value
Hypoxanthine	O(10)	0.173	O (10)	0.169	N(9)	0.136	N(9)	0.154
Guanine	O(11)	0.137	O(11)	0.131	O(11)	0.113	N(9)	0.130
Adenine	C(8)	0.124	C(8)	0.134	N(3)	0.158	N(3)	0.186
Xanthine	O(8)	0.126	O(8)	0.121	O(13)	0.127	O(13)	0.123



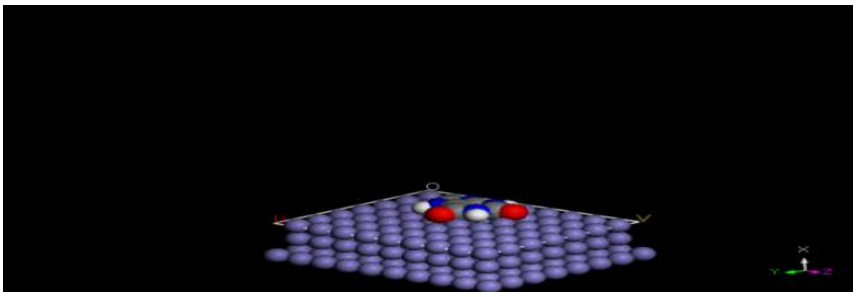
adenine(AD)



guanine(GU)

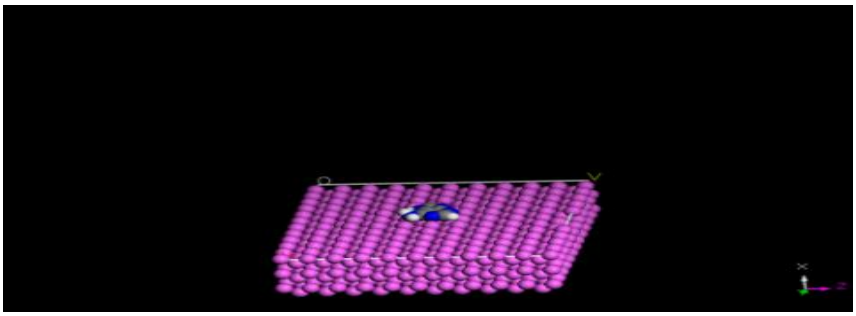


hypoxanthine(HYP)

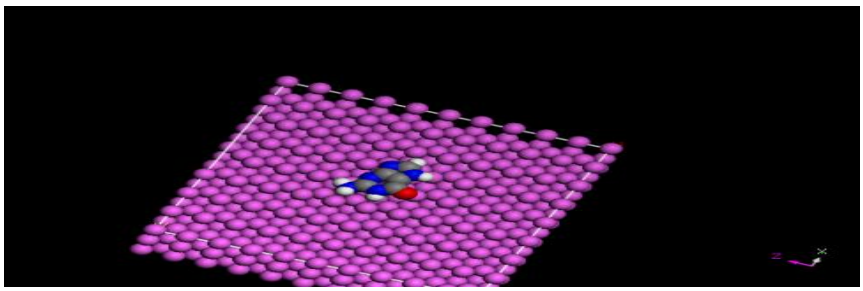


xanthine(XN)

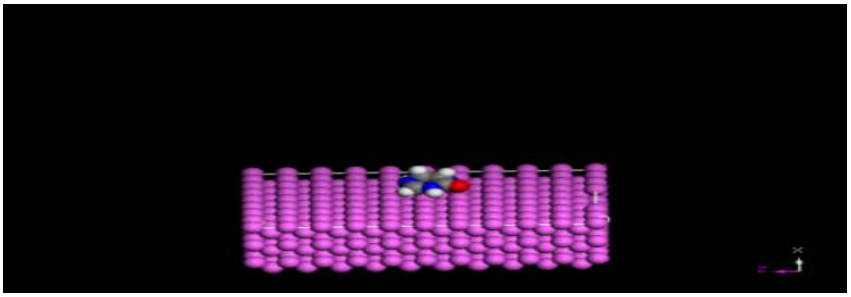
Figure 4.35. Adsorption of single molecules of adenine (AD), guanine (GU), hypoxanthine (HYP) and xanthine (XN) on a Fe (110) surface.



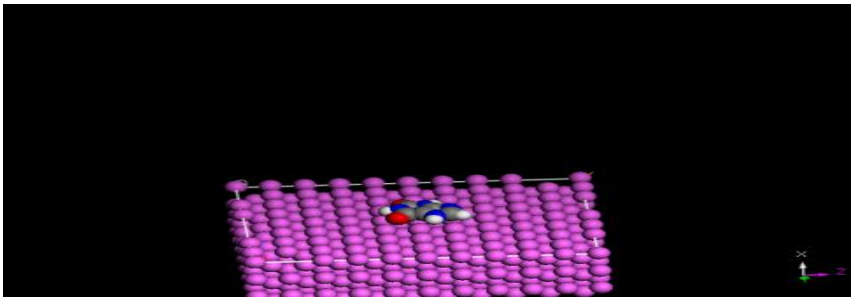
adenine(AD)



guanine(GU)

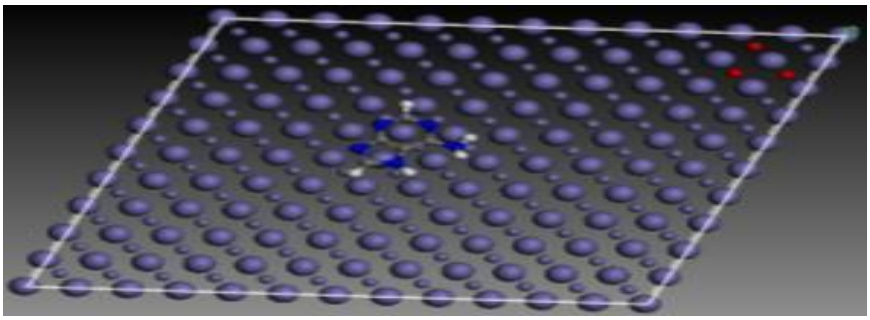


hypoxanthine(HYP)

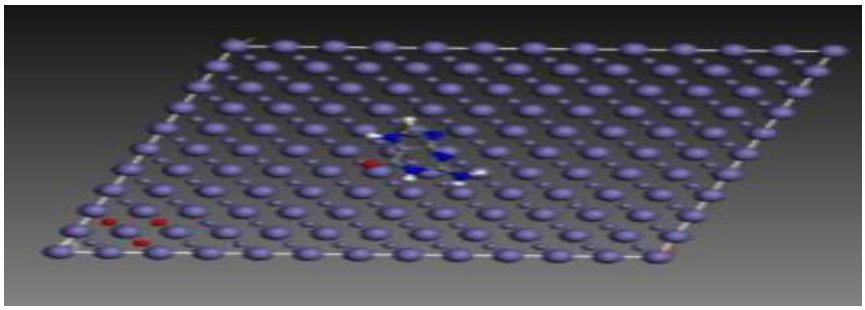


xanthine(XN)

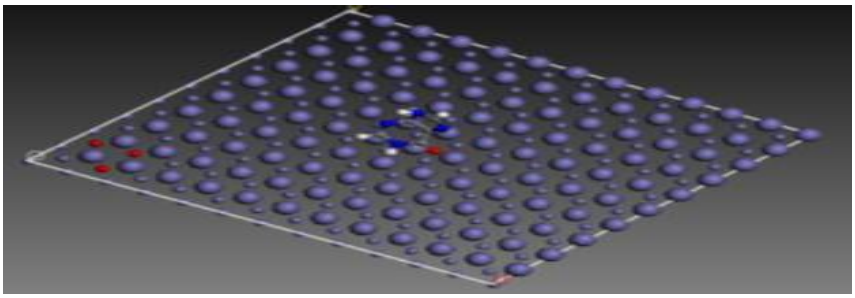
Figure 4.36. Adsorption of single molecules of adenine (AD), guanine (GU), hypoxanthine (HYP) and xanthine (XN) on Al (110) surface.



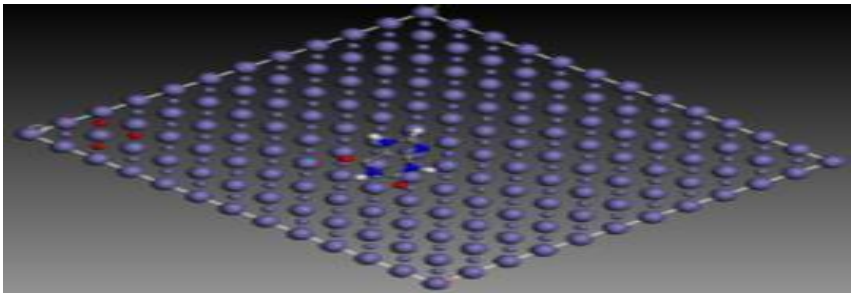
adenine(AD)



guanine(GU)

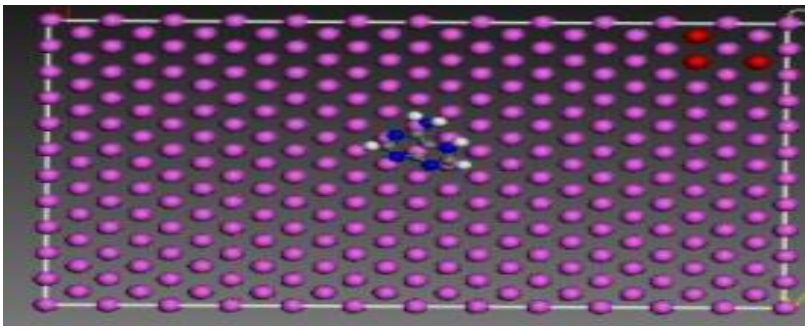


hypoxanthine(HYP)

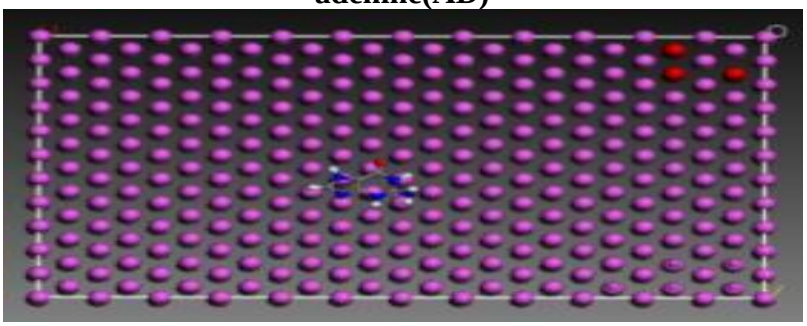


xanthine(XN)

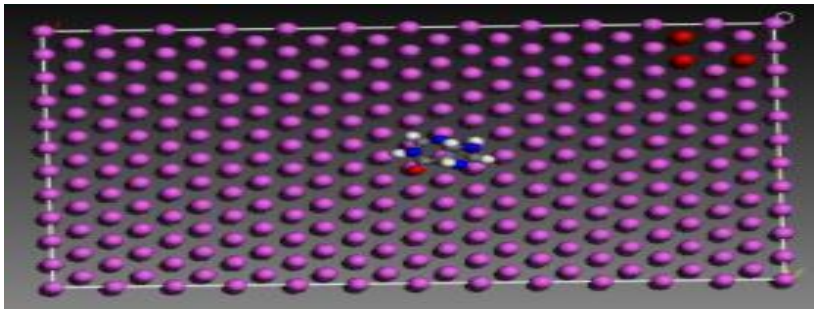
Figure 4.37. Representative snapshots of the on-top views of adenine (AD), guanine (GU), hypoxanthine (HYP) and xanthine (XN) on Fe (110) surface.



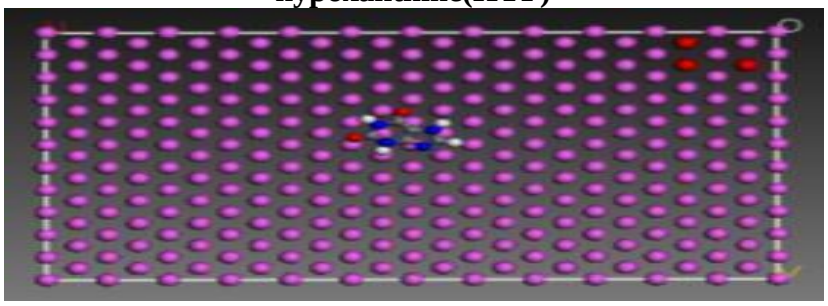
adenine(AD)



guanine(GU)



hypoxanthine(HYP)



xanthine(XN)

Figure 4.38. Representative snapshots of the on-top views of adenine (AD), guanine (GU), hypoxanthine (HYP) and xanthine (XN) on Al (110) surface.

Table 4.17. Caculated binding energies of the adsorption of adenine (AD), guanine (GU), hypoxanthine (HYP) and xanthine (XN) molecules on Fe (110) using Forcite quench molecular dynamics.

Molecule	Total P.E (kcal mol^{-1})	$E_{molecule}$ (kcal mol^{-1})	E_{Fe} (kcal mol^{-1})	Binding Energy (kcal mol^{-1})
AD	-93.08	-20.61	0.00	-72.47
GU	-326.73	-242.90	0.00	-83.82
HYP	-125.08	-58.11	0.00	-66.97
XN	-257.27	-172.73	0.00	-84.53

Table 4.18 Calculated binding energies of the adsorption of adenine (AD), guanine (GU), hypoxanthine (HYP) and xanthine (XN) molecules on Al (110) using Forcite quench molecular dynamics.

Molecule	TotalP.E (kcal mol^{-1})	$E_{molecule}$ (kcal mol^{-1})	E_{Fe} (kcal mol^{-1})	Binding Energy (kcal mol^{-1})
AD	-51.23	-20.64	0.00	-30.60
GU	-282.63	-242.93	0.00	-39.69
HYP	-92.80	-57.80	0.00	-34.82
XN	-210.82	-172.63	0.00	-38.19

CHAPTER FIVE

DISCUSSION

5.1 Gravimetric Measurements

From the plots obtained (Figures 4.1 – 4.16) it is evident that the degradation of mild steel in the absence of adenine (AD), guanine (GU), hypoxanthine (HYP) and xanthine (XN) is highest in H_3PO_4 at both 303 and 333 K, while the rate of corrosion of aluminium appeared to be highest in HCl at both temperatures. The observed difference in the behaviours of mild steel and aluminium in 0.1 M HCl, H_2SO_4 and H_3PO_4 can be explained on the basis of the different nature of the metals and their relative positions on the galvanic series (Appendix IX). The Galvanic series provides a guide to the corrosion resistance of metals and alloys. It is clear from the Galvanic series on Appendix IX that aluminium with a more negative potential should corrode more readily than mild steel. This may be responsible for higher corrosion rates for aluminium compared to those of mild steel in HCl solutions (Tables 4.1 and 4.3). However, higher corrosion rates were observed for mild steel in H_2SO_4 and H_3PO_4 than those for aluminium in the same acid solutions (Tables 4.1 and 4.3).

The high resistance to corrosion of aluminium media may be due to the naturally formed oxide film on aluminium surface which protects it in air or neutral solutions. Even upon immersion in acidic and alkaline media, this film is preserved for long periods of time (Pourbaix, 1974). Since the potential of zero charge (pzc) for aluminium oxide (Al_2O_3) occurs from pH 9.0 to 9.1 (Cabot *et al.*, 1991; Fouda *et al.*, 2000), chloride or any aggressive anion is likely to be adsorbed at pH values <9.0. This leads to localization of the corrosion attack by preferential adsorption at weak sites on the passive film. The lower corrosion rates observed for aluminium in H_2SO_4 and H_3PO_4

solutions are indications that these media do not readily dissolve the passive oxide film on the aluminium surface, so that the corrosion rates are lower.

Solubility of the corrosion products is another factor that may be responsible for the different behaviours of mild steel and aluminium in the different acid media. From the knowledge of chemical equilibria, a soluble corrosion product signifies more dissolution of the metal in the acid medium resulting in higher corrosion rates and lower inhibition efficiencies.

The nature of the different counter-anions of the different acids may also interact with the corroding Fe/Al atoms in different ways at the metal/solution interface thus influencing the overall corrosion process in different ways (Oguzie, 2008; Lashgari *et al*. 2010).

It can also be deduced from Figures 4.1 – 4.16 that the weight loss of mild steel and aluminium hence, the corrosion rates, increased with immersion time at the higher temperature of 333 K compared to 303 K. This could be attributed to increase in the rates of ionisation and diffusion of the aggressive ions to the electrodes thereby accelerating the corrosion reaction.

From Figures 4.1 – 4.8 and Table 4.1, it is evident that weight loss, hence corrosion rate of mild steel in the presence of AD, GU, HYP and XN was reduced indicating the inhibiting action of the compounds. It was also observed that weight loss of mild steel varied linearly with immersion time and concentration of the purines at both 303 and 333 K. However, weight loss was more pronounced at 333 K in the different acids.

From Figures 4.9 – 4.16 and Table 4.3, it was observed that the corrosion rate of aluminium decreased with increase in concentrations of AD, GU, HYP and XN only in HCl, and in the presence of HYP in H_2SO_4 signifying the ability of these compounds to reduce the rate of corrosion of aluminium in HCl and only HYP in H_2SO_4. The other purines namely AD, GU, XN (with the exception of HYP) were observed to promote the corrosion of aluminium in H_2SO_4. Moreover, none of the purines showed any inhibiting property against the corrosion of aluminium in H_3PO_4, rather, they acted as catalyts by enhancing the corrosion process with a resultant increase in weight loss of the aluminium coupons.

In general, the chemical stability of a metal exposed to a solution is a function of the potential of the metal with respect to the pH of the solution. This also explains the difference in weight losses hence corrosion rates of mild steel (a ferrous metal) and aluminium (a non ferrous metal) in 0.1 M HCl, H_2SO_4 and H_3PO_4. The inhibition efficiencies (IE%) obtained for AD, GU, HYP and XN for the corrosion of mild steel and aluminium in the three acid media are presented on Tables 4.2 and 4.4. From Table 4.2, it was observed that IE% of the purine derivatives for the corrosion of mild steel increased with increasing concentrations in the three acid media in the order: AD > HYP > GU > XN in HCl; HYP > AD > GU > XN in H_2SO_4 and GU > AD > HYP > XN in H_3PO_4. This is an indication that AD, HYP, GU and XN inhibited the corrosion of mild steel in HCl, H_2SO_4 and H_3PO_4 while in the case of aluminium, from Table 4.2, it can be observed that IE% of all the purine derivatives increased with concentration in HCl in the order: GU > HYP > AD and XN. Although negative inhibition efficiencies (IE%) were obtained in H_2SO_4 and H_3PO_4 at both temperatures, however, the addition

of HYP to aluminium in H_2SO_4 retarded the corrosion of aluminium with an IE% of about 82 and 61 at the optimum concentration of 0.01 M at 303 and 333 K respectively.

Negative inhibition efficiencies (IE%) have been obtained by other researchers such as Chen *et al.* (2000) in the application of imidazoline at high temperature/pressure corrosion inhibition of mild steel in brine. Phanasgaonkar *et al.* (1997) also obtained negative inhibition efficiencies (IE%) for 0.01 M sodium nitrite as corrosion inhibitor for concrete in marine environments. Better inhibitions were however obtained with higher concentrations of sodium nitrite.

From the plots of weight loss as a funtion time and inhibition efficiencies (IE%) obtained, it can be inferred that the inhibition process depended on the amount of inhibiting species present in the system resulting in increased surface coverage, θ, due to the increase in the number of adsorbed molecules on the mild steel surface and the stability of the corrosion products formed.

Higher inhibition efficiencies (IE%) signify higher surface coverage by the purine derivatives on the metal surface as well as better stability of the corrosion products formed. The driving force for the corrosion of a metal is the thermodynamic instability of the metal in its surrounding environment. A metal tend to corrode faster when its dissolution potential is negative. In the absence of any surface active compound, the oxidation of the metal is the primary anodic reaction. The fact that some of the selected purines functioned as catalysts with negative inihibition efficiencies (IE%) in aluminium systems could mean that their corrosion products were not thermodynamically stable leading to their solubilities and formations of chemical

species that actually enhanced the anodic oxiation or dissolution of the aluminium electrode instead of inhibiting it.

5.2 Half Lives ($t_{1/2}$) of Mild Steel and Aluminium in the Test Solutions

The plots of / versus time are linear and are presented in Figures 5.1 – 5.16.

From Figures 5.1 – 5.8 and Tables 4.5-4.6, it is evident that the half lives of mild steel in solutions of HCl, H_2SO_4 and H_3PO_4 containing various concentrations of the inhibitors are higher than the half lives of mild steel in the blank solutions indicating thatAD, GU, HYP and XN increased the half life of mild steel in solutions of HCl, H_2SO_4 and H_3PO_4 thereby, reducing the rate of dissolution of the mild steel coupons at 303 and 333 K.

In the case of aluminium, it was observed that only aluminium coupons in HCl solutions containing various concentrations of the purines and H_2SO_4 solutions containing HYP, had higher half lives values compared to aluminium coupons in the blank solutions of HCl, H_2SO_4 and H_3PO_4 (Figures 5.9 – 5.16, Tables 4.7-4.8). This implies that aluminium in H_2SO_4 in the presence of AD, GU and XN had lower half lives than aluminium coupons in the absence of these purines. A similar observation was made for the calculated half lives of aluminium in H_3PO_4 in the presence of AD, GU, HYP and XN in H_3PO_4. Lower half lives were obtained compared to those for aluminium coupons in blank solutions of H_3PO_4. These signify the inability of the purines to inhibit the corrosion of aluminium in these media.

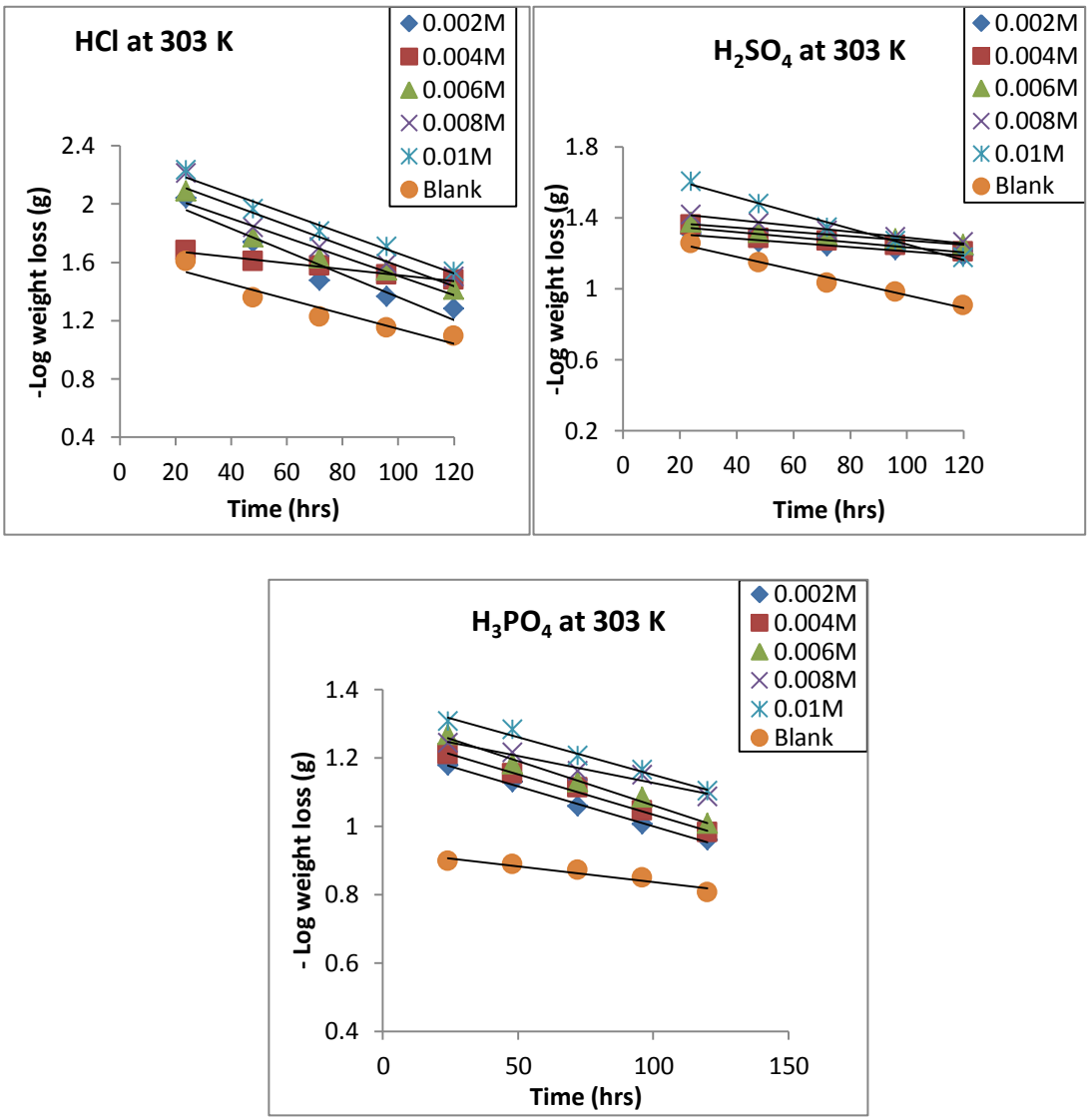


Figure 5.1. Plots of –log weight loss (g) versus time (hrs) for the corrosion of mild steel in 0.1 M HCl, H_2SO_4 and H_3PO_4 containing various concentrations of adenine (AD) at 303 K.

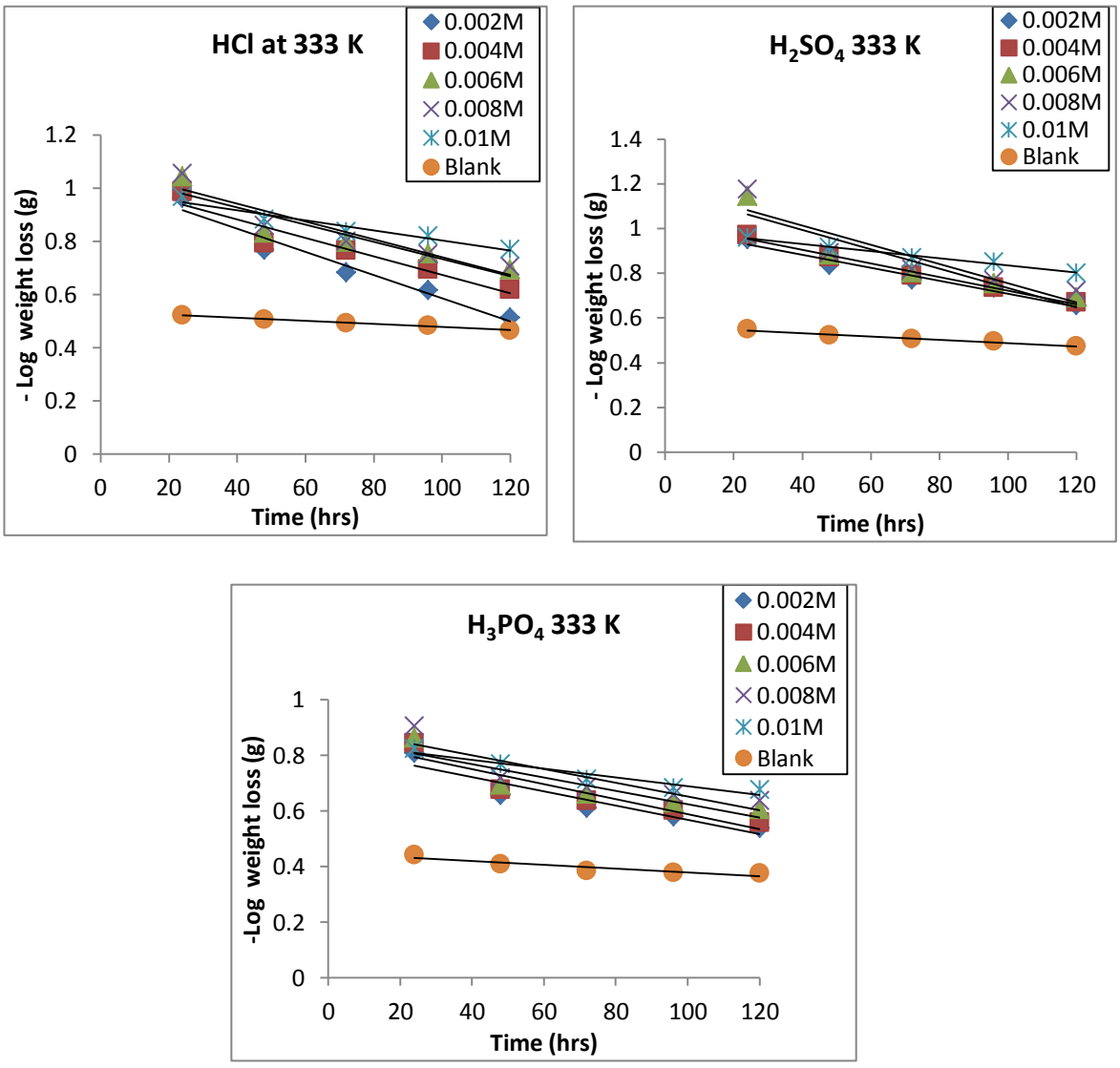


Figure 5.2. Plots of –log weight loss (g) versus time (hrs) for the corrosion of mild steel in 0.1 M HCl, H_2SO_4 and H_3PO_4 containing various concentrations of adenine (AD) at 333 K.

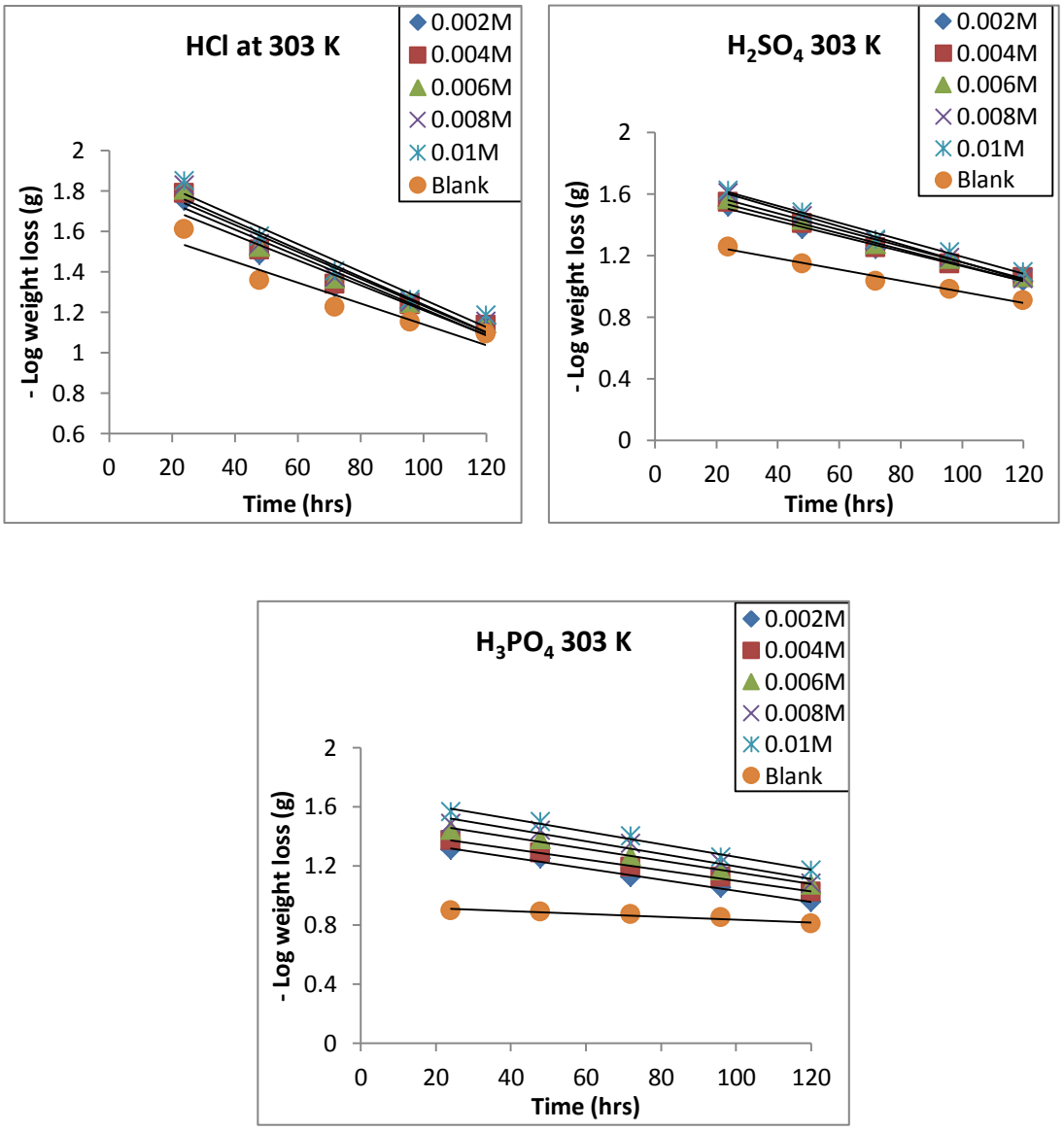


Figure 5.3. Plots of –log weight loss (g) versus time (hrs) for the corrosion of mild steel in 0.1 M HCl, H_2SO_4 and H_3PO_4 containing various concentrations of guanine (GU) at 303 K.

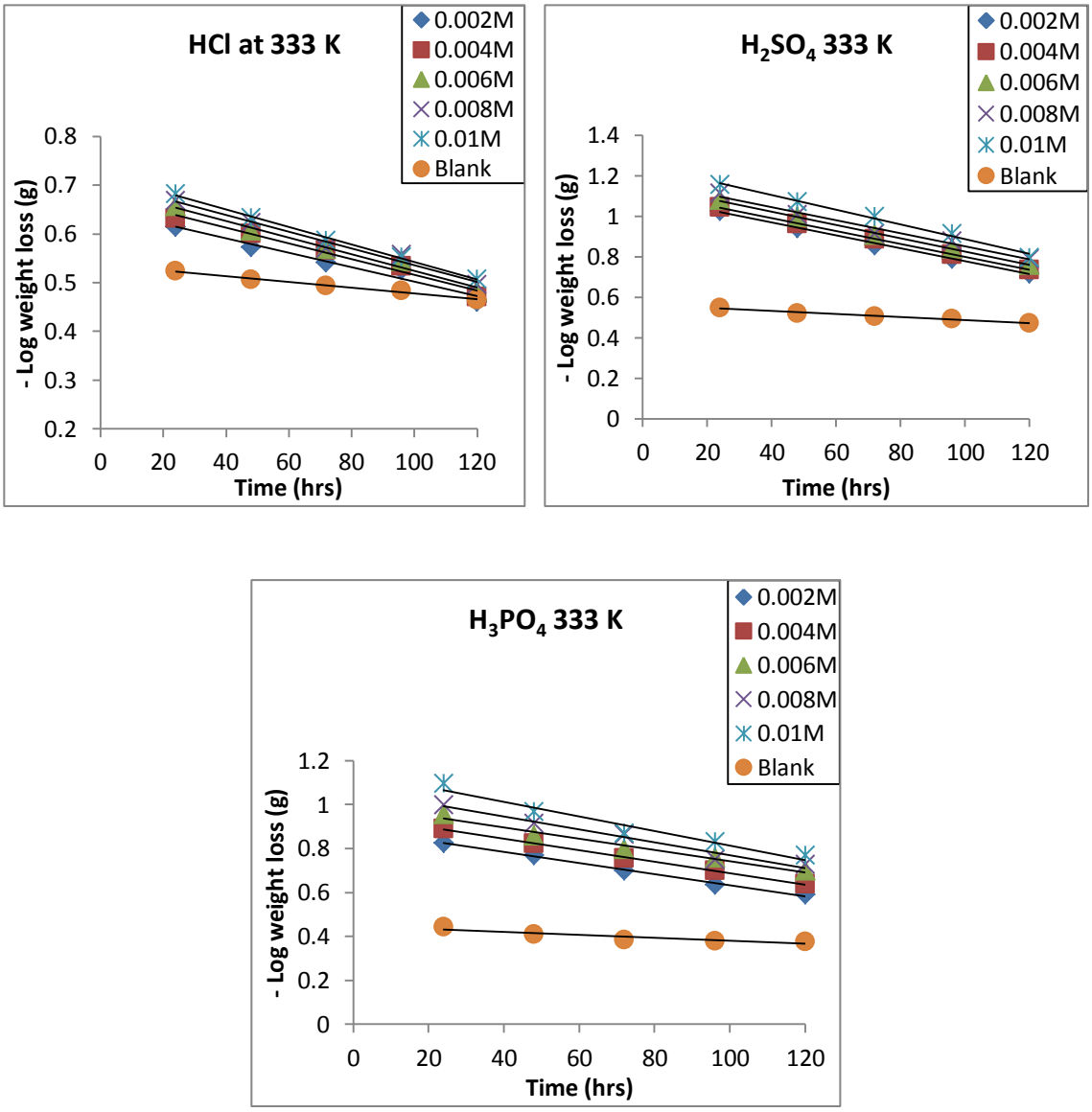


Figure 5.4. Plots of –log weight loss (g) versus time (hrs) for the corrosion of mild steel in 0.1 M HCl, H_2SO_4 and H_3PO_4 containing various concentrations of guanine (GU) at 333 K.

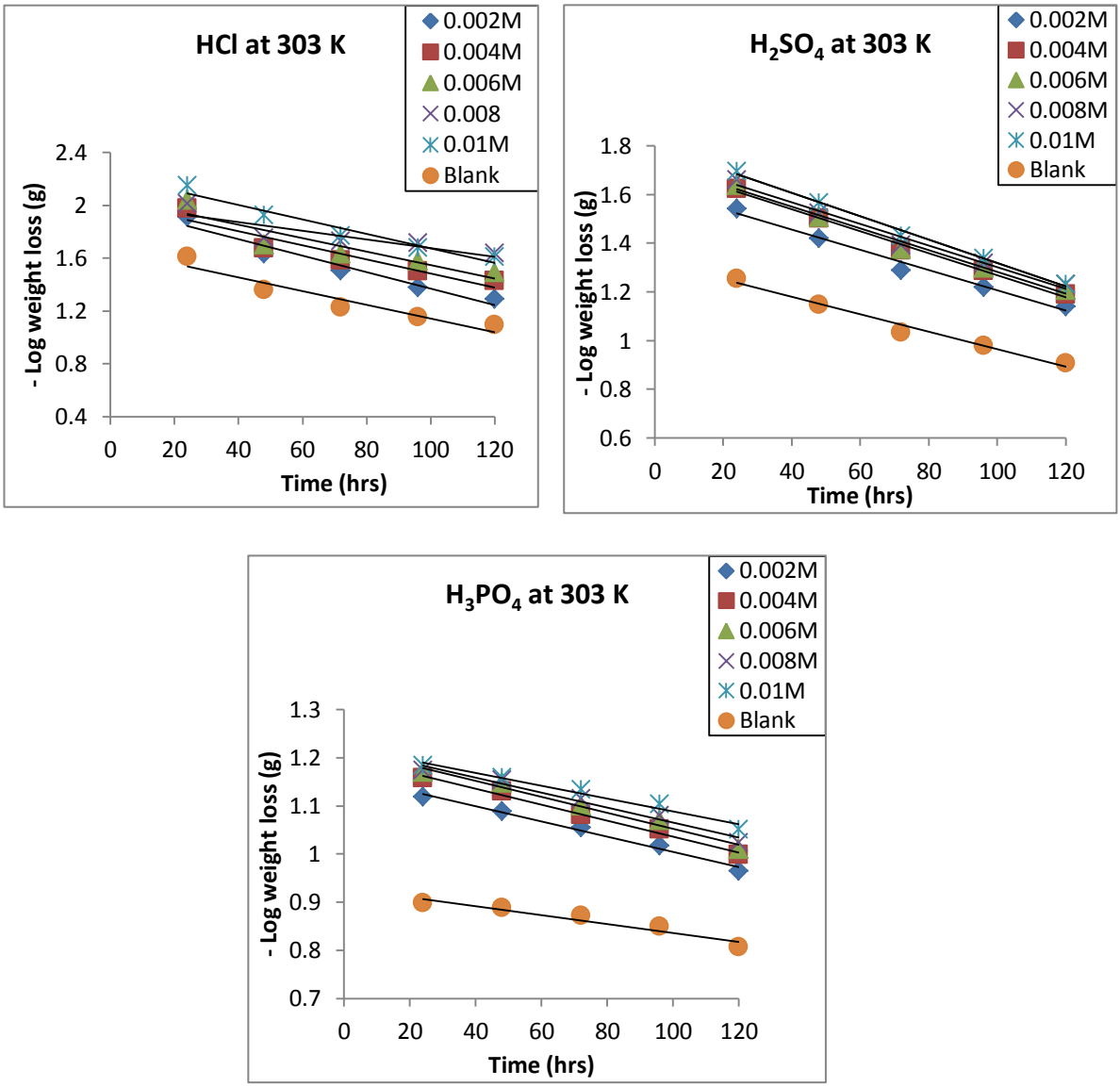


Figure 5.5. Plots of –log weight loss (g) versus time (hrs) for the corrosion of mild steel in 0.1 M HCl, H_2SO_4 and H_3PO_4 containing various concentrations of hypoxanthine (HYP) at 303 K.

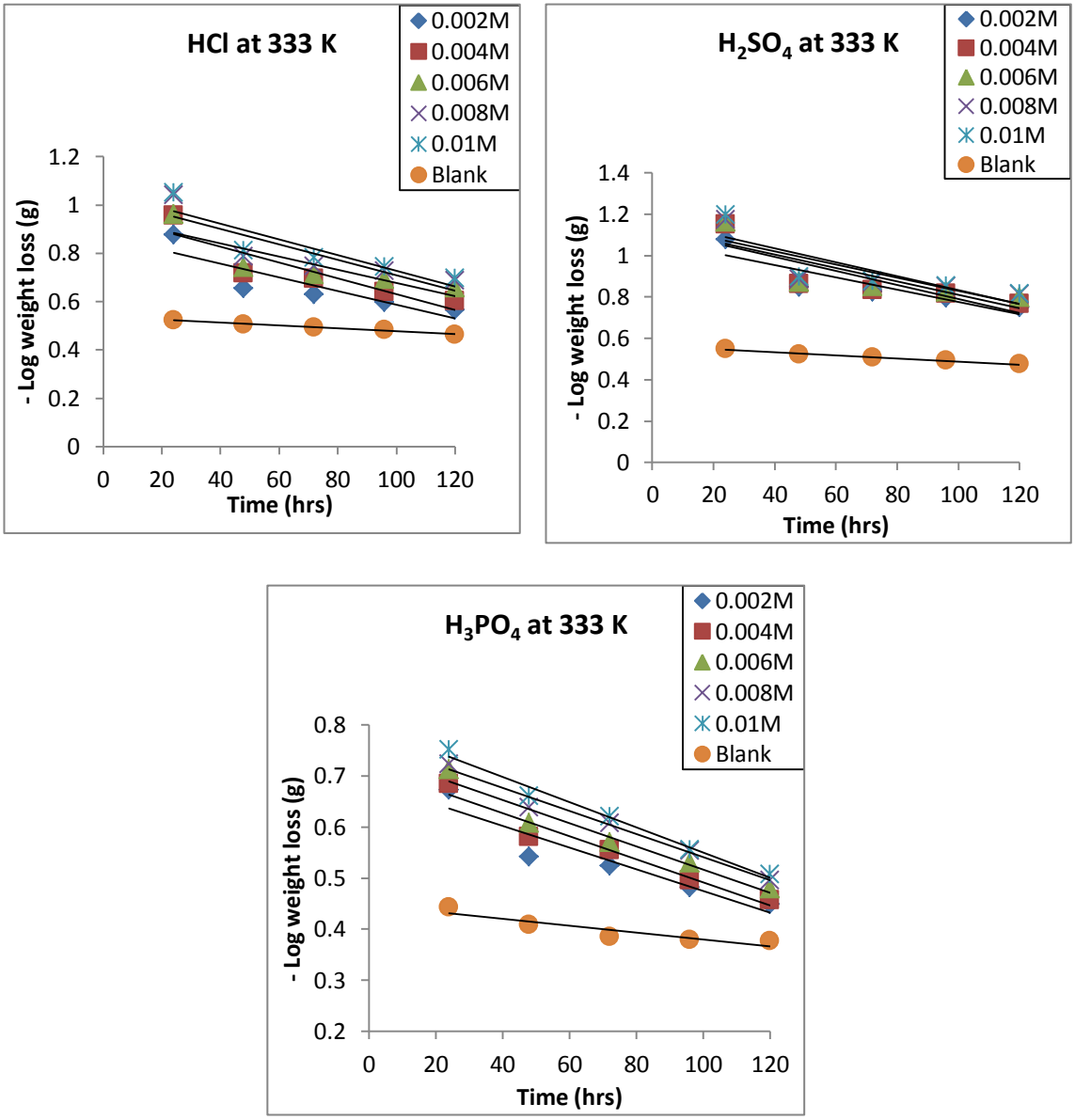


Figure 5.6. Plots of –log weight loss (g) versus time (hrs) for the corrosion of mild steel in 0.1 M HCl, H_2SO_4 and H_3PO_4 containing various concentrations of hypoxanthine (HYP) at 333 K.

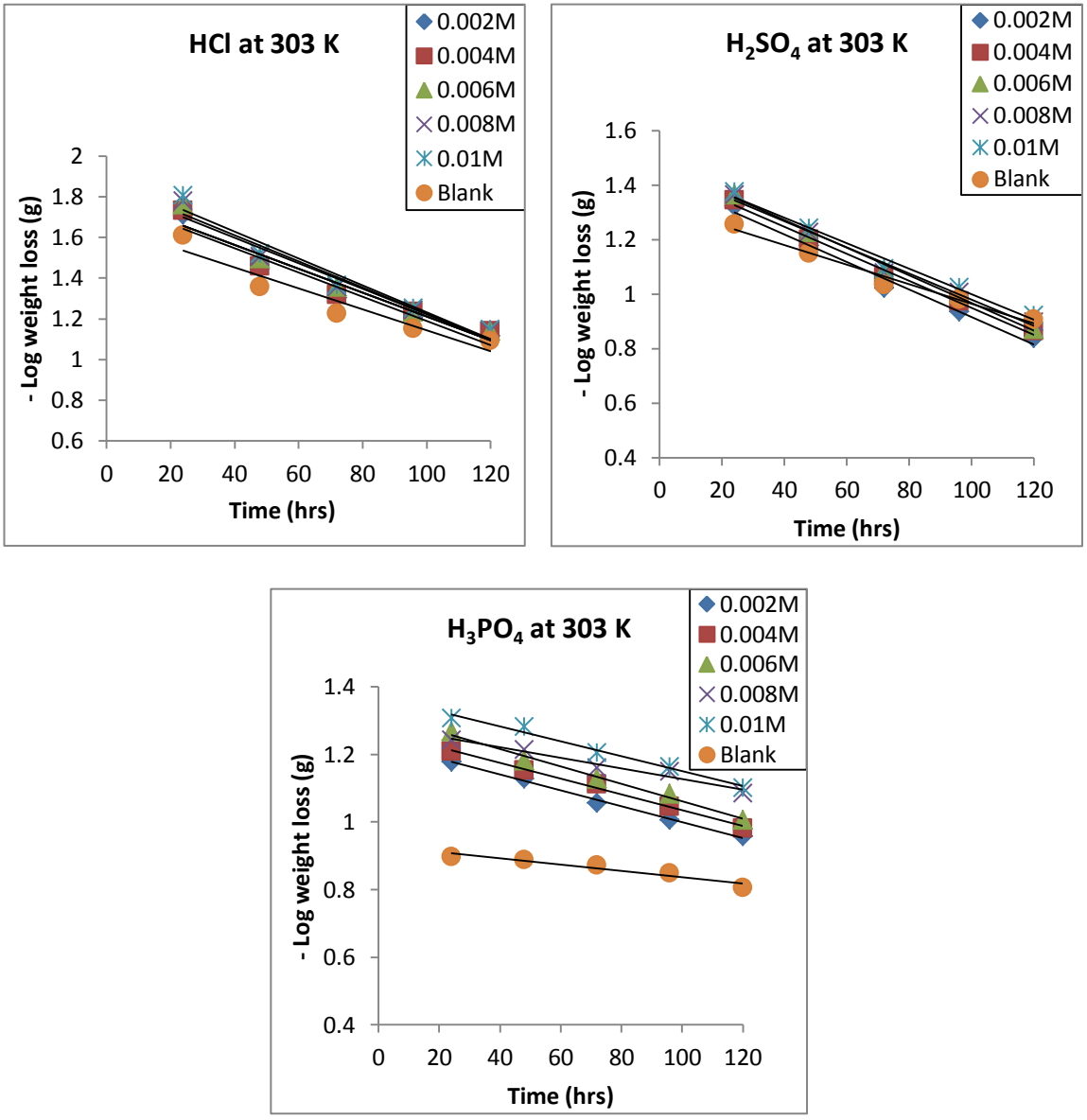


Figure 5.7. Plots of –log weight loss (g) versus time (hrs) for the corrosion of mild steel in 0.1 M HCl, H_2SO_4 and H_3PO_4 containing various concentrations of xanthine (XN) at 303 K.

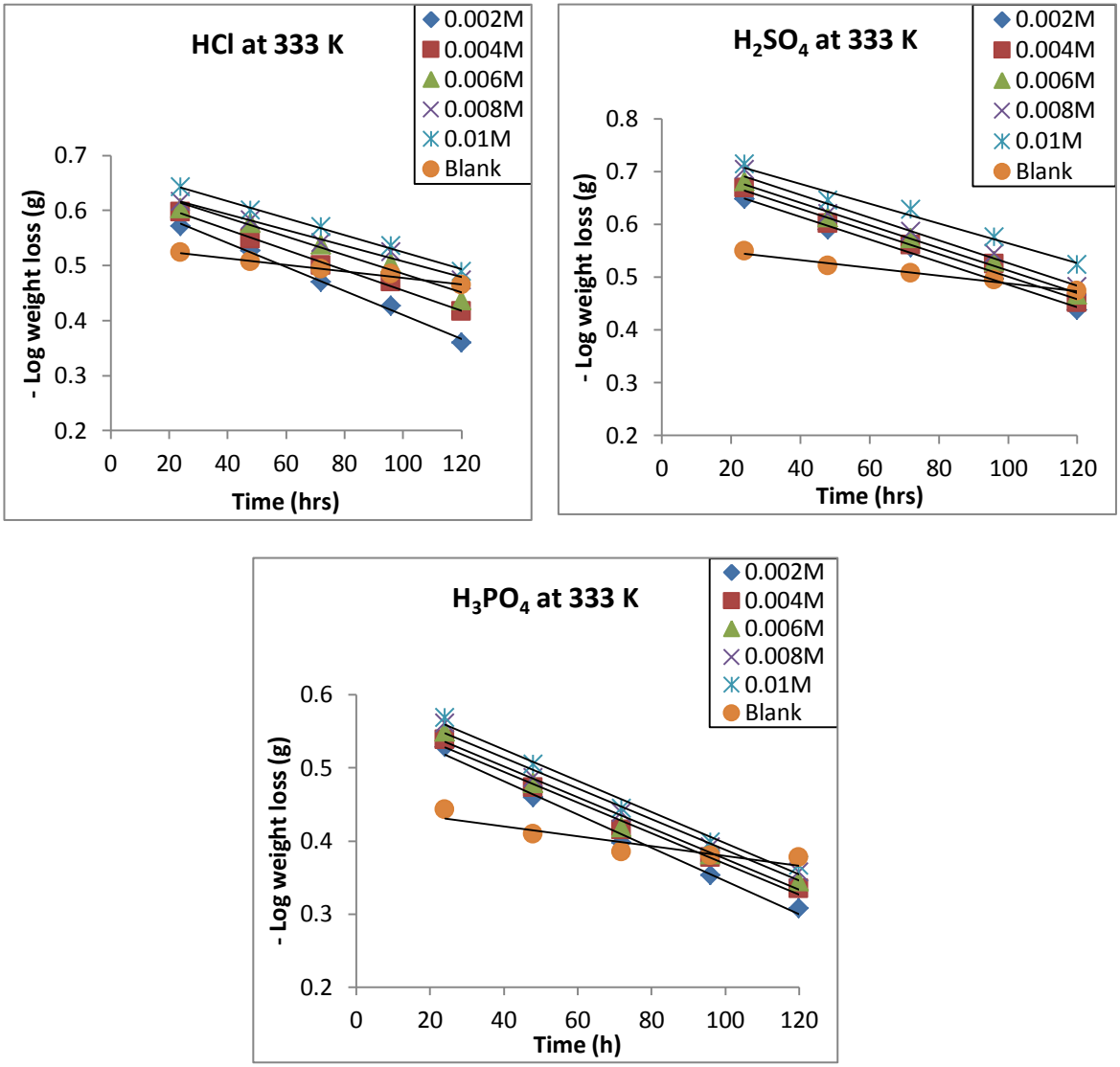


Figure 5.8. Plots of –log weight loss (g) versus time (hrs) for the corrosion of mild steel in 0.1 M HCl, H_2SO_4 and H_3PO_4 containing various concentrations of xanthine (XN) at 333 K.

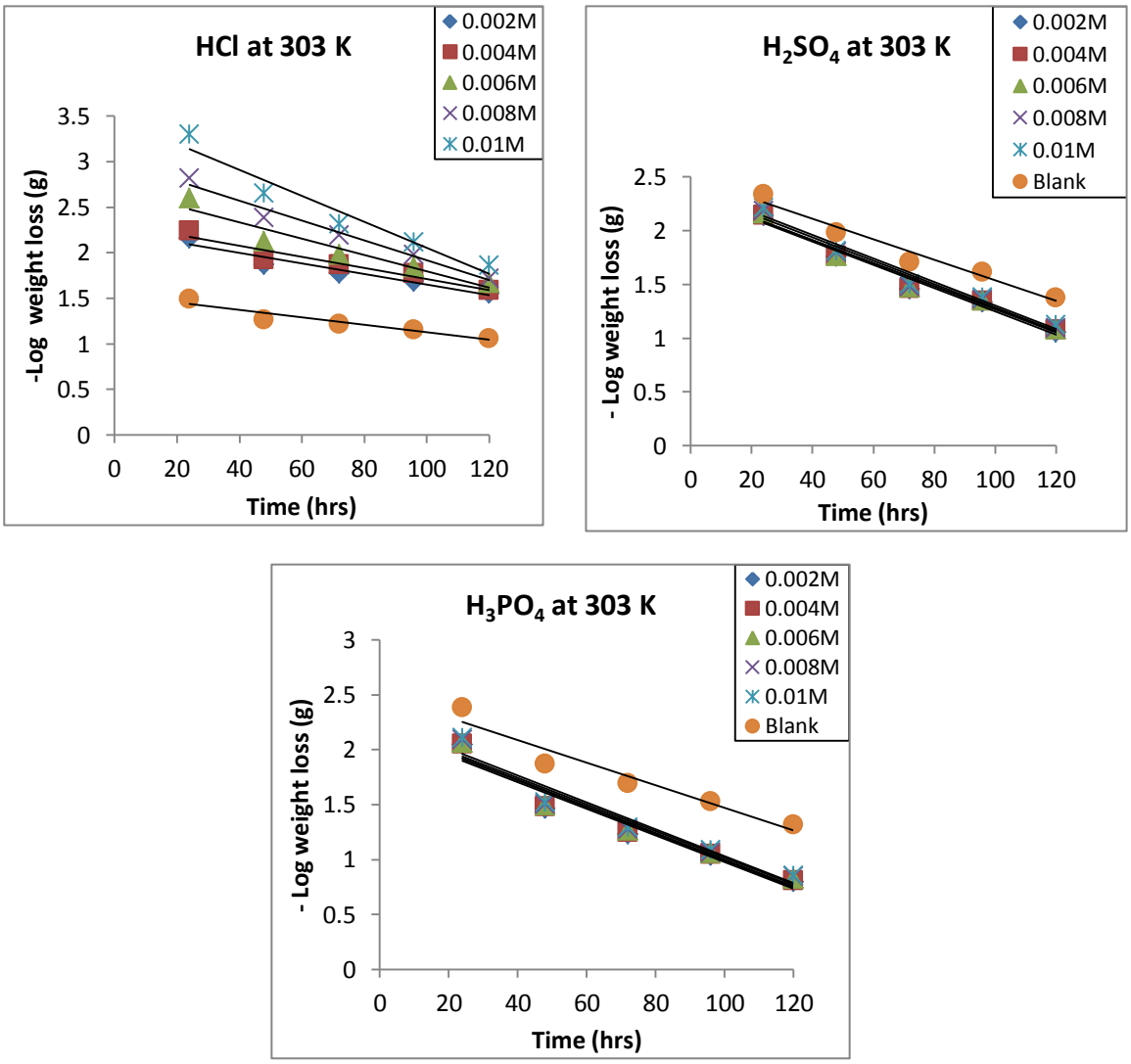


Figure 5.9. Plots of –log weight loss (g) versus time (hrs) for the corrosion of aluminium in 0.1 M HCl, H_2SO_4 and H_3PO_4 containing various concentrations of adenine (AD) at 303 K.

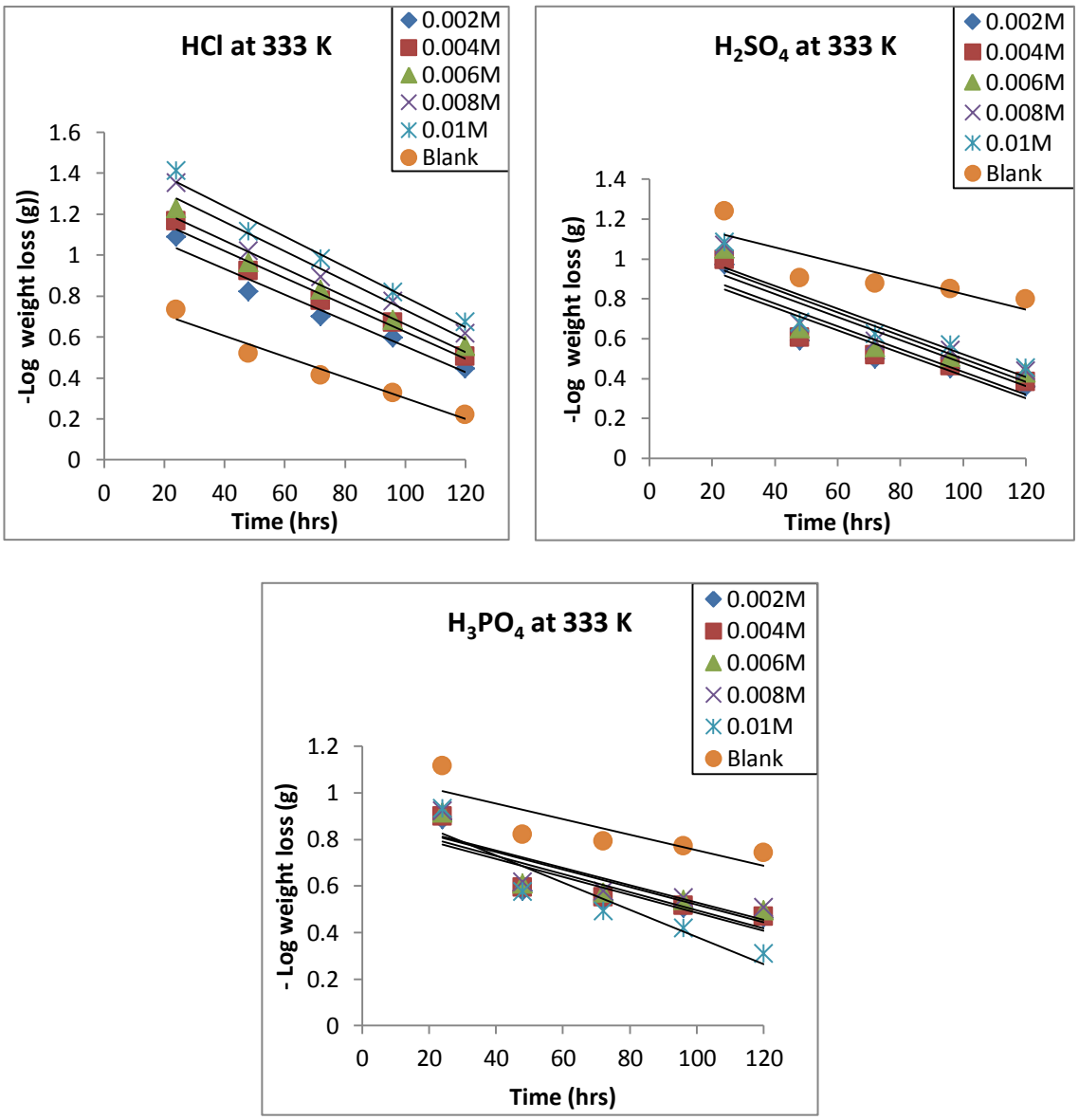


Figure 5.10. Plots of –log weight loss (g) versus time (hrs) for the corrosion of aluminium in 0.1 M HCl, H_2SO_4 and H_3PO_4 containing various concentrations of adenine (AD) at 333 K.

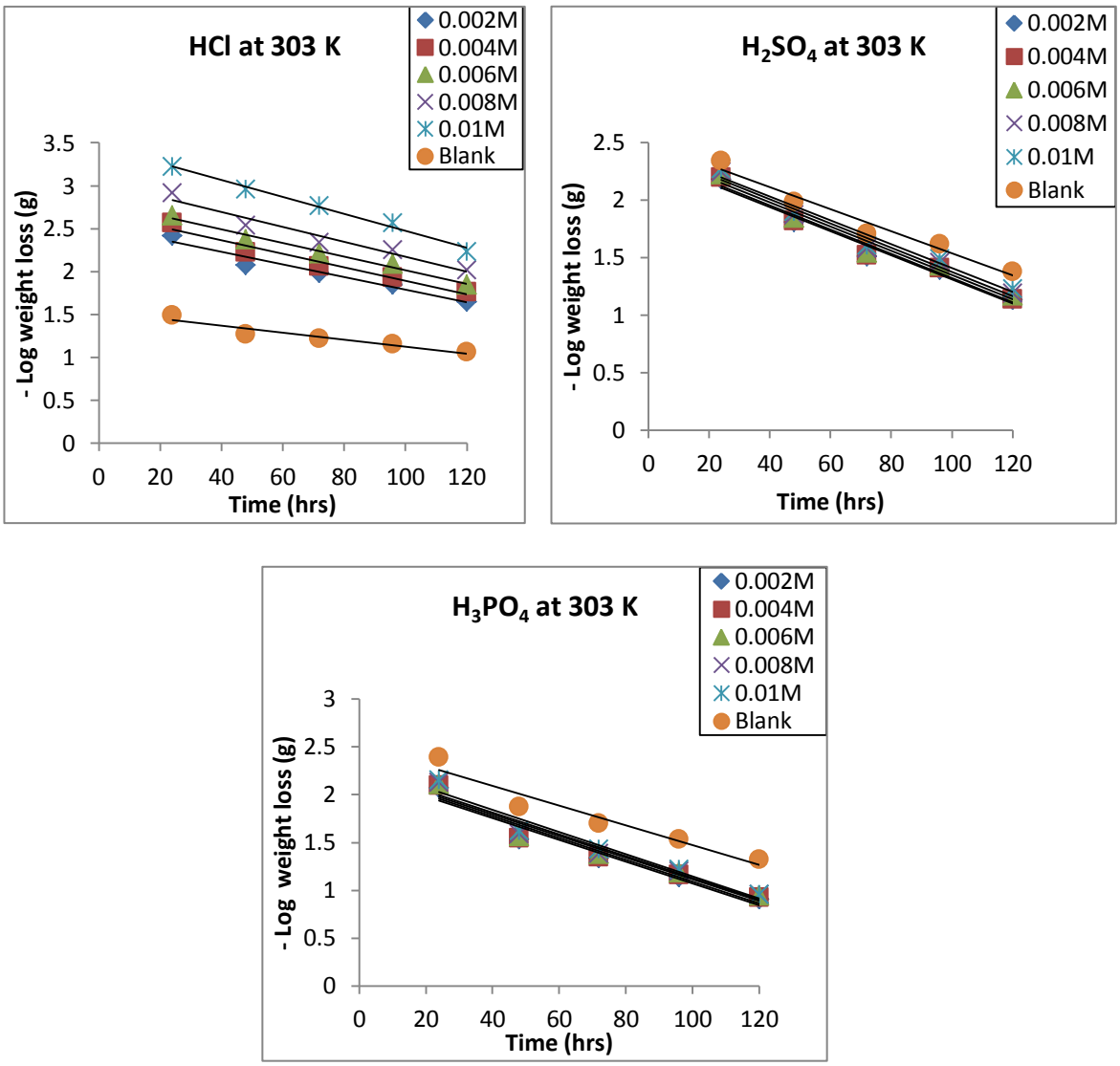


Figure 5.11. Plots of –log weight loss (g) versus time (hrs) for the corrosion of aluminium in 0.1 M HCl, H_2SO_4 and H_3PO_4 containing various concentrations of guanine (GU) at 303 K.

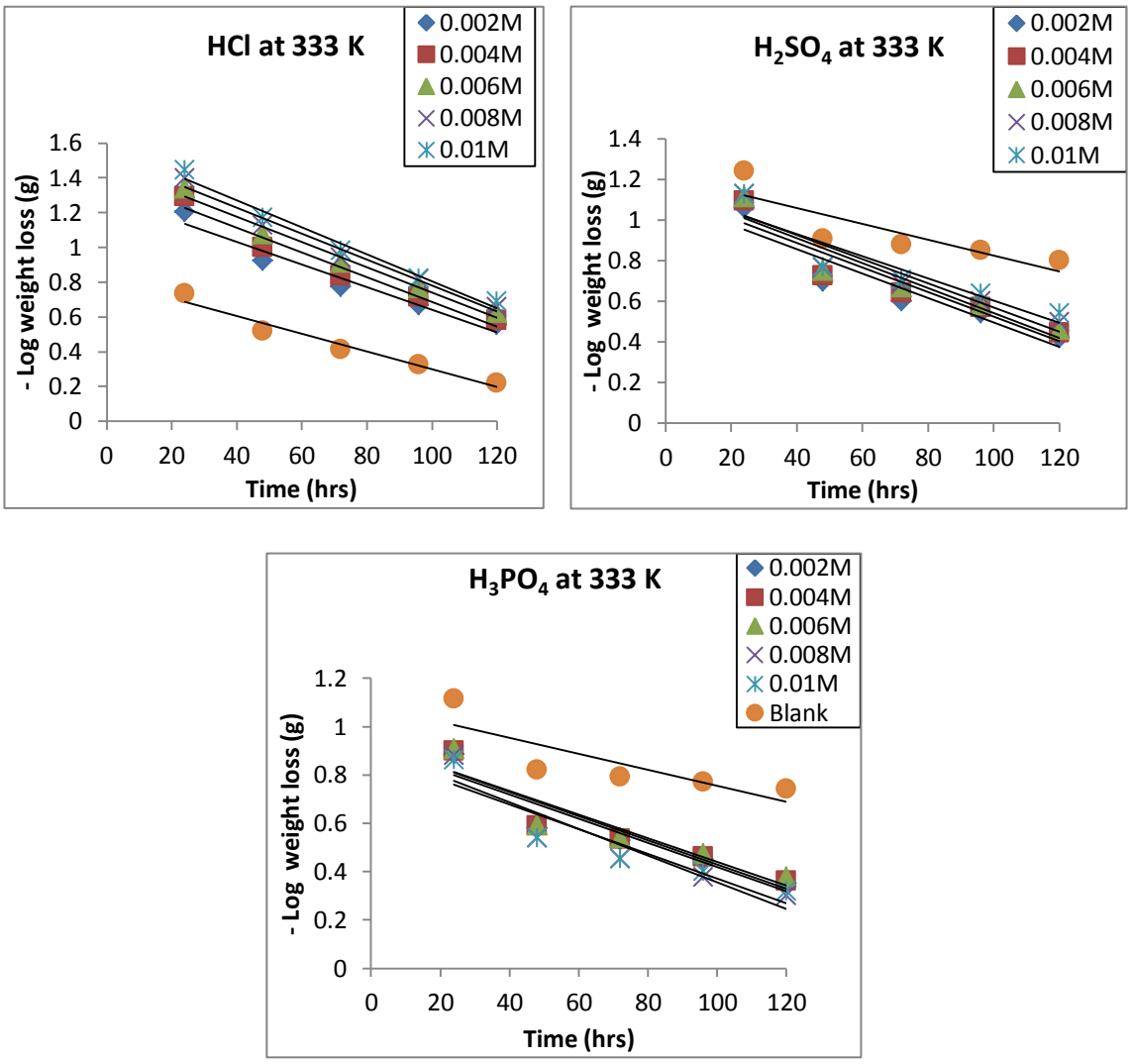


Figure 5.12. Plots of –log weight loss (g) versus time (hrs) for the corrosion of aluminium in 0.1 M HCl, H_2SO_4 and H_3PO_4 containing various concentrations of guanine (GU) at 333 K.

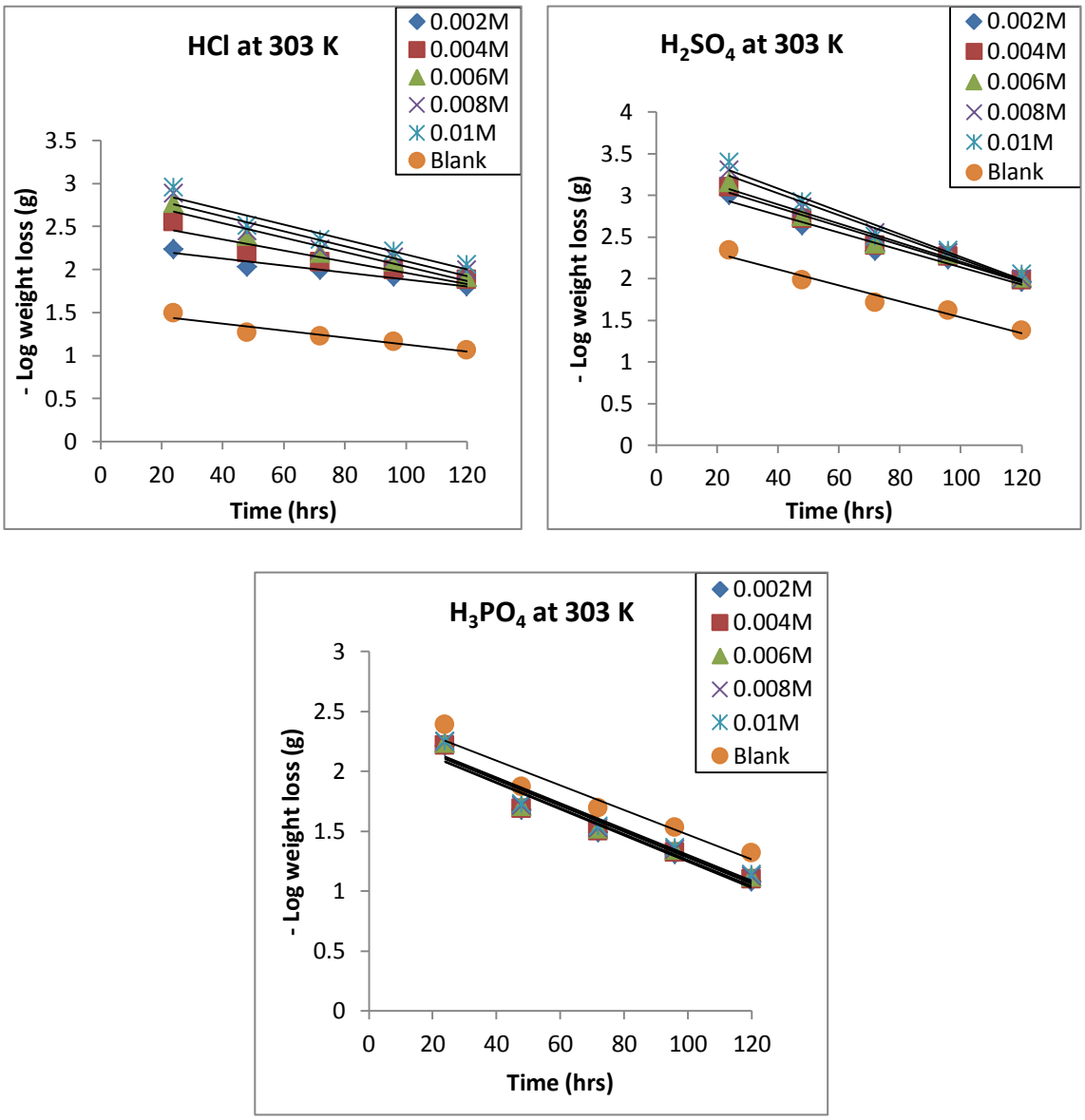


Figure 5.13. Plots of –log weight loss (g) versus time (hrs) for the corrosion of aluminium in 0.1 M HCl, H_2SO_4 and H_3PO_4 containing various concentrations of hypoxanthine (HYP) at 303 K.

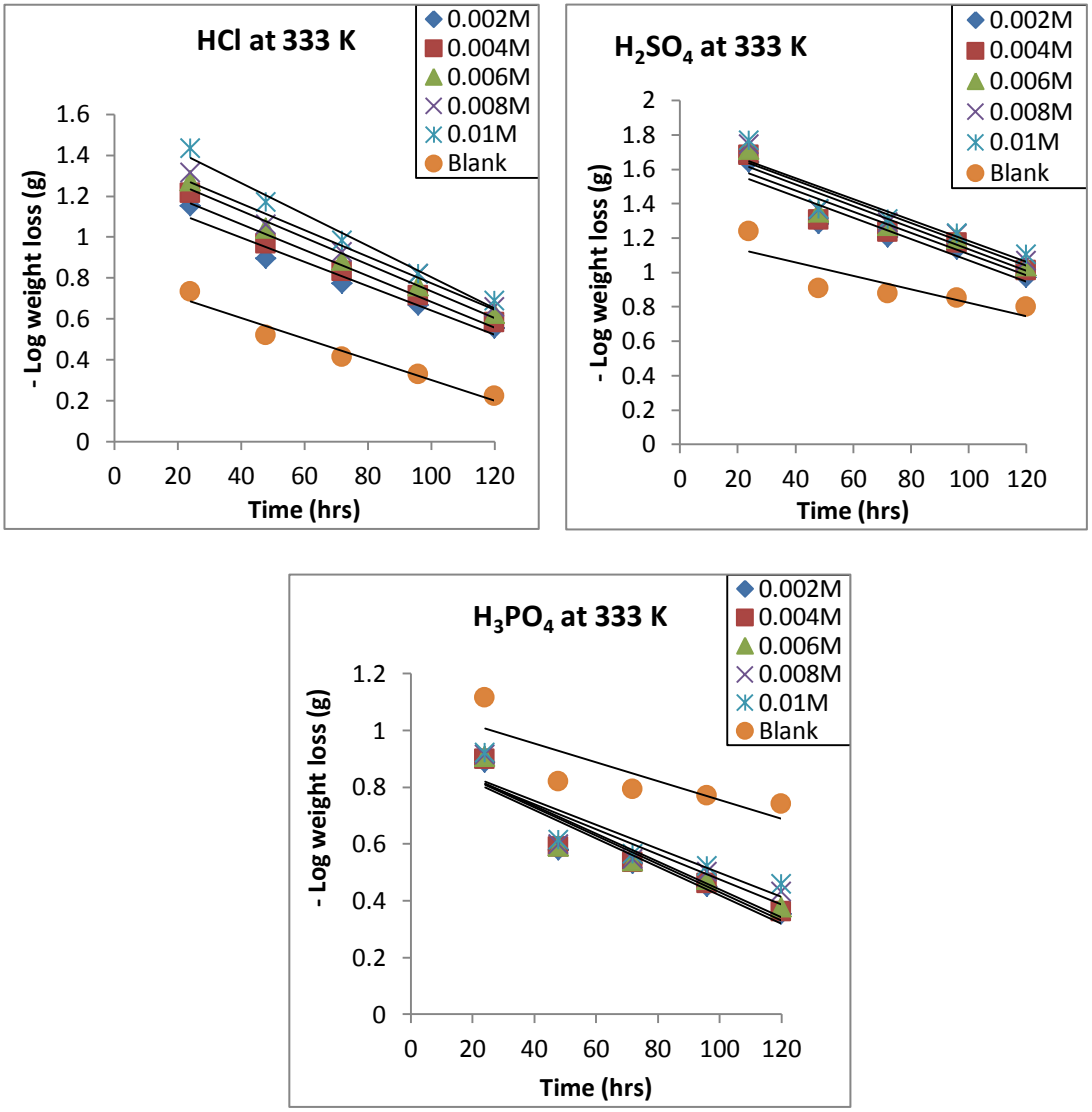


Figure 5.14. Plots of –log weight loss (g) versus time (hrs) for the corrosion of aluminium in 0.1 M HCl, H_2SO_4 and H_3PO_4 containing various concentrations of hypoxanthine (HYP) at 333 K.

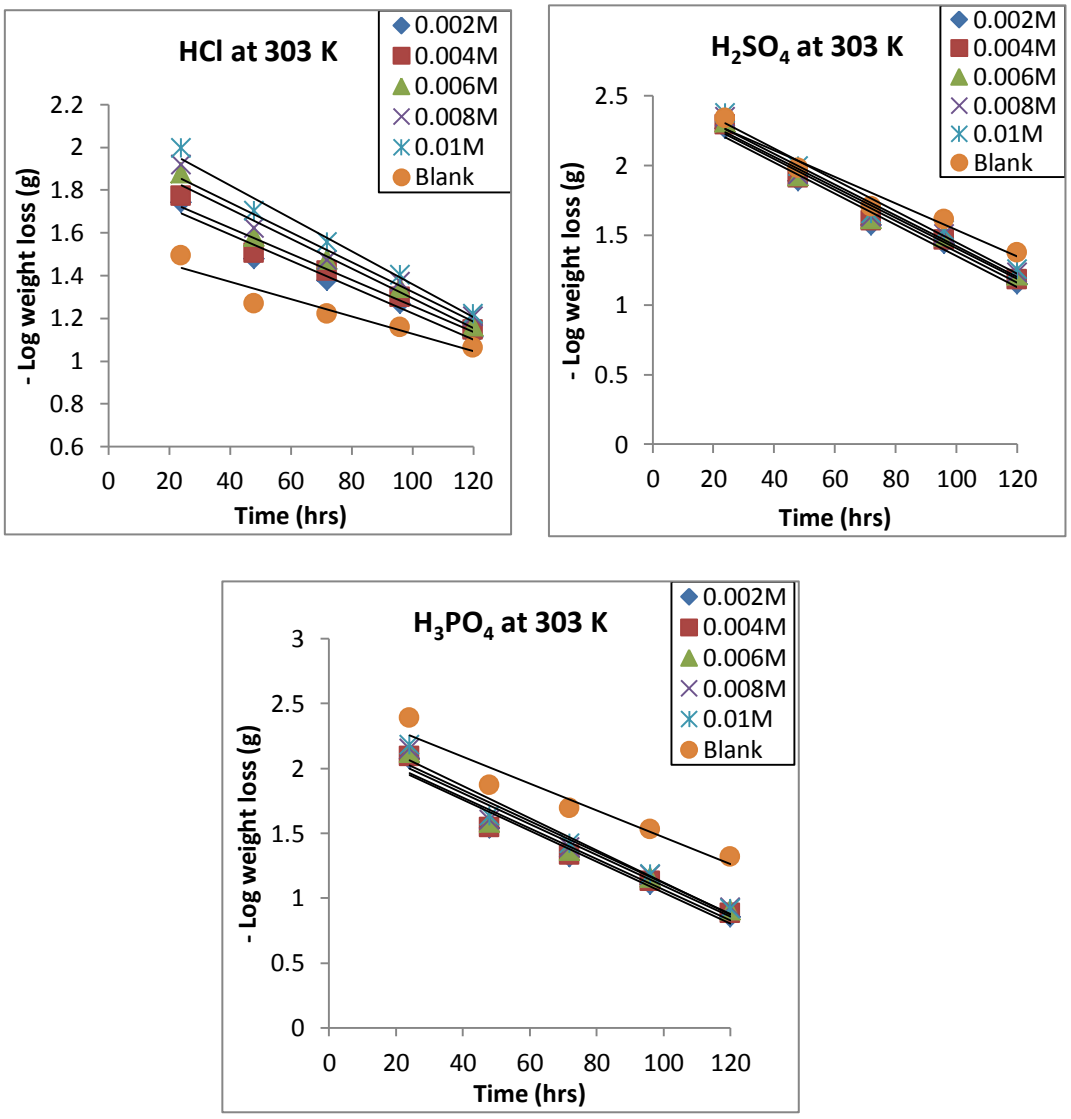


Figure 5.15. Plots of –log weight loss (g) versus time (hrs) for the corrosion of aluminium in 0.1 M HCl, H_2SO_4 and H_3PO_4 containing various concentrations of xanthine (XN) at 303 K.

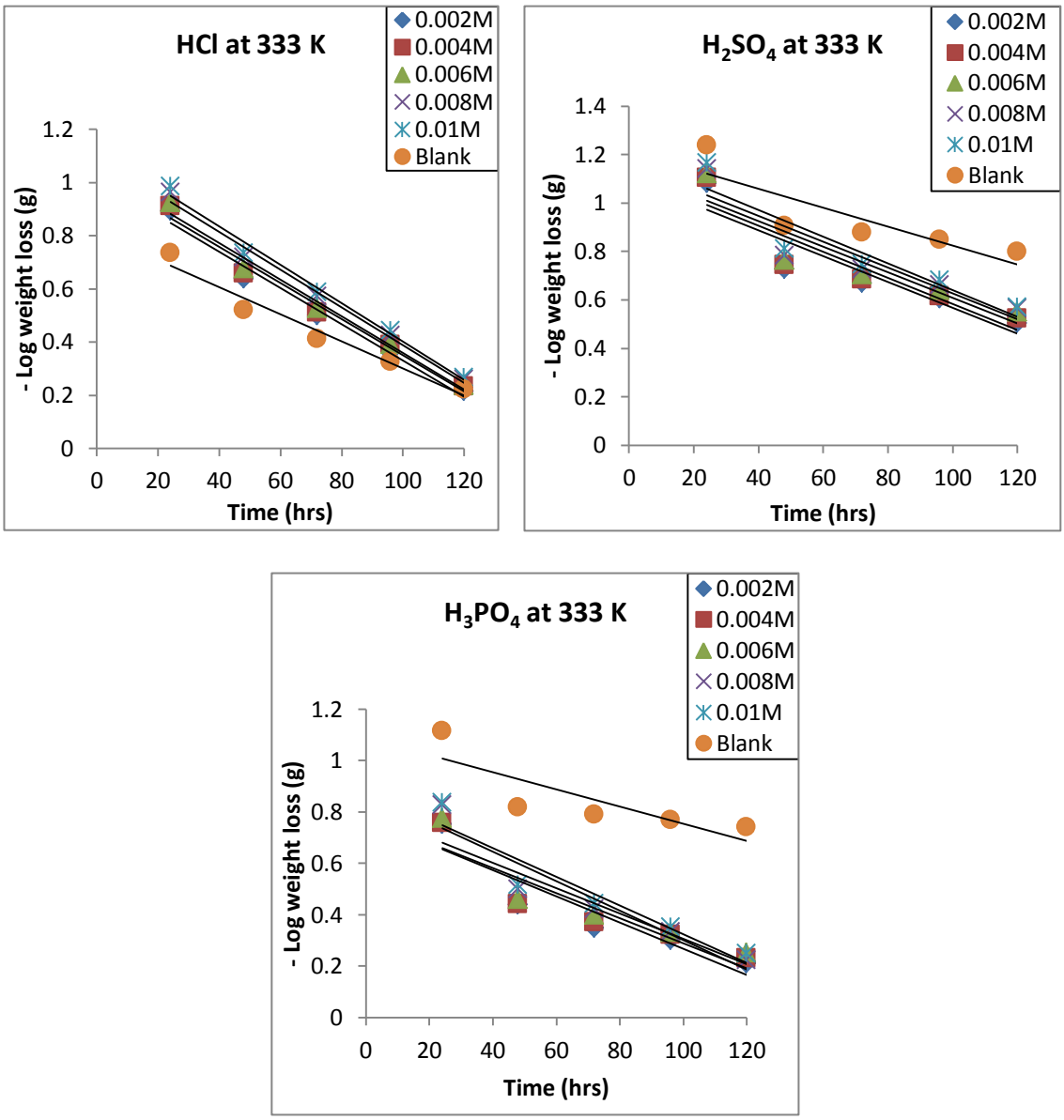


Figure 5.16. Plots of –log weight loss (g) versus time (hrs) for the corrosion of aluminium in 0.1 M HCl, H_2SO_4 and H_3PO_4 containing various concentrations of xanthine (XN) at 333 K.

The ability of the inhibitors to increase the half lives ($t_{½}$) of mild steel and aluminium in any of the acid media is a good indicator of their inhibitive properties as good corrosion inhibitors, therefore, the purine derivatives functioned as good corrosion inhibitors for mild steel in solutions of HCl, H_2SO_4 and H_3PO_4. However, for aluminium, all the purine derivatives inhibited the corrosion of aluminium in HCl while only HYP retarded the rate of aluminium dissolution in H_2SO_4. In H_3PO_4 solution, the purine derivatives acted as corrosion catalysts, accelerating the rate of corrosion of aluminium at both 303 and 333 K.

5.3 Effect of Temperature /Thermodynamics Study

A given inhibitor functions through a specific mechanism, depending on the type and composition of metal and corrodent, inhibitor structure and concentration as well as temperature. To assess the effect of temperature on corrosion and corrosion inhibition processes of mild steel and aluminium in HCl, H_2SO_4 and H_3PO_4, gravimetric experiments were performed at 303 and 333 K in the absence and presence of inhibitors in acid solutions containing 0.002- 0.01 M of the selected purines. The results obtained from weight losses, corrosion rates and IE% had been presented in Figures 4.1- 4.16 and Tables 4.1-4.4 which showed that corrosion rates in the absence and presence of inhibitors in acids increased at the higher temperature of 333 K. This implies that,

The effect of temperature on the inhibition of any metal by inhibitors is highly complex, because many changes may occur on the metal surface including rapid etching,

desorption of the inhibitor, and the inhibitor may undergo decomposition and/or rearrangement (Obot *et al.,* 2012).

From the results presented on Tables 4.1- 4.4 and Figures 4.1- 4.16, it is evident that corrosion rates in acid solutions and in the presence of inhibitors increased at the higher temperature of 333 K. Figures 4.1 – 4.8 showed that all the purine compounds were observed to maintain their inhibiting effects at both temperatures in all the acid media for mild steel systems while for aluminium systems (Figures 4.9-4.16), with the exception of hypoxanthine (HYP) in H_2SO_4, the other purines functioned as catalysts in H_2SO_4 and all the purines increased the corrosion of aluminium in H_3PO_4 solutions at both temperatures hence, resulting in negative inhibition efficiencies (%IE).

It is obvious from Figures 4.1 and 4.8 that corrosion rates were higher at 333 K for all systems. This is because a rise in temperature exponentially accelerates the rates of corrosion processes in media where hydrogen gas evolution accompanies corrosion, resulting in higher dissolution rates of metals. Higher rates of hydrogen gas generation increasingly agitate the metal/corrodent interface and could hinder inhibitor adsorption or perturb already adsorbed inhibitor, especially when the interaction between the metal and the inhibitor is relatively weak (Oguzie, 2012a,b). As a result, the efficiency of a considerable number of organic inhibitors is significantly reduced when the temperature of the system is increased, a trend often attributed to physical rather than chemical adsorption of the inhibiting species on the corroding metal surface (Eddy *et al.,* 2010; Adejo *et al.,* 2012). Figures 4.1-4.16 clearly show that the efficiency of the selected purines decreased at all concentrations studied with a rise in temperature in HCl acid for mild steel and aluminium systems, while the efficiencies of the purines improved at 333

K in H_2SO_4 and H_3PO_4 acid for only mild steel systems. This means that the interaction between each of AD, GU and XN with mild steel surface in H_2SO_4 and H_3PO_4 scaled up at a higher temperature. Improvement in inhibition efficiency with increasing temperature has been attributed to a change in the nature of adsorption, wherein the inhibitor is physically adsorbed at lower temperatures whilst chemisorption is favoured at higher temperatures (Popova *et al*., 2003).

The rate of a reaction is dependent on the rate constant, k. The higher the value of k, the higher the reaction rate. A modified form of the Arrhenius-type relationship between the corrosion rate (*CR*) of a metal in acidic media and temperature (*T)*, which can be written according to equation 5.3 (Eddy *et al*, 2009),

was used to determine the activation energies (E_a) of the corrosion and corrosion inhibition processes of mild steel and aluminium in the different acid media where *CR* is the corrosion rate of the metal, *A* is the Arrhenius or pre-exponential factor, E_a is the activation energy (i.e the minimum energy needed before the corrosion reaction of the metal can proceed), *R* is the universal gas constant and *T* is the absolute temperature of the system in Kelvin *(K).*

Taking logarithm of both sides of equation 5.3, equation 5.4 is obtained,

If the corrosion rates of the metal at two temperatures, T_1 (303 K) and T_2 (333 K) are known, (i.e CR_1 and CR_2 respectively), then equation 5.4 can be transformed to equation 5.5,

The activation energies calculated from equation 5.5 are presented on Tables 5.1 and 5.2 for mild steel and aluminium respectively.

From Tables 5.1 and 5.2, activation energies (E_a) have been observed to increase in solutions of HCl acid containing inhibitors for both mild steel and aluminium systems and decreased in solutions of H_2SO_4 and H_3PO_4 acids containing inhibitors for mild steel systems only compared to systems without inhibitors (blanks). The occurence of decreasing and increasing inhibition efficiencies at higher temperatures are evidence of specific physisorptive and chemisorptive interactions respectively, between the purine species and the metal surfaces (Oguzie *et al.,* 2005; Popova, 2007; Ekanem *et al.,* 2010).

This reasoning is corroborated by Yurt *et al* (2006), who suggested that the corrosion process in the presence of weak inhibitors is characterised by higher activation energies compared to that in the absence of the inhibitor while powerful inhibitors are characterized by lower activation energies compared to that in the absence of the inhibitor. Nevertheless, the adsorption of an organic molecule may not strictly be physical or chemical adsorption. A wide spectrum of conditions ranging from the dominance of chemisorption or electrostatic effects from other adsorption experimental data (Moretti *et al.,* 2004; Ahamad *et al.,* 2010; Döner *et al.,* 2011). Szauer and Brand (1981) explained that the increase in activation energy can be attributed to an appreciable decrease in the adsorption of the inhibitor on the mild steel surface with increase in temperature.

Table 5.1: Calculated activation energies (E_a) and heats of adsorption (Q_{ads}) for the corrosion of mild steel in 0.1 M HCl, H_2SO_4 and H_3PO_4 in the absence and presence of various concentrations of adenine (AD), guanine (GU), hypoxanthine (HYP) and xanthine (XN).

Inhibitor	Concentration (M)	Activation Energy, E_a (kJ mol^{-1})			Heat of Adsorption, Q_{ads} (kJ mol^{-1})		
		HCl	H_2SO_4	H_3PO_4	HCl	H_2SO_4	H_3PO_4
	Blank	49.02	34.86	29.87			
AD	0.002	52.96	29.96	27.67	-3.86	4.49	2.19
	0.004	53.23	30.59	28.38	-2.58	3.51	1.35
	0.006	53.32	30.40	28.58	-3.00	3.39	1.13
	0.008	57.45	30.96	29.34	-5.46	2.78	1.08
	0.01	60.81	30.63	30.62	-7.00	2.98	0.66
GU	0.002	51.40	26.04	27.88	-5.82	7.10	1.84
	0.004	52.05	25.70	28.36	-6.64	7.12	0.72
	0.006	52.34	22.21	28.76	-6.30	9.13	0.70
	0.008	52.07	21.34	29.11	-5.33	9.44	0.64
	0.01	52.26	18.99	29.87	-5.18	10.47	0.40
HYP	0.002	52.93	29.47	30.36	-3.98	3.98	-0.58
	0.004	52.34	30.59	30.16	-2.50	2.50	-0.35
	0.006	51.46	31.18	30.48	-1.68	1.68	-0.52
	0.008	55.51	31.96	30.53	-3.88	3.88	-0.54
	0.01	55.70	31.05	30.94	-3.86	3.86	-0.92
XN	0.002	53.21	32.15	27.73	-19.39	9.81	-38.63
	0.004	53.29	32.98	26.97	-15.83	9.11	-29.48
	0.006	54.32	34.18	26.99	-15.43	2.48	-26.49
	0.008	53.83	33.83	27.44	-11.05	2.99	12.27
	0.01	49.02	33.90	27.79	-10.58	2.31	9.27

Table 5.2: Calculated activation energies (E_a) and heats of adsorption (Q_{ads}) for the corrosion of aluminium in 0.1 M HCl, H_2SO_4 and H_3PO_4 in the absence and presence of various concentrations of adenine (AD), guanine (GU), hypoxanthine (HYP) and xanthine (XN).

Inhibitor	Concentration (M)	Activation Energy, E_a (kJ mol^{-1})			Heat of adsorption, Q_{ads} (kJ mol^{-1})		
		HCl	H_2SO_4	H_3PO_4	HCl	H_2SO_4	H_3PO_4
	Blank	52.13	50.54	52.08			
AD	0.002	69.10	58.67	55.78	-10.58	NIL	NIL
	0.004	68.31	59.67	55.40	-9.15		
	0.006	73.44	58.04	55.71	-11.20		
	0.008	74.66	57.83	55.80	-10.84		
	0.01	78.94	61.19	55.88	-12.28		
GU	0.002	72.34	55.04	54.73	-10.48	NIL	NIL
	0.004	76.39	53.68	55.03	-12.01		
	0.006	77.46	53.38	55.45	-14.72		
	0.008	82.39	53.60	54.96	-18.18		
	0.01	84.55	54.27	55.05	-24.37		
HYP	0.002	78.69	70.94	56.01	-14.19	-12.03	NIL
	0.004	82.35	71.05	55.47	-15.23	-11.43	
	0.006	85.18	71.30	55.31	-15.86	-11.33	
	0.008	86.93	71.09	56.22	-16.21	-10.93	
	0.01	88.98	72.19	55.76	-16.69	-11.21	
XN	0.002	56.39	55.46	55.62	-7.08	NIL	NIL
	0.004	57.28	56.17	55.81	-7.52		
	0.006	60.29	56.18	56.47	-10.15		
	0.008	60.10	56.15	57.10	-8.44		
	0.01	61.51	55.59	56.99	-8.86		

NOTE:

NIL- No surface coverage (ie, θ = negative values)

However, Vracar and Drazic (2002) opined that the criteria of adsorption type obtained from the change of activation energy cannot be conclusive due to competing adsorption of water molecules, whose removal from the metal surface also involves some activation energy. In other words, the so-called physical adsorption process may contain chemisorption process simultaneously and vice versa as reported by other investigators (Döner *et al*, 2011; Obot *et al.*, 2012; Oguzie *et al.*, 2012a).

Another thermodynamic parameter which can further be used to verify adsorption mechanisms in a corrosion inhibition process is the heat of adsorption, Q_{ads}. Its relationship with the degree of surface coverage, θ , is given by equation 5.6

where θ_1 and θ_2 are values of the degree of surface coverage at temperatures T_1 and T_2, respectively.

From the calculated values of Q_{ads} presented on Tables 5.1 and 5.2, negative Q_{ads} values indicate an exothermic process with a decrease in inhibition efficiency at a higher temperature while positive Q_{ads} values indicate an endothermic process resulting in an increase in the inhibition efficiency with a rise in temperature (Khaled, 2003; Oguzie *et al.*, 2012b).

Negative Q_{ads} values were obtained for the inhibition of steel and aluminium by the following selected purines: AD, GU, HYP and XN in HCl acid for both mild steel and aluminium systems (Tables 5.1 and 5.2), HYP in H_2SO_4 acid for mild steel and

aluminum systems (Tables 5.1 and 5.2), and HYP in H_3PO_4 acid for mild steel (Table 5.1). This implies that the inhibition efficiencies of these purines decreased at 333 K in these media which is a good indication of an electrostatic kind of interaction between these purines and the metal surfaces. Chemisorption was observed for the inhibition mechanism of AD, GU and XN in H_2SO_4 and H_3PO_4 acids on mild steel.

The purine compounds functioned as catalysts in H_2SO_4 (except for HYP in H_2SO_4) and H_3PO_4 solutions for aluminium systems hence, there was no surface coverage of the aluminium surface by these compounds resulting in negative inhibition efficiencies.

5.4 Adsorption Study

Assuming a direct relationship between inhibition efficiency and the degree of surface coverage (θ) for different inhibitor concentrations, data obtained from gravimetric measurements were used to determine the fit to some well-known adsorption isotherms including the Langmuir, Freundlich, Temkin, Flory–Huggins, the kinetic–thermodynamic model of El-Awady (El-Awady *et al.,* 1992) and Frumkin isotherms. The generalised expression for the common adsorption isotherms is of the form of equation 5.7 (El-Awady *et al.,* 1992; Martinez, 2003; Ashassi-Sorkhabi *et al.,* 2008; Oguzie *et al.,* 2012b):

where $f(\theta, x)$ is the configuration factor, which depends on the physical model adopted and the assumptions made to derive isotherm equations. The parameter x is the size ratio which represents the relative size of the adsorbed molecule to the solvent molecule. Specifically, in the case of corrosion inhibitors in aqueous solutions, x represents the number of water molecules replaced by adsorbed inhibitor as shown in equation 5.8

where α is the molecular interaction parameter which accounts for the lateral interaction between adsorbed species (Shibli and Saji, 2005), whilst the quantity *C* is the inhibitor concentration and *k* is the adsorption equilibrium constant. The functional and linear forms of the isotherm equations tested in this study are given in Appendix X.

The degrees of surface coverage, θ, at various concentrations of the selected purines at 303 and 333 K were the data used for plotting the isotherms. The data were tested with the different adsorption isotherm equations viz Langmuir (Figures 5.17 – 5.22), Freundlich (Figures 5.23 -5.28), Temkin (Figure 5.29 – 5.34), Flory-Huggins (Figures 5.35 – 5.40), El-Awady (Figures 5.41 – 5.46) and Frumkin models (Figures 5.47 – 5.52). Appendices XI -XV show the parameters of linearisation of each adsorption model.

The surface coverage obtained from IE% values fitted all the adsorption models since the values of the regression coefficient, R^2, were greater than 0.9 (Saratha *et al.*, 2009). The calculated values of the adsorption equilibrium constant, k_{ads}, were very high especially for the Temkin isotherm reflecting the high adsorption ability of the purines on the aluminium and mild steel surfaces.

Sometimes, it may be sufficient to confirm inhibitor adsorption from data which fit the isotherms. Often times, it is also desirable to extend the scope to include deduction of thermodynamic parameters associated with the adsorption process using the relationship between the adsorption equilibrium constant (k_{ads}) and the standard free energy of adsorption, $\Delta G_{ads}°$ using equation 5.9

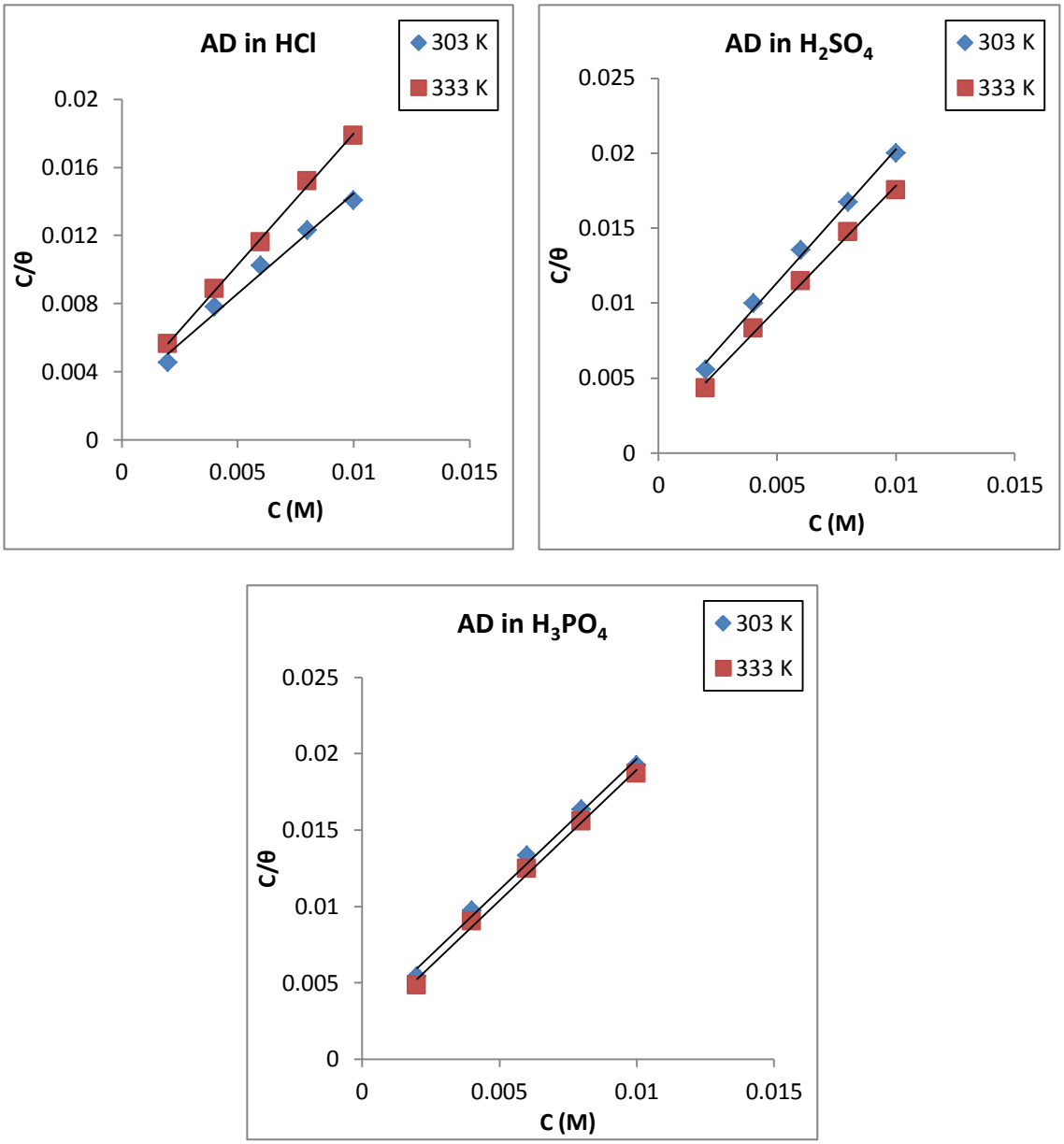


Figure 5.17. Langmuir isotherm for the adsorption of adenine (AD) on mild steel surface in 0.1 M solutions of HCl, H_2SO_4 and H_3PO_4 at 303 and 333 K.

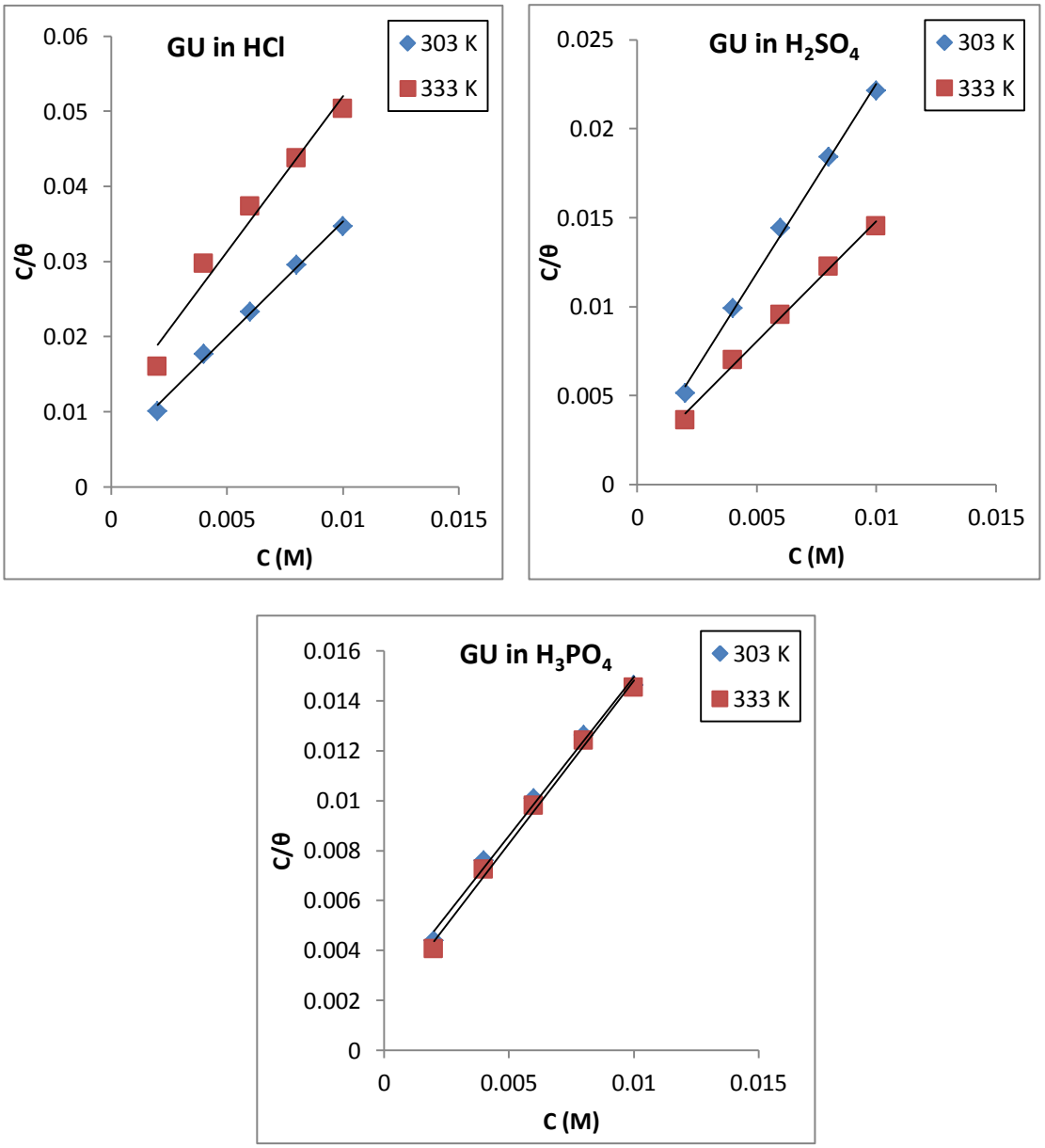


Figure 5.18. Langmuir isotherm for the adsorption of guanine (GU) on mild steel surface in 0.1 M solutions of HCl, H_2SO_4 and H_3PO_4 at 303 and 333 K.

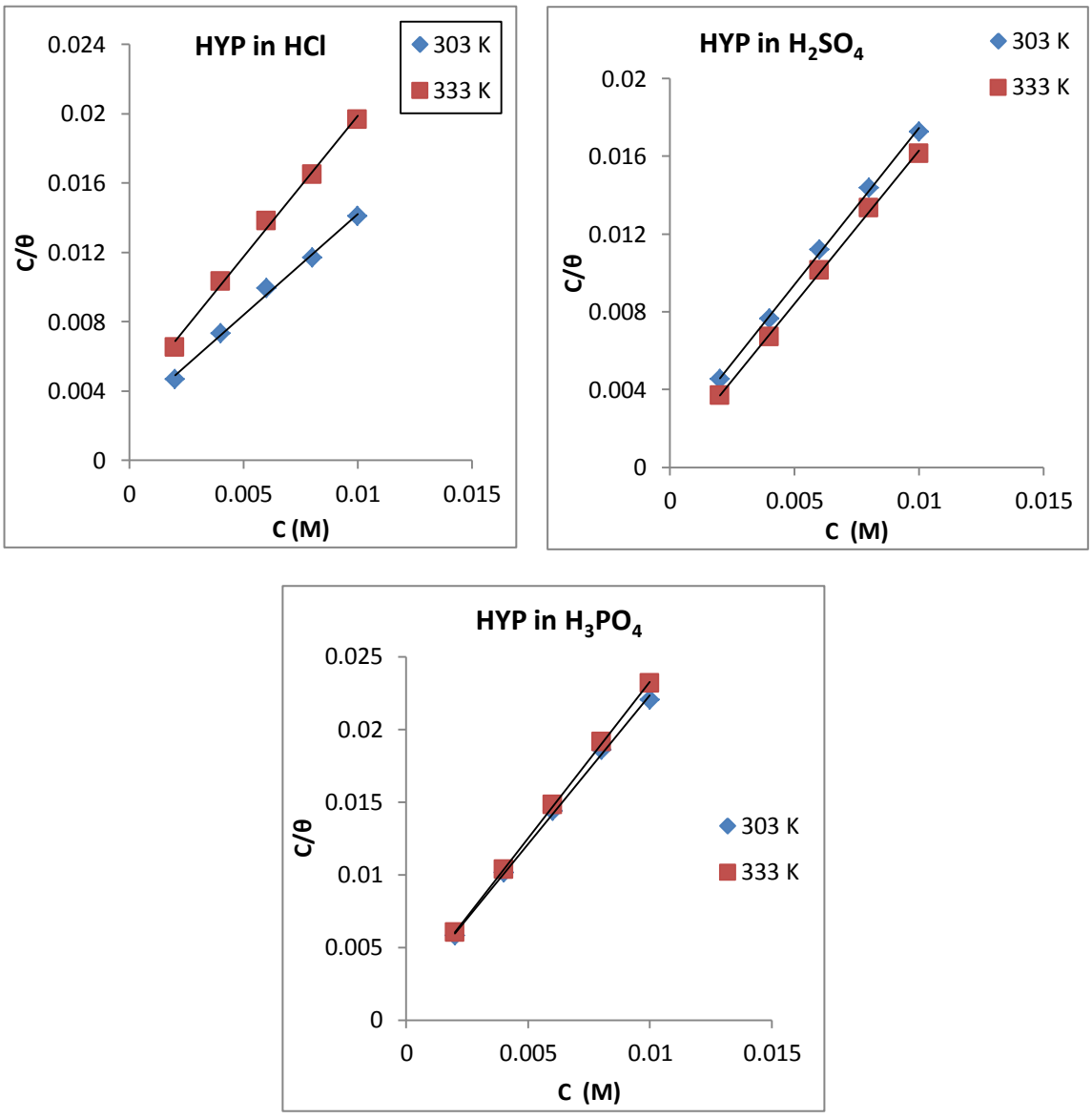


Figure 5.19. Langmuir isotherm for the adsorption of hypoxanthine (HYP) on mild steel surface in 0.1 M solutions of HCl, H_2SO_4 and H_3PO_4 at 303 and 333 K.

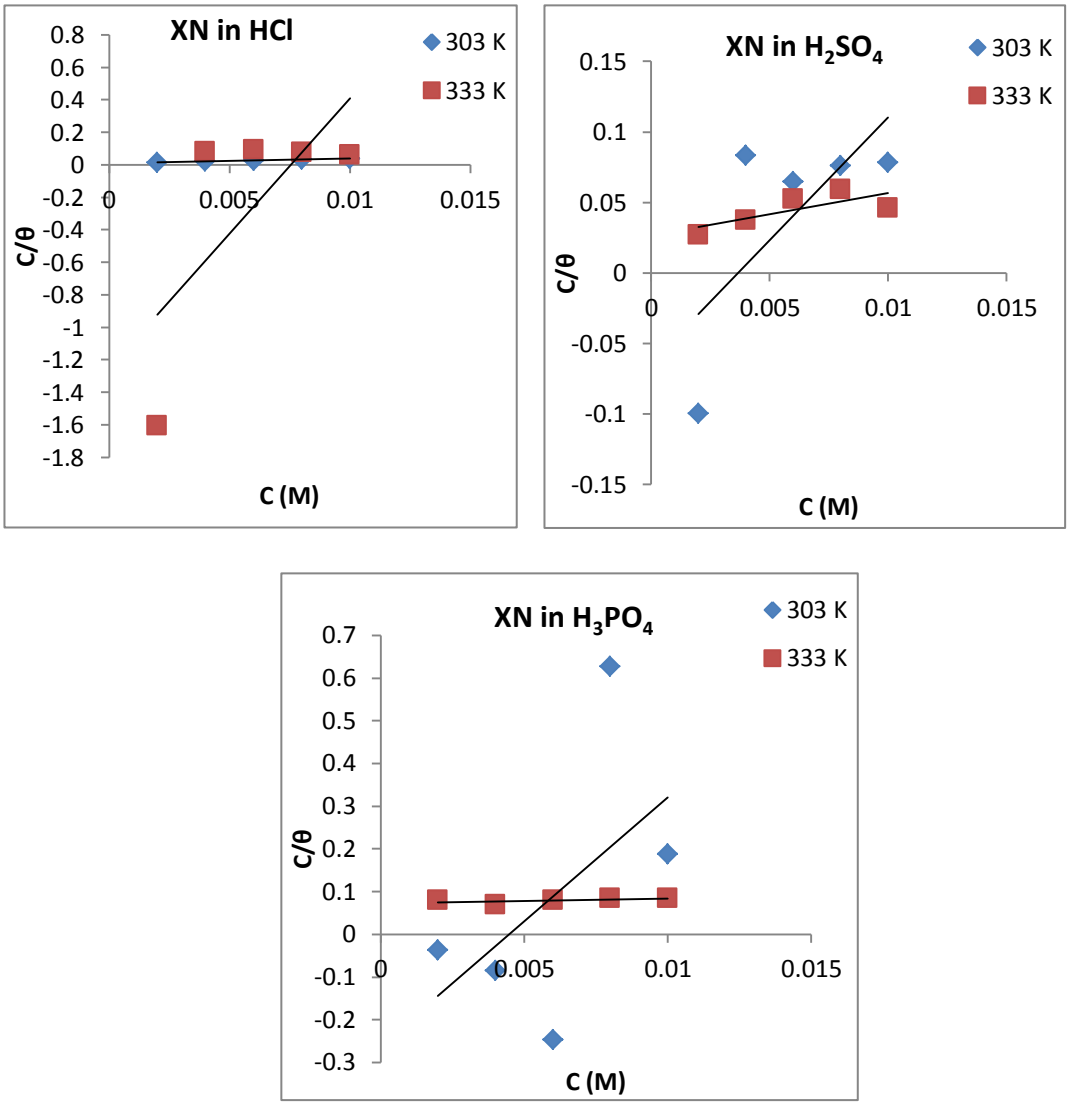


Figure 5.20. Langmuir isotherm for the adsorption of xanthine (XN) on mild steel surface in 0.1 M solutions of HCl, H_2SO_4 and H_3PO_4 at 303 and 333 K.

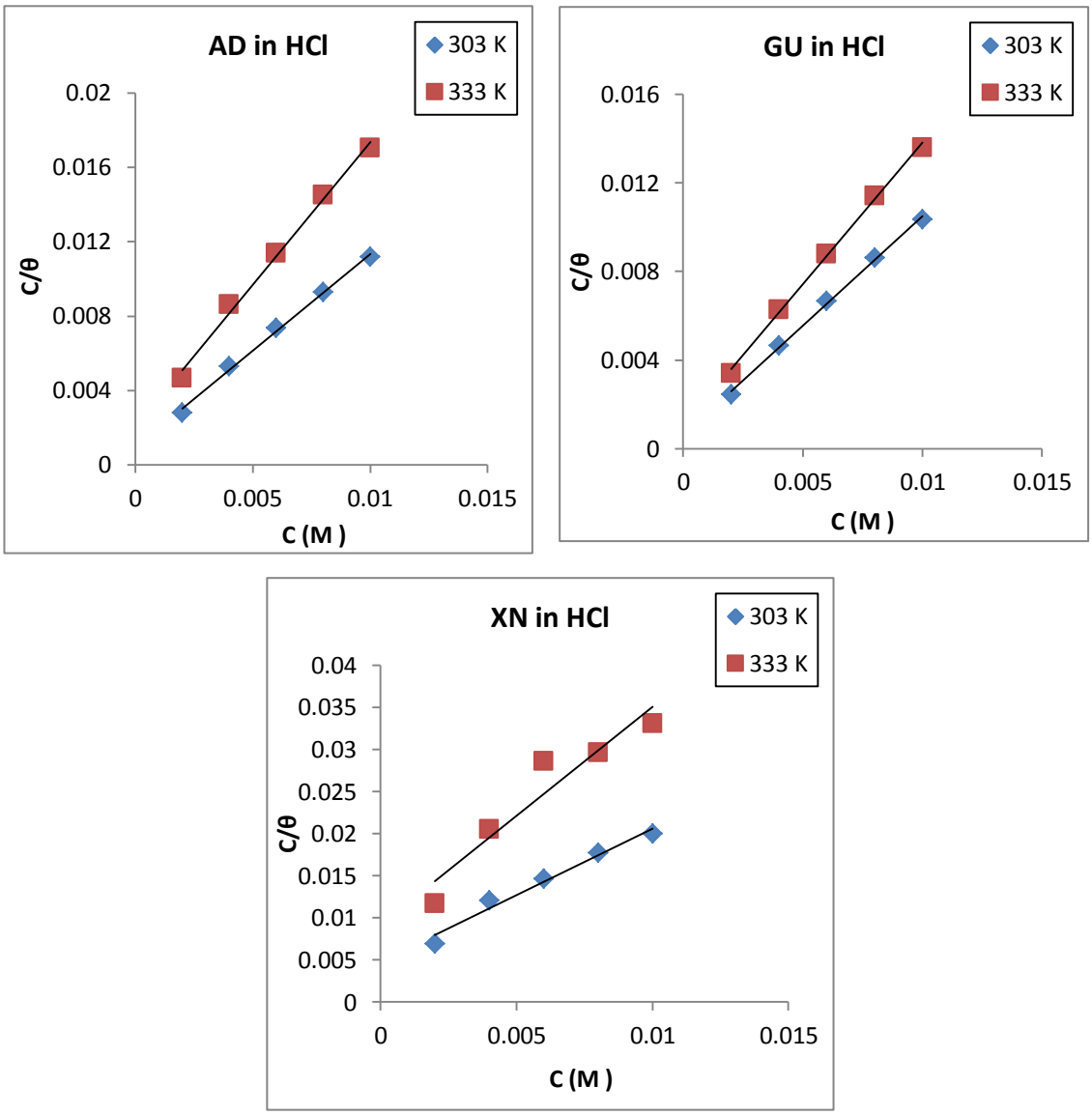
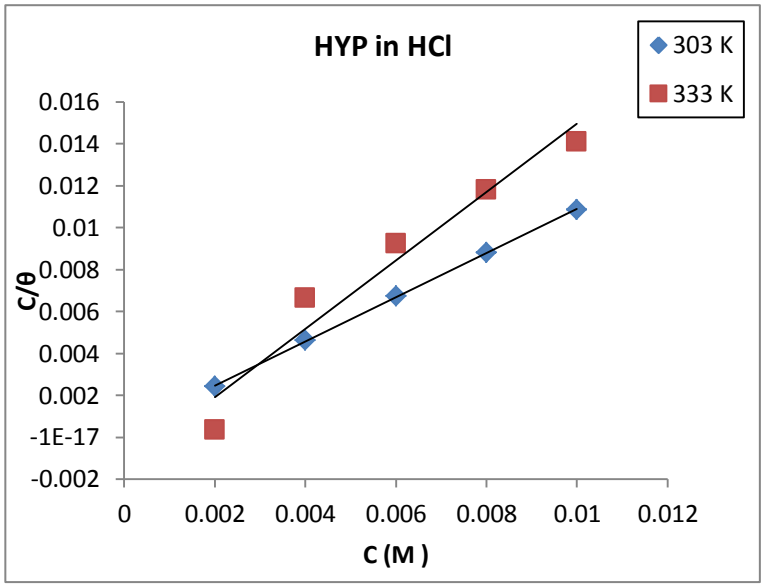


Figure 5.21. Langmuir isotherm for the adsorption of adenine (AD), guanine (GU) and xanthine (XN) on aluminium surface in 0.1 M solution of HCl, H_2SO_4 and H_3PO_4 at 303 and 333 K.



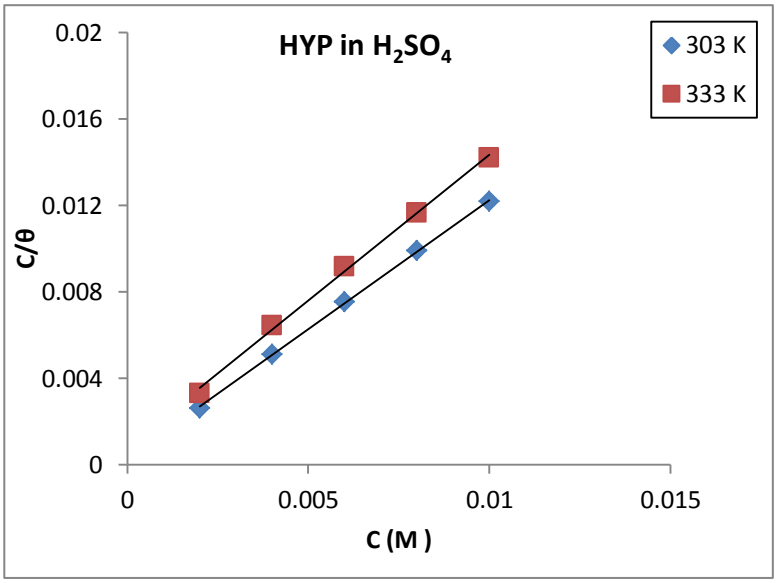


Figure 5.22. Langmuir isotherm for the adsorption of hypoxanthine (HYP) on aluminium surface in 0.1 M solutions of HCl and H_2SO_4 at 303 and 333 K.

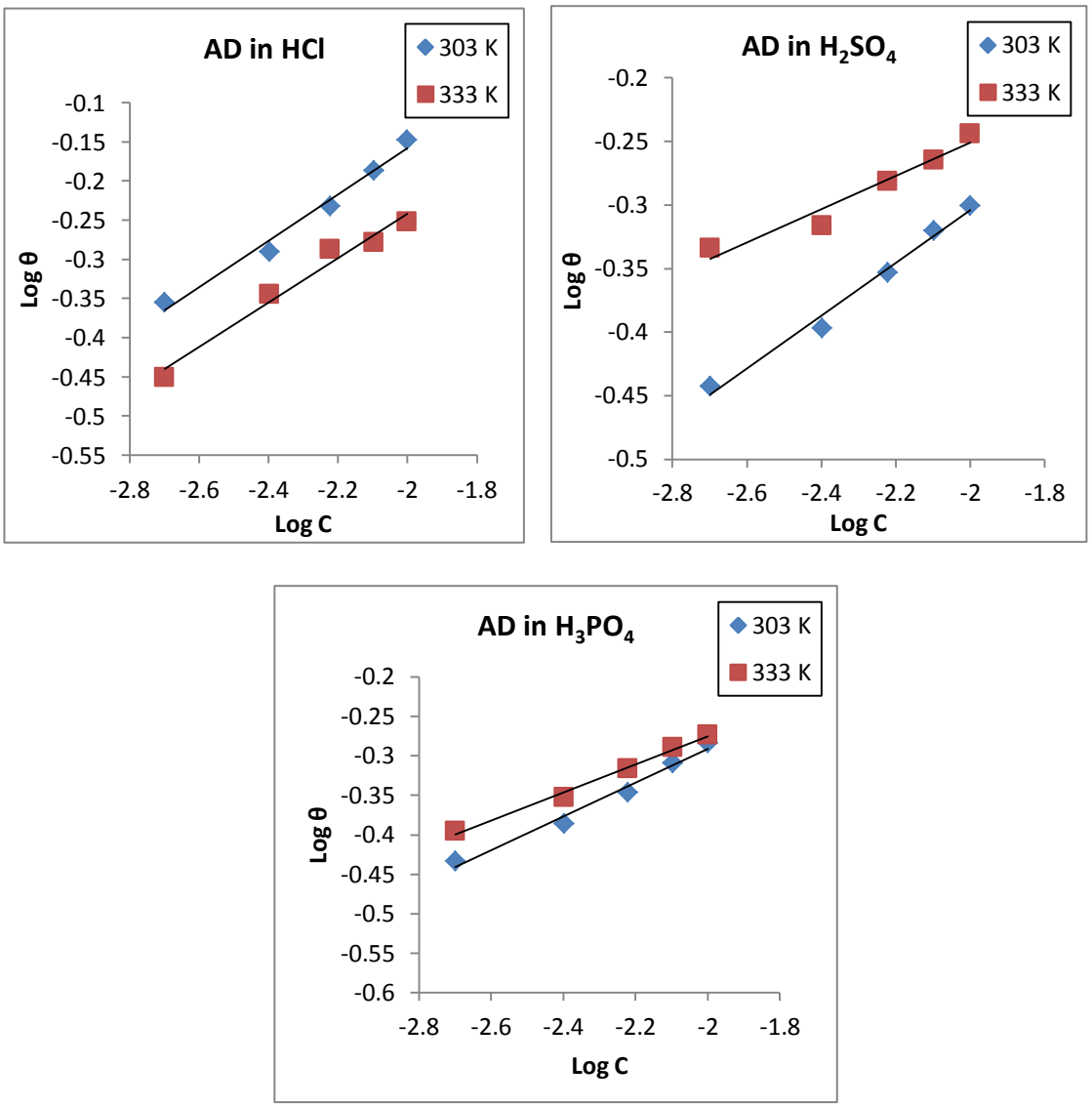


Figure 5.23. Freundlich isotherm for the adsorption of adenine (AD) on mild steel surface in 0.1 M solutions of HCl, H_2SO_4 and H_3PO_4 at 303 and 333 K.

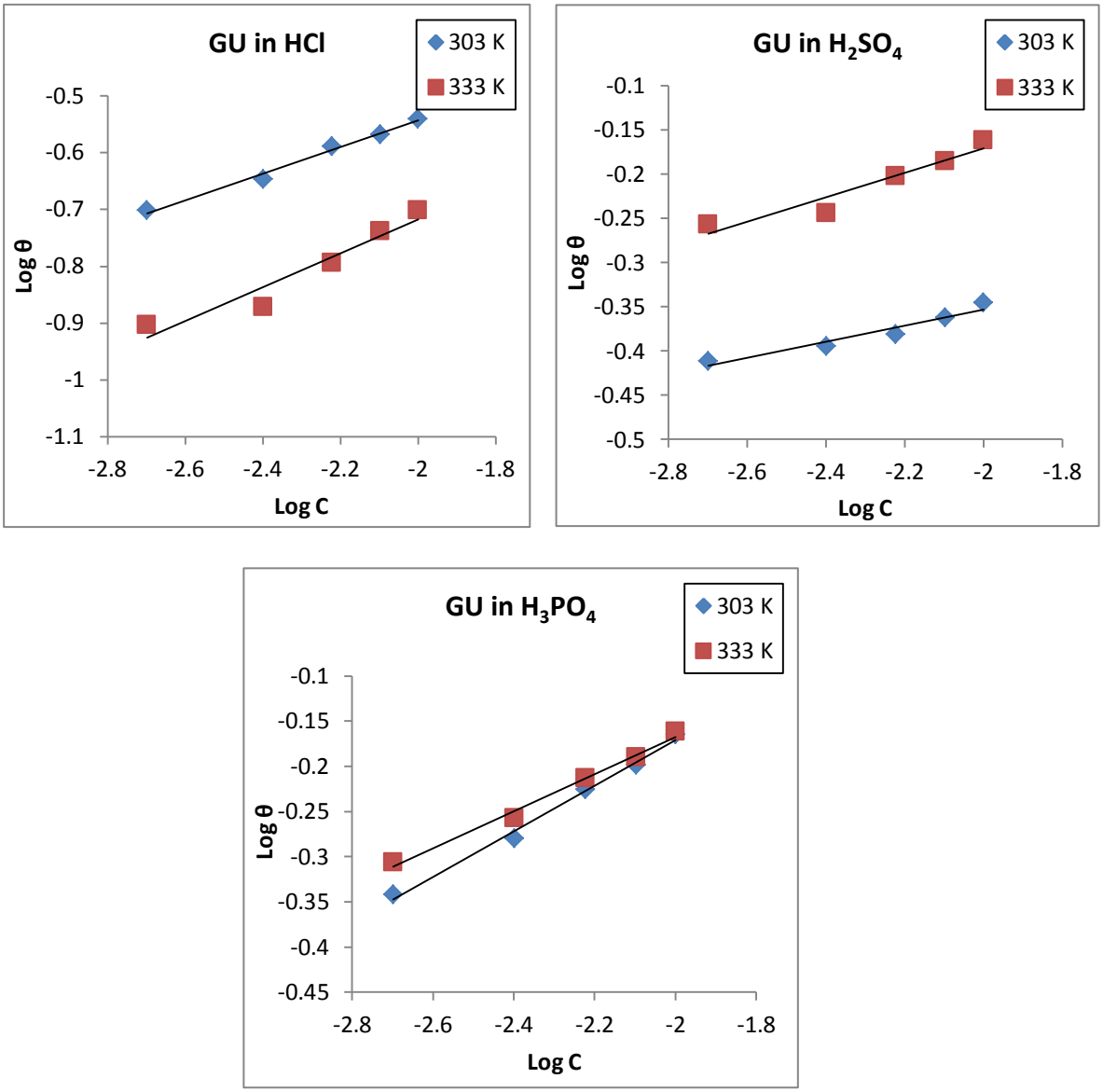


Figure 5.24. Freundlich isotherm for the adsorption of guanine (GU) on mild steel surface in 0.1 M solutions of HCl, H_2SO_4 and H_3PO_4 at 303 and 333 K.

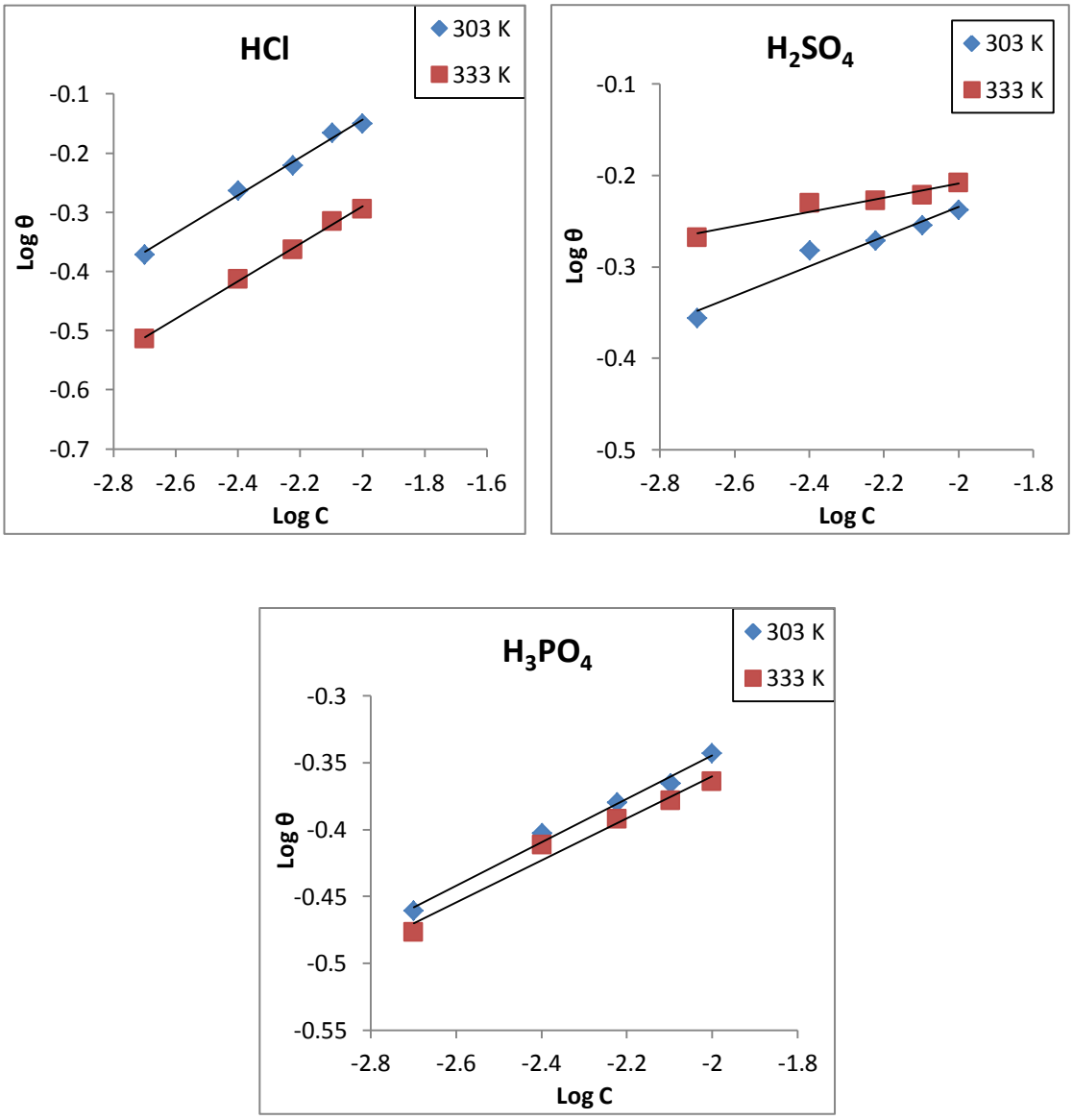


Figure 5.25. Freundlich isotherm for the adsorption of hypoxanthine (HYP) on mild steel surface in 0.1 M solutions of HCl, H_2SO_4 and H_3PO_4 at 303 and 333 K.

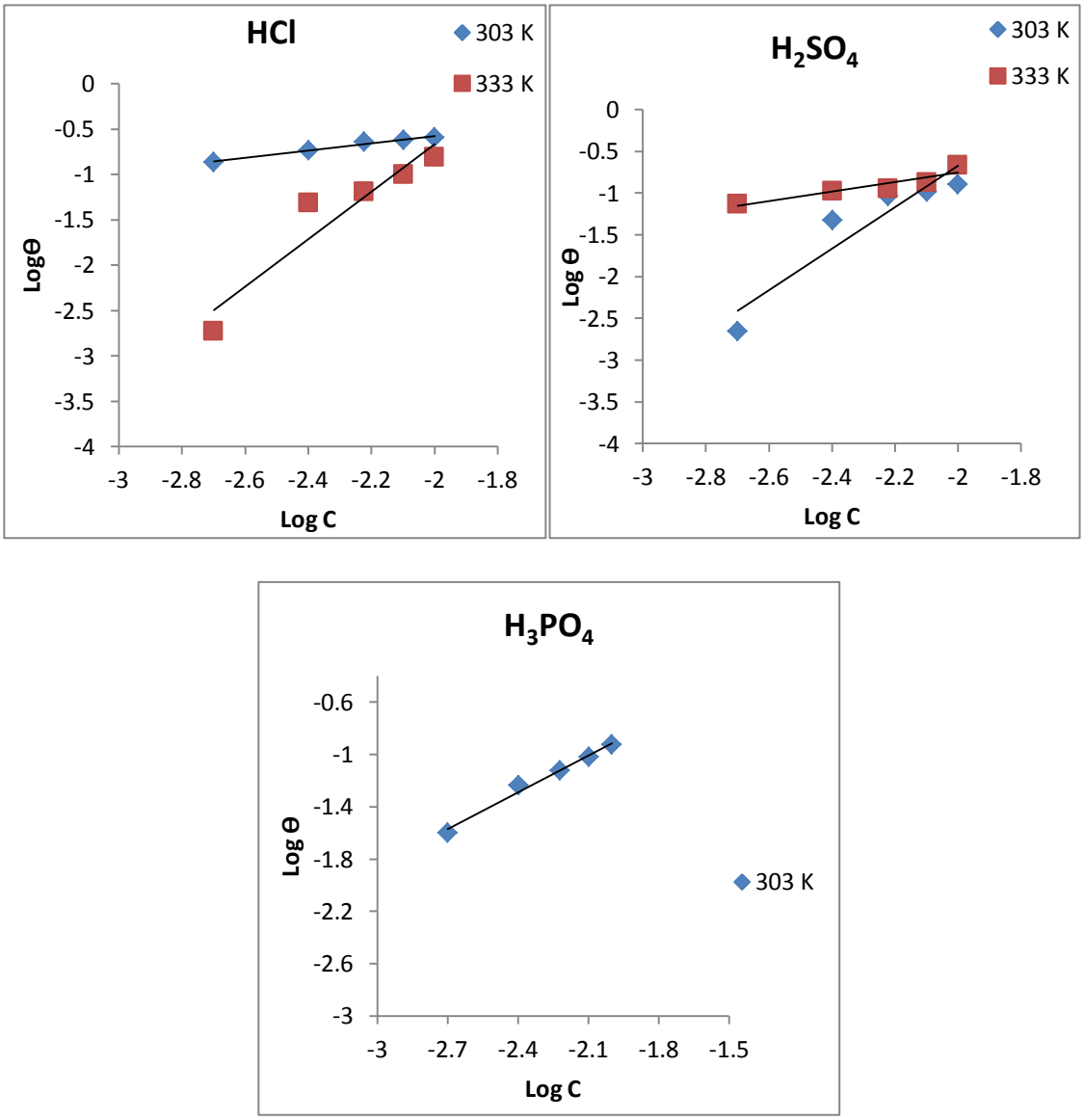


Figure 5.26. Freundlich isotherm for the adsorption of xanthine (XN) on mild steel surface in 0.1 M solutions of HCl, H_2SO_4 and H_3PO_4 at 303 and 333 K.

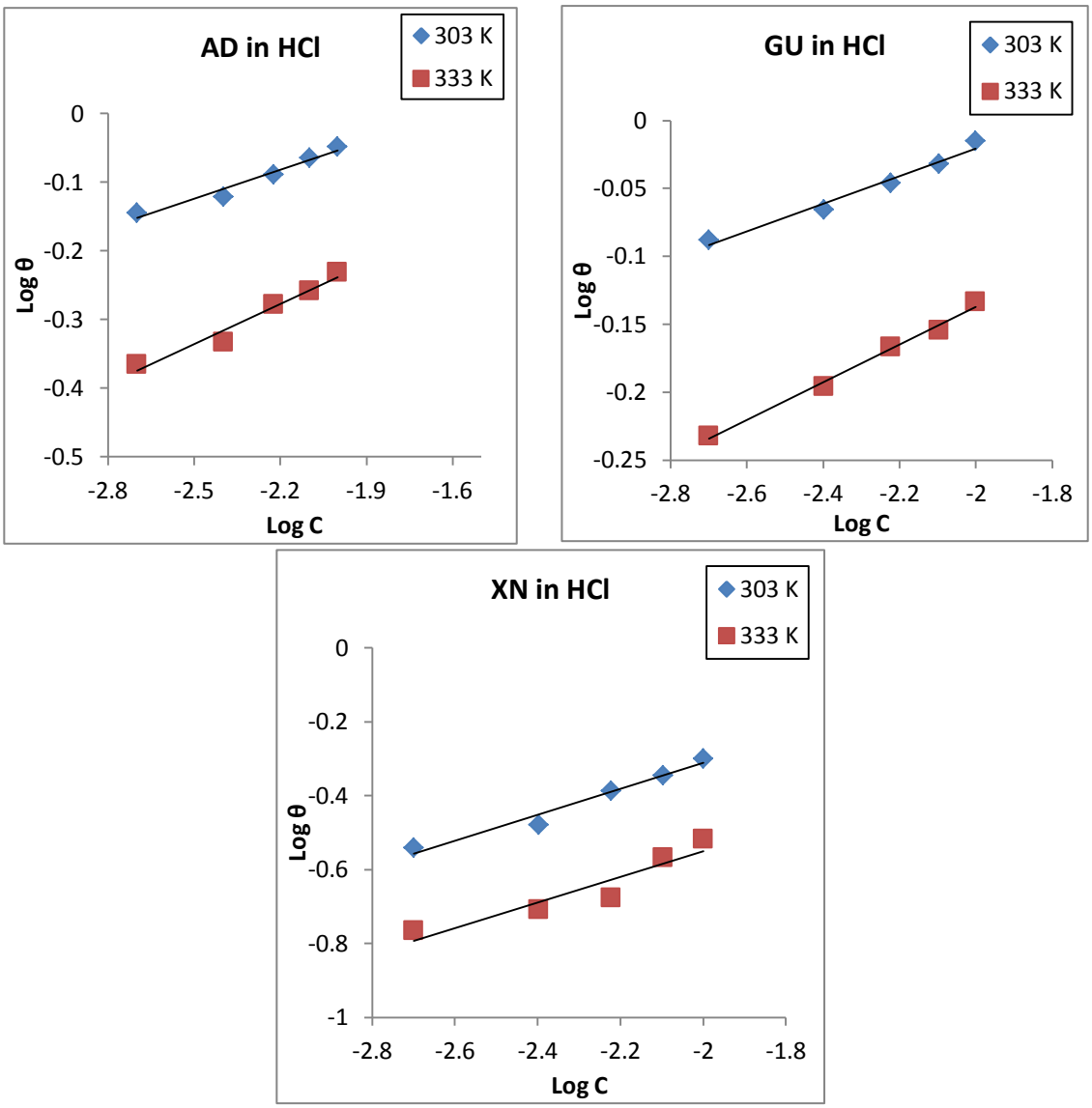
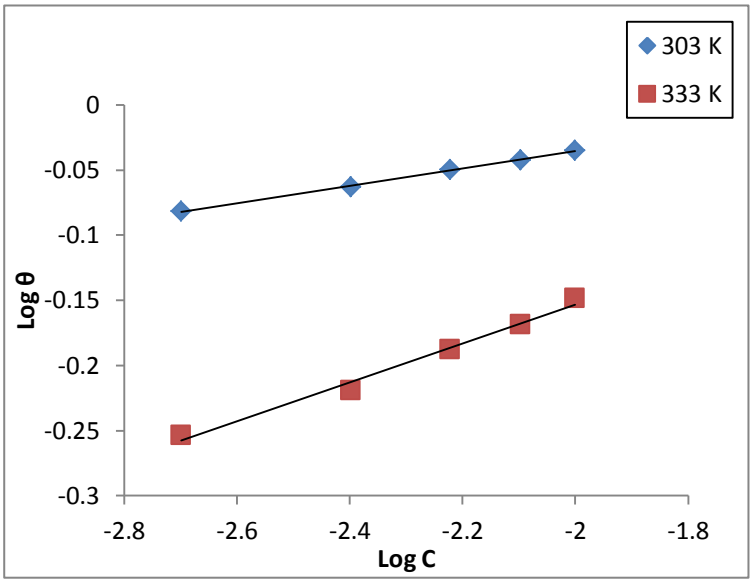


Figure 5.27. Freundlich isotherm for the adsorption of adenine (AD), guanine (GU) and xanthine (XN) on aluminium surface in 0.1 M solutions of HCl at 303 and 333 K.



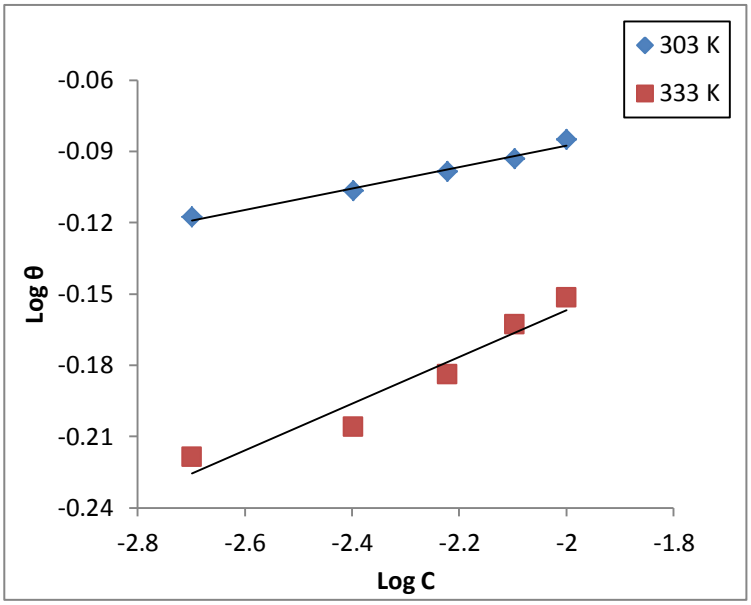


Figure 5.28. Freundlich isotherm for the adsorption of hypoxanthine (HYP) on aluminium surface in 0.1 M solutions of HCl and H_2SO_4 at 303 and 333 K.

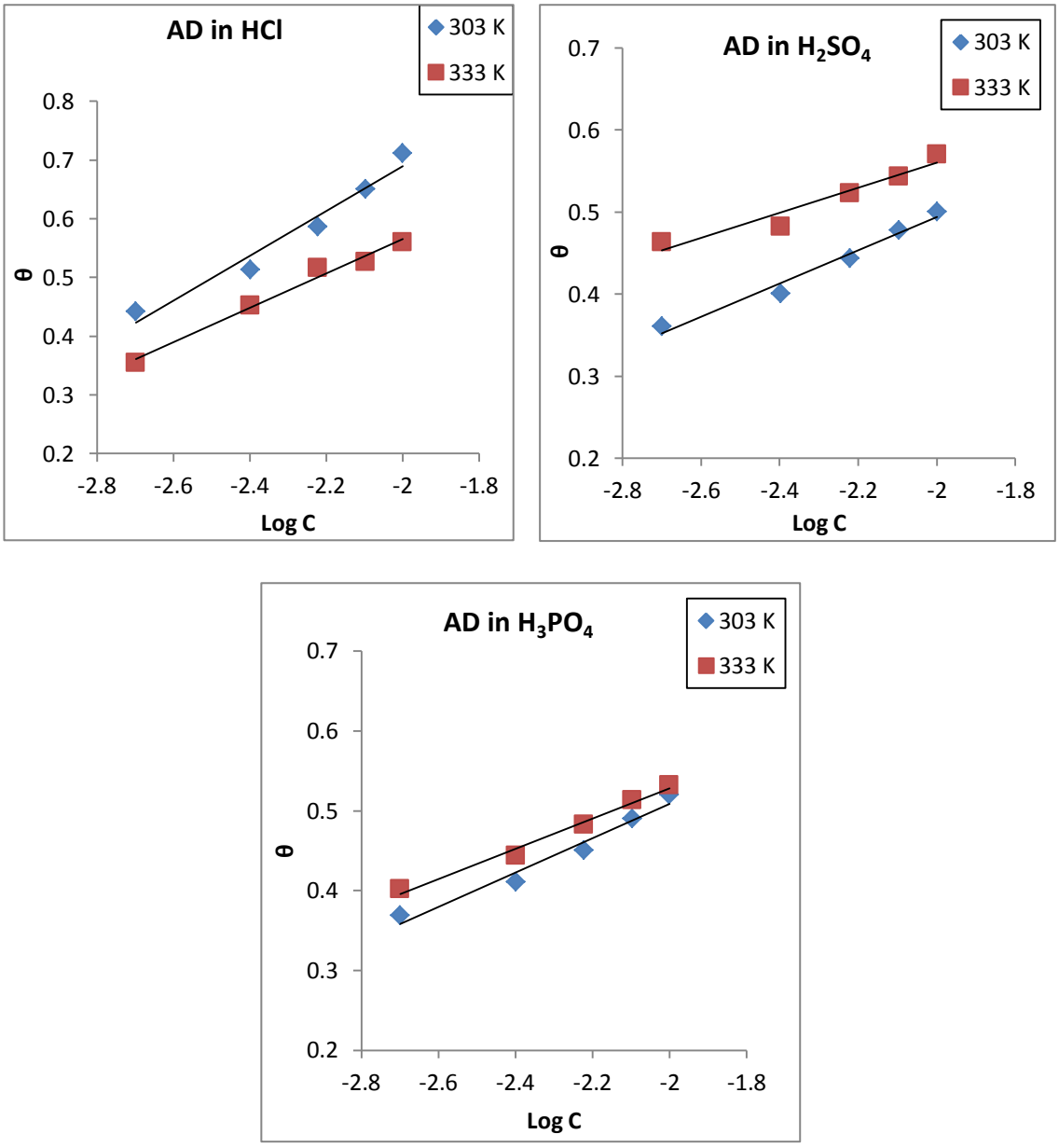


Figure 5.29. Temkin isotherm for the adsorption of adenine (AD) on mild steel surface in 0.1 M solutions of HCl, H_2SO_4 and H_3PO_4 at 303 and 333 K.

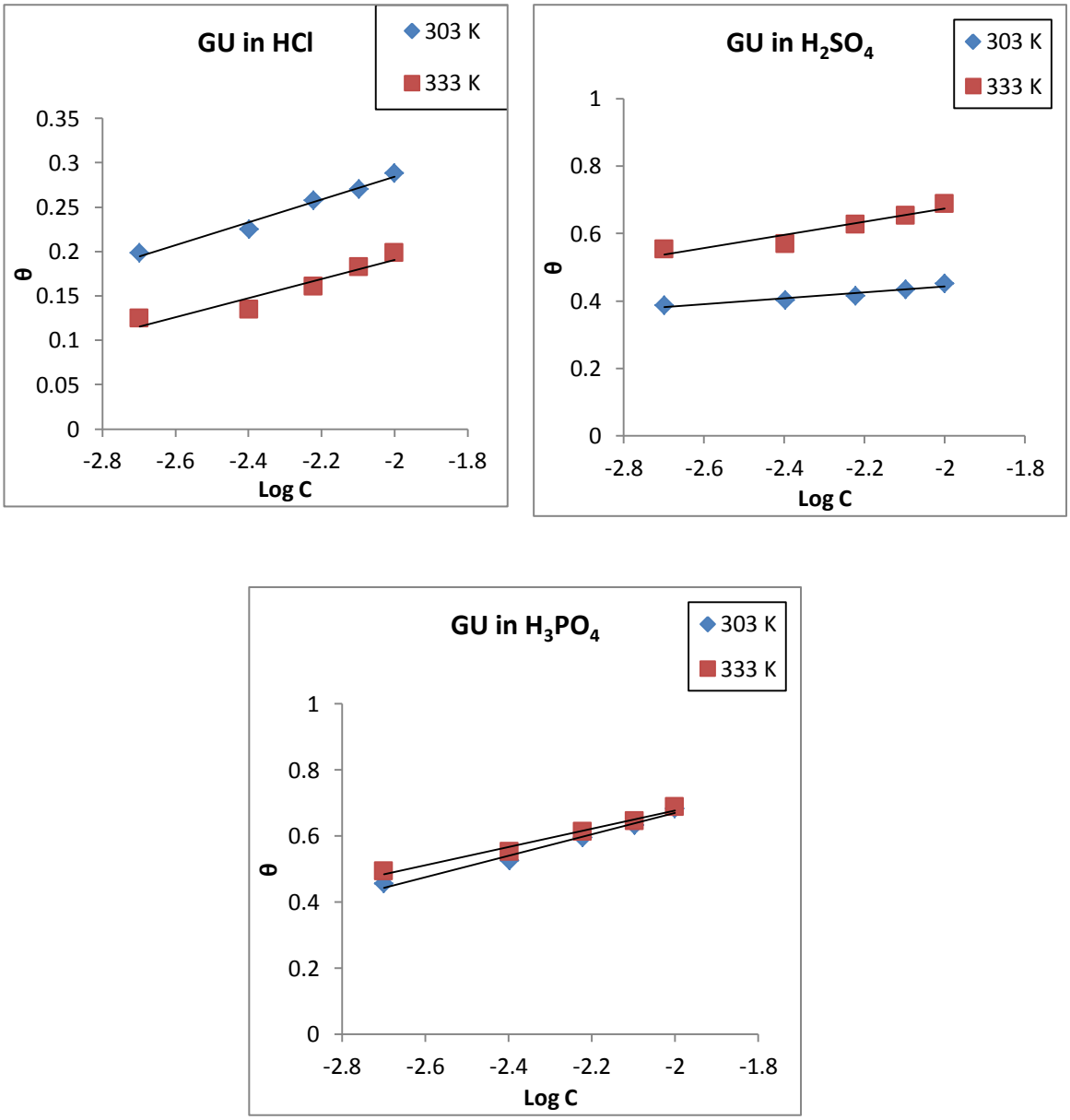


Figure 5.30. Temkin isotherm for the adsorption of guanine (GU) on mild steel surface in 0.1 M solutions of HCl, H_2SO_4 and H_3PO_4 at 303 and 333 K.

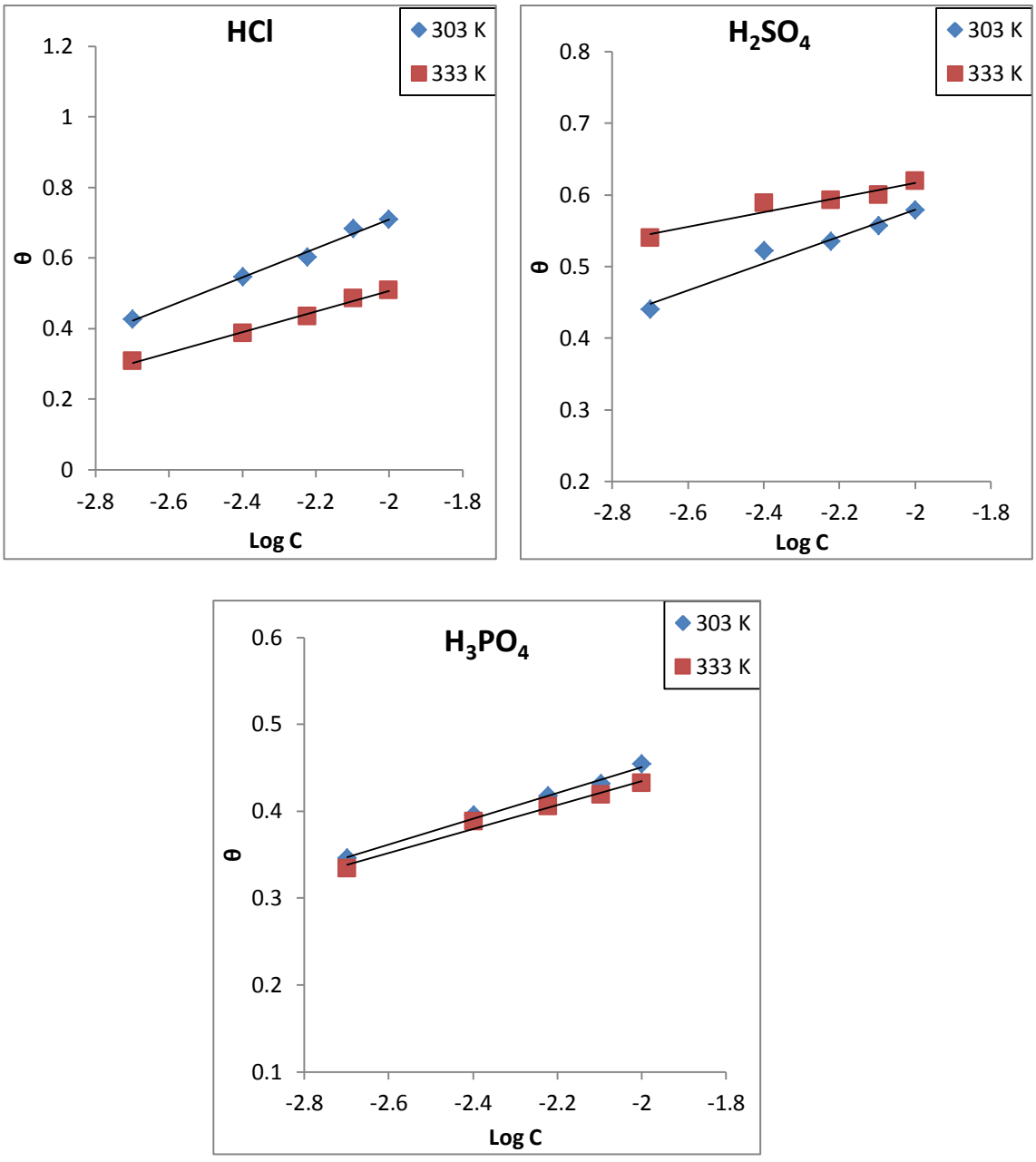


Figure 5.31. Temkin isotherm for the adsorption of hypoxanthine (HYP) on mild steel surface in 0.1 M solutions of HCl, H_2SO_4 and H_3PO_4 at 303 and 333 K.

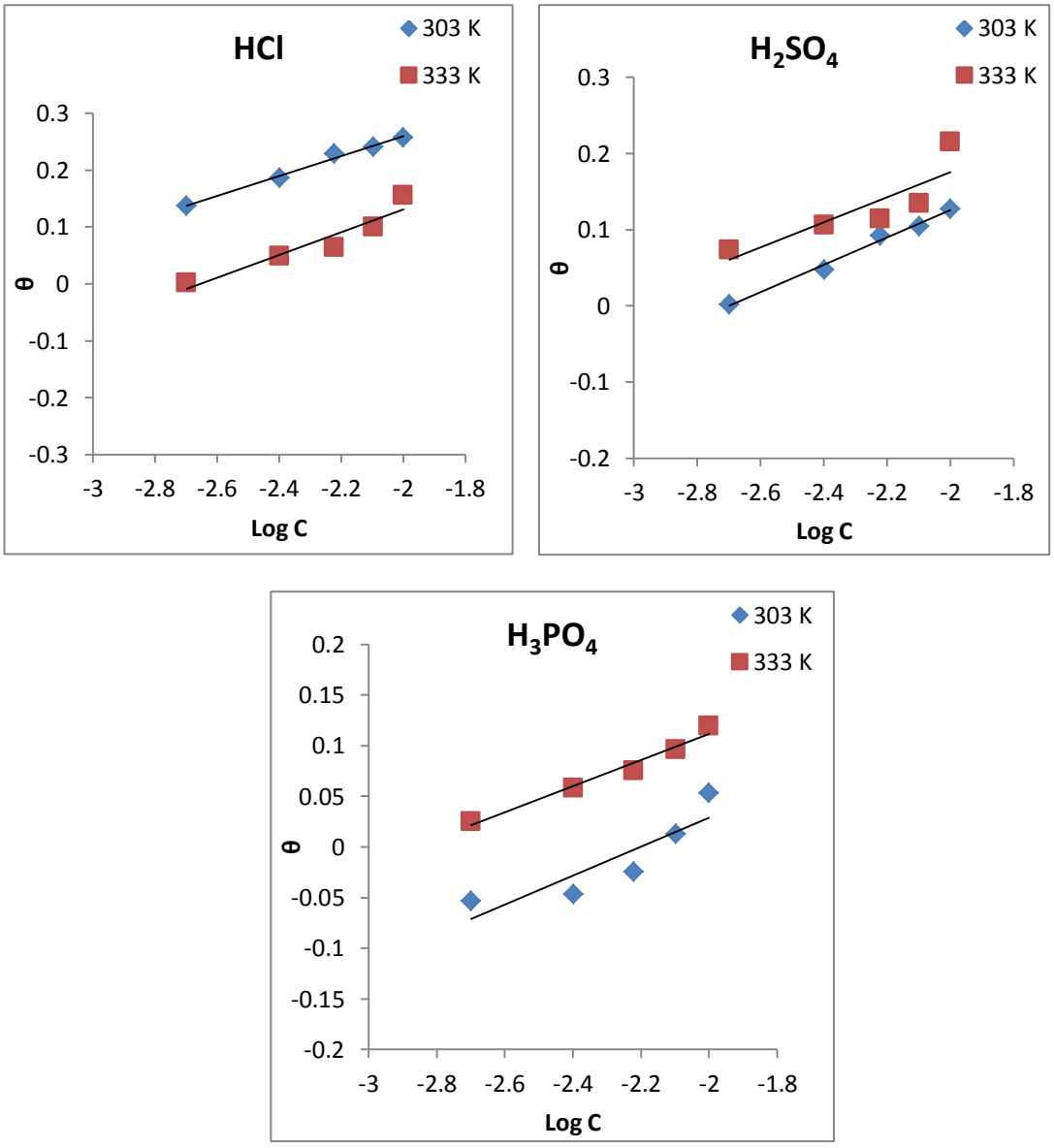


Figure 5.32. Temkin isotherm for the adsorption of xanthine (XN) on mild steel surface in 0.1 M solutions of HCl, H_2SO_4 and H_3PO_4 at 303 and 333 K.

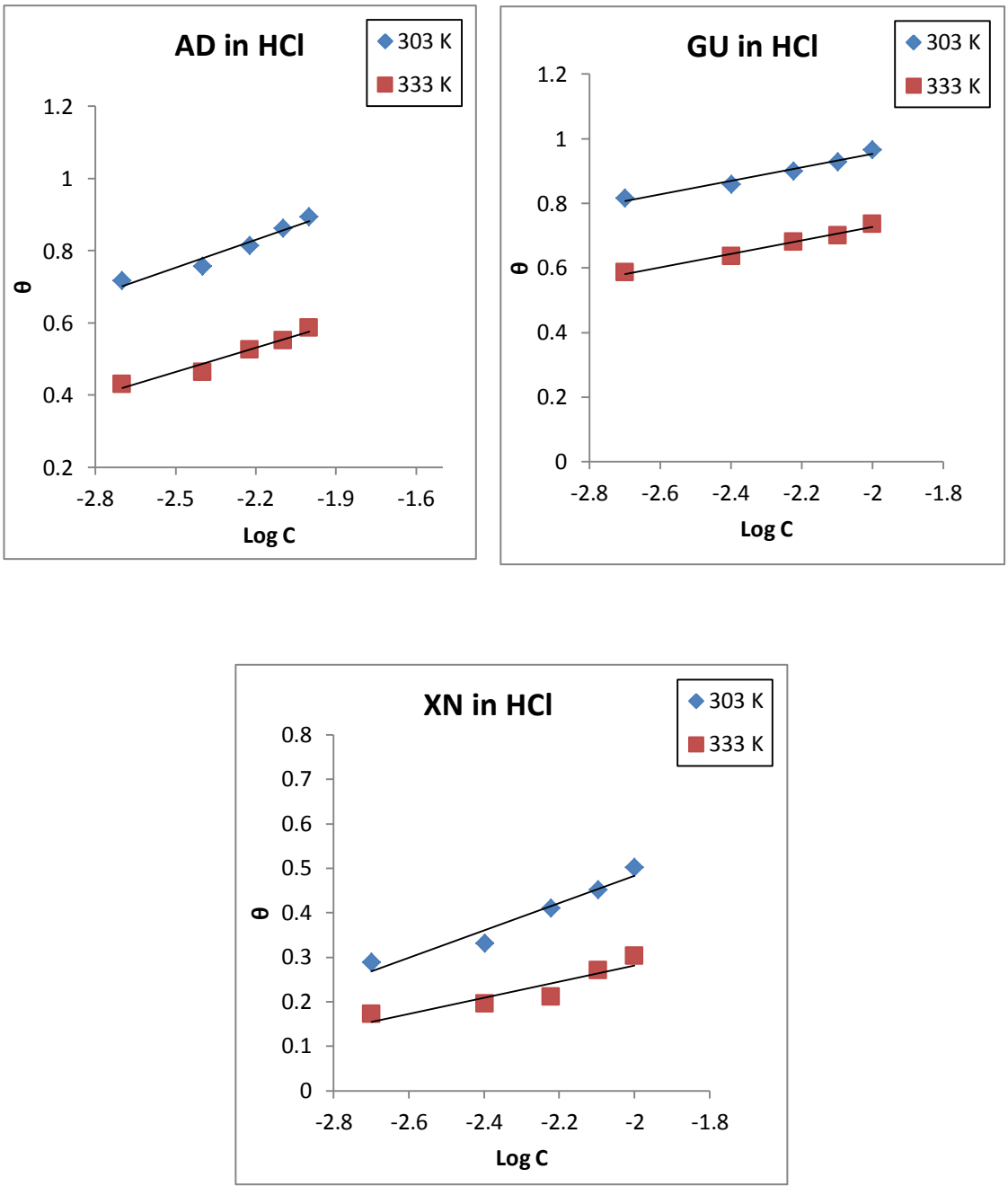
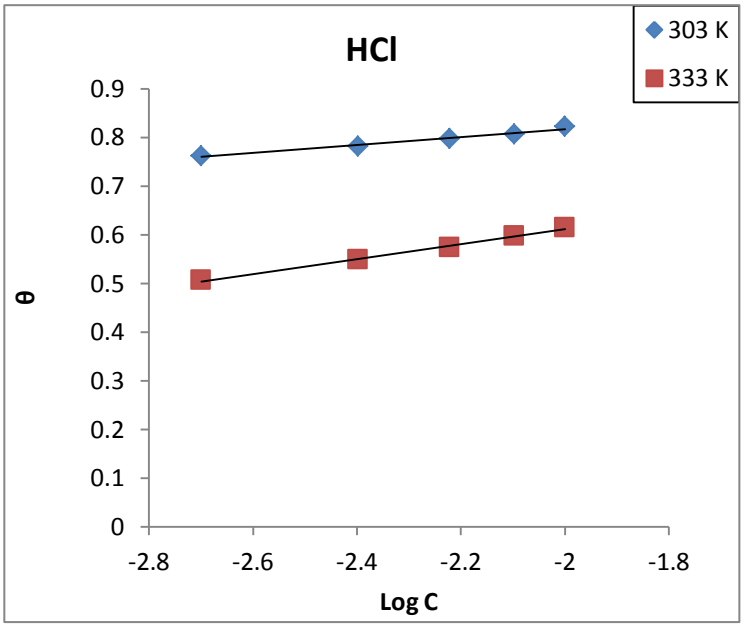


Figure 5.33. Temkin isotherm for the adsorption of adenine (AD), guanine (GU) and xanthine (XN) on aluminium surface in 0.1 M solutions of HCl at 303 and 333 K.



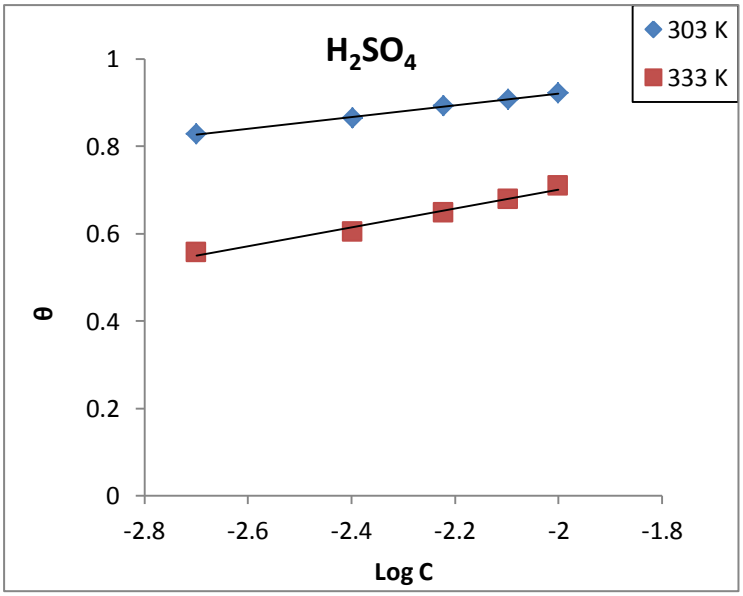


Figure 5.34. Temkin isotherm for the adsorption of hypoxanthine (HYP) on aluminium surface in 0.1 M solutions of HCl and H_2SO_4 at 303 and 333 K.

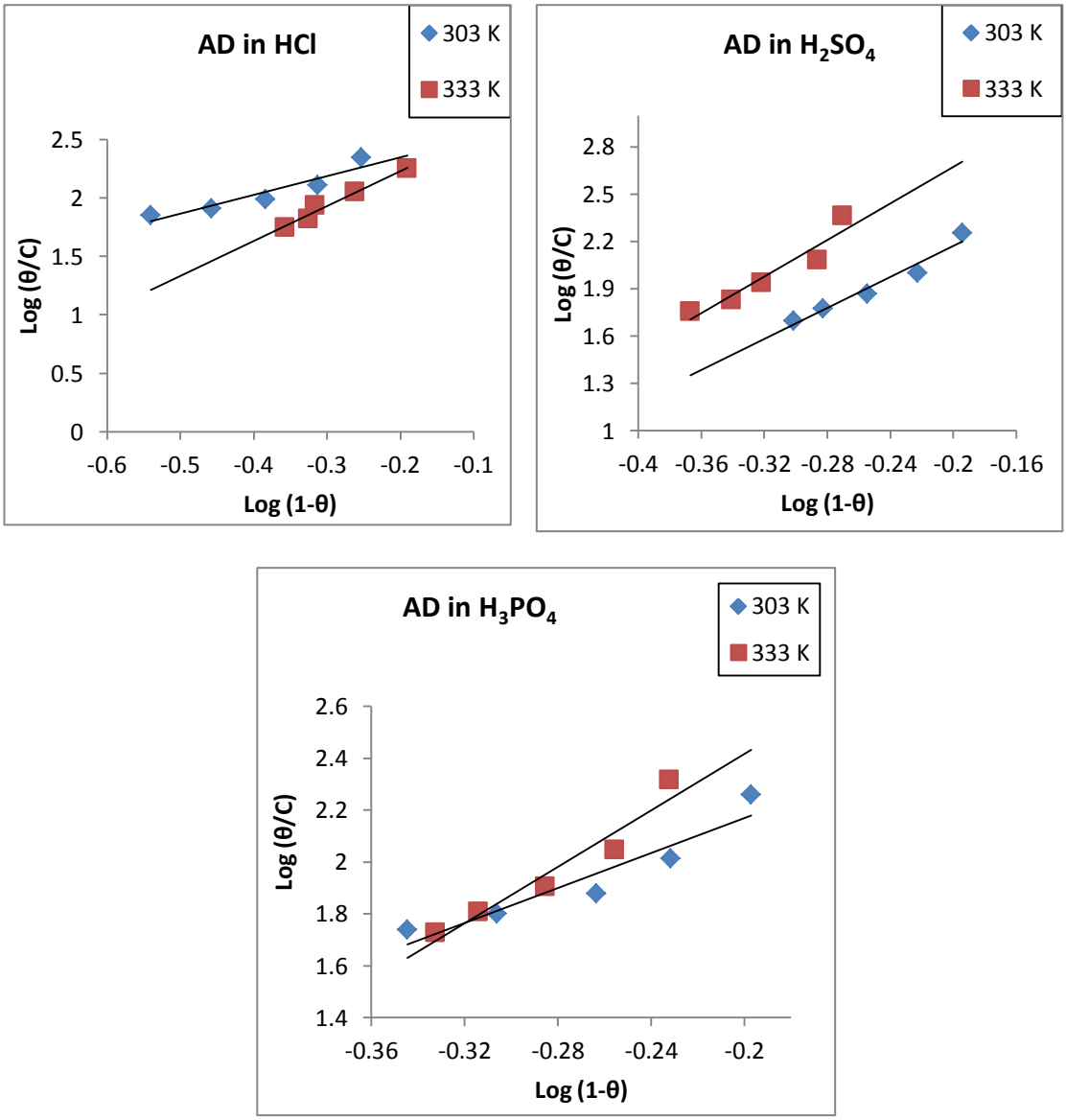


Figure 5.35. Flory Huggins isotherm for the adsorption of adenine (AD) on mild steel surface in 0.1 M solutions of HCl, H_2SO_4 and H_3PO_4 at 303 and 333 K.

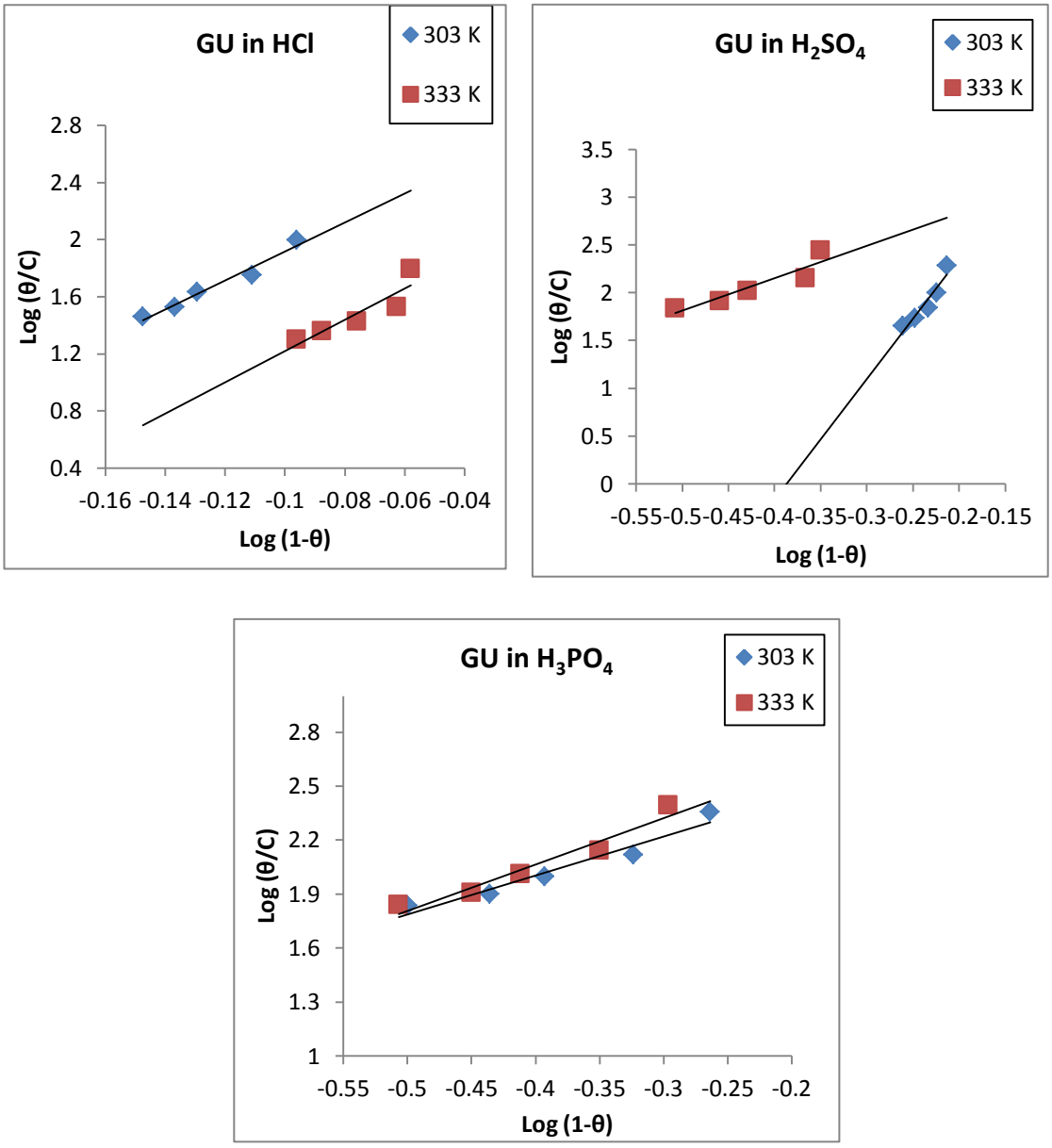


Figure 5.36. Flory Huggins isotherm for the adsorption of guanine (GU) on mild steel surface in 0.1 M solutions of HCl, H_2SO_4 and H_3PO_4 at 303 and 333 K.

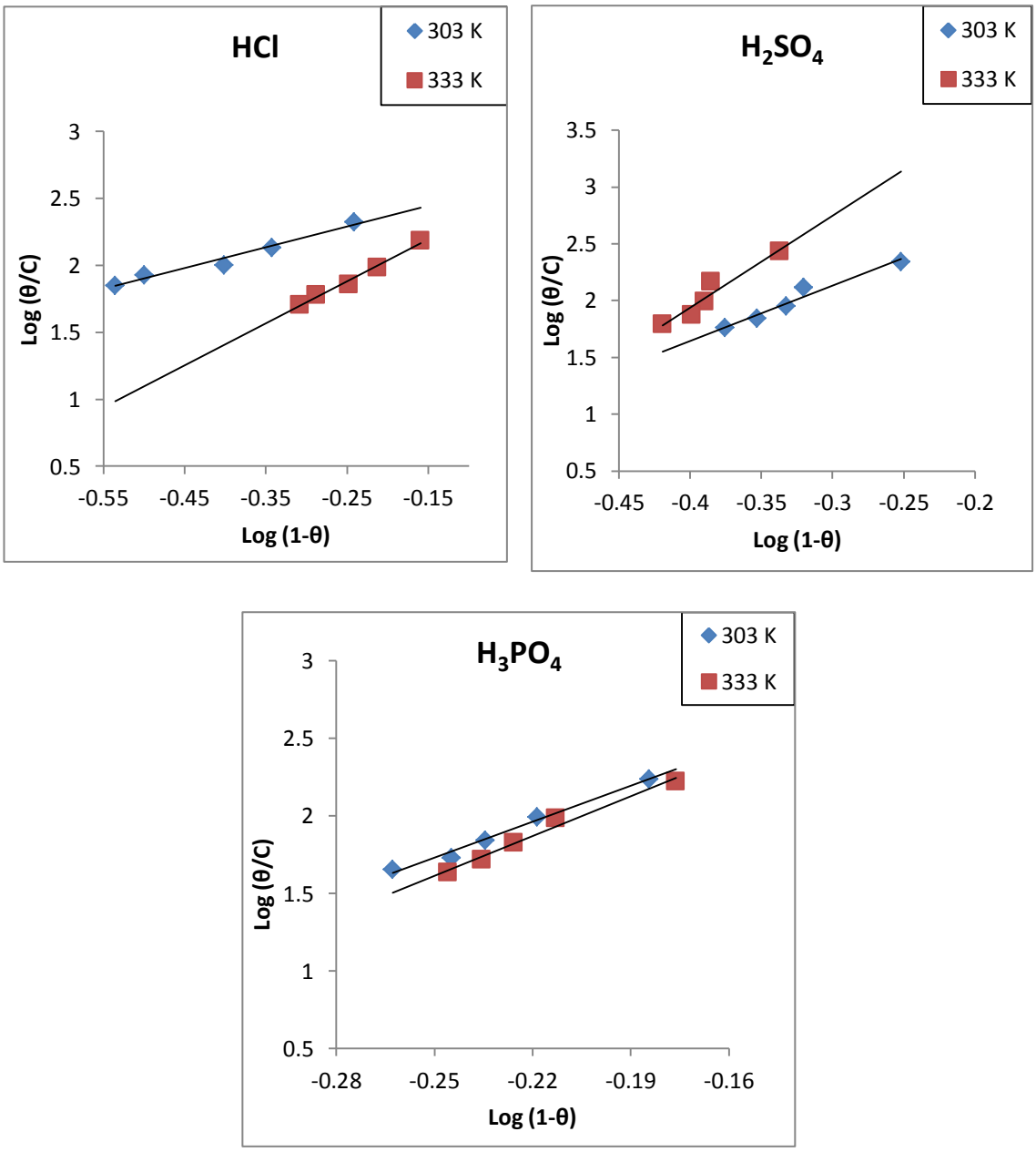


Figure 5.37. Flory Huggins isotherm for the adsorption of hypoxanthine (HYP) on mild steel surface in 0.1 M solutions of HCl, H_2SO_4 and H_3PO_4 at 303 and 333 K.

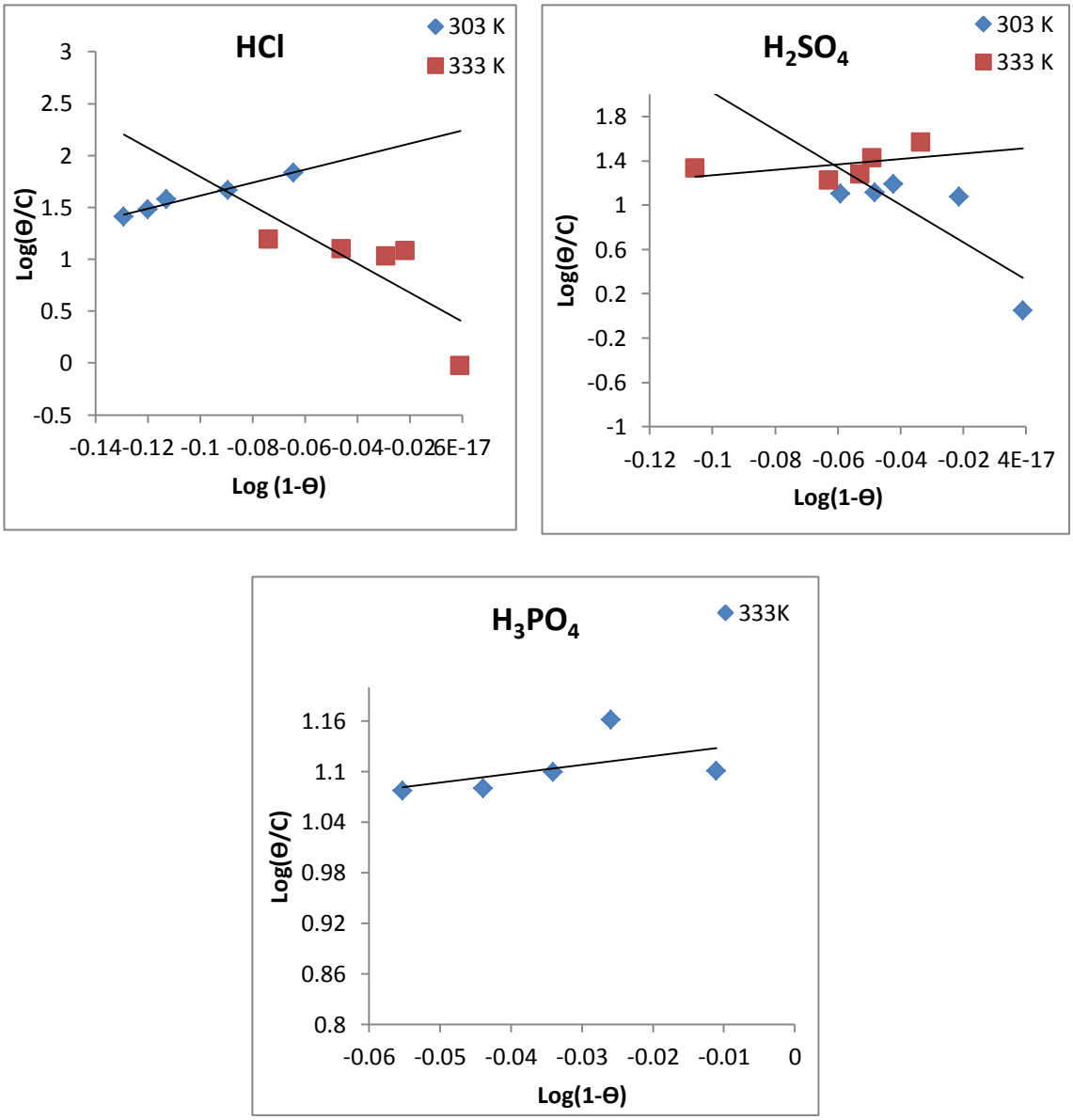


Figure 5.38. Flory Huggins isotherm for the adsorption of xanthine (XN) on mild steel surface in 0.1 M solutions of HCl, H_2SO_4 and H_3PO_4 at 303 and 333 K.

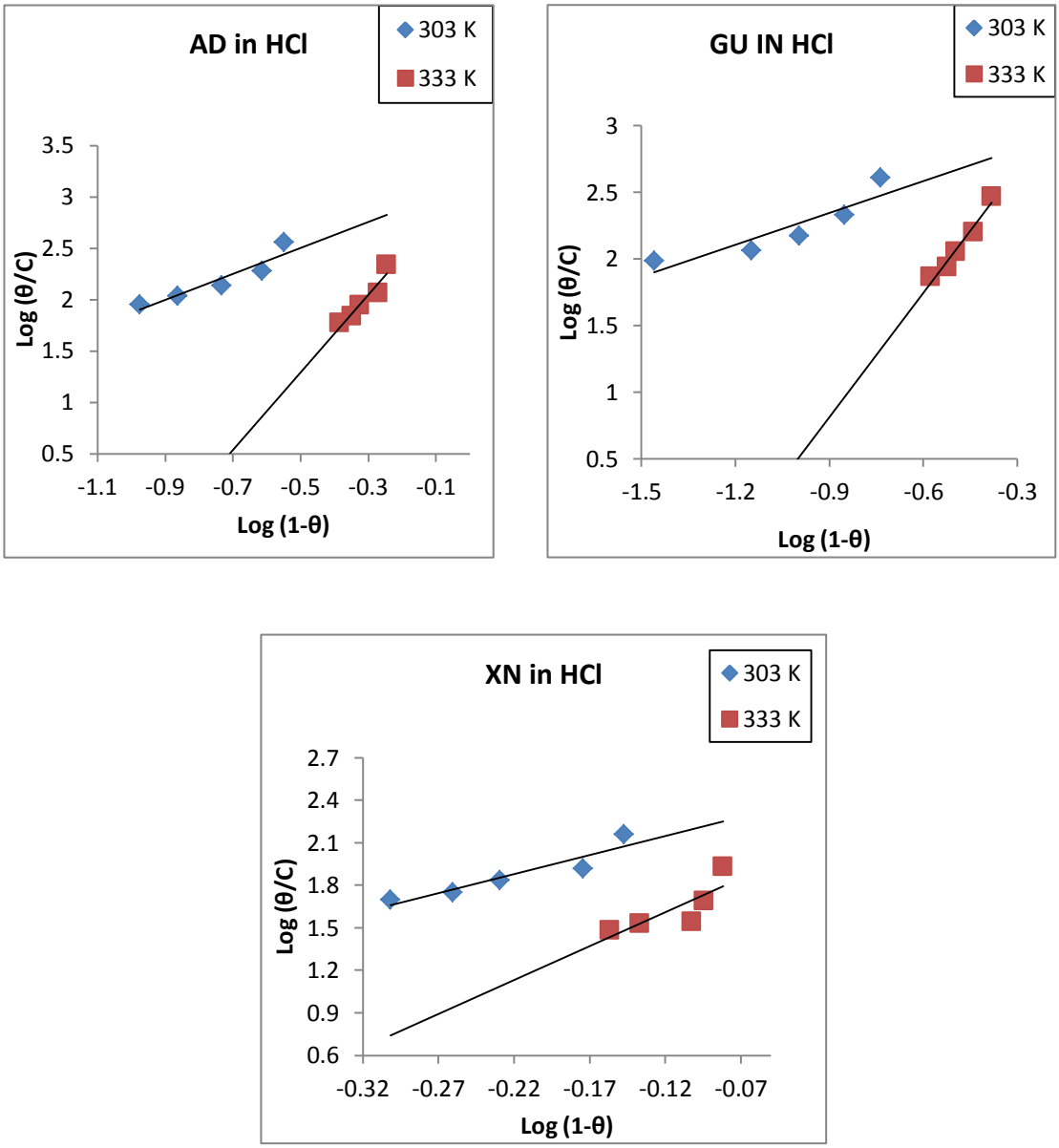
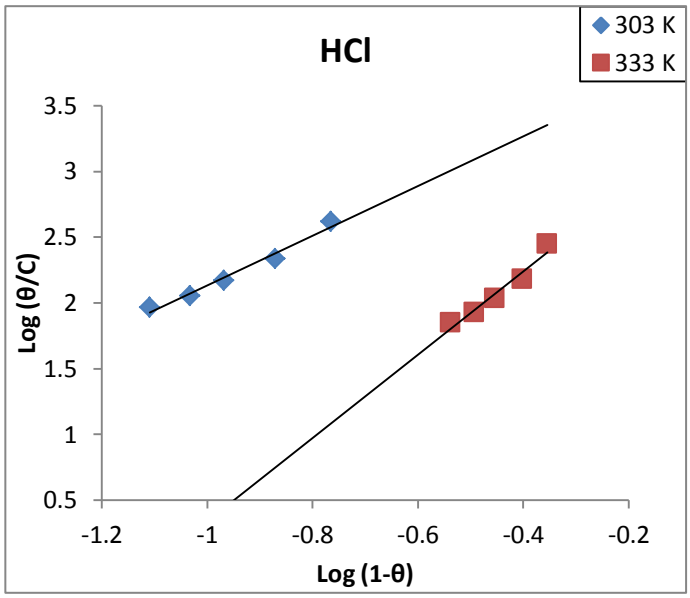


Figure 5.39. Flory Huggins isotherm for the adsorption of adenine (AD), guanine (GU) and xanthine (XN) on aluminium surface in 0.1 M solutions of HCl at 303 and 333 K.



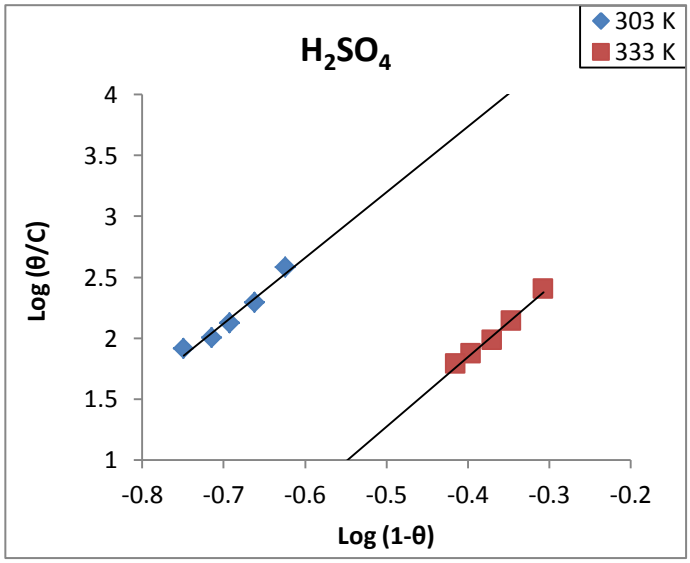


Figure 5.40. Flory Huggins isotherm for the adsorption of hypoxanthine (HYP) on aluminium surface in 0.1 M solutions of HCl and H_2SO_4 at 303 and 333 K.

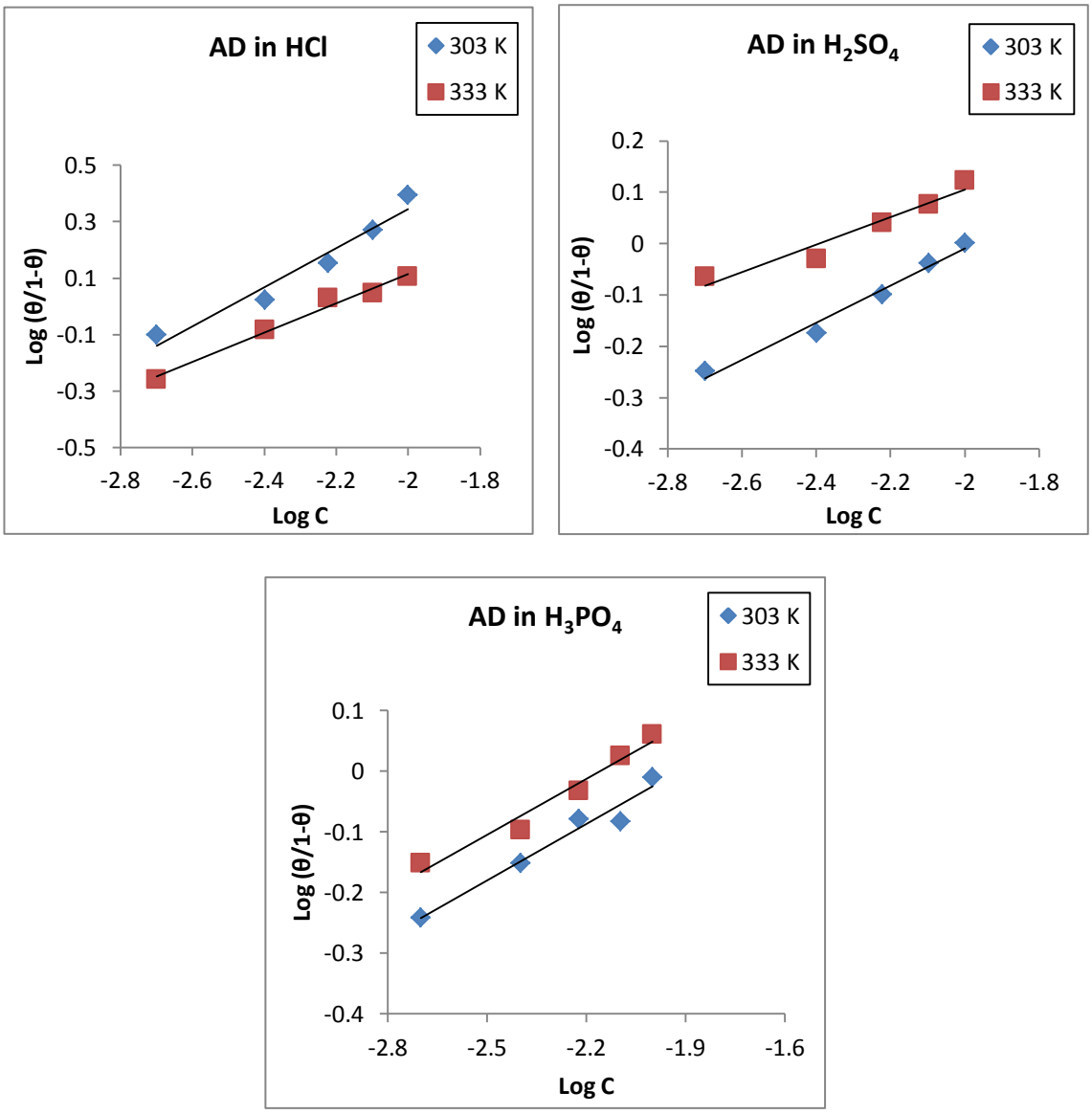


Figure 5.41. El-Awardy isotherm for the adsorption of adenine (AD) on mild steel surface in 0.1 M solutions of HCl, H_2SO_4 and H_3PO_4 at 303 and 333 K.

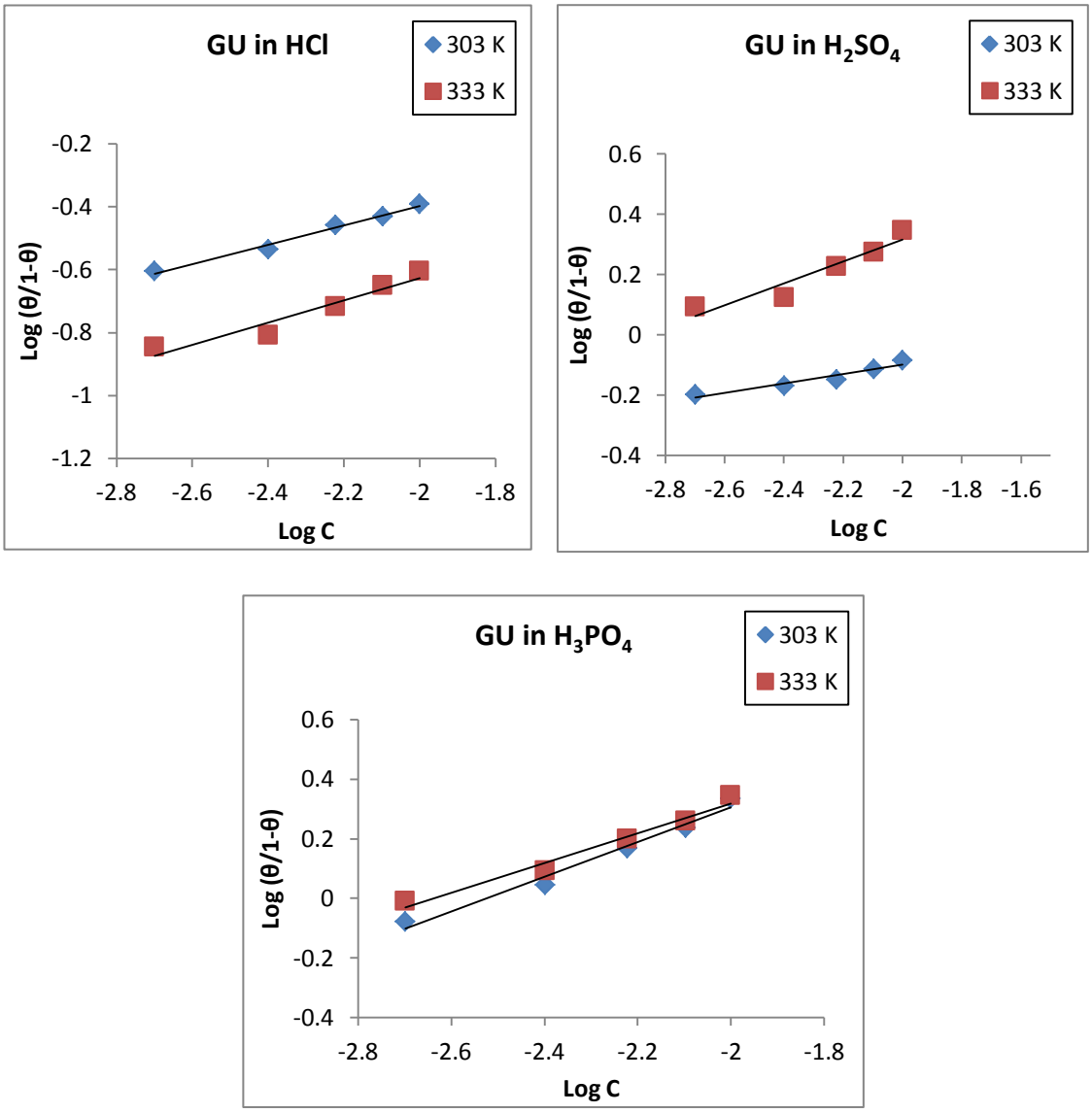


Figure 5.42. El-Awardy isotherm for the adsorption of guanine (GU) on mild steel surface in 0.1 M solutions of HCl, H_2SO_4 and H_3PO_4 at 303 and 333 K.

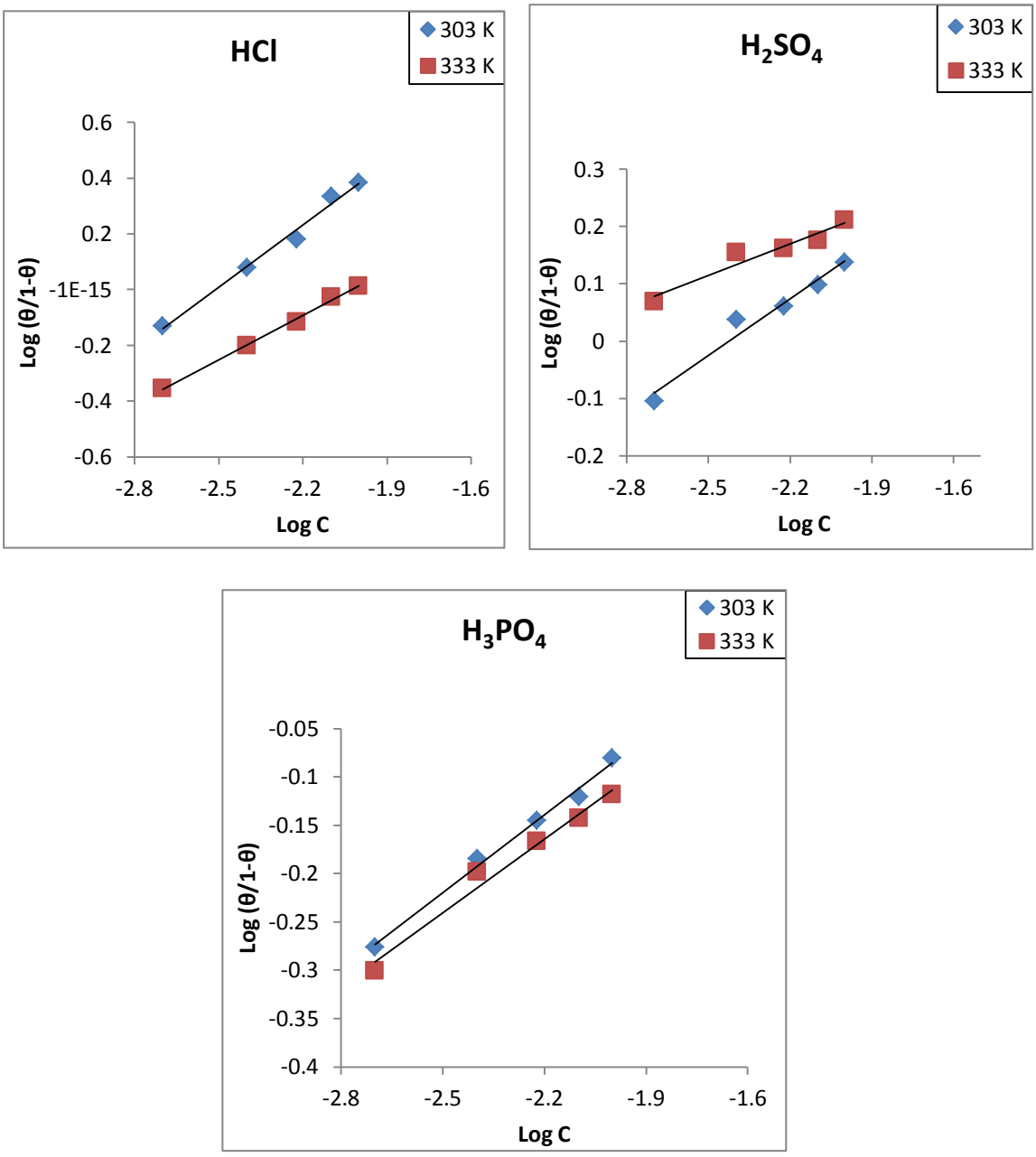


Figure 5.43. El-Awardy isotherm for the adsorption of hypoxanthine (HYP) on mild steel surface in 0.1 M solutions of HCl, H_2SO_4 and H_3PO_4 at 303 and 333 K.

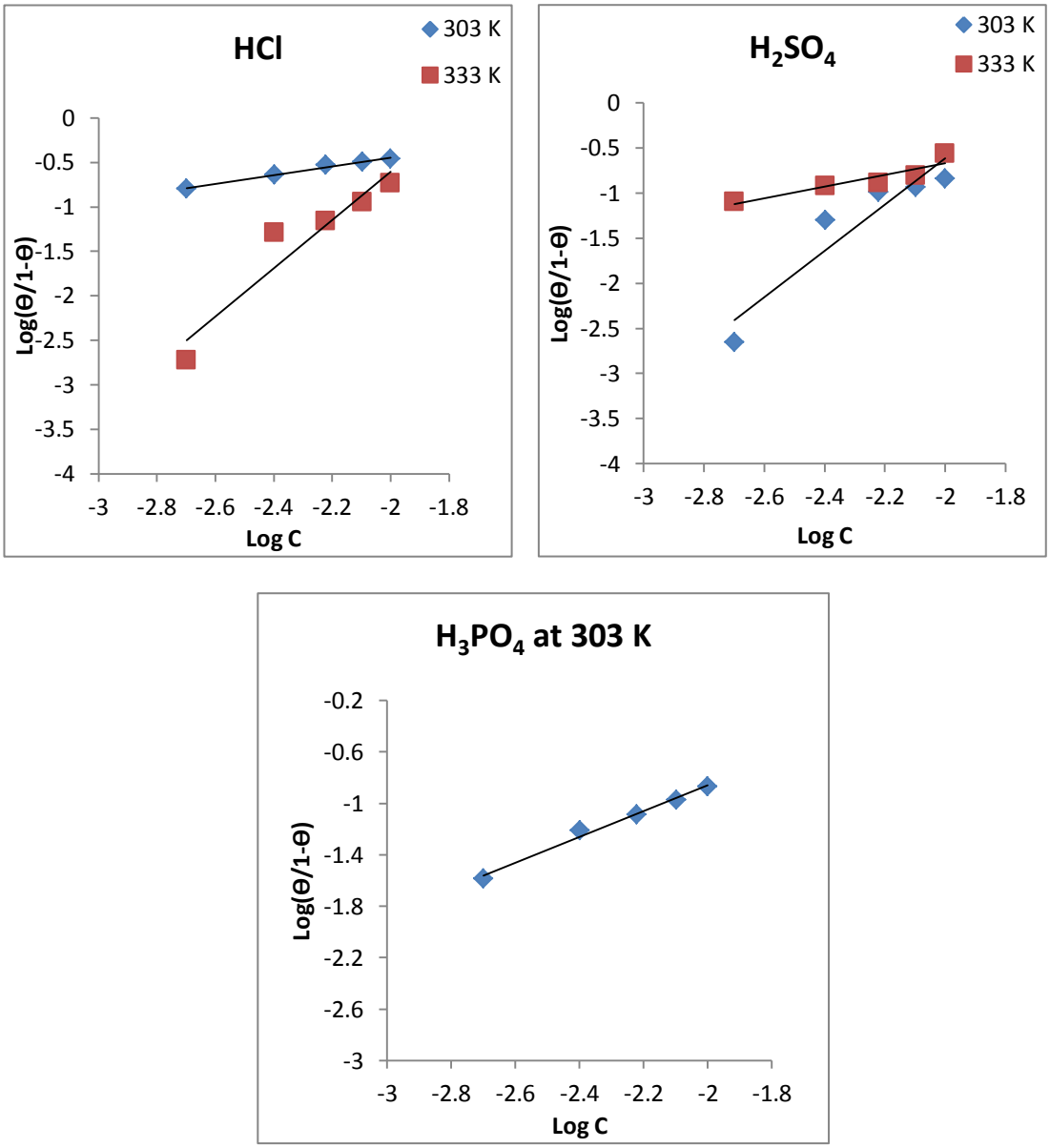


Figure 5.44. El-Awardy isotherm for the adsorption of xanthine (XN) on mild steel surface in 0.1 M solutions of HCl, H_2SO_4 and H_3PO_4 at 303 and 333 K.

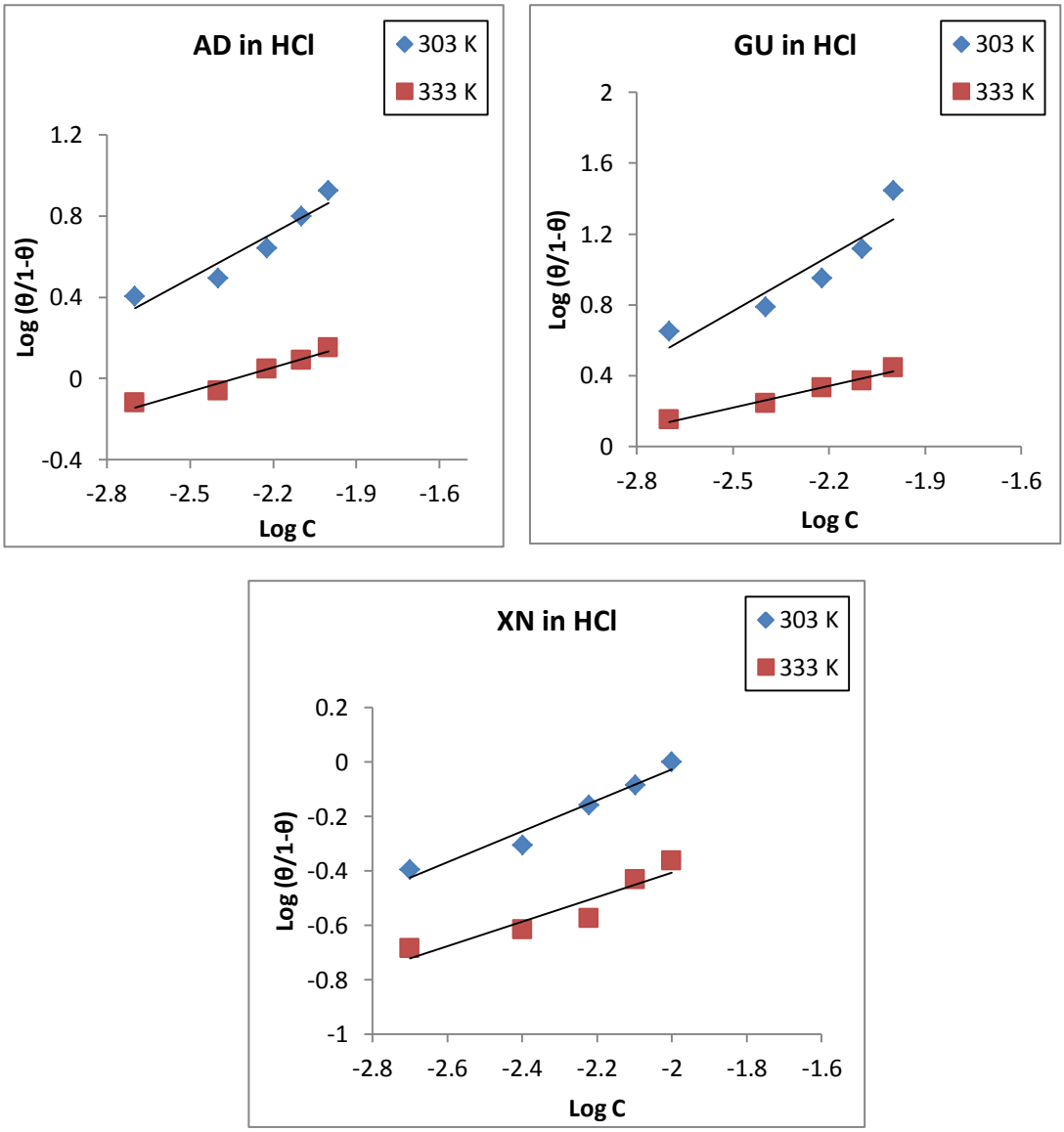
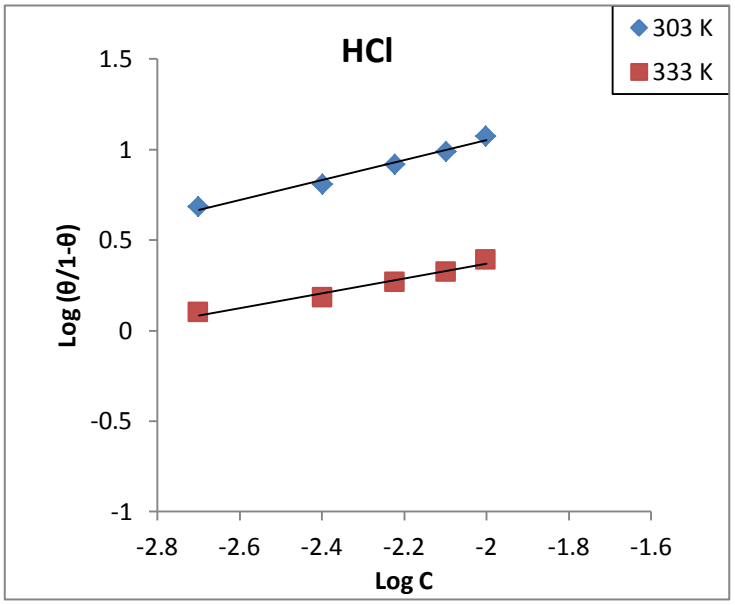


Figure 5.45. El-Awardy isotherm for the adsorption of adenine (AD), guanine (GU) and xanthine (XN) on aluminium surface in 0.1 M solutions of HCl at 303 and 333 K.



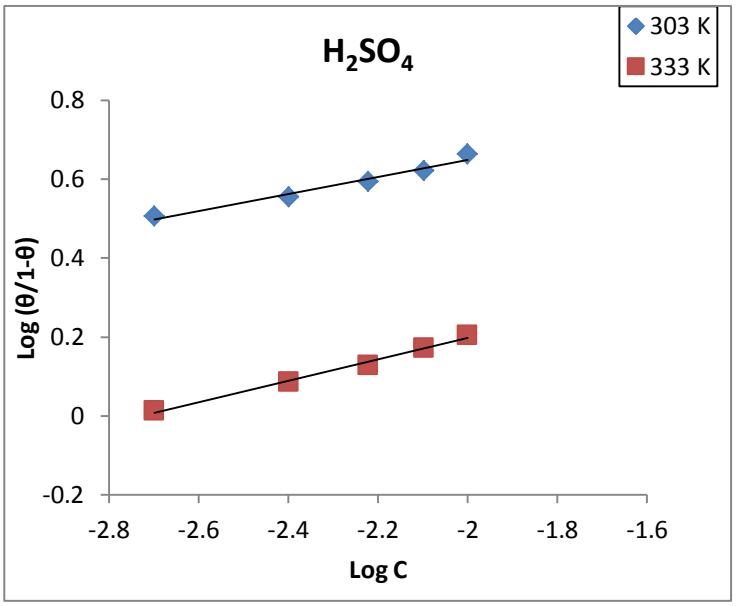


Figure 5.46. El-Awardy isotherm for the adsorption of hypoxanthine (HYP) on aluminium surface in 0.1 M solutions of HCl and H_2SO_4 at 303 and 333 K.

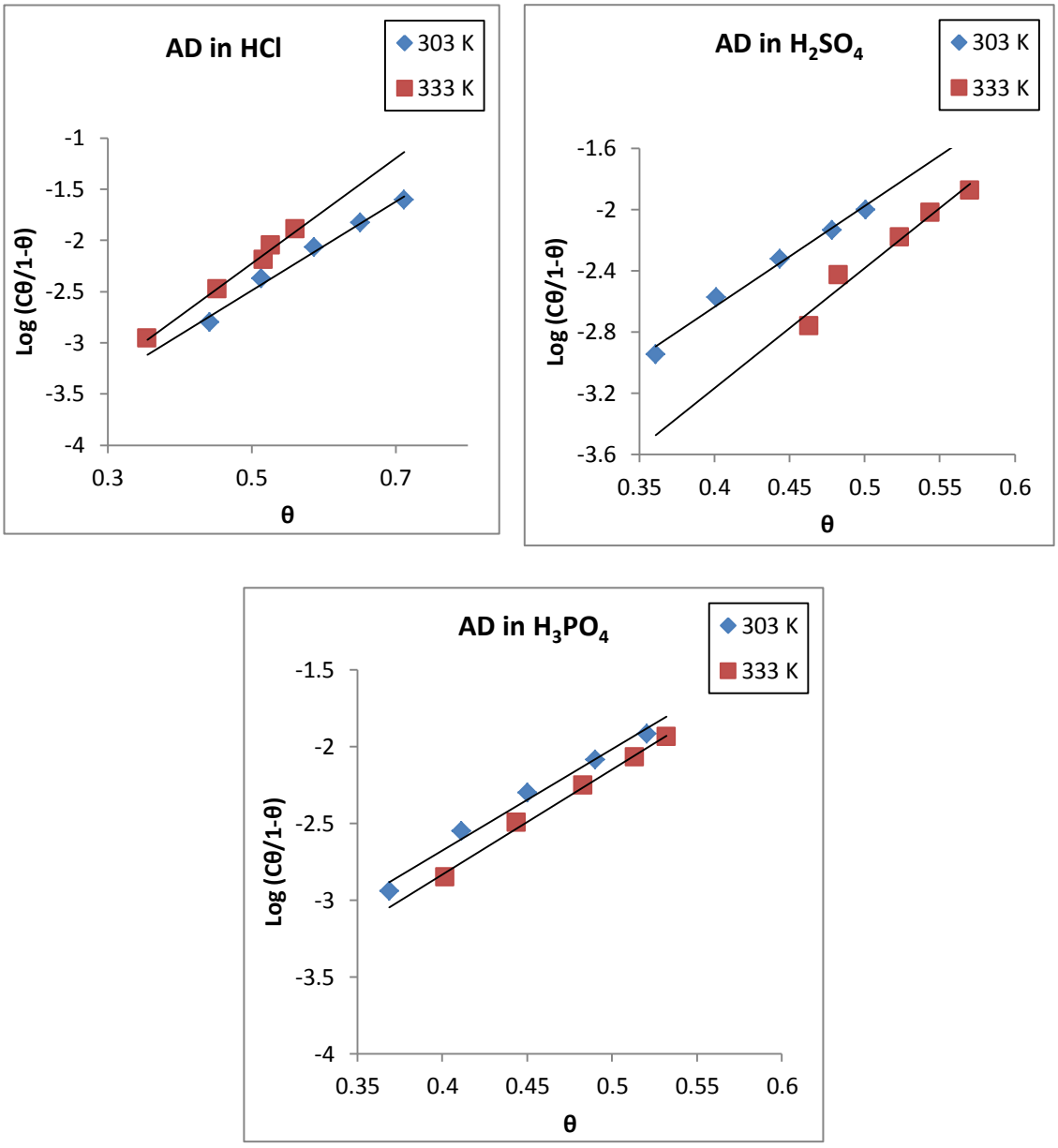


Figure 5.47. Frumkin isotherm for the adsorption of adenine (AD) on mild steel surface in 0.1 M solutions of HCl, H_2SO_4 and H_3PO_4 at 303 and 333 K.

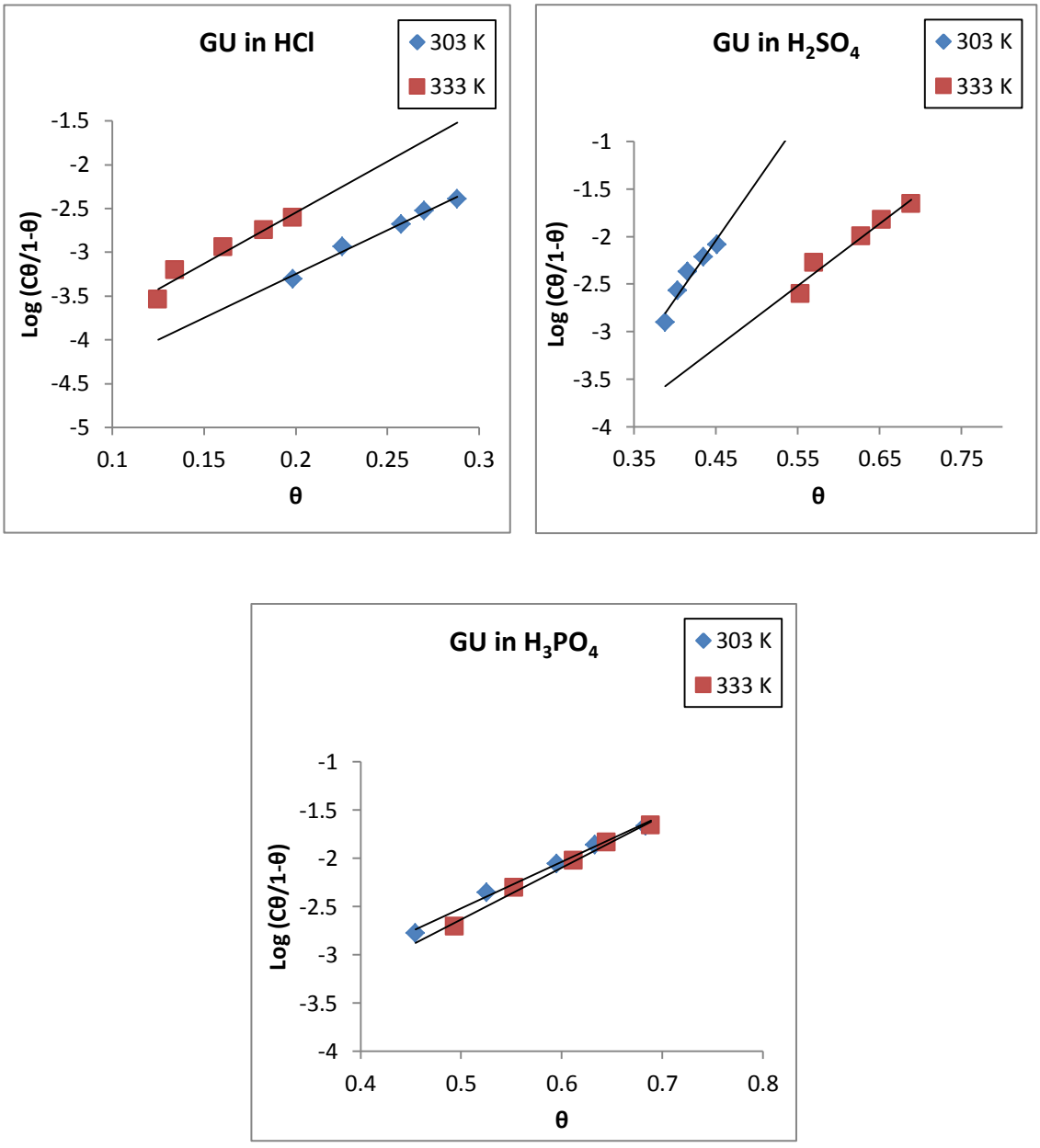


Figure 5.48. Frumkin isotherm for the adsorption of guanine (GU) on mild steel surface in 0.1 M solutions of HCl, H_2SO_4 and H_3PO_4 at 303 and 333 K.

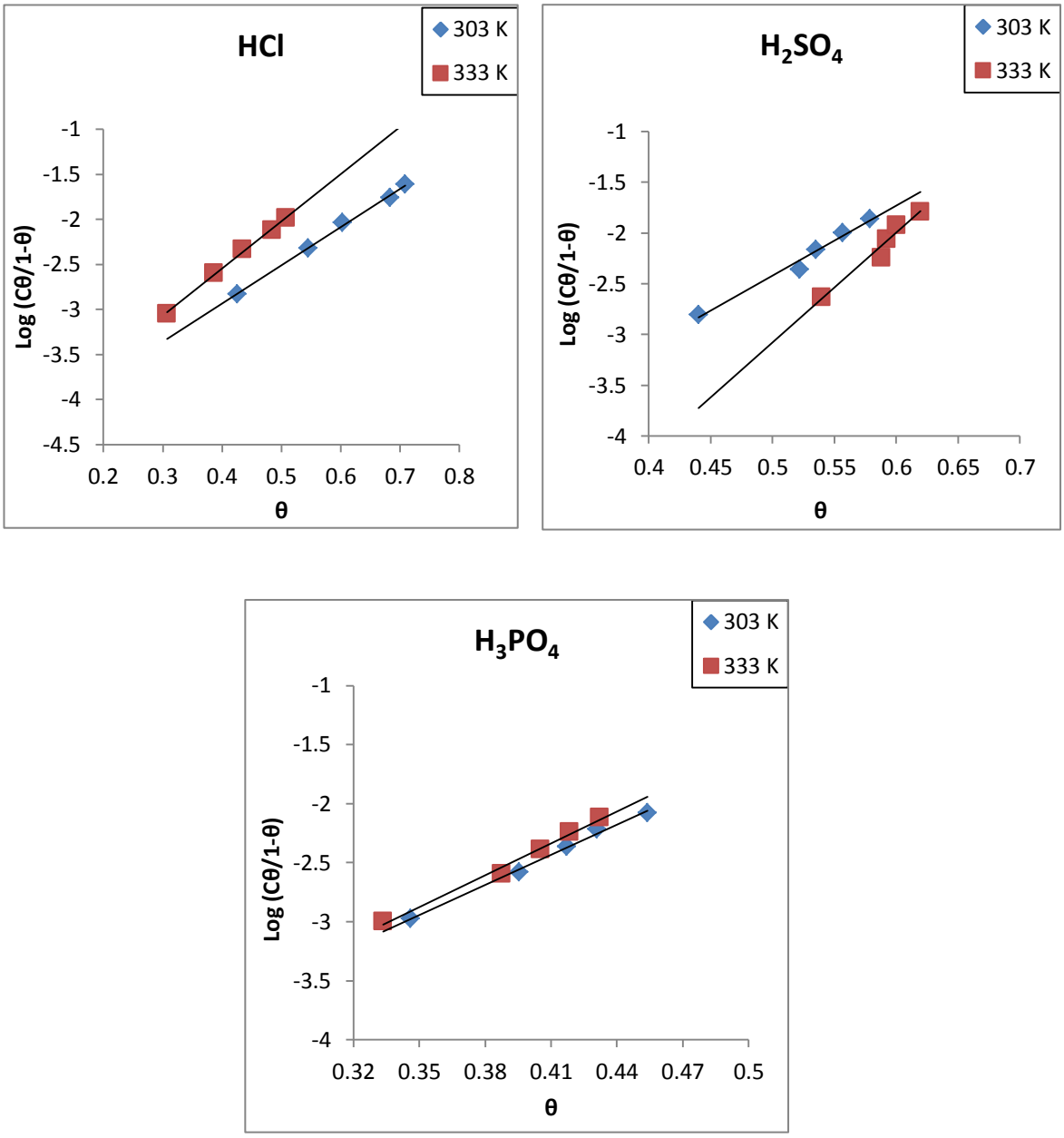


Figure 5.49. Frumkin isotherm for the adsorption of hypoxanthine (HYP) on mild steel surface in 0.1 M solutions of HCl, H_2SO_4 and H_3PO_4 at 303 and 333 K.

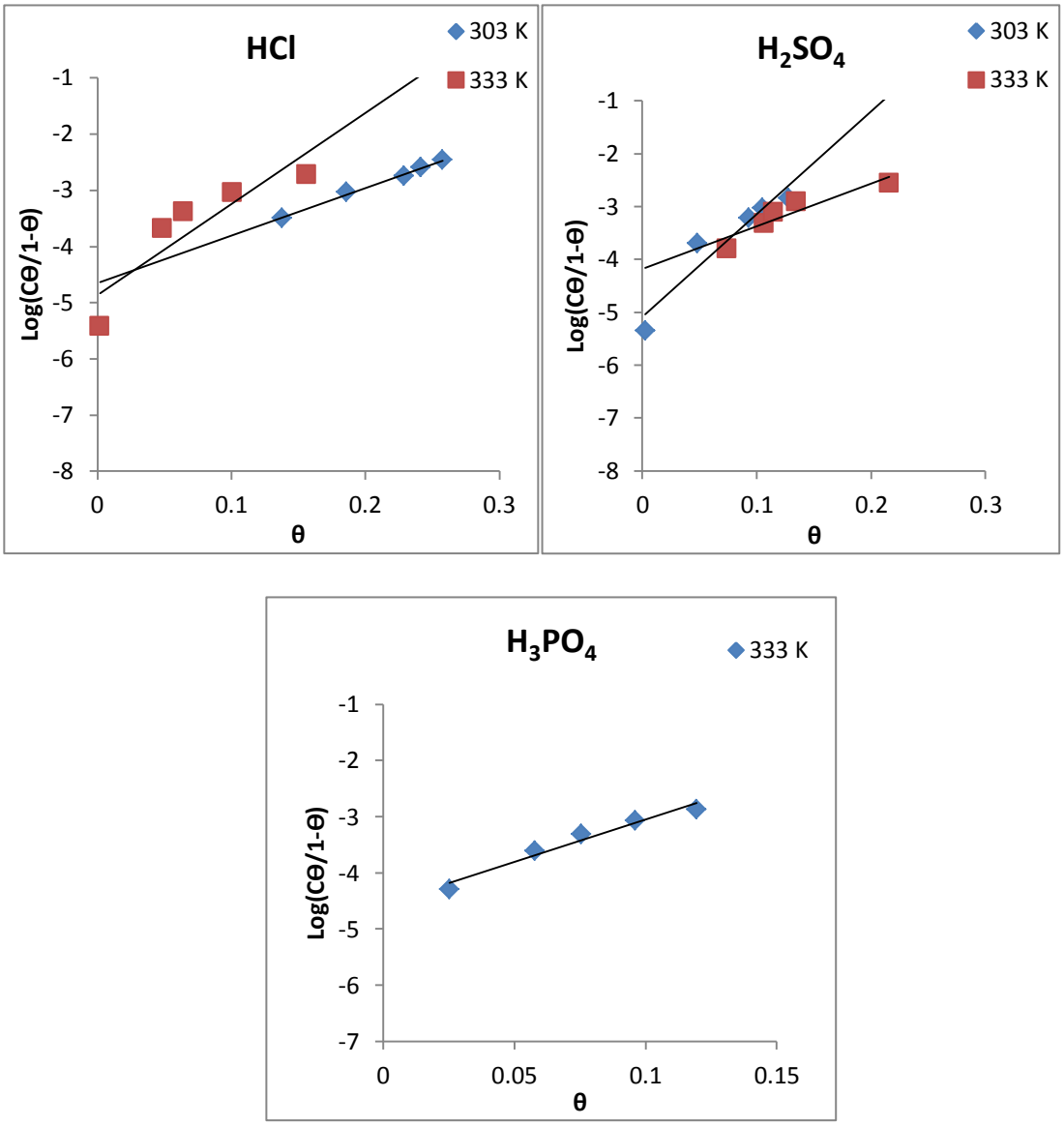


Figure 5.50. Frumkin isotherm for the adsorption of xanthine (XN) on mild steel surface in 0.1 M solutions of HCl, H_2SO_4 and H_3PO_4 at 303 and 333 K.

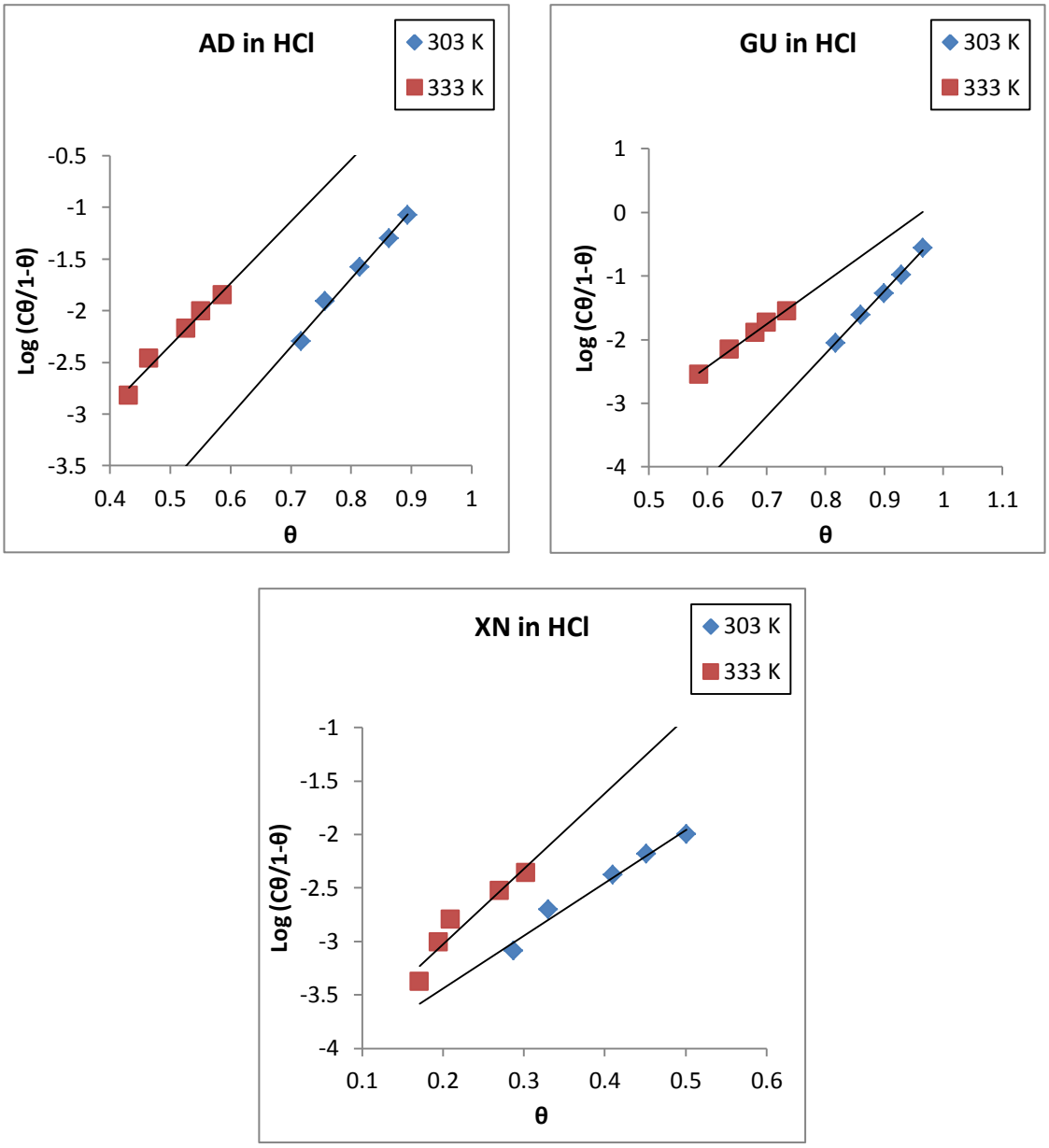
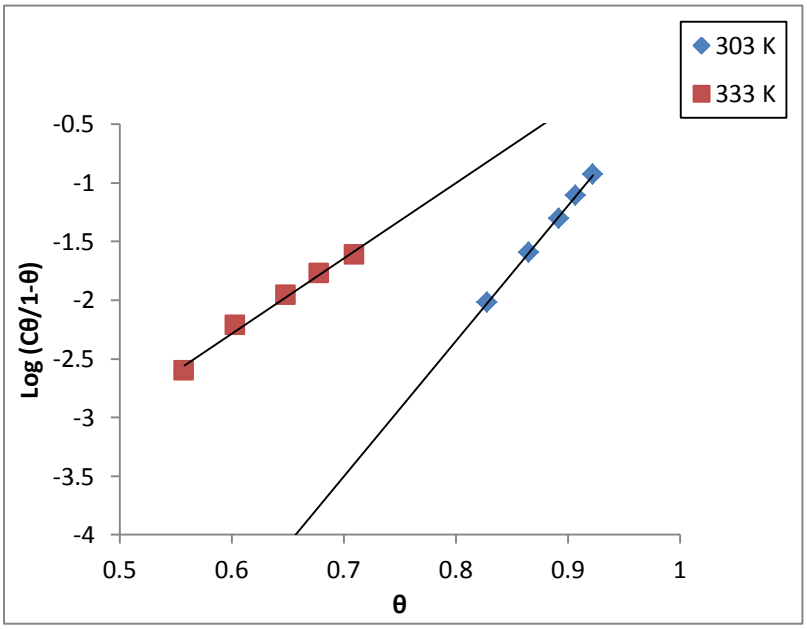


Figure 5.51. Frumkin isotherm for the adsorption of adenine (AD), guanine (GU) and xanthine (XN) on aluminium surface in 0.1 M solutions of HCl at 303 and 333 K.



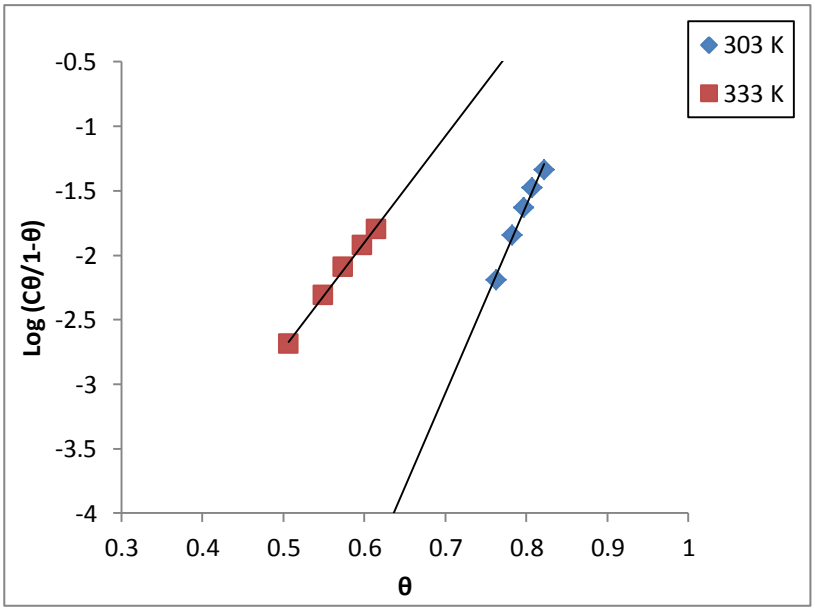


Figure 5.52. Frumkin isotherm for the adsorption of hypoxanthine (HYP) on aluminium surface in 0.1 M solutions of HCl and H_2SO_4 at 303 and 333 K.

Negative ΔG_{ads} values indicate spontaneity of the adsorption process (Avci, 2008; Bahrami *et al.,* 2010). Generally, ΔG_{ads} values with magnitude much less than 40 kJ mol^{-1} have typically been correlated with the electrostatic interactions between organic molecules and charged metal surface (physisorption), whilst those of magnitude greater than 40 kJ mol^{-1} are associated with charge sharing or transfer from the organic molecules to the metal surface (chemisorption) (Popova, 2003).

The standard free energy of adsorption, ΔG_{ads} values were evaluated from the different isotherms at 303 and 333 K for selected purines at various concentrations. The corresponding results are presented in Appendices XI-XV. Except for the Frumkin isotherm, all the other isotherms gave negative ΔG_{ads} values, implying that the adsorption of the purines on both mild steel and aluminium surfaces in HCl, H_2SO_4 and H_3PO_4 was a spontaneous process. Also, from Appendices XI-XV, it is evident that more negative ΔG_{ads} values were obtained in HCl, H_2SO_4 and H_3PO_4 acids for mild steel systems than aluminium systems at 333 K, suggesting that the higher temperature was more favourable for the adsorption of AD, GU, HYP and XN on mild steel. However, only the Temkin isotherm gave the highest ΔG_{ads} values for the purines in H_2SO_4 and H_3PO_4 acids at 333 K, which is within the range of values often expected for the chemisorptive interactions suggested by the experimental data (> -40 kJ mol^{-1}). ΔG_{ads} from all the other tested isotherms were well below this value, implying that they do not

adequately describe the experimental data in this regard. This is despite the relatively good linear fit to all the isotherms (R^2= 0.9).

As far as corrosion inhibition studies are concerned, a large number of experimental adsorption data fit the Langmuir isotherm [ ], at least qualitatively (i.e. good linear fit). Similar linear fit has been obtained for AD, GU and HYP on mild steel and aluminium at 303 and 333 K (Figures 4.38 - 4.43). Often, however, the linear fits intercept the y-axis (C/θ) or the x-axis (C) and the slope deviates substantially from unity, contrary to the isotherm prediction. Similar results have been reported by Yan *et al.* (2008) for purines in 1 M HCl solution, including studies by Döner *et al.* (2011). This anomaly may be attributed to interactions between adsorbate species on the metal surface as well as changes in the heat of adsorption with increasing surface coverage, factors that might not have been taken into consideration in derivation of the isotherm. A number of modifications to the Langmuir equation have been suggested, with the molecular interaction term included (Villamil *et al.*, 1999). Nonetheless, the possibility of adapting the Langmuir isotherm to describe chemisorption and physisorption processes (at least qualitatively) may account for its widespread applicability.

The adsorption of uncharged molecules on a heterogeneous surface is appropriately described by the Temkin isotherm , where θ is a linear function of '*lnC'* (Fuchs-Godec and Zerjav, 2009). This isotherm contains a factor (f= -2α) that clearly takes into account adsorbent-adsorbate interactions and considers the fact that the heat of adsorption of all molecules in the layer decreases with coverage due to the adsorbate–adsorbent interaction. This makes the isotherm quite suitable for systems where chemical interaction of inhibiting species with the metal surface is more

pronounced as observed for the purines on mild steel surface in H_2SO_4 and H_3PO_4 acids at 333 K in this study. The linear plots of θ versus log C shown in Figures 5.29-5.34 are well in agreement with the Temkin equation. More importantly, the trend of ΔG_{ads} values obtained from the Temkin isotherm with temperature for mild steel systems in H_2SO_4 and H_3PO_4 acids is evident that the observed improvement in inhibition efficiency at the higher temperature may have resulted from a change in the nature of adsorption from physisorption at the lower temperature (303 K) to chemisorption at the higher temperature (333 K). This corresponds to an improvement in the rate of chemisorption of non-protonated species with increasing temperature suggested earlier. Therefore, whereas all the tested isotherms qualitatively describe the experimental data by provided proofs of the adsorption of the purines on the mild steel and aluminium surfaces, only the Langmuir and Temkin isotherms have provided exact (quantitative per say) interpretation, whereoff the regression coefficients, R^2, the trend of the free energy values, ΔG_{ads} and adsorption equilibrium constants, k_{ads} corroborate the experimental data.

5.5 Electrochemical Tests

5.5.1. Electrochemical impedance measurements

Impedance measurements were undertaken to provide insight into the characteristics and kinetics of electrochemical processes occurring at the metal/acid interface. The impedance responses of these systems are given in Figures 4.17 - 4.18 as Nyquist plots. The Nyquist plots generally have the form of only one depressed semicircle in the high frequency region, which shows that the process is under charge-transfer control (Martinez and Stern, 2001). The depression of the Nyquist semicircle with center under the real axis is typical for solid metal electrodes that show frequency dispersion of the impedance data. The transfer function can be represented by a solution resistance R_s,

shortned by a capacitor (C) placed parallel to the charge transfer resistance R_{ct} according to equation 5.10 (Quraishi, 2004)

$$Z_{(\omega)} = R_s + \left(\frac{1}{R_{ct}} + j\omega C \right)^{-1} \qquad 5.10$$

where $Z_{(\omega)}$= a combination of real and imaginary impedance, $j = (-1)^{1/2}$ is an imaginary number, ω is the angular frequency in rad s^{-1}, ($\omega = 2\pi f$), when f is the frequency in Hz (Quraishi, 2004). This transfer function is however only applicable for homogeneous systems with one time constant when the centre of the semicircle lies on the abscissa and cannot account for the depression of the capacitive loop. When a non ideal frequency response is present, the capacitor is replaced by a constant phase element (CPE). The use of such a CPE accounts for the deviations from ideal dielectric behaviour and is related to surface inhomogeneities. The impedance, Z of the CPE is given by Kliskic *et al* (2000) as equation 5.11

$$Z_{CPE} = Q^{-1}(j\omega)^{-n} \qquad 5.11$$

where Q and n stand for the CPE constant and exponent respectively The impedance spectra for the Nyquist plots were appropriately analyzed by fitting the data into the equivalent circuit model $R_s(C_{dl}R_{ct})$, which has been previously used to model the metal/acid interface (Zucchi and Omar, 1985; Mu and Li, 2005; Oguzie *et. al.*, 2009, 2010).The corresponding electrochemical parameters derived from the impedance spectra are presented on Tables 4.5 and 4.6.

Impedance measurements revealed how the kinetics of the electrochemical processes at the metal/acid interface was modified by the presence of the purines. Nyquist plots for

mild steel and aluminium corrosion in 0.1 M solutions of HCl, H_2SO_4 and H_3PO_4 in the absence and presence of 0.01 M AD, GU, HYP and XN had been given in Figures 4.17 and 4.18.

The corresponding impedance parameters are presented on Tables 4.5 and 4.6. The increase in R_{ct} values in inhibited systems which signifies an increase in the diameters of the Nyquist semicircles with a corresponding decrease in the double layer capacitance (C_{dl}), confirms the corrosion inhibiting properties of the purines . The observed decrease in C_{dl} values, which normally corresponds to alteration of the double-layer thickness can be attributed to the adsorption of the purines (with lower dielectric constant compared to the displaced adsorbed water molecules) on the metal/acid interface, thereby protecting the metals from the corrosive effect of the aggressive acids.

The magnitude and trend of the obtained inhibition efficiencies %IE presented are in agreement with those determined from gravimetric measurements.

5.5.2 Potentiodynamic polarization measurements

The corrosion current is a function of the reactivity of a metal in an aqueous environment. The higher the values of i_{corr}, the higher the dissolution of the metal and vice versa.

Typical potentiodynamic polarization curves for mild steel and aluminium in 0.1 M solutions of HCl, H_2SO_4 and H_3PO_4 in the absence and presence of 0.01 M AD, GU, HYP and XN are shown in Figures 4.19 - 4.20 while the electrochemical parameters derived from the polarization curves and inhibition efficiencies are summarized on Tables 4.7 and 4.8.

Addition of the purines is seen to affect the anodic as well as the cathodic partial reactions, shifting the corrosion potential (E_{corr}) slightly toward more positive (anodic) values and reducing the anodic and cathodic current densities and the corresponding corrosion current density (i_{corr}). This is an indication of a mixed-type corrosion inhibition mechanism. However, the anodic inhibiting effect of AD and HYP is slightly more pronounced for mild steel in HCl system, whereas the cathodic inhibiting effect is more pronounced for aluminium in HCl system for all the inhibitors (Figures 4.19 - 4.20). Polarisation curves in Figure 4.76 show that only HYP reduced the corrosion current density for aluminium in H_2SO_4 system while none of the inhibitors inhibited the corrosion process for aluminium in H_3PO_4 system.

The obtained IE% values presented on Tables 4.7 and 4.8 follow the same trend as the gravimetric and impedance data confirming the corrosion inhibiting efficacy of the purines.

5.6 Synergistic Considerations

Purines are organic bases which depending on the pH, can be present in aqueous solutions as protonated cationic species, neutral molecules, or dissociated anionic species. Literature findings reveal that the protonated cationic forms are in solution within the pH range of 0-2 while the neutral molecules are the dominant species in the pH range of 5-9 (Katritzky, 1984; Scendo, 2007a, 2007b; Amin *et al.*, 2009).

The results obtained on addition of iodide ions to the test solutions indicate that the iodide ions slightly enhanced the inhibition efficiencies of GU, XN, AD and HYP in HCl and GU and XN in H_3PO_4 for mild steel (Table 4.9) while for aluminium, synergism was evidence with only AD, GU and XN in H_2SO_4 solutions (Table 4.10).

It is well-known that the protective properties of a cation type of an inhibitor in any aggressive environment can be improved with the addition of halide ions to the solution (Hackerman, 1962; Obot *et al,* 2009a; Umoren *et al,* 2009). Corrosion inhibition synergism results from increased surface coverage arising from ion-pair interactions between the protonated purine species and the iodide ions (Oguzie, 2004). The acid anions might however compete with iodide ions for active sites on the metal surface leading to a lower synergistic effect depending on the pH of the bulk solution and that which is obtainable at the metal/acid interface (Oguzie *et al.,* 2007; Amin *et al.,* 2009).

Iodide ion (I^-) is characterized by its strong adsorbability onto the metal surface due to its large ionic radius. This process changes the electrical double layer at the solution side of the interface from positive to negative. This change in the electrical double layer facilitates physical adsorption of the inhibitor cations. Thus, the protonated purine molecules are able to be electrostatically adsorbed on the electrode surface covered primarily by adsorbed I^-ions. From the results obtained (Tables 4.9 and 4.10), it is obvious that I^- ions probably promoted the physical adsorption of purine on the metal surfaces particularly in HCl and H_3PO_4 solutions for mild steel and only in H_2SO_4 solution for aluminium. This was not the case for aluminium in HCl media; this may be because of repulsion between Cl^- and I^- ions (excess negative charge) at the oxide/solution interface in HCl media resulting in relatively lower IE% values. The inhibition efficiencies obtained from the different techniques are very similar (Tables 4.9 and 4.10).

5.7 Infrared Spectroscopic Analysis

From Figures 4.21- 4.28 and Appendices XVI - XXVII, it can be observed that most of the peaks for the purine powders were also noticed in the surface films of the inhibitors on the mild steel surface, suggesting that most of the functional groups within the purine powders are also present in the surface film. This further confirms the fact that the purines were actually adsorbed on the metal surfaces. Moreover, some of the peaks for the adsorbed film diminished or even vanished indicating that the functional groups responsible for these peaks could have been used for the formation of the inhibitor-metal complex which further protected the metal from corrosion.

Examination of the spectra of AD and that of the products of corrosion of mild steel in the presence of AD show that the C-H "oop" aromatic at 722.37cm^{-1} shifted to 717.54 cm^{-1}, the C-N stretch at 1276.92 cm^{-1} due to aromatic amines shifted to 1369.5 cm^{-1}, the C-C stretch in the ring at 1425.44 cm^{-1} shifted to 1482.34 cm^{-1}, N-H bend at 1600.97 cm^{-1} and 3262.7 cm^{-1} shifted to 1634.73 cm^{-1} and 3211.59 cm^{-1} respectively while, O-H stretch at 2804.59 cm^{-1} and 3598.33 cm^{-1} shifted to 2790.12 cm^{-1} and 3533.71 cm^{-1} respectively. The missing functional groups in the spectrum of the corrosion products include C-H "oop" at 894.04 cm^{-1}, C-N stretches at 1031.95 cm^{-1} and 1146.72 cm^{-1} and O-H stretches at 2576.98 cm^{-1} and 2677.98 cm^{-1}.

For the corrosion products of aluminium in the presence of AD, C-H "oop" at 894.04 cm^{-1} shifted to 828.45 cm^{-1} and C-N stretches at 1031.95 cm^{-1} and 1276.92 cm^{-1} shifted to 1022.31 cm^{-1} and 1323.21 cm^{-1} respectively. The C-H wag and stretch at 1146.72 cm^{-1} and 3076.56 cm^{-1} shifted to 1177.58 cm^{-1} and 3196.15 cm^{-1} respectively, the C-C stretch in the ring at 1425.44 cm^{-1} shifted to 1419.66 cm^{-1}, N-H bend at

1600.97 cm^{-1} shifted to 1604.83cm^{-1} while the O-H stretches at 2576.98 cm^{-1}, 2677.29cm^{-1}, 2804.59 cm^{-1}, 2893.32 cm^{-1} , 3262.7 cm^{-1}, and 3358.18 cm^{-1} shifted to 2522.01 cm^{-1},2639.67cm^{-1}, 2740.94 cm^{-1}, 2859.56 cm^{-1}, 3196.15 cm^{-1} and 3380.36 cm^{-1} respectively. Functional groups that were absent in the spectrum of the corrosion products of aluminium in the presence of AD include C-H "oop" at 722.37 cm^{-1} and O-H stretch at 3598.33 cm^{-1}.

For the spectra of GU, C-H "oop" at 857.39 cm^{-1} shifted to 733.94 cm^{-1}, C-O stretch at 1220.02 cm^{-1} shifted to 1153.47cm^{-1}, N-O stretch at 1367.58cm^{-1} shifted to 1372.4 cm^{-1}, the C-N stretch due to aromatic amines at 1367.58 cm^{-1} shifted to 1372.4 cm^{-1}, C-C stretch at 1599.04 cm^{-1} shifted to 1629.9 cm^{-1}, C-H stretches at 2445.82 cm^{-1} and 3034.13 cm^{-1} shifted to 2399.53 cm^{-1} and 3086.21 cm^{-1} respectively while the O-H stretches at 2665.71 cm^{-1}, 2834.49 cm^{-1} and 3357.22 cm^{-1} shifted to 2673.43 cm^{-1}, 2812.31 cm^{-1} and 3396.76 cm^{-1} respectively. The missing functional groups include C=O stretching frequency at 1730.21 cm^{-1} and the O−H stretching frequencies at 2579.88 cm^{-1} and 3153.72 cm^{-1}.

For the corrosion products of aluminium in the presence of GU, C-H "oop" at 857.39 cm^{-1} shifted to 890.18 cm^{-1}, C-O stretch at 1220.02 cm^{-1} shifted to 1021.34 cm^{-1}, C-N at 1367.58 cm^{-1} shifted to 1313.57 cm^{-1}, C-C in the ring stretch at 1599.04 cm^{-1} shifted to 1407.12 cm^{-1}, C=O stretch at 1730.21 cm^{-1} shifted to 1605.79 cm^{-1}, C-H stretches at 2445.82 cm^{-1}, 2665.71 cm^{-1}, 2834.49 cm^{-1} and 3034.13 cm^{-1} shifted to 2442.93 cm^{-1}, 2650.28 cm^{-1}, 2851.85 cm^{-1} and 3080.42 cm^{-1} respectively. The O-H stretch at 3357.22 cm^{-1} also appeared at 3357.22 cm^{-1}. The missing functional groups include C-Br stretch at 645.21 cm^{-1} and C-H stretch at 3153.72 cm^{-1}.

For the corrosion products of mild steel in the presence of HYP shows C-H "oop" at 886.32 cm^{-1} shifted to 700.18 cm^{-1}, C-O stretch at 1132.25 cm^{-1} shifted to 1010.73 cm^{-1}, N-O stretch at 1362.75 cm^{-1} shifted to 1373.36 cm^{-1}, C-C stretch in the ring at 1449.55 cm^{-1} and 1606.76cm^{-1} shifted to 1487.17 cm^{-1} and 1654.01cm^{-1} respectively, C-H stretch at 3049.56 cm^{-1} shifted to 3056.31 cm^{-1} while O-H stretch at 3459.45 cm^{-1} shifted to 3382.29 cm^{-1}.

For the corrosion products of aluminium in the presence of HYP, C-H "oop" at 886.32 cm^{-1} shifted to 822.67 cm^{-1}, C-O stretches at 1194.94 cm^{-1} and 1362.75 cm^{-1} shifted to 1164.08 cm^{-1} and 1312.6 cm^{-1} respectively.The C-C in-ring stretches at 1449.55 cm^{-1} and 1606.76 cm^{-1} shifted to 1428.34 cm^{-1} and 1600.01 cm^{-1} respectively while the C=O stretches at 1672.34 cm^{-1} and 1844.97 cm^{-1} shifted to 1755.28 cm^{-1} and 1898.98 cm^{-1}. The O-H stretches at 2475.72 cm^{-1}, 2580.84 cm^{-1}, 2648.35 cm^{-1}, 2796.88 cm^{-1}, 2902.96 cm^{-1} and 3459.45 cm^{-1} shifted to 2417.85 cm^{-1}, 2508.51 cm^{-1}, 2605.92 cm^{-1}, 2753.48 cm^{-1}, 2949.26 cm^{-1} and 3403.51 cm^{-1} and C-H stretch at 3049.53 cm^{-1} shifted to 3068.85 cm^{-1}. Missing functional groups include C-Br stretch at 538.16 cm^{-1} and 636.53 cm^{-1}.

For XN, examination of the spectra of its powder together with the products of corrosion in the presence of mild steel reveals that C-H "oops" at 755.16 cm^{-1} and 872.82 cm^{-1} shifted to 745.51 cm^{-1} and 838.1 cm^{-1}, C-N stretch at 1149.61 cm^{-1} shifted to 1155.40cm^{-1}, C-C stretches at 1415.80 cm^{-1} and 1600.97 cm^{-1} shifted to 1475.59 cm^{-1} and 1634.73 cm^{-1}, O-H stretches at 2521.05 cm^{-1}, 2681.14 cm^{-1} and 3216.41 cm^{-1} shifted to 2591.45 cm^{-1}, 2701.40 cm^{-1} and 3282.95 cm^{-1} respectively. The missing functional

groups include C-Br stretch at 499.58 cm^{-1}, C-N stretch at 1351.18 cm^{-1}, C=O stretch at 1776.50 cm^{-1}, and O-H stretches at 2867.28 cm^{-1} and 3139.25 cm^{-1}.

The spectra of the corrosion products of aluminium in the presence of XN show that C- H "oop" at 872.82 cm^{-1} shifted to 800.49 cm^{-1}, C-N stretches at 1149.61 cm^{-1} and 1351.18 cm^{-1} shifted to 1171.79 cm^{-1} and 1299.1 cm^{-1}, C-C stretches at 1415.80 cm^{-1} and 1600.97 cm^{-1} shifted to 1398.44 cm^{-1} and 1598.08 cm^{-1}, O-H stretches at 2681.14 cm^{-1}, 2867.28 $cm^{-1}$and 3216.41 cm^{-1} shifted to 2600.13 cm^{-1}, 2865.35 $cm^{-1}$and 3265.59 cm^{-1} respectively. Again, the missing functional groups include C-Br stretch at 499.58 cm^{-1}, C-H "oop" at 755.16 cm^{-1}, C=O stretch at 1776.50cm^{-1}, O-H stretches at 2521.05 cm^{-1} and 3139.25 cm^{-1}.

5.8 Scanning Electron Microscopy

The surface morphologies of mild steel and aluminium in solutions of HCl were studied using scanning electron microscopy. Figures 4.29 and 4.30 show the scanning electron micrographs of mild steel and aluminium (at x5000 magnification) in the absence and presence of adenine (AD), guanine (GU) and hypoxanthine (HYP) respectively. From Figures 4.29(a) and Figure 4.30(a), flakes showing corrosion products of mild steel and aluminium in the absence of the purines indicate that the surfaces were strongly damaged but in the presence of AD, GU and HYP on mild steel (Figures 4.29(b), (c) and (d)), it can be seen that the damaging effect of the acid on the mild steel is greatly reduced giving rise to more ordered corrosion products as surface coatings. It can also be seen from Figures 4.30(b)-(d) that the surface of the aluminium electrode was modified by AD, GU and HYP through the formation of a thin protective layer (Oguzie, 2012a).

The results obtained from the scanning electron micrographs of AD, GU and HYP are consistent with those obtained from the FTIR spectra of the corrosion products of the metals and impedance spectra of mild steel and aluminium in the presence of these purines, showing that these compounds inhibited the corrosion of mild steel and aluminium to varying degrees through the mechanism of adsorption (Enenebeaku, 2011; Oguzie *et al.*, 2012a).

5.9 Quantum Chemical Calculations

Figures 4.31 – 4.34 illustrate the highest occupied molecular orbital (HOMO), lowest unoccupied molecular orbital (LUMO), as well as the total electron density of adenine (AD), guanine (GU), hypoxanthine (HYP) and xanthine (XN); while the corresponding quantum chemical parameters are presented in Tables 4.15 and 4.16. Interestingly, the HOMO-LUMO locations are actually almost identical for all the molecules, which should lead to some similarities in their adsorption characteristics. The region of highest electron density, HOMO, are the sites at which electrophiles (metal surface) attack and represents the active sites with the utmost ability to bond to the metal surface, whereas the LUMO orbital can accept electrons from the 3d orbital of the Fe atom or 3p orbital of the aluminium, to form feedback bonds. The HOMO energy (E_{HOMO}) expresses the intrinsic electron donating tendency to an appropriate acceptor i.e., any molecule with lower HOMO energy and empty molecular orbital; while the energy of LUMO (E_{LUMO}) is directly related to the electron affinity and characterizes the susceptibility of the molecule toward attack by nucleophiles (Martinez, 2003; Rodriguez-Valdez, 2005; Chi and Zhao, 2009). Low values of the gap ($\Delta E = E_{LUMO\ -\ HOMO}$), will render good inhibition efficiencies since the energy to remove an electron from the last occupied orbital will be minimized.

The E_{HOMO} and E_{LUMO} values do not vary significantly for all the molecules, probably because the functional groups that comprise their HOMO and LUMO locations are comparable. The ΔE values again do not vary so much which means that any observed differences in their adsorption strengths would result from molecular size parameters rather than electronic structure parameters. The seemingly low values of ΔE (approximately 5 eV) suggest that interaction of the molecules with the metal surface would likely involve electron transfer processes (Enenebeaku, 2011). The Mulliken charges were calculated and the charges of representative atoms are listed in Table 4.12.

5.10 Molecular Dynamics Simulations

The adsorption of adenine (AD), guanine (GU), hypoxanthine (HYP) and xanthine (XN) molecules on the mild steel and aluminium surfaces were analyzed at a molecular level by molecular dynamics simulations, using Forcite quench molecular dynamics to sample many different low energy configurations and to identify the low energy minima (Casewit *et al.,* 1992a,1999b). Optimised structures of AD, GU, HYP and XN were used for the simulation. Solvent and charge effects were neglected in all the simulations and calculations were performed at the metal/vacuum interface. Although this is clearly an oversimplification of the actual situation, it is adequate to qualitatively illustrate the differences in the adsorption behaviour of the molecules and provide sufficient insight to the study objectives.

Figure 4.35 shows representative snapshots of the crosssection of the lowest energy adsorption configurations for the single molecules on the Fe (110) surface from the simulations, while Figure 4.36 shows the representative snapshots for the single molecules on the Al (110) surface. The molecules can be seen to maintain a flat-lying adsorption orientation on the metal surfaces thereby maximizing contact and enhancing

the degree of surface coverage. This parallel adsorption orientation also facilitates interaction of π - electrons of the pyrimidine and imidazole nucleus and the hetero-atoms (N and O) in the molecules with the metal surfaces.

The binding energy (E_{bind}) between the metal surface and the inhibitor molecules are presented on Tables 4.17-4.18. In each case, the potential energies were calculated by averaging the energies of the five structures of lowest energy. As can be seen from the data, the binding energies are all negative suggesting stable adsorption structures however, the magnitude of the calculated binding energies is < 100 kcal mol^{-1} this is despite the fact that the simulations did not take into consideration the specific covalent interactions between the molecules and the Fe surface. This value has been reported by Akalezi *et al.* (2012) to be in the range of physisorptive interactions.

From Tables 4.17 and 4.18, it is observed that the binding energies for the purine molecules on Fe (110) slab are of higher magnitude (-66.97 to -84.53 kcal mol^{-1}) than those obtained for Al (110) slab (-30.60 to -39.69 kcal mol^{-1}). This implies that the molecules are more strongly adsorbed on Fe than Al.

A detailed analysis of the on-top view of the adsorbed molecules on Fe (110) and Al (110) emphasizing the soft epitaxial adsorption mechanism with accommodation of the molecular backbone in characteristic epitaxial grooves on the metal surface are presented in Figures 4.37- 4.38. The on-top view reveal a very clear trend in the adsorption configuration in which polarizable atoms along the molecular backbone appear to align with vacant sites on the face-centered cubic lattice atop the metal surface. In other words, the pyrimidine and imidazole nucleus seem to avoid contact

with the Fe atoms on the surface plane (larger spheres on the Fe/Al slab) and is preferentially accommodated in characteristic epitaxial grooves on the metal surface. Such epitaxial adsorption configuration, which is associated with a minimum free energy of adsorption, has also been reported for some compounds like amino acids, peptides, etc. (Heinz *et al.*, 2009; Feng *et al.*, 2010; Feng *et al.*, 2011) and accounts for the stable adsorption structures (Dai and Zhang, 2011).

5.11 Mechanism of Inhibition

Results from impedance studies, infra red spectroscopy scanning electron microscopy and molecular dynamics show that some of the inhibitors are adsorbed to varying degrees on the mild steel and aluminium surfaces. In acid solutions, organic inhibitors may interact with the corroding metal surface and affect the corrosion reaction in more than one way, sometimes simultaneously. It is therefore often difficult to assign a single general inhibition mechanism, since the mechanism may change with experimental conditions. The adsorption mechanism for a given inhibitor depends on such factors as the nature of metal, surface charge, corrosive medium, pH of the metal/solution interface, the concentration of the inhibitor as well as the functional groups in the inhibitors, since different groups are adsorbed to different extents.

Physical adsorption requires the presence of both electrically charged surface of the metal and charged species in the bulk solution. Chemisorption process involves charge sharing or charge-transfer from the inhibitor molecules to the metal surface to form a coordinate type of bond. The presence of a transition metal, having vacant, low-energy electron orbital and of an inhibitor molecule having relatively loosely bound electrons or hetero atoms with lone pairs of electrons is necessary for this to occur (Reinhard and Rammet, 1985; Obot *et al*, 2009a, 2009b).

It has been reported that purines exist in protonated forms in acidic media (Katritzky, 1984; Ould-Moulaye *et al.,* 2001). Therefore AD, GU, HYP and XN can exist as protonated species (cations) as well as molecular species (neutral molecules) in acidic medium, depending on the concentration (pH) of the acid. Katritzky (1984) reported that protonated cationic species of purines, are the dominant inhibiting species in the range of pH of 0–2.

where *Inh* corresponds to AD, GU, HYP and XN.

If physisorption is the dominant adsorbtion mechanism, one expects the electrostatic interaction involving protonated species to be more significant. This may have been the case in the adsorption of AD, GU, HYP and XN on the metal surfaces in HCl. Increased activation energy in inhibited solutions compared to the blank suggests physisorption while either unchanged or lower E_a in the presence of inhibitor suggests chemisorptions (Popova et al., 2003; Obot et al., 2009). From Tables 4.3 and 4.4, E_a values were higher in the presence of AD, GU, HYP and XN compared to their absence in the corrosion of mild steel in HCl. On the other hand, if chemisorption is dominant, one expects electron transfer or sharing involving molecular species to be the most important. Also, from Tables 4.3 and 4.4, it can be observed that E_a values for the corrosion of mild steel in 0.1 M H_2SO_4 and H_3PO_4 in the presence of AD, GU and HYP were higher than the values obtained for the blank. It can therefore be concluded that the corrosion inhibition of mild steel in 0.1 M H_2SO_4 and H_3PO_4 by AD, GU and HYP is afforded by adsorption of neutral molecules on the steel surface rather than protonated species. Similar results have been reported by Oguzie (2007) and Umoren (2007).

The cathodic hydrogen evolution reaction may be given by equations 5.13-5.15

This implies that the protonated inhibitor molecules may have also been adsorbed at cathodic sites of mild steel/aluminium in competition with hydrogen ions reduced to H_2 gas (Lagrenee *et al.*, 2002; Yurt *et al.*, 2004; Solmaz *et al.*, 2008). The adsorption of protonated purine molecules at the cathode may have therefore reduced the rate of hydrogen evolution reaction. The adsorption of the purines on the mild steel/aluminium surface at both anodic and cathodic sites on the metal surface may therefore account for mixed-type inhibition mechanism observed from the polarization curves.

In addition, the chemical structures of AD, GU, HYP and XN indicate the presence of carbonyl (–C=O) group in GU, HYP and XN and amino ($–NH_2$) group for all the compounds. The purines may be adsorbed on the mild steel/aluminium surface by the formation of an iron–nitrogen or aluminium-nitrogen coordination bond. Also, the unshared electron pairs on N and/or O atoms of the purines may interact with vacant d-orbitals or p-orbitals of iron and aluminium respectively, to provide a protective chemisorbed/physisorbed film. This is seen from the on-top view of the adsorbed molecules on Fe (110) and Al (110), as presented in Figures 4.37 and 4.38. From Figures 4.37 and 4.38, the adsorption configuration is such that the polarizable atoms

along the molecular backbone appear to align with vacant sites on the face-centered cubic lattice atop the metal surface.

It is generally accepted that the presence of halide ions in acidic media yield enhancement of inhibition efficiencies of some organic compounds (Umoren *et al*, 2006). It is also assumed that the halide ions are able to improve adsorption of organic cations by forming intermediate bridges between the positively charged metal surface and the positive end of the organic inhibitor thereby increasing surface coverage of the inhibitors (Obot *et al*, 2009a).

The addition of I^- ions to the test solutions may have changed the charge on the electrical double layer from positive to negative. This change in the charge of the solution side of the interface facilitates physical adsorption of the purine cations. Thus, protonated purine molecules may have been electrostatically adsorbed on the electrode surface covered primarily by adsorbed I^- ions justifying the mechanism of physisorption with accompanying higher %IE values. Lower %IE values in the presence of I^- ions on the other hand could imply that the neutral molecular species are dominant in the system thereby favouring chemisorption.

CHAPTER SIX

SUMMARY, CONCLUSIONS AND RECOMMENDATIONS

6.1 Summary and Conclusions

The results from the study show that some of the purines studied possess good inhibition properties for the corrosion of mild steel and aluminium in 0.1 M HCl, H_2SO_4 and H_3PO_4. The inhibition efficiencies increased with increasing concentrations of the inhibitors. The inhibition efficiencies of purines for the corrosion of mild steel in 0.1M HCl, H_2SO_4 and H_3PO_4 solutions decreased in the order: AD > HYP > GU > XN (in HCl); HYP > AD > GU > XN (in H_2SO_4); and GU > AD > HYP > XN (in H_3PO_4), respectively. For aluminium in 0.1 M HCl, H_2SO_4 and H_3PO_4 solutions, the inhibition efficiencies decreased in the order: GU > AD > HYP > XN (in HCl). However, only HYP inhibited the corrosion of aluminium in H_2SO_4 solution. Their was no evidence of corrosion inhibition by AD, GU and XN in H_2SO_4 or any of the purines in H_3PO_4 solutions as they rather enhanced the corrosion of aluminium thereby functioning as corrosion catalysts. It was also observed that the inhibition efficiencies decreased with inmersion time for all the systems and for some of the systems at 333 K. Moreover, IE% of the selected purines was slightly enhanced in the presence of KI for some of the systems investigated.

The results obtained revealed that AD, GU, HYP and XN are good corrosion inhibitors for the corrosion of mild steel in HCl, H_2SO_4 and H_3PO_4. All the purines inhibit the corrosion of aluminium in HCl while only HYP inhibit the corrosion of aluminium in H_2SO_4.

Impedance measurements show that the inhibitors functioned by adsorption of the purines on the metal/corrodent interface while polarization measurements show that the adsorbed purines inhibited the corrosion process via mixed inhibition mechanism, affecting both the anodic metal dissolution reaction and the cathodic hydrogen evolution reaction.

Furthermore, the inhibition efficiencies of the purines obtained from gravmetric, polarization and impedance studies were observed to be similar and in good agreement.

From the activation energies (E_a), heats of adsorption (Q_{ads}) and standard free energies of adsorption (ΔG_{ads}) obtained from the study, it is evident that the inhibitors are adsorbed on the steel and aluminium surfaces through both physical and chemical interactions suggesting that both molecular as well as protonated purine species were responsible for the observed inhibiting actions of the compounds in the different acid media. Adsorption characteristics of the purines fitted both the Langmuir and Temkin isotherms.

SEM micrographs, FTIR and impedance spectra showed the presence of protective layers over the mild steel and aluminium surfaces, providing evidence for the corrosion inhibitory effects of the inhibitors. While DFT-based quantum chemical computations of parameters associated with the electronic structures of the purine molecules confirmed their inhibiting potential, which was further corroborated by molecular dynamics modeling of the adsorption of the single molecules on the metal surface.

6.2 RECOMMENDATIONS

Further study is required to assess the following:

i. Use of purine derivatives as corrosion inhibitors in coatings on metallic implants in the field of medicine should be explored under *in vitro* and *in vivo* conditions.

ii. Synergistic studies involving two or more of the studied purine derivatives should be undertaken.

iii. Corrosion inhibition studies by purines should be carried out under field conditions to simulate operational conditions including the effects of flow, pressure, a wider temperature range and pH of the aqueous systems so as to explore the possibility of using them as inhibitor formulations in industries.

iv. Quantum chemical calculations and molecular dynamics involving a rigorous modeling of inhibitor-metal surface, water-metal surface, and inhibitor-water interactions should be investigated. This is because inhibition effectiveness depends on the interplay between them.

REFERENCES

Abdallah, M. (2004). Guar gum as corrosion inhibitor for carbon steel in sulphuric acid solutions. *Portugaliae Electrochimica Acta*, **22:**161-175.

Abdeli, M., Ahmadi, N. P. and Khosroshahi, R. A. (2009). Nile blue and indigo carmine organic dyes as corrosion inhibitor of mild steel in hydrochloric acid. *Journal of Solid State Electrochemistry*, **14(7):** 1317-1324.

Achebe, C.H., Nneke, U.C. and Anisiji, O. E. (2012). Analysis of oil pipeline failures in the oil and gas industries in the Niger Delta area of Nigeria. Proceedings of the International MultiConference of Engineers and Computer Scientists, IMECS (Vol II, pp. 14 – 16). Hong Kong.

Adejo, S.O., Ekwenchi, M.M., Momoh, F. and Odiniya, E. (2012). Adsorption characterization of ethanol extract of leaves of *Portulaca oleracea* as green corrosion inhibitor for corrosion of mild steel in sulphuric acid medium. *International Journal of Modern Chemistry*, **1(3):** 125-134.

Ahamad, I., Prasad, R. and Quraishi, M.A. (2010). Experimental and quantum chemical characterization of the adsorption of some Schiff base compounds of phthaloyl thiocarbohydrazide on the mild steel in acid solutions. *Materials Chemistry Physics*, 124: 1155-1165.

Akalezi, C.O., Enenebaku, C.K. and Oguzie, E.E. (2012). Application of aqueous extracts of coffee senna for control of mild steel corrosion in acidic environments. *International Journal of Industrial Chemistry,* 3:13-25.

American Society for Testing Materials (ASTM) G96-90. (2001). Standard Guide for On-Line Monitoring of Corrosion in Plant Equipment (Electrical and Electrochemical Methods). Annual Book of ASTM Standards, Vol. 03.02, ASTM, Philadelphia, PA.

Amin, M. A., Moshen, Q. and Omar, A. H . (2009). Synergistic effect of I^- ions on the corrosion inhibition of Al in 1.0 M phosporic acid solutions by purine. *Materials Chemistry and Physics,* 123: 1023-1035

Ashassi-Sorkhabi, H., Seifzadeh, D. and Hosseini, M.G. (2008). EN, EIS and polarization studies to evaluate the inhibition effect of 3H-phenothiazin-3-one, 7-dimethylamin on mild steel corrosion in 1 M HCl solution. *Corrosion Science,* 50(12): 3363-3370.

Ashassi-Sorkhabi, H., Shaabani, B., Aligholipour, B. and Seifzadeh , D. (2006). The effect of some schiff bases on the corrosion of aluminium in HCl solution. *Applied Surace Sci*ence, **252** : 4039-4047.

Avci, G. (2008). Inhibitor effect of N,N-methylenediacrylamide on corrosion behaviour of mild steel in 0.5 M HCl. *Materials Chemistry and Physics,* 112: 234–238.

Baboian, R., Bellante, E. L. and Cliver, E. B. (1990). *The Statue of Liberty Restauration,* Houston, Tex., NACE International.

Bahrami, M.J., Hosseini, S.M.A. and Pilvar, P. (2010). Experimental and theoretical investigation of organic compounds as inhibitors for mild steel corrosion in sulfuric acid medium. *Corrosion Science*, 52: 2793–2803.

Cabot, P.L., Centellas, F.A., Garrido, J.A., Perez, E. and Vidal, H. (1991). "Electrochemical Study of Aluminium Corrosion in Acid Chloride Solutions". *Electrochimica Acta.*, **36**: 171-187.

Casewit, C.J., Colwell, K.S. and Rappé, A. K. (1992a). Application of a universal force field to organic molecules. *Journal of the American Chemical Society,* 114:10035–10046.

Casewit, C.J., Colwell, K. S. and Rappé, A. K. (1992b). Application of a universal force field to main group compounds. *Journal of the American Chemical Society,* 114:10046–1005.3

Chen, H.J., Hong, T. and Jepson, P. (2000). High temperature corrosion inhibition performance of imidazoline and amide. *Corrosion 2000,* Paper 00035.

Chi, M. and Zhao, Y.P. (2009). Adsorption of formaldehyde molecule on the intrinsic and Al-doped grapheme: A first principle study. *Computional Materials Science,* 48:1085–1090.

Dai, W. and Zhang, Y.Y. (2012). Molecular dynamics simulation of the adsorption behaviour of amino acid corrosion inhibitor on Cu (1 0 0) surface. *Applied Mechanics and Materials,* **121-126:** 226-230.

Dean, S.W. (2003). Corrosion monitoring for industrial processes. In: D.S Cramer, B.S Covino (eds.), Corrosion: Fundamentals, Testing and Protection (Vol. 13A, pp. 533-541) Metals Park, OH, ASM International.

Delley, B. (1990). An All-Electron Numerical Method for Solving the Local Density Functional for Polyatomic Molecules. *Journal of Chemical Physics*, 92:508–517.

Delley, B. (2000). From molecules to solids with the $DMol^3$ approach. *Journal of Chemical Physics*, 113:7756–7764.

Denny, J. (2004). Principles and Preventions of Corrosion, Upper Saddle River, New Jersey Prentice Hall. ISBN 0-13-359993-0.

Döner, A., Solmaz, R., Özcan, M. and Kardas, G. (2011). Experimental and theoretical studies of thiazoles as corrosion inhibitors for mild steel in sulphuric acid solution. *Corrosion Science*, 53: 2902–2913.

Ebenso, E.E., Eddy, N.O. and Odiongenyi, A.O. (2008). Corrosion inhibitive properties and adsorption behaviour of ethanol extract of *Piper guinensis* as a green corrosion inhibitor for mild steel in H_2SO_4. *African Journal of Pure and Applied Chemistry*, **2(11):** 107-115.

Eddy, N. O. (2008). Inhibition of the corrosion of mild steel in H_2SO_4 by some antibiotics. Ph.D Thesis, University of Calabar, Calabar.

Eddy, N.O. (2010). Part 3: Theoretical study on some amino acids and their potential activity as corrosion inhibitors for mild steel in HCl. *Molecular Simulations*, **36(5):** 354-363.

Eddy, N.O. and Ebenso, E.E. (2008). Adsorption and inhibitive properties of ethanol extracts of *Musa sapientum* peels as a green corrosion inhibitor for mild steel in H_2SO_4. *African Journal of Pure and Applied Chemistry*, **2(6):** 046-054.

Eddy, N.O. and Ebenso, E.E. (2010). Corrosion inhibition and adsorption properties of ethanol extract of *Gongronema latifolium*on mild steel in H_2SO_4. *Pigment and Resin*, **39(2):** 77-83.

Eddy, N. O., Ebenso, E. E. and Ibok, U. J. (2010). Adsorption, synergistic inhibitive effect and quantum chemical studies of ampicillin (AMP) and halides for the corrosion of mild steel in H_2SO_4. *Journal of Applied Electrochem*istry, **40**: 445-456.

Eddy, N. O. and Ita, B. I. (2010). Experimental and theoretical studies on the inhibition potentials of some derivatives of cyclopenta-1,3-diene for the corrosion of mild steel in HCl solutions. *International Journal of Quantum Chemistry*, **DOI:** 104152/pea.200904443.

Eddy, N.O. and Odiongenyi, A.O. (2010). Corrosion inhibition and adsorption properties of ethanol extract of *Heinsia crinata* on mild steel in H_2SO_4. *Pigment and Resin Technol*ogy, **39(5):** 288-295.

Eddy, N.O. and Odoemelam, S.A. (2008). Inhibition of the corrosion of mild steel in acidic medium by Penicillin V potassium. *Advances in Natural and Applied Sci*ence, **2(3):**225-232.

Eddy, N.O., Odoemelam, S.A. and Odiongenyi, A.O. (2009). Inhibitive, adsorption and synergistic studies on ethanol extract of *Gnetum africana* as green corrosion inhibitor for mild steel in H_2SO_4. *Green Chemistry Letters and Reviews,***2(2):** 111-119.

Ekanem, U.F., Umoren, S.A., Udousoro I.I. and Udoh, A.P. (2010). Inhibition of mild steel corrosion in HCl using pineapple leaves (*Ananas comosus L.*) extract. *Journal of Materials Science*. **45(20):** 5558-5566.

EI-Awady, A.A., Abd-EI-Nabey, B.A. and Aziz, S.G. (1992). Kinetic-thermodynamic and adsorption isotherms analyses for the inhibition of the acid corrosion of steel by cyclic and open-chain amines. *Journal of the Electrochemical Society*, 139(8):2149-2154.

El-Rabiee, M. M., Helal, N. H., Abd El-Hafez, G. M. and Badawy, G. A. (2008). Corrosion control of vanadium in aqueous solutions by amino acids. *Journal of Alloys and Compounds*,**459:** 466–471.

Enenebeaku, C.K. (2011). Electrochemical studies of the inhibitory effects of selected plant extracts on the acid corrosion of mild steel. Ph.D Thesis. Federal University of Technology, Owerri.

Feng, J., Pandey, R.B., Berry, R.J., Farmer, B.L., Naik, R.R. and Heinz, H. (2010). Adsorption mechanism of single amino acid and surfactant molecules to Au{111} surfaces in aqueous solutions: Design rules for metal-binding molecules. *Soft Matter*. 7: 2113-2120

Feng, L., Yang, H. and Wang, F. (2011). Experimental and theoretical studies for corrosion inhibition of carbon steel by imidazoline derivative in 5% NaCl saturated $Ca(OH)_2$ solution. *Electochimica Acta*, **58:** 427-436

Fiaud, C. (1994). Theory and Practice of Vapour Phase Inhibitors, in *A Working Party Report on Corrosion Inhibitors*, London, U.K., The Institute of Materials, pp.1–11.

Fontana, M.G. (1986). Corrosion Engineering, New York, McGraw-Hill Book Company.

Fox, D.L. (1979). Biochromy, natural colouration of living things. University of California Press.

Fuchs-Godec, R. and Zerjav, G. (2009). Inhibition properties of triton X100 on ferritic stainless steel in sulphuric acid at increasing temperature. *Acta Chimica Slovenica*, 56:78-85.

Gasparac, R., Martin, C.R. and Stupnisek-Lisac, E. (2000a). *In situ* studies of imidazole and its derivatives as copper corrosion inhibitors I. Activation Energies and Thermodynamics of Adsorption. *Journal of the Electrochemical Society*, **147(2):** 548-551.

Gasparac, R., Martin, C.R., Stupnisek-Lisac, E. and Mandic, Zoran. (2000b). *In situ* and *ex situ* studies of imidazole and its derivatives as copper corrosion inhibitors II. AC Impedance, XPS, and SIMS Studies. *Journal of the Electrochemical Society*, **147(3):** 991-998.

Gopi, D., Govindaraju, K.M., Manimozhi, S., Ramesh, S. and Rajeswari, S. (2007). Inhibitors with biocidal functionalities to mitigate corrosion on mild steel in natural aqueous environment. *Journal of Applied Electrochemistry*, 37(6): 681-689.

Günter, S. (2009). Global needs for knowledge dissemination, research and development in materials deterioration and corrosion control. *The World Corrosion Organisation*, 5: 3

Hackerman, N. (1962). Recent advances on understanding of organic inhibitors. *Corrosion*, **18 (9):** 332-337.

Hackerman, N. and Snaveley, E. S. (1984). Corrosion Basics, NACE, Texas, USA.

Heinz, H., Farmer, B.L., Pandey, R.B., Slocik, J.M., Patnaik, S.S., Pachter, R. and Naik R.R. (2009). *Journal of American Chemical Society, 131:9704–9714*

Hosseini, M.G., Khalilpur, H., Ershad, S. and Saghatforoush, L. (2009). Protection of mild steel corrosion with new thia-derivative salens in 0.5 M H_2SO_4 solution. *Journal of Applied Electrochemistry*,40(2): 215-223.

James, A.O., Oforka, N.C. and Abiola, O. K. (2006). Inhibition of aluminium (3SR) corrosion in hydrochloric acid by pyridoxol hydrochloride. *Bulletin of Electrochemistry*, **22:** 111 116.

Jones, D.A. (1982). Forms of corrosion, recognition and prevention. Dillon C.P. edited. NACE, Houston. Reprinted by permission of the National Association of Corrosion Engineers.

Jones, L. W. (1988). *Corrosion and Water Technology for Petroleum Producers.* Tulsa, Oklahoma, Oil and Gas Consultants International.

Jorge, E.C. and Leandro, E. (2005). Corrosion and corrosion control. *Concrete Repair Bulletin*, (Sept/Oct): 2

Katritzky, A.R. (1984). Comprehensive Heterocyclic Chemistry: The structure, reaction, synthesis and uses of heterocyclic compounds. London, Pergamon Press Ltd.

Khadom, A.A., Yaro, A.S., Altaie, A.S. and Khadum, A.A.H. (2009). Electrochemical, activations and adsorption studies for the corrosion inhibition of low carbon steel in acidic media. *Portugaliae Electrochimica Acta*, **27(6):** 699-712.

Khaled, K.F. (2003). The inhibition of benzimidazole derivative on corrosion of iron in 1 M HCl solutions. *Electrochimica Acta*, 48: 2493-2503.

Khaled, K. F. (2010a).Studies of iron corrosion inhibition using chemical, electrochemical and computer simulation techniques. *Electrochimica Acta*, **55:** 6523−6532.

Khaled, K.F. (2010b). Corrosion of copper in nitric acid solutions using some amino acids: A combined experimental and theoretical study. *Corrosion Science*, 52:3225–3234.

Kliskic, M., Radosevic, J., Gudic, S. and Katalinic, V. (2000). Aqueous extract of *Rosmarinus officinalis L*. as inhibitor of Al-Mg alloy corrosion in chloride solution. *Journal of Applied Electrochemistry,* **30:** 823-30.

Lagrenee, M., Mernari, B., Bouanis, M., Traisnel, M. and Bentiss, F. (2002). Study of the mechanism and inhibiting efficiency of 3,5-bis(4-methylthiophenyl)-4H-1,2,4-triazole on mild steel corrosion in acidic media. *Corrosion Science*, 44: 573–588.

Lagrenée, M., Mernari, B., Chaibi, N., Traisnel, M., Vezin, H. and Bentiss, F. (2001). Investigation of the inhibitive effect of substituted oxadiazoles on the corrosion of mild steel in HCl medium. *Corrosion Science,* **43:** 951–962.

Lashgari, M., Arshadi, M. R. and Biglar, M. J. (2010). Experimental and theoretical studies of media effects on copper corrosion in acidic environments containing 2-amino-5-mercapto-1,3,4-thiadiazole. *Iranian Chemical Soc*iety, ***7*:** 478-486.

Li, X., Shuduan, D., Hui, F. and Guannan, M. (2009a). Inhibition effect of 6-benzylaminopurine on the corrosion of cold rolled steel in H_2SO_4 solution. *Corrosion Science,***51(3):** 620 -634.

Li, X., Shuduan, D., Hui, F. and Guannan, M. (2009b). Adsorption and inhibition effect of 6-benzylaminopurine on cold rolled steel in 1.0 M HCl . *Electrchimica Acta,* **54(16):** 4089 -4098.

Li, X., Shuduan,D., Hui,F. and Guannan, M .(2009c). Synergism between red tetrazolium and uracil on the corrosion of cold rolled steel in H_2SO_4 solution. *Corrosion Science,* **51(6):** 1344 -1355.

Li, X., Shuduan, D., Hui, F. and Guannan, M. (2009d). Synergistic inhibition effect of red tetrazolium and uracil on the corrosion of cold rolled steel in H_3PO_4 solutions: Weight loss, electrochemical and AFM approaches. *Materials Chemistry and Phys*ics, **115(2):** 815 -824.

Li, W., Hu, L., Tao, Z., Tian, H. and Hou, B. (2011). Experimental and quantum chemical studies on two triazole derivatives as corrosion inhibitors for mild steel in acid media. *Materials and Corros*ion, 62: n/a. doi: 10.1002/maco.201005965.

Li, Y., Umoren, S.A. and Wang, F.H. (2010). Electrochemical study of corrosion inhibition and adsorption behaviour for pure iron by polyacrylamide in H_2SO_4: Synergistic effect of iodide ions. *Corrosion Science,* 52: 1777–1786.

Martinez, S. (2003). Inhibitory mechanism of mimosa tannin using molecular modeling and substitutional adsorption isotherms. *Materials Chemistry and Physics*, 77(1):97-102

Martinez .S. and Stern. I. (2001). Inhibitory mechanism of low-carbon steel corrosion by mimosa tannin in sulphuric acid solutions. *Journal of Applied Electrochemistry*, **31:**973-978.

Matheswaran, P. and Ramasamy, A. K. (2010). Influence of benzotriazole on corrosion inhibition of mild steel in citric acid medium. *Electronanalytical Journal of Chemistry*, **7(3):** 1090-1094.

Mercer, A. D. (1994). Corrosion Inhibition: Principles and Practice. In: Shreir, L. L., Jarman, R. A. and Burstein, G.T. (Eds.). *Corrosion Control*, Oxford, UK, ButterworthsHeinemann.

Miksic, B. A. (1993). Use of Vapour Phase Inhibitors for Corrosion Protection of MetalProducts. In Raman, A. and Labine, P. (Eds.). *Reviews on Corrosion Inhibitor Scienceand Technology,* Houston, Tex., NACE International.

Moniz, B. J. (1986). Process industries corrosion. In: Moniz, B.J. and Pollock (Ed). NACE. Houston. Reprinted by permission of the National Association of Corrosion Engineers.

Moore, J. J. (1996). Chemical metallurgy. 2nd edition. London. Butterworths.

Morgan, W. M. (1984). Outline of Paint Technology. England: Charles Griffins Ltd.

Moretti, G. Guidi, F. and Grion, G. (2004). Tryptamine as a green iron corrosion inhibitor in 0.5 M deaerated sulphuric acid. *Corrosion Science*, **46:** 387–403.

Mu, G. and Li, X. (2005).Inhibition of cold rolled steel corrosion by Tween-20 in sulfuric acid: Weight loss, electrochemical and AFM approaches. *Journal of Colloid and Interface Science,* **289:** 184-192.

NACE. (1999). Techniques for monitoring corrosion and related parameters in field applications, NACE, 3T199, NACE International, Houston, TX.

Noor, E.A. (2009). Potential of aqueous extract of *Hibiscus sabdariffa* leaves for inhibiting the corrosion of aluminium in alkaline solutions. *Journal of Applied Electrochemistry,* **39**: 1465-1475.

Obot, I.B., Ebenso, E.E., Akpan, I.A., Z. M. Gasem, Z.M. and Afolabi, A.S.(2012). Thermodynamic and density functional theory investigation of sulphathiazole as green corrosion inhibitor at mild steel/hydrochloric acid interface. *International Journal of Electrochemical Science,***7:** 1978 – 1996.

Obot, I.B., Obi-Egbedi, N.O. and Umoren, S.A. (2009a). Experimental and theoretical investigation of clotrimazole as corrosion inhibitor for aluminium in hydrochloric acid and effect of iodide ion addition. *Der Pharma Chemica*, **1(1):** 151-166 .

Obot, I.B., Umoren, S.A., Ebenso, E.E. and Obi-Egbedi, N.O. (2009b). The Inhibition of aluminium corrosion in hydrochloric acid solution by exudate gum from Raphia hookeri. *Desalination*, 250: 225–236.

Odoemelam, S.A., Ibiam, N.A. and Eddy, N.O. (2009). Adsorption and inhibitive effects of ethanol extracts of *Costus afer* on the corrosion of mild steel in H_2SO_4. *Journal of Surface Science and Technology*, **25(3-4):**1-14.

Ogoko, E.C., Odoemelam, S.A., Ita, B.I. and Eddy, N.O. (2009). Adsorption and inhibitive properties of clarithromycin for the corrosion of zinc in 0.01 to 0.05M H_2SO_4. *Portugaliae Electrochimica Acta*, **27(6):** 713-724.

Oguzie, E.E.(2004). Influence of halide ions on the inhibitive effect of congo red dye on the corrosion of mild steel in sulphuric acid solution. *Materials Chemistry and Physics*, **87(1):** 212-217.

Oguzie, E.E. (2005). Inhibition of acid corrosion of mild steel by *Telfaria occidentalis* extract. *Pigment and Resin Technology*, 34(6): 321–326.

Oguzie, E. E. (2008). Corrosion inhibitive effect and adsorption behaviour of *Hibiscus sabdariffa* extract on mild steel in acidic media. *Portugaliae Electrochimica Acta*, **2:**303-314. http://dx.doi.org/10.4152/pea.200803303

Oguzie, E.E., Adindu, C.B., Enenebeaku, C.K., Ogukwe, C.E., Chidiebere, M.A. and Oguzie, L.L. (2012a). Natural products for materials protection: Mechanism of corrosion inhibition of mild steel by acid extracts of Piper guineense. *Journal of Physical Chemistry*, dx.doi.org/10.1021/jp300791s

Oguzie, E.E. and Ebenso, E.E., (2005). Corrosion inhibition of mild steel in acidic media by some organic dyes. *Materials Letters*, **59:**2163–2165.

Oguzie, E.E., Enenebeaku, C.K., Akalezi, C.O., Okoro, S.C., Ayuk, A.A. and Ejike, E.N. (2010). Adsorption and corrosion inhibiting effect of *Dacryodis edulis* extract on low carbon steel corrosion in acidic media. *Journal of Colloid and Interface Science*, **349:** 283-292. http://dx.doi.org/10.1016/j.jcis.2010.05.027

Oguzie, E.E., Li, Y. and Wang, F.H. (2007). Corrosion inhibition and adsorption behaviour of methionine on mild steel in sulphuric acid and synergistic effect of iodide ions. *Journal of Colloid and Interface Science*, 310: 90-98.

Oguzie, E.E., Mejeha, I.M., Nwandu, M.C., Okeoma, K.B., Nnanna, L.A., Chidiebere, M.A. and Eze, F.C. (2012b). Experimental and theoretical assessment of the inhibiting action of *Aspilia africana* extract on corrosion of aluminium alloy AA3003 in hydrochloric acid. *Journal of Materials Science*,**47:** 2559-2572.

Oguzie, E. E., Onuchukwu, A.I., Okafor, P.C. and Ebenso, E.E. (2006). Corrosion inhibition and adsorption behaviour of *Occimum basiclicum* extract on aluminium. *Pigment and Resin technology*, **35(2):** 63-70.

Oguzie, E.E., Onuoha, G.N. and Onuchukwu, A.I. (2005). Inhibitory mechanism of mild steel corrosion in 2 M sulphuric acid solution by methylene blue dye. *Materials Chemistry and Physics,* **89(2-3):** 305-311.

Oguzie, E.E., Unaegbu, C., Ogukwe, C.N., Okolue, B.N. and Onuchukwu, A.I. (2004). Inhibition of mild steel corrosion in sulphuric acid using indigo dye and synergistic halide additives. *Materials Chemistry and Physics*, **84(2-3):**363-368.

Oguzie, E.E., Wang, S.G., Li, Y. and Wang, F.H. (2009). Influence of iron microstructure on corrosion inhibitor performance in acidic media. *Journal of Physical Chemistry C*, **113:** 8420-8429.

Okafor, P. C. and Ebenso, E. E. (2007). Inhibitive action of *Carica papaya* extracts on the corrosion of mild steel in acidic media and their adsorption characteristics. *Pigment and Resin Technology*, **36(3):** 134-140.

Olasehinde, E.F., Olusegun, S.J., Adesina, A.S., Omogbehin, S. A. and Momoh-Yahaya, H. (2012). Inhibitory action of *Nicotiana tabacum* extracts on the corrosion of mild steel in HCl: Adsorption and Thermodynamics Study. *Nature and Science*, 10(12): 21-34.

Oldfield, J. W. (1988). Electrochemical theory of galvanic corrosion. In: Hack, H. P. (Ed.). *Galvanic Corrosion* (pp. 5–22). Philadelphia, Penn., American Society for Testing of Materials.

Olivares-Xometl, O., Likhanova, N.V., Domı´nguez-Aguilar, M.A., Hallen, J.M., Zamudio, L.S. and Arce, E. (2006). Surface analysis of inhibitor films formed by imidazolines and amides on mild steel in an acidic environment. *Applied Surface Science*, **252:** 2139–2152.

Ould-Moulaye, C.B., Dussap, C.G. and Gros, J.B. (2001). A consistent set of formation properties of nucleic acid compounds purines and pyrimidines in the solid state and in aqueous solution. *Thermochimica Acta*, **375:** 93-107.

Parker, W.B., Allan, P.W., Waud W.R., Hong J.S. and Sorscher, E.J. (2010). Effect of expression of adenine phosphoribosyltransferase on the *in vivo* anti-tumor activity of prodrugs activated by *E. coli* purine nucleoside phosphorylase. *Cancer Gene Therapy*, **18:** 390-398.

Phanasgaonkar, A., Forsyth, M. and Cherry, B. (1997). "Organic corrosion inhibitors; How do they inhibit and can they really migrate through concrete?" Proceedings of Corrosion and Prevention (November, paper No. 54) Australasian Corrosion Association Inc: Brisbane.

Popova A., Christov, M. and Zwetanova, A. (2007). Effect of the molecular structure on the inhibitor properties of azoles on mild steel corrosion in 1 M hydrochloric acid. *Corrosion Science*, **49:** 2131-2143.

Popova, A., Sokolova, E., Raicheva, S. and Christov, M. (2003). AC and DC study of the temperature effect on mild steel corrosion in acid media in the presence of benzimidazole derivatives. *Corrosion Science,* **45(1):** 33-58.

Pourbaix, M. (1974). Atlas of Electrochemical Equilibria in Aqueous Solutions. 2nd edition, National Association of Corrosion Engineers, Houston TX.

Qiao, G. M., Zhang, J., Ren, Z. J., Hu, S. Q., Yan, Y. G. and Ti, Y. (2010). Molecular dynamics simulation of corrosive medium diffusion in corrosion inhibitor membrane. *Acta Physico-Chimica Sinica,* **26(11):** 3041-3046.

Quraishi, M.A. (2004). Naturally occurring products as corrosion inhibitors. Paper No. 04411, NACE International, Houston, TX, Corrosion.

Quraishi, M.A., Rafiquee, M.Z.A., Saxena, N. and Khan, S. (2008). Inhibition of mild steel corrosion in presence of fatty acid imidazolines in hydrochloric acid, *Protection of Metals,* **44(1):** 91-98.

Quraishi, M.A and Singh, A.K. (2010). Piroxicam: A novel corrosion inhibitor for mild steel corrosion in HCl acid solution. *Journal of Materials and Environment Science,* **1(2):** 101-110.

Reinhard, G. and Rammet, U. (1985). In: Proceedings of the 6th European Symposium on Corrosion Inhibitors (pp.831), Ferrara.

Roberge, P. R. (1999). Handbook of Corrosion Engineering (2nd ed., pp 833-861). The McGraw-Hill Companies Inc., USA.

Rodriguez-Valdez LM, Martinez-Villafane A, Martinez L, Glossman-Mitnik D. (2005) . Computational simulation of the molecular structure and properties of heterocyclic organic compounds with possible corrosion inhibition properties. *Journal of Molecular Structure (THEOCHEM),* **713:** 65–70.

Saratha, R., Priya, S.V and Thilagavathy, P. (2009). Investigation of *Citrus aurantiifolia* leaves extract as corrosion inhibitor formild steel in 1 M HCl. *E-Journal of Chemistry,* **6(3):** 785-795.

Sastri, V. S. (1998). Corrosion Inhibitors: Principles and Applications. New York: John Wiley & Sons Ltd. West Sussex.

Sastri, V.S. (2011). Green Corrosion Inhibitors: Theory and Practice. John Wiley & Sons, Inc., Hoboken, New Jersey.

Sayed, S.A., Omar, A.H., Mohammed, A.A. and Khaled, F.K. (2008). On the corrosion inhibition of low carbon steel in concentrated sulphuric acid solutions. Part 1: Chemical and electrochemical (AC and DC) studies. *Corrosion Science,* **50:** 2258-2271.

Scendo, M .(2007a). An investigation of copper corrosion inhibition in sodium nitrate solutions by purine and adenine. *Corrosion Science,* **49(10):** 3953 – 3968.

Scendo, M .(2007b). Inhibitive action of purine and adenine for copper corrosion in sulphate solutions. *Corroion Science,* **49(7):** 2985 -3000.

Scendo, M .(2008). The influence of adenine on corrosion of copper in chloride solutions. *Corrosion Sci*ence, **50(7):** 2070 -2077.

Selvi, S.T., Raman, V. and Rajendran, N. (2003).Corrosion inhibition of mild steel by benzotriazole derivatives in acidic medium. *Journal of Applied Electrochemistry,* **33(12):** 1175-1182.

Shibli, S.M.A. and Saji, V.S. (2005). Co-inhibition characteristics of sodium tungstate with potassium iodate on mild steel corrosion. *Corrosion Science,* **47(9):** 2213-2224.

Silva, A.B., Agostinho, S.M.l., Barcia, O.E., Cordeiro, G. G. O. and D'Elia, E. (2006). The effect of cysteine on the corrosion of 304L stainless steel in sulphuric acid. *Corrosion Science,* **48:** 3668–3674.

Solmaz, R., Kardas, G., Culha, M., Yazici, B. and Erbil, M. (2008). Investigation of adsorption and inhibitive effect of 2-mercaptothiazoline on corrosion of mild steel in hydrochloric acid media. *Electrochimica Acta,* **53(20):** 5941–5952.

SPE, (2008). *Society of Petroleum Engineers Journal* (Vol. 8, pp. 35). Philips Publishing Inc. Company.

Spiller, G.A. (1998). Caffeine. Boca Ration: CRC Press

Staehle, R.W. (1989). Understanding "Situation-Dependent Strength:" A Fundamental Objective in *Assessing the History of Stress Corrosion Cracking. Environment-Induced Cracking of Metals*. Houston, Tex., NACE International.

Szauer, T. and Brand, A. (1981). Mechanism of inhibition of electrode reactions at high surface coverages—II. *Electrochimica Acta*, **26(9):** 1219-1224.

Szklarska-Smialowska, Z. (1986). *Pitting Corrosion,* Houston, Tex., NACE International.

Thomas, J.G.N. (1994). The Mechanism of Corrosion, In: Shreir, L. L., Jarman, R. A., and Burstein, G. T. (Ed). *Corrosion Control,* Oxford, UK, Butterworths Heinemann.

Umoren, S. A. and Ebenso, E. E. (2008). Studies of anti-corrosive effect of Raphia hiikeri exudates gum-halide mixtures for aluminiumcorrosion in acidic medium. *Pigment and Resin Technol*ogy, **37(3):** 173-182.

Umoren S.A., Ebenso, E.E., Okafor, P.C., Ekpe, U.J. and Ogbobe, O. (2007). Effect of halide ions on the corrosion inhibition of aluminium in alkaline medium using polyvinyl alcohol. *Journal of Applied Polymer Science*, **103**: 2810-2816.

Umoren, S.A., Obot, I.B. and Igwe, I.O. (2009). Synergistic inhibition between polyvinylpyrollidone and iodide ions on corrosion of aluminium in HCl. *The Open Corrosion Journal,* **2:** 1-7

Umoren, S.A., Ogbobe, O., Ebenso, E.E. and Ekpe, U. J. (2006). Effect of halide ions on the corrosion inhibition of mild steel in acidic medium using polyvinyl alcohol. *Pigment and Resin Technology,* **35:** 284 – 292.

Upadhyay, S. K., Tehlan, S. and Mathur, P. (2007). Synthesis, Spectral and oxidase studies of a new diamide copper(II) complex with pendant benzimidazolyl groups. *Spectrochimica Acta part A,* **66:** 347-352.

Van, A.C. and Orden, A.C. (1998). Applications and problem solving using the polarization technique, Corrosion, Paper No. 301, NACE International, Houston, TX.

Villamil, R.F.V., Corio, P., Agostinho, S.M.L. and Rubim, J.C. (1999). Effect of sodium dodecylsulphate on copper corrosion in sulphuric acid media in the absence and presence of benzotriazole. *Journal of Electroanalytical Chemistry,* **472(2):** 112-119.

Vracar, L.M. and Drazic, D.M. (2002). Adsorption and corrosion inhibitive properties of some organic molecules on iron electrode in sulphuric acid. *Corrosion Science*, **44:** 1669-1680.

Wilson, J.M., Baugher, B.W., Mattes, P.M., Daddona, P.E. and Kelley, W.N. (1982). Human hypoxanthine-guanine phosphoribosyltransferase. Demonstration of structural variants in lymphoblastoid cells derived from patients with a deficiency of the enzyme. *The Journal of Clinical Investigation*, **69(3):** 706-715.

WWARN (*In Vitro* Module). (2012). 3H-hypoxanthine uptake inhibition assay to evaluate *P. Falciparium ex vivo* isolate susceptibility to antimalarial drugs. WWARN Procedure.

Xia, S., Qiu, M., Yu, L., Liu, F. and Zhao, H. (2008). Molecular dynamics and density functional theory study of relationship between structure of imidazoline derivatives and inhibition performance. *Corrosion Science,* **50:** 2021-2029.

Yan, Y., Weihua, L., Lankun, C. and Baorong, H. (2008). Electrochemical and quantum chemical study of purines as corrosion inhibitors for mild steel in 1 M HCl solution. *Corrosion Science*, **53:** 5953-5960.

Yurt, A., Balaban, A., Kandemir, S.U., Bereket, G. and Erk, B. (2004). Investigation on some Schiff bases as HCl corrosion inhibitors for carbon steel. *Materials Chemistry and Physics,* **85(2-3):** 420–426.

Yurt, A., Ulutas, S. and Dal, H. (2006). Electrochemical and theoretical investigation on the corrosion of aluminium in acidic solution containing some Schiff bases. *Applied Surface Science*, **253(2):** 919-925.

Zhang, D., Cai, Q., He, X., Gao, L. and Zhou, G. (2008). Inhibition effect of some amino acids on copper corrosion in HCl solution. *Materials Chemistry and Physics*, **112:** 353–358.

Zhang, D., Gao, L.and Zhou, G. (2004). Inhibition of copper corrosion in aerated hydrochloric acid solution by heterocyclic compounds containing a mercapto group. *Corrosion Science*, **46:** 3031–3040.

Zhang, D., Gao, L.X. and Zhou, G.D. (2006). Inhibition of copper corrosion by bis-(1,1-benzotriazoly)-α, ω-diamide compounds in aerated sulfuric acid solution, *Applied Surface Science*, **252:** 4975-4981.

Zhang, Q.B. and Hua, Y.X. (2009). Corrosion inhibition of mild steel by alkylimidazolium ionic liquids in hydrochloric acid. *Electrochimica Acta,* **54:** 1881-1887.

Zucchi, F. and Omar, I.H.(1985). Plant extracts as corrosion inhibitors of mild steel in HCl solutions. *Surface Technology*, **24(4):**391-399.

APPENDICES

Appendix I: Data for average weight loss as a function of time (hrs) for the corrosion of mild steel in 0.1 M HCl, H_2SO_4 and H_3PO_4 in the absence and presence of various concentrations of adenine (AD) at 303 and 333 K respectively.

System	Acid (0.1M)	Time (hrs)	Weight Loss (g)					
			Blank	0.002 M	0.004 M	0.006 M	0.008 M	0.01 M
AD with mild steel at 303 K	HCl	24	0.0246	0.0091	0.0209	0.0081	0.0061	0.0058
		48	0.0440	0.0182	0.0248	0.0168	0.0144	0.0108
		72	0.0596	0.0333	0.0265	0.0234	0.0198	0.0154
		96	0.0704	0.0433	0.0307	0.0285	0.0257	0.0195
		120	0.0809	0.0521	0.0331	0.0387	0.0315	0.0290
	H_2SO_4	24	0.0555	0.0492	0.0436	0.0421	0.0381	0.0248
		48	0.0711	0.0544	0.0519	0.0483	0.0426	0.0333
		72	0.0925	0.0572	0.0538	0.0498	0.0471	0.0451
		96	0.1046	0.0601	0.0570	0.0523	0.0511	0.0536
		120	0.1238	0.0651	0.0617	0.0565	0.0544	0.0667
	H_3PO_4	24	0.1267	0.0664	0.0618	0.0541	0.0573	0.0493
		48	0.1294	0.0744	0.0703	0.0659	0.0611	0.0522
		72	0.1346	0.0877	0.0773	0.0744	0.0692	0.0623
		96	0.1417	0.0987	0.0902	0.0825	0.0708	0.0686
		120	0.1564	0.1103	0.1044	0.0986	0.0821	0.0791
AD with mild steel at 333 K	HCl	24	0.2997	0.1089	0.1031	0.0904	0.0883	0.1079
		48	0.3115	0.171	0.1611	0.1473	0.1381	0.1313
		72	0.3213	0.2076	0.1711	0.1597	0.1586	0.1453
		96	0.3281	0.2414	0.2021	0.1758	0.1771	0.1509
		120	0.3434	0.3061	0.2406	0.2018	0.1964	0.1696
	H_2SO_4	24	0.2824	0.1117	0.1074	0.0715	0.0668	0.1098
		48	0.3015	0.1461	0.1347	0.1308	0.1283	0.1219
		72	0.3113	0.1695	0.1625	0.1574	0.1523	0.1351
		96	0.3205	0.1844	0.1837	0.1765	0.1702	0.1413
		120	0.3358	0.2208	0.2142	0.2033	0.1904	0.1584
	H_3PO_4	24	0.3611	0.1552	0.1431	0.1366	0.1243	0.1501
		48	0.3901	0.2205	0.2104	0.202	0.1914	0.1701
		72	0.4126	0.2453	0.2305	0.2181	0.2066	0.1928
		96	0.4176	0.2622	0.2504	0.2342	0.2191	0.2076
		120	0.4201	0.2898	0.2771	0.2471	0.2301	0.2104

Appendix II: Data for average weight loss as a function of time (hrs) for the corrosion of mild steel in 0.1 M HCl, H_2SO_4 and H_3PO_4 in the absence and presence of various concentrations of guanine (GU) at 303 and 333 K respectively.

System	Acid (0.1 M)	Time (hrs)	Weight loss (g)					
			Blank	0.002 M	0.004 M	0.006 M	0.008 M	0.01 M
GU with mild steel at 303 K	HCl	24	0.0246	0.0177	0.0163	0.0156	0.0148	0.0141
		48	0.0440	0.0328	0.0311	0.0299	0.0289	0.0278
		72	0.0596	0.0475	0.0456	0.0429	0.0434	0.0431
		96	0.0704	0.0603	0.0579	0.0567	0.0561	0.0557
		120	0.0809	0.0719	0.0728	0.0714	0.0698	0.0677
	H_2SO_4	24	0.0555	0.0303	0.0285	0.0271	0.0247	0.0238
		48	0.0711	0.0424	0.0391	0.0368	0.0348	0.0329
		72	0.0925	0.0573	0.0562	0.0532	0.0506	0.0499
		96	0.1046	0.0679	0.0711	0.0665	0.0653	0.0601
		120	0.1238	0.0924	0.0875	0.0866	0.0891	0.0805
	H_3PO_4	24	0.1267	0.0493	0.0426	0.0361	0.0327	0.0271
		48	0.1294	0.0564	0.0518	0.0418	0.0364	0.0319
		72	0.1346	0.0753	0.0642	0.0542	0.0446	0.0397
		96	0.1417	0.0887	0.0756	0.0675	0.0603	0.0551
		120	0.1564	0.1114	0.0955	0.0844	0.0831	0.0675
GU with mild steel at 333 K	HCl	24	0.2997	0.2429	0.2331	0.2204	0.2143	0.2075
		48	0.3115	0.2671	0.2511	0.2473	0.2381	0.2329
		72	0.3213	0.2876	0.2711	0.2697	0.2686	0.2591
		96	0.3281	0.2974	0.2921	0.2858	0.2771	0.2801
		120	0.3434	0.3461	0.3381	0.3288	0.3191	0.3111
	H_2SO_4	24	0.2824	0.0937	0.0904	0.0831	0.0768	0.0698
		48	0.3015	0.1141	0.1087	0.1008	0.0983	0.0849
		72	0.3113	0.1385	0.1291	0.1229	0.1213	0.1001
		96	0.3205	0.1624	0.1537	0.1435	0.1322	0.1213
		120	0.3358	0.1908	0.1842	0.1733	0.1614	0.1594
	H_3PO_4	24	0.3611	0.1492	0.1291	0.1106	0.1003	0.0801
		48	0.3901	0.1705	0.1504	0.1382	0.1214	0.1081
		72	0.4126	0.2003	0.1755	0.1591	0.1366	0.1348
		96	0.4176	0.2312	0.2004	0.1742	0.1781	0.1476
		120	0.4201	0.2568	0.2301	0.2001	0.1871	0.1704

Appendix III: Data for average weight loss as a function of time (hrs) for the corrosion of mild steel in 0.1 M HCl, H_2SO_4 and H_3PO_4 in the absence and presence of various concentrations of hypoxanthine (HYP) at 303 and 333 K respectively.

System	Acid (0.1 M)	Time (hrs)	Weight loss (g)					
			Blank	0.002 M	0.004 M	0.006 M	0.008 M	0.01 M
HYP with mild steel at 303 K	HCl	24	0.0246	0.0123	0.0106	0.0091	0.0097	0.0071
		48	0.044	0.0234	0.0211	0.0198	0.0178	0.0119
		72	0.0596	0.0313	0.0262	0.0232	0.0186	0.017
		96	0.0704	0.0421	0.0316	0.0265	0.0193	0.021
		120	0.0809	0.0514	0.0375	0.0324	0.0231	0.0245
	H_2SO_4	24	0.0555	0.0287	0.0237	0.0229	0.0218	0.0201
		48	0.0711	0.038	0.0315	0.0311	0.0298	0.0271
		72	0.0925	0.0513	0.0426	0.042	0.0403	0.0371
		96	0.1046	0.0602	0.0516	0.0501	0.0479	0.0457
		120	0.1238	0.0723	0.0646	0.0619	0.0587	0.0585
	H_3PO_4	24	0.1267	0.0761	0.0696	0.0677	0.0671	0.0655
		48	0.1294	0.0815	0.0742	0.0712	0.0702	0.0694
		72	0.1346	0.0881	0.0831	0.0794	0.0767	0.0735
		96	0.1417	0.0961	0.0891	0.0853	0.0833	0.0787
		120	0.1564	0.1087	0.1005	0.0979	0.0947	0.0891
HYP with mild steel at 333 K	HCl	24	0.2997	0.1328	0.1108	0.1093	0.0912	0.0887
		48	0.3115	0.2207	0.1921	0.1812	0.1634	0.1538
		72	0.3213	0.2343	0.2024	0.1938	0.1792	0.1652
		96	0.3281	0.2523	0.2286	0.2031	0.1873	0.1802
		120	0.3434	0.2714	0.2501	0.2201	0.2054	0.2011
	H_2SO_4	24	0.2824	0.0833	0.0708	0.0687	0.0668	0.0633
		48	0.3015	0.1417	0.1374	0.1346	0.1297	0.1267
		72	0.3113	0.1501	0.1463	0.1405	0.1343	0.1331
		96	0.3205	0.1604	0.1532	0.1494	0.1409	0.1398
		120	0.3358	0.1785	0.1713	0.1593	0.1538	0.1526
	H_3PO_4	24	0.3611	0.2122	0.2065	0.1937	0.1888	0.1771
		48	0.3901	0.2872	0.2626	0.2465	0.2298	0.2183
		72	0.4126	0.2988	0.2786	0.2687	0.2464	0.2397
		96	0.4176	0.3297	0.3195	0.2948	0.2798	0.2778
		120	0.4201	0.3561	0.3488	0.3318	0.3192	0.3106

Appendix IV: Data for average weight loss as a function of time (hrs) for the corrosion of mild steel in 0.1 M HCl, H_2SO_4 and H_3PO_4 in the absence and presence of various concentrations of xanthine (XN) at 303 and 333 K respectively.

System	Acid (0.1 M)	Time (hrs)	Weight loss (g)					
			Blank	0.002 M	0.004 M	0.006 M	0.008 M	0.01 M
XN with mild steel at 303 K	HCl	24	0.0246	0.0195	0.0186	0.0173	0.0166	0.0156
		48	0.044	0.0359	0.0349	0.0319	0.0312	0.0302
		72	0.0596	0.0499	0.0481	0.044	0.0441	0.0431
		96	0.0704	0.0619	0.0581	0.0581	0.0571	0.0561
		120	0.0809	0.0767	0.0727	0.0727	0.0719	0.0709
	H_2SO_4	24	0.0555	0.0489	0.0476	0.0454	0.0438	0.0418
		48	0.0711	0.0684	0.0667	0.0638	0.0608	0.0588
		72	0.0925	0.0928	0.0898	0.0821	0.0821	0.0819
		96	0.1046	0.1137	0.1057	0.0997	0.0987	0.098
		120	0.1238	0.1469	0.1328	0.1292	0.1212	0.1167
	H_3PO_4	24	0.1267	0.1231	0.1201	0.1141	0.1103	0.1103
		48	0.1294	0.1328	0.1271	0.1241	0.1178	0.1178
		72	0.1346	0.1448	0.1428	0.1405	0.1297	0.1297
		96	0.1417	0.1594	0.1571	0.1566	0.1466	0.1466
		120	0.1564	0.1861	0.1833	0.1821	0.1751	0.1751
XN with mild steel at 333 K	HCl	24	0.0246	0.0195	0.0186	0.0173	0.0166	0.0156
		48	0.0440	0.0359	0.0349	0.0319	0.0312	0.0302
		72	0.0596	0.0499	0.0481	0.044	0.0441	0.0431
		96	0.0704	0.0619	0.0581	0.0581	0.0571	0.0561
		120	0.0809	0.0767	0.0727	0.0727	0.0719	0.0709
	H_2SO_4	24	0.0555	0.0489	0.0476	0.0454	0.0438	0.0418
		48	0.0711	0.0684	0.0667	0.0638	0.0608	0.0588
		72	0.0925	0.0928	0.0898	0.0821	0.0821	0.0819
		96	0.1046	0.1137	0.1057	0.0997	0.0987	0.098
		120	0.1238	0.1469	0.1328	0.1292	0.1212	0.1167
	H_3PO_4	24	0.1267	0.1231	0.1201	0.1141	0.1103	0.1103
		48	0.1294	0.1328	0.1271	0.1241	0.1178	0.1178
		72	0.1346	0.1448	0.1428	0.1405	0.1297	0.1297
		96	0.1417	0.1594	0.1571	0.1566	0.1466	0.1466
		120	0.1564	0.1861	0.1833	0.1821	0.1751	0.1751

Appendix V: Data for average weight loss as a function of time (hrs) for the corrosion of aluminium in 0.1 M HCl, H_2SO_4 and H_3PO_4 in the absence and presence of various concentrations of adenine (AD) at 303 and 333 K respectively.

System	Acid (0.1 M)	Time (hrs)	Weight Loss (g)					
			Blank	0.002 M	0.004 M	0.006 M	0.008 M	0.01 M
AD with aluminium at 303 K	HCl	24	0.0321	0.0069	0.0057	0.0025	0.0015	0.0005
		48	0.054	0.0135	0.0118	0.0075	0.0041	0.0022
		72	0.0601	0.0167	0.0134	0.0104	0.0064	0.0048
		96	0.0694	0.0205	0.0167	0.0143	0.0104	0.0076
		120	0.0869	0.0279	0.0259	0.0213	0.0191	0.0137
	H_2SO_4	24	0.0046	0.0072	0.0071	0.0069	0.0065	0.0061
		48	0.0104	0.0174	0.0171	0.0171	0.0157	0.0153
		72	0.0196	0.0348	0.0342	0.0336	0.0329	0.0311
		96	0.0243	0.0462	0.0451	0.0442	0.0431	0.0412
		120	0.0421	0.0878	0.0836	0.0827	0.0796	0.0754
	H_3PO_4	24	0.0041	0.009	0.0088	0.0086	0.0081	0.0078
		48	0.0135	0.0343	0.0329	0.0322	0.0314	0.0302
		72	0.0202	0.0583	0.0561	0.0544	0.0528	0.0507
		96	0.0296	0.0916	0.0889	0.0868	0.0857	0.0815
		120	0.0481	0.1585	0.1542	0.1494	0.1415	0.1391
AD with aluminium at 333 K	HCl	24	0.1847	0.0815	0.0681	0.0591	0.0445	0.0386
		48	0.3026	0.1505	0.1191	0.1081	0.0951	0.0764
		72	0.3872	0.1988	0.1671	0.1472	0.1282	0.1044
		96	0.4717	0.2521	0.2131	0.2081	0.1681	0.1512
		120	0.6013	0.3591	0.3126	0.2776	0.2411	0.2119
	H_2SO_4	24	0.0577	0.1068	0.1008	0.0891	0.0853	0.0823
		48	0.1244	0.2574	0.2479	0.2223	0.2111	0.2082
		72	0.1328	0.3167	0.3033	0.2769	0.2592	0.2382
		96	0.1417	0.3547	0.3435	0.3109	0.2868	0.2694
		120	0.1589	0.4383	0.4133	0.3719	0.3655	0.3518
	H_3PO_4	24	0.0767	0.1298	0.1265	0.1221	0.1198	0.1171
		48	0.1515	0.2642	0.2546	0.2465	0.2418	0.2666
		72	0.1616	0.2902	0.2816	0.2687	0.2637	0.3227
		96	0.1697	0.3137	0.3055	0.2898	0.2828	0.3825
		120	0.1815	0.3451	0.3402	0.3199	0.3102	0.4904

Appendix VI: Data for average weight loss as a function of time (hrs) for the corrosion of aluminium in 0.1 M HCl, H_2SO_4 and H_3PO_4 in the absence and presence of various concentrations of guanine (GU) at 303 and 333 K respectively.

System	Acid (0.1 M)	Time (hrs)	Weight loss (g)					
			Blank	0.002 M	0.004 M	0.006 M	0.008 M	0.01 M
GU with aluminium at 303 K	HCl	24	0.0321	0.0038	0.0027	0.0022	0.0012	0.0006
		48	0.0540	0.0084	0.0059	0.0042	0.0029	0.0011
		72	0.0601	0.0104	0.0086	0.0061	0.0046	0.0017
		96	0.0694	0.0141	0.0116	0.0081	0.0056	0.0027
		120	0.0869	0.0223	0.0172	0.0141	0.0095	0.0058
	H_2SO_4	24	0.0046	0.0066	0.0064	0.006	0.0057	0.0054
		48	0.0104	0.0157	0.0152	0.0144	0.0134	0.0127
		72	0.0196	0.0311	0.0304	0.0287	0.0265	0.0249
		96	0.0243	0.0405	0.0391	0.0372	0.0352	0.0326
		120	0.0421	0.0738	0.0731	0.0677	0.0645	0.0594
	H_3PO_4	24	0.0041	0.0086	0.0081	0.0078	0.0075	0.0071
		48	0.0135	0.0295	0.0289	0.0274	0.0259	0.0242
		72	0.0202	0.0469	0.0452	0.0421	0.0415	0.0377
		96	0.0296	0.0739	0.0691	0.0654	0.0637	0.0605
		120	0.0481	0.1251	0.1202	0.1143	0.1113	0.1111
GU with aluminium at 333 K	HCl	24	0.1847	0.0625	0.0511	0.0459	0.0401	0.0360
		48	0.3026	0.1195	0.0998	0.0841	0.0745	0.0675
		72	0.3872	0.1688	0.1461	0.1221	0.1142	0.1042
		96	0.4717	0.2151	0.1931	0.1711	0.1519	0.1508
		120	0.6013	0.2791	0.2626	0.2366	0.2201	0.2042
	H_2SO_4	24	0.0577	0.0871	0.0805	0.0771	0.0745	0.0743
		48	0.1244	0.2004	0.1886	0.1778	0.1719	0.1701
		72	0.1328	0.2507	0.2289	0.2141	0.2061	0.1971
		96	0.1417	0.2868	0.2698	0.2611	0.2509	0.2299
		120	0.1589	0.3807	0.3583	0.3468	0.3191	0.2878
	H_3PO_4	24	0.0767	0.1298	0.1265	0.1241	0.1318	0.1374
		48	0.1515	0.2642	0.2579	0.2565	0.2878	0.2882
		72	0.1616	0.2952	0.2916	0.2887	0.3531	0.3524
		96	0.1697	0.3547	0.3455	0.3358	0.4208	0.3985
		120	0.1815	0.4451	0.4342	0.4201	0.5005	0.4784

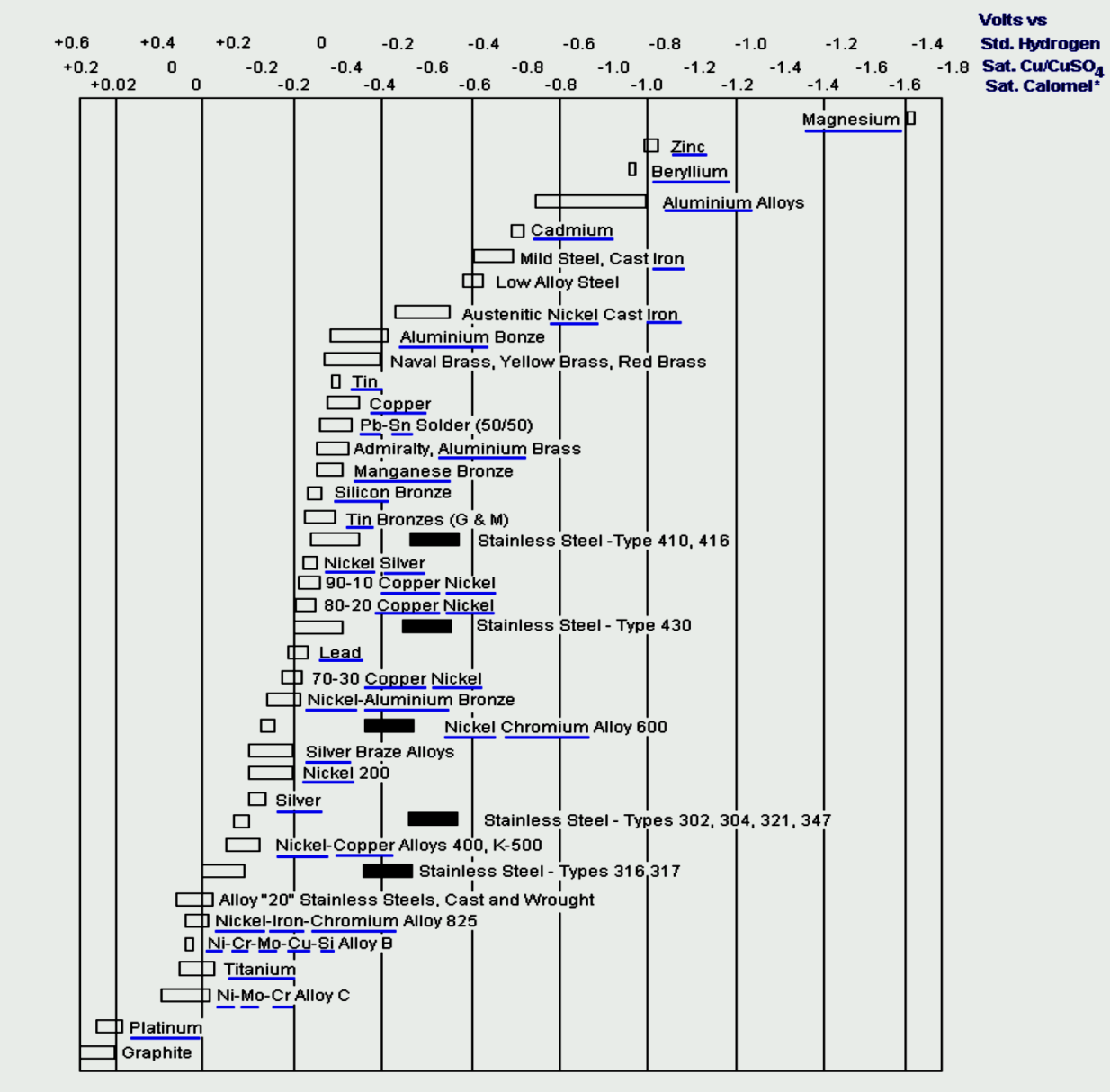
Appendix VII: **Data for average weight loss as a function of time (hrs) for the corrosion of aluminium in 0.1 M HCl, H_2SO_4 and H_3PO_4 in the absence and presence of various concentrations of hypoxanthine (HYP) at 303 and 333 K respectively.**

System	Acid (0.1 M)	Time (hrs)	Weight loss (g)					
			Blank	0.002 M	0.004 M	0.006 M	0.008 M	0.01 M
HYP with aluminium at 303 K	HCl	24	0.0321	0.0045	0.0028	0.0017	0.0013	0.0011
		48	0.054	0.0094	0.0064	0.0041	0.0036	0.0031
		72	0.0601	0.0102	0.0082	0.0064	0.0058	0.0045
		96	0.0694	0.0121	0.0101	0.0081	0.0072	0.0061
		120	0.0869	0.0157	0.0132	0.0123	0.0102	0.0087
	H_2SO_4	24	0.0046	0.001	0.0008	0.0007	0.0005	0.0004
		48	0.0104	0.0023	0.0019	0.0018	0.0014	0.0012
		72	0.0196	0.0047	0.004	0.0038	0.0028	0.0031
		96	0.0243	0.0059	0.0054	0.0051	0.0049	0.0046
		120	0.0421	0.0111	0.0104	0.0098	0.0101	0.0089
	H_3PO_4	24	0.0041	0.0062	0.0061	0.0058	0.0057	0.0056
		48	0.0135	0.021	0.0206	0.0196	0.0194	0.0188
		72	0.0202	0.0324	0.0317	0.0301	0.0298	0.0288
		96	0.0296	0.0492	0.0479	0.0455	0.0448	0.0432
		120	0.0481	0.0831	0.0801	0.0763	0.0751	0.0725
HYP with aluminium at 333 K	HCl	24	0.1847	0.0705	0.0611	0.0534	0.0485	0.0368
		48	0.3026	0.1275	0.1081	0.0908	0.0868	0.0675
		72	0.3872	0.1688	0.1471	0.1301	0.1182	0.1044
		96	0.4717	0.2151	0.1931	0.1731	0.1519	0.1512
		120	0.6013	0.2791	0.2626	0.2366	0.2211	0.2046
	H_2SO_4	24	0.0577	0.0229	0.0208	0.0194	0.0181	0.0171
		48	0.1244	0.0524	0.0497	0.0448	0.0433	0.0428
		72	0.1328	0.0627	0.0583	0.0537	0.0512	0.0492
		96	0.1417	0.0738	0.0678	0.0639	0.0598	0.0594
		120	0.1589	0.1077	0.0973	0.0919	0.0861	0.0788
	H_3PO_4	24	0.0767	0.1298	0.1265	0.1241	0.1218	0.1201
		48	0.1515	0.2642	0.2579	0.2565	0.2528	0.2436
		72	0.1616	0.2952	0.2916	0.2887	0.2841	0.2724
		96	0.1697	0.3547	0.3455	0.3358	0.3158	0.3005
		120	0.1815	0.4451	0.4342	0.4201	0.3695	0.3484

Appendix VIII: **Data for average weight loss as a function of time (hrs) for the corrosion of aluminium in 0.1 M HCl, H_2SO_4 and H_3PO_4 in the absence and presence of various concentrations of xanthine (XN) at 303 and 333 K respectively.**

System	Acid (0.1 M)	Time (hrs)	Weight loss (g)					
			Blank	0.002 M	0.004 M	0.006 M	0.008 M	0.01 M
XN with aluminium at 303 K	HCl	24	0.0321	0.0181	0.0169	0.0132	0.0121	0.0101
		48	0.054	0.0332	0.0312	0.0262	0.0239	0.0199
		72	0.0601	0.042	0.0379	0.0335	0.0338	0.0278
		96	0.0694	0.0538	0.0504	0.0454	0.0426	0.0396
		120	0.0869	0.0773	0.0715	0.0685	0.0621	0.0601
	H_2SO_4	24	0.0046	0.0054	0.0051	0.0049	0.0045	0.0042
		48	0.0104	0.0129	0.0122	0.0119	0.0116	0.0101
		72	0.0196	0.0267	0.0249	0.0241	0.0232	0.0221
		96	0.0243	0.0365	0.0341	0.0321	0.0311	0.0292
		120	0.0421	0.0706	0.0654	0.0611	0.0584	0.0554
	H_3PO_4	24	0.0041	0.0085	0.0081	0.0076	0.0071	0.0066
		48	0.0135	0.0289	0.0284	0.0261	0.0249	0.0232
		72	0.0202	0.0479	0.0466	0.0429	0.0408	0.0378
		96	0.0296	0.0787	0.0742	0.0691	0.0659	0.0651
		120	0.0481	0.1398	0.1303	0.1241	0.1183	0.1205
XN with aluminium at 333 K	HCl	24	0.1847	0.1282	0.1228	0.1191	0.1092	0.1036
		48	0.3026	0.2301	0.2202	0.2112	0.1907	0.1845
		72	0.3872	0.3172	0.3092	0.2972	0.2678	0.2584
		96	0.4717	0.4375	0.4095	0.4055	0.3767	0.3612
		120	0.6013	0.6085	0.5856	0.5776	0.5502	0.5399
	H_2SO_4	24	0.0577	0.0828	0.0788	0.0755	0.0723	0.0683
		48	0.1244	0.1875	0.1801	0.1724	0.1642	0.1542
		72	0.1328	0.2141	0.2067	0.1972	0.1872	0.1792
		96	0.1417	0.2482	0.2422	0.2298	0.2178	0.2084
		120	0.1589	0.3143	0.2993	0.2814	0.2718	0.2698
	H_3PO_4	24	0.0767	0.1767	0.1748	0.1671	0.1488	0.1451
		48	0.1515	0.3642	0.3606	0.3466	0.3166	0.3046
		72	0.1616	0.4474	0.4241	0.3987	0.3767	0.3597
		96	0.1697	0.4987	0.4763	0.4652	0.4635	0.4445
		120	0.1815	0.6152	0.5858	0.5603	0.5963	0.5634

Appendix IX: **Corrosion Potentials in Flowing Seawater (8-13 ft/s), Temperature Range 10-27 °C.**



Appendix X: Functional and linear forms of adsorption isotherm equations tested.

Isotherm	Functional form	Linear form
Langmuir		
Freundlich	**with 0<n<1**	
Temkin	**with**	
Flory-Huggins		
El-Awady		
Frumkin		

Appendix XI: **Adsorption isotherm parameters obtained from the corrosion data for mild steel in 0.1 M HCl containing various concentrations of adenine (AD), guanine (GU), hypoxanthine (HYP) and xanthine (XN).**

Isotherm	Inhibitor	303 K					333 K					
		Intercept	Slope		Log K_{ads}	R^2	ΔG_{ads}(kJmol^{-1})	Intercept	Slope		Log K_{ads}	R^2	ΔG_{ads}(kJmol^{-1})
Langmuir			1.176				-25.78	0.002	1.537		2.70	0.998	-28.33
			3.058				-24.04	0.010	4.137		2.00	0.969	-23.87
			1.160				-25.78	0.003	1.624		2.52	0.996	-27.19
			3.011				-22.30	-1.257	166.6		-0.90	0.489	-5.38
Freundli-ch			0.295				-12.63	0.323	0.282		0.323	0.972	-13.18
			0.233				-9.68	-0.122	0.297		-0.122	0.924	-10.34
			0.320				-13.01	0.344	0.317		0.344	0.997	-13.31
			0.398	***a***			-11.41	4.576	2.620	**a**	4.576	0.897	-40.30
Temkin			0.381	-3.02			-32.19	1.149	0.292	-3.943	3.934	0.983	-36.20
			0.128	-9.00			-34.65	0.405	0.107	-10.762	3.785	0.902	-35.25
			0.410	*-2.81*			-31.78	1.088	0.291	-3.957	3.739	0.994	-34.96
			0.174	-6.62			-30.43	0.528	0.199	-5.786	2.653	0.897	-28.03
Flory-Huggins	AD	2.668	1.609		2.668	0.886	-25.60	2.827	2.987		2.827	0.972	-29.14
	GU	2.930	10.12		2.930	0.968	-27.12	2.312	10.92		2.312	0.814	-25.86
	HYP	2.675	1.550		2.675	0.968	-25.64	2.666	3.138		2.666	0.986	-28.12
	XN	2.243	6.273	**K'**	2.243	0.973	-23.13	0.397	-13.95	**K'**	0.397	0.565	-13.65
El-Awady	AD	1.725	0.691	53.09	2.50	0.951	-24.62	1.151	0.518	14.16	2.222	0.982	-25.29
	GU	0.216	0.307	1.64	0.700	0.987	-14.18	0.079	0.352	1.20	0.225	0.920	-12.55
	HYP	1.873	0.746	74.64	2.510	0.988	-24.68	1.077	0.531	11.94	2.028	0.996	-24.05
	XN	0.538	0.491	3.45	1.096	0.986	-16.48	4.823	2.714	66,527	1.775	0.906	-22.44
Frumkin	AD	4.659	4.344		4.659	0.988	-37.15	-4.794	5.139		-4.794	0.993	19.45
	GU	-5.250	10.01		-5.250	0.987	20.34	-4.878	11.66		-4.878	0.942	19.98
	HYP	-4.625	4.234		-4.625	0.997	16.71	-4.642	5.242		-4.642	0.997	18.48
	XN	-4.650	8.474		-4.650	0.995	16.86	-4.864	16.23		-4.864	0.8	19.89

Appendix XII: Adsorption isotherm parameters obtained from the corrosion data for mild steel in 0.1 M H_2SO_4 containing various concentrations of adenine (AD), guanine (GU), hypoxanthine (HYP) and xanthine (XN).

Isotherm	Inhibitor	303 K						333 K					
		Intercept	Slope		Log K_{ads}	R^2	ΔG_{ads}(kJmol^{-1})	Intercept	Slope		Log K_{ads}	R^2	ΔG_{ads}(kJmol^{-1})
Langmuir			1.781				-25.78	0.001	1.643		1.00	0.996	-17.50
			2.123				-27.52	0.001	1.352		1.00	0.994	-17.50
			1.609				-27.52	0.000	1.575		0.00	0.999	-11.12
			17.44				-3.19	0.026	3.034		1.58	0.571	-21.19
Freundli-ch			0.207				-10.76	0.009	0.130		0.009	0.945	-11.18
			0.091				-9.13	0.106	0.138		0.106	0.917	-11.80
			0.320				-13.01	0.344	0.317		0.344	0.997	-13.31
			2.476	**a**			-34.95	0.380	0.567	**a**	0.380	0.861	-13.54
Temkin			0.203	-5.67			-35.83	0.866	0.153	-7.526	5.660	0.936	-47.21
			0.087	-13.23			-51.31	1.064	0.195	-5.905	5.456	0.908	-45.91
			0.410	-2.81			-31.78	1.088	0.291	-3.957	3.739	0.994	-34.96
			0.18	-6.40			-25.79	0.504	0.164	-7.021	3.073	0.731	-30.71
Flory-Huggins	AD	3.155	4.916		3.155	0.954	-28.42	3.836	5.803		3.836	0.904	-35.58
	GU	4.884	12.63		4.884	0.900	38.45	3.504	3.389		3.504	0.858	-33.46
	HYP	2.675	1.550		2.675	0.968	-25.64	2.666	3.138		2.666	0.986	-28.12
	XN	0.324	-16.95	**K'**	0.324	0.665	-12.00	1.517	2.473	**K'**	1.517	0.248	-26.89
El-Awady	AD	0.715	0.362	5.19	1.975	0.979	-21.58	0.639	0.267	4.35	2.39	0.935	-26.36
	GU	0.214	0.156	1.64	1.377	0.927	-18.11	1.036	0.360	10.86	2.88	0.901	-29.48
	HYP	1.873	0.746	74.64	2.510	0.988	-24.68	1.077	0.531	11.94	2.028	0.996	-24.05
	XN	4.505	2.560	31,988	1.761	0.883	-20.33	0.630	0.650	4.27	0.970	0.844	-17.30
Frumkin	AD	-5.273	6.590		-5.273	0.986	20.47	-6.309	7.848		-6.309	0.960	29.11
	GU	-7.591	12.34		-7.591	0.943	33.92	-6.092	6.501		-6.092	0.952	27.72
	HYP	-4.625	4.234		-4.625	0.997	16.71	-4.642	5.242		-4.642	0.997	18.48
	XN	-5.082	19.42		-5.082	0.913	19.37	-4.183	8.092		-4.183	0.863	15.55

Appendix XIII: Adsorption isotherm parameters obtained from the corrosion data for mild steel in 0.1 M H_3PO_4 containing various concentrations of adenine (AD), guanine (GU), hypoxanthine (HYP) and xanthine (XN).

Isotherm	Inhibitor	303 K					333 K					
		Intercept	Slope		Log K_{ads}	R^2	ΔG_{ads}(kJmol^{-1})	Intercept	Slope		Log K_{ads}	R^2	ΔG_{ads}(kJmol^{-1})
Langmuir			1.709				-25.78	0.001	1.714		3.00	0.996	-30.25
			1.274				-25.78	0.001	1.305		3.00	0.995	-30.25
			2.047				-27.52	0.001	2.153		3.00	0.999	-30.25
			58.05				-6.70	0.072	1.155		1.14	0.381	-18.39
Freundli-ch			0.214				-10.91	0.081	0.178		0.081	0.992	-11.63
			0.205				-11.52	0.333	0.252		0.333	0.992	-13.24
			0.162				-10.01	-0.045	0.157		-0.045	0.974	-10.83
			0.942	**a**			-15.75			**a**			
Temkin			0.215	-5.36			-35.50	0.907	0.189	-6.092	4.798	0.985	-41.71
			0.323	-3.56			-33.72	1.226	0.274	-4.202	4.474	0.979	-39.65
			0.147	-7.83			-39.55	0.709	0.137	-8.405	5.175	0.983	-44.11
			0.142	*-8.11*			-22.94	0.368	0.128	-8.996	2.875	0.971	-29.45
Flory-Huggins	AD	2.84	3.356		2.840	0.894	-26.59	3.505	5.444		3.505	0.935	-33.47
	GU	2.871	2.167		2.871	0.945	-26.77	3.096	2.579		3.096	0.945	-30.86
	HYP	3.668	7.754		3.668	0.987	-31.40	3.754	8.558		3.754	0.980	-35.06
	XN			**K'**				1.139	1.054	**K'**	1.139	0.275	-18.38
El-Awady	AD	0.594	0.31	3.92	1.914	0.958	-21.22	0.664	0.307	4.61	2.162	0.963	-24.90
	GU	1.465	0.580	29.17	2.526	0.976	-24.77	1.314	0.498	20.61	2.639	0.973	-27.95
	HYP	0.453	0.269	2.84	1.685	0.991	-19.89	0.394	0.254	2.48	1.553	0.980	-21.02
	XN							1.142	1.002	13.87	1.140	0.989	-18.39
Frumkin	AD	-5.312	6.593		-5.312	0.985	20.70	-5.565	6.831		-5.565	0.994	24.36
	GU	-4.939	4.836		-4.939	0.993	18.54	-5.329	5.384		-5.329	0.992	22.86
	HYP	-5.930	8.529		-5.930	0.995	24.29	-6.024	8.992		-6.024	0.990	27.29
	XN							-4.558	15.09		-4.558	0.964	17.94

Appendix XIV: Adsorption isotherm parameters obtained from the corrosion data for aluminium in 0.1 M HCl containing various concentrations of adenine (AD), guanine (GU), hypoxanthine (HYP) and xanthine (XN).

Isotherm	Inhibitor	303 K					333 K					
		Intercept	Slope		Log K_{ads}	R^2	ΔG_{ads}(kJmol^{-1})	Intercept	Slope		Log K_{ads}	R^2	ΔG_{ads}(kJmol^{-1})
Langmuir			1.038				-10.12	0.002	1.534		2.70	0.993	-28.33
			0.989				-10.12	0.001	1.275		3.00	0.998	-30.25
			1.052				-10.12	-0.001	1.630		-3.00	0.946	8.01
			1.582				-24.04	0.009	2.591		2.05	0.908	-24.19
Freundli-ch			0.140				-11.43	0.152	0.195		0.152	0.963	-12.09
			0.101				-11.18	0.140	0.138		0.140	0.992	-12.01
			0.066				-10.69	0.145	0.149		0.145	0.987	-12.04
			0.351	**a**			-12.39	0.144	0.347	**a**	0.144	0.881	-12.04
Temkin			0.257	-4.48			-41.67	1.025	0.224	-5.141	4.576	0.953	-40.30
			0.207	-5.617			-48.80	1.145	0.209	-5.51	5.479	0.987	-46.05
			0.134	-8.59			-61.58	1.133	0.216	-5.331	5.245	0.979	-44.56
			0.306	-3.763			-30.88	0.643	0.181	-6.362	3.552	0.838	-33.77
Flory-Huggins	AD	3.137	1.269		3.137	0.876	-28.32	3.176	3.769		3.176	0.916	-31.34
	GU	3.063	0.798		3.063	0.822	-27.89	3.611	3.109		3.611	0.965	-34.14
	HYP	4.021	1.889		4.021	0.978	-33.45	3.505	3.163		3.505	0.951	-31.29
	XN	2.467	2.676	**K'**	2.467	0.872	-24.43	2.18	4.769	**K'**	2.180	0.659	-25.02
El-Awady	AD	2.345	0.740	221.31	3.169	0.911	-28.50	0.919	0.393	8.30	2.338	0.953	-26.03
	GU	3.35	1.034	2,238.72	3.239	0.853	-28.91	1.236	0.406	17.22	3.044	0.979	-30.53
	HYP	2.151	0.550	141.58	3.910	0.982	-32.80	1.180	0.406	15.13	2.906	0.972	-29.65
	XN	1.114	0.570	13.00	1.954	0.955	-21.45	0.493	0.450	3.11	1.095	0.869	-18.10
Frumkin	AD	-6.980	6.611		-6.980	0.990	30.38	-5.329	5.988		-5.329	0.975	22.86
	GU	-10.10	9.855		-10.10	0.997	48.48	-6.434	6.674		-6.434	0.994	29.90
	HYP	-11.58	11.54		-11.58	0.999	57.06	-6.137	6.419		-6.137	0.991	28.01
	XN	-4.438	7.053		-4.438	0.915	15.63	-4.427	4.938		-4.427	0.975	17.11

Appendix XV: Adsorption isotherm parameters obtained from the corrosion data for mild steel in 0.1 M H_2SO_4 containing various concentrations of hypoxanthine (HYP).

Isotherm	Inhibitor	303 K					333 K				
		Intercept	Slope		Log K_{ads}	R^2	ΔG_{ads}(kJmol^{-1})	Intercept	Slope	Log K_{ads}	R^2	ΔG_{ads}(kJmol^{-1})
Langmuir			1.194				-10.12	0.000	1.348	0	0.997	-11.12
Freundli-ch			0.045				-10.13	0.040	0.098	0.040	0.932	-11.38
Temkin			0.081	-14.216			-80.37	0.918	0.153	-7.526	6.000	0.994	-49.38
Flory-Huggins	HYP	5.895	5.393		5.895	0.963	-44.32	4.135	5.724	4.135	0.987	-37.48
El-Awady	HYP	1.080	0.215	12.02	5.023	0.969		0.740	0.271	5.50	2.732	0.993	
Frumkin	HYP	-13.29	14.60		-13.29	0.987	66.98	-6.853	8.251	-6.853	0.997	32.57

Appendix XVI: Frequencies, intensities and functional groups associated with adsorption of IR by adenine (AD) powder.

Frequency (cm^{-1})	Intensity	Assignments
722.37	29.6969	C-H "oop" aromatic
894.04	24.2767	C-H "oop" aromatic
1031.95	30.7365	C-N stretch
1146.72	24.72	C-H wag
1276.92	22.1414	C-N stretch aromatics
1425.44	22.2724	C-C stretch aromatics
1600.97	22.0731	N-H bend
1899.95	46.2814	C=O stretch
2576.98	22.1412	O-H stretch
2677.29	22.1993	O-H stretch
2804.59	21.1172	O-H stretch
2893.32	22.139	O-H stretch
3076.56	22.4901	C-H stretch
3262.70	24.2595	O-H stretch
3358.18	25.2162	O-H stretch
3598.33	42.2905	O-H stretch

Appendix XVII: Frequencies, intensities and functional groups associated with adsorption of IR by the corrosion product of mild steel in the presence of adenine (AD) as an inhibitor.

Frequency (cm^{-1})	Intensity	Assignments
717.54	33.62	C-H "oop" aromatics
1369.50	45.49	N-O symmetric stretch
1482.34	42.66	C-C stretch (in-ring)
1634.73	35.36	N-H bend
2790.12	24.79	O-H stretch
2939.61	23.94	C-H stretch aromatics
3068.85	24.38	C-H stretch aromatics
3211.59	25.62	N-H stretch
3339.86	26.34	N-H stretch
3448.84	28.13	O-H stretch
3533.71	29.70	O-H stretch
3798.93	39.01	O-H stretch

Appendix XVIII: Frequencies, intensities and functional groups associated with adsorption of IR by the corrosion product of aluminium in the presence of adenine (AD) as an inhibitor.

Frequency (cm^{-1})	Intensity	Assignments
650.03	37.61	C-Br stretch
828.45	33.28	C-H "oop" aromatics
1022.31	31.96	C-N stretch
1177.58	31.04	C-H wag
1323.21	30.27	C-N stretch aromatics
1419.66	30.89	C-C stretch(in-ring) aromatics
1604.83	29.70	N-H bend
1795.79	31.48	C=O stretch
1998.32	32.32	C=O stretch
2095.73	30.79	C-N stretch
2271.26	30.25	C-N stretch
2428.46	28.20	O-H stretch
2522.01	29.18	O-H stretch
2639.67	29.40	O-H stretch
2740.94	28.64	O-H stretch
2859.56	28.78	O-H stretch
3002.30	28.83	C-H stretch
3196.15	30.36	O-H stretch
3380.36	33.70	O-H stretch
3497.06	33.81	O-H stretch
3608.93	34.14	O-H stretch
3788.32	36.93	O-H stretch
3957.10	34.79	O-H stretch

Appendix XIX: Frequencies, intensities and functional groups associated with adsorption of IR by guanine (GU).

Frequency (cm^{-1})	Intensity	Assignments
645.21	40.47	C-Br stretch
857.39	30.83	C-H "oop" aromatics
1220.02	25.72	C-O stretch
1367.58	24.56	C-N stretch
1599.04	25.24	C=O stretch
1730.21	24.63	C=O stretch
2445.82	24.59	C-H stretch
2579.88	23.27	O-H stretch
2665.71	24.03	O-H stretch
2834.49	24.26	O-H stretch
3034.13	26.12	C-H stretch aromatics
3153.72	25.96	C-H stretch aromatics
3357.22	29.59	O-H stretch

Appendix XX: Frequencies, intensities and functional groups associated with adsorption of IR by the corrosion product of mild steel in the presence of guanine (GU) as an inhibitor.

Frequency (cm^{-1})	Intensity	Assignments
733.94	29.58	C-H "oop" aromatics
1016.52	36.58	C-O stretch
1153.47	44.20	C-O stretch
1372.40	36.41	C-N stretch
1473.66	34.92	C-C stretch (in-ring)
1629.90	28.94	N-H bend
1684.88	28.76	C=O stretch
1995.43	29.20	C=O stretch
2237.50	28.99	C-N stretch
2399.53	26.35	C-N stretch
2673.43	22.85	O-H stretch
2812.31	25.03	C-H stretch
2879.82	24.41	C-H stretch
2998.44	24.79	C-H stretch
3086.21	24.27	C-H stretch
3269.45	25.29	O-H stretch
3396.76	26.81	O-H stretch
3494.17	26.83	O-H stretch
3664.87	31.13	O-H stretch
3797.96	31.35	O-H stretch
3957.10	30.22	O-H stretch

Appendix XXI: Frequencies, intensities and functional groups associated with adsorption of IR by the corrosion product of aluminium in the presence of guanine (GU) as an inhibitor.

Frequency (cm^{-1})	Intensity	Assignments
890.18	32.38	C-H "oop" aromatics
1021.34	28.22	C-O stretch
1313.57	26.68	C-N stretch
1407.12	28.21	C-C sretch (in-ring)
1605.79	25.88	C=O stretch
1809.29	27.11	C=O stretch
1931.77	26.73	C=O stretch
2093.80	26.14	C-C stretch
2257.75	26.26	C-N stretch
2442.93	26.66	C-H stretch
2650.28	27.04	C-H stretch
2747.69	28.38	C-H stretch
2851.85	28.03	C-H stretch
2948.29	28.49	C-H stretch
3080.42	28.14	C-H stretch
3357.70	31.72	O-H stretch
3452.70	31.78	O-H stretch
3627.26	33.33	O-H stretch
3796.04	36.04	O-H stretch
3932.02	32.75	O-H stretch

Appendix XXII: Frequencies, intensities and functional groups associated with adsorption of IR by hypoxanthine (HYP) powder

Frequency (cm^{-1})	Intensity	Assignments
538.16	60.53	C-Br stretch
636.53	63.22	C-Br stretch
886.32	34.38	C-H "oop" aromatics
1132.25	39.95	C-O stretch
1194.94	47.03	C-O stretch
1362.75	41.58	N-O symmetric stretch
1449.55	41.35	C-C stretch aromatics
1606.76	27.63	C-C stretch aromatics
1672.34	25.88	C=C stretch
1844.97	44.43	C=O stretch
2475.72	23.65	O-H stretch
2580.84	23.13	O-H stretch
2648.35	23.49	O-H stretch
2796.88	23.95	O-H stretch
2902.96	24.03	O-H stretch
3049.56	25.66	C-H stretch aromatics
3459.45	62.67	O-H stretch

Appendix XXIII: Frequencies, intensities and functional groups associated with adsorption of IR by the corrosion product of mild steel in the presence of hypoxanthine (HYP) as an inhibitor.

Frequency (cm^{-1})	Intensity	Assignments
700.18	32.85	C-H "oop"
1010.73	63.89	C-O stretch
1373.36	55.57	N-O stretch
1487.17	51.90	C-C stretch aromatics
1654.01	39.12	C=C stretch
3056.31	24.49	C-H stretch
3202.91	24.38	O-H stretch
3290.67	25.27	O-H stretch
3382.29	23.91	N-H stretch
3512.49	25.68	O-H stretch
3825.93	45.59	O-H stretch
3971.56	44.11	O-H stretch

Appendix XXIV: Frequencies, intensities and functional groups associated with adsorption of IR by the corrosion product of aluminium in the presence of hypoxanthine (HYP) as an inhibitor

Frequency (cm^{-1})	Intensity	Assignments
822.67	35.34	C-H "oop" aromatics
962.51	30.61	C-H bend
1164.08	31.58	C-O stretch
1312.60	29.85	C-O stretch
1428.34	30.52	C-C stretch
1600.01	30.40	C-C stretch
1755.28	30.07	C=O stretch
1898.98	28.38	C=O stretch
2030.15	28.04	C-C stretch
2140.09	29.02	C-C stretch
2263.54	28.73	C-N stretch
2417.85	29.18	O-H stretch
2508.51	28.48	O-H stretch
2605.92	28.63	O-H stretch
2753.48	29.81	O-H stretch
2858.6	30.82	O-H stretch
2949.26	31.51	O-H stretch
3068.85	31.25	C-H stretch
3139.25	31.17	C-H stretch
3256.91	32.93	N-H stretch
3403.51	33.51	N-H stretch
3489.34	33.47	N-H stretch
3688.98	38.21	O-H stretch
3791.21	36.01	O-H stretch
3918.52	38.27	O-H stretch

Appendix XXV: Frequencies, intensities and functional groups associated with adsorption of IR by xanthine (XN) powder

Frequency (cm^{-1})	Intensity	Assignments
499.58	49.52	C-Br stretch
755.16	35.70	C-H "oop" aromatics
872.82	35.12	C-H "oop" aromatics
1149.61	30.35	C-N stretch
1351.18	30.54	C-N stretch
1415.8	30.00	C-C stretch aromatics
1600.97	28.96	C-C stretch aromatics
1776.50	28.81	C=O carbonyls
2521.05	28.36	O-H stretch
2681.14	28.44	O-H stretch
2867.28	28.83	O-H stretch
3030.27	30.42	C-H stretch aromatics
3139.25	31.37	C-H stretch aromatics
3216.41	31.03	O-H stretch

Appendix XXVI: Frequencies, intensities and functional groups associated with adsorption of IR by the corrosion product of mild steel in the presence of xanthine (XN) as an inhibitor

Frequency (cm^{-1})	Intensity	Assignments
646.17	41.29	C-Br stretch
745.51	37.34	C-H "oop" aromatics
838.10	40.51	C-H "oop" aromatics
1011.70	48.92	C-N stretch
1155.40	57.79	C-N stretch
1475.59	45.79	C-C stretch aromatics
1634.73	34.17	C-C stretch aromatics
2026.29	42.12	C-N stretch aromatics
2210.50	40.56	C-N stretch
2591.45	32.39	O-H stretch
2701.40	29.59	O-H stretch
2787.23	28.57	O-H stretch
2906.82	28.84	C-H stretch aromatics
3092.96	29.65	C-H stretch aromatics
3282.95	32.17	O-H stretch
3379.40	32.86	N-H stretch
3504.77	33.25	O-H stretch
3708.27	41.96	O-H stretch
3812.43	43.42	O-H stretch
3942.63	40.01	O-H stretch

Appendix XXVII: Frequencies, intensities and functional groups associated with adsorption of IR by the corrosion product of aluminium in the presence of xanthine (XN) as an inhibitor

Frequency (cm^{-1})	Intensity	Assignments
800.49	31.799	C-H "oop" aromatics
1052.20	26.59	C-N stretch
1171.79	27.72	C-N stretch
1299.10	25.49	C-N stretch aromatics
1398.44	26.29	C-C stretch
1598.08	25.44	C-C stretch
1973.24	24.62	C-N stretch
2152.63	24.65	C-C stretch
2226.89	24.67	C-N stretch
2419.78	25.30	O-H stretch
2600.13	24.25	O-H stretch
2757.33	25.65	O-H stretch
2865.35	26.02	O-H stretch
3093.92	26.86	C-H stretch
3265.59	28.86	O-H stretch
3362.04	28.96	N-H stretch
3466.20	29.86	O-H stretch
3687.05	33.56	O-H stretch
3784.46	33.01	O-H stretch
3942.63	31.67	O-H stretch